

STUDIES IN THE OPTIMIZATION OF THE SUZUKI-MIYAJIMA REACTION

by

EMILY ANNE MITCHELL

A thesis submitted to the Department of Chemistry  
in conformity with the requirements for  
the Degree of Doctor of Philosophy

Queen's University  
Kingston, Ontario, Canada

December 5, 2008

Copyright © Emily Anne Mitchell, 2008

## ABSTRACT

Enormous efforts have been made to optimize the Pd-catalyzed Suzuki-Miyaura reaction, but there is to date no generally useful protocol and forcing conditions are often required. One reaction variable that has often been neglected is the extent to which the supposed catalysts, bisphosphinepalladium(0) complexes, are actually formed from the variety of popular precatalysts used. There is in fact little evidence that these precursors produce bis-ligated Pd(0) complexes and it is possible that the rate limiting factor may be catalyst formation. If so, then the development of an optimized method for forming these catalytic species would be a significant contribution to this field. The following work describes research efforts to determine the optimum conditions to generate PdL<sub>2</sub> (L = PCy<sub>3</sub>, PMeBu<sup>t</sup><sub>2</sub>, PBu<sup>t</sup><sub>3</sub>) cleanly and quantitatively from Pd(η<sup>3</sup>-C<sub>3</sub>H<sub>5</sub>)(η<sup>5</sup>-C<sub>5</sub>H<sub>5</sub>) and Pd(η<sup>3</sup>-1-Ph-C<sub>3</sub>H<sub>5</sub>)(η<sup>5</sup>-C<sub>5</sub>H<sub>5</sub>).

Furthermore, the conditions under which PdL<sub>3</sub> species may exist in equilibrium with the PdL<sub>2</sub> species are defined. NMR studies indicate that while Pd(PBu<sup>t</sup><sub>3</sub>)<sub>2</sub> shows no inclination to increase its coordination number, Pd(PCy<sub>3</sub>)<sub>2</sub> and Pd(PMeBu<sup>t</sup><sub>2</sub>)<sub>2</sub> react with added phosphine to form 3:1 compounds. Equilibrium constants for dissociation of the PdL<sub>3</sub> compounds were measured over a range of temperatures, yielding the thermodynamic parameters of dissociation and estimated Pd-P bond dissociation energies. Additionally, the generation of heteroleptic species serve to confirm the existence of 3:1 compounds.

A kinetic study of the oxidative addition of PhBr to Pd(PCy<sub>3</sub>)<sub>2</sub> was also performed. It was found that oxidative addition was first order in palladium, but that added bromide had no effect on the rate of oxidative addition. Added PCy<sub>3</sub> inhibited oxidative addition, possibly due to the conversion of palladium(0) into the less active 3:1 compound.

The formation of the catalytically less active 3:1 compounds has serious implications for many catalytic cross-coupling processes which involve catalyst formation via the slow reduction of palladium(II) in the presence of excess phosphine; for many systems, relatively little of the added palladium may actually be present as the active bisphosphinepalladium(0) compound.

## ACKNOWLEDGEMENTS

I would like to thank Dr. M.C. Baird for the opportunity to participate in his research. I am sincerely grateful for his guidance, patience and friendship and for the privilege of working under his supervision. I would also like to gratefully acknowledge the continued support of Dr. C. Crudden, Dr. P. Jessop and Dr. F. Sauriol for their contributions to my research and education. In addition, I would like to acknowledge the financial support of NSERC and Queen's University.

I would also like to thank the Baird Lab members, past and present, and so many members of the Department of Chemistry, who have made my stay at Queen's so enjoyable. I will always recollect on my time in the Baird Lab with the fondest of memories.

I would also like to acknowledge many of those I have met while at Queen's for their kindness and friendship. I would like to thank Shirley, as well as John and Eva, for their unfailing support. I would also like to thank Eggy and Rea: I will always cherish our unforgettable antics and your enduring friendship. I would especially like to thank Goran, for his constant patience. In difficult times, you have always reminded me to enjoy each day, one at a time. I am forever grateful for having met you.

Lastly, I would like to thank my dear family, who has provided me with so much love and encouragement over the years. I have been truly blessed to have you in my life. Thank you mom, dad and grandma for your continued belief in me. I love you all more than words can say.

## STATEMENT OF ORIGINALITY

The research discussed in this work was carried out by the author in the Department of Chemistry at Queen's University under the supervision of Dr. M. C. Baird. The kinetic portion of this research was conducted under the guidance of Dr. P. Jessop at Queen's University.

## TABLE OF CONTENTS

	Page
ABSTRACT.....	i
ACKNOWLEDGEMENTS.....	iii
STATEMENT OF ORIGINALITY.....	iv
TABLE OF CONTENTS.....	v
LIST OF TABLES.....	xi
LIST OF FIGURES.....	xiii
LIST OF SCHEMES.....	xxi
LIST OF SYMBOLS AND ABBREVIATIONS.....	xxiv
CHAPTER 1. INTRODUCTION.....	1
1.1 Historical Development of Cross-coupling Reactions.....	2
1.1.1 “First Generation” Palladium Catalyzed Cross-coupling.....	3
1.1.2 “Second Generation”.....	5
1.2 The Suzuki-Miyaura (SM) Reaction.....	7
1.2.1 Mechanistic Features of the SM Reaction.....	8
1.2.1.1 Oxidative Addition.....	9
1.2.1.2 Transmetallation.....	14
1.2.1.3 Reductive Elimination.....	16
1.2.2 Common Conditions for SM Reactions.....	19
1.2.2.1 Generally Used Precatalysts.....	19
1.2.2.2 Organoboron Reagents.....	21
1.2.2.3 Aryl Electrophile.....	23
1.3 Challenges to “Textbook” SM Catalysis.....	24

1.3.1	Consequences Associated with Choice of Precatalyst.....	25
1.3.1.1	Pd(PPh <sub>3</sub> ) <sub>4</sub> .....	25
1.3.1.2	Pd(dba) <sub>2</sub> /Pd <sub>2</sub> (dba) <sub>3</sub> .....	26
1.3.1.3	Monophosphine Complexes.....	31
1.3.1.4	Pd(OAc) <sub>2</sub> + nPPh <sub>3</sub> .....	40
1.3.1.5	Pd(PPh <sub>3</sub> ) <sub>2</sub> Cl <sub>2</sub> .....	42
1.4	Research Objectives.....	43
1.4.1	Optimization of PdL <sub>2</sub> Generation.....	44
1.4.2	Assessment of the Relevance of Species of the Type PdL <sub>1,2,3</sub> .....	47
1.4.3	Kinetics of Oxidative Addition with Pd(PCy <sub>3</sub> ) <sub>2</sub> .....	48
1.4.4	Studies in Transmetalation and Reduction of Pd(II).....	49
1.5	References.....	51
CHAPTER 2. EXPERIMENTAL .....		60
2.1	Physical Methods.....	60
2.2	Chemical Supplies.....	61
2.3	Preparation of Palladium Compounds.....	62
2.3.1	Preparation of [PdCl(η <sup>3</sup> -C <sub>3</sub> H <sub>5</sub> )] <sub>2</sub> .....	62
2.3.2	Preparation of [PdCl(η <sup>3</sup> -1-Ph-C <sub>3</sub> H <sub>4</sub> )] <sub>2</sub> .....	63
2.3.3	Preparation of Pd(η <sup>3</sup> -C <sub>3</sub> H <sub>5</sub> )(η <sup>5</sup> -C <sub>5</sub> H <sub>5</sub> ).....	64
2.3.4	Preparation of Pd(η <sup>3</sup> -1-Ph-C <sub>3</sub> H <sub>4</sub> )(η <sup>5</sup> -C <sub>5</sub> H <sub>5</sub> ).....	65
2.3.5	Preparation of PdL <sub>2</sub> (L = PCy <sub>3</sub> , PBU <sup>t</sup> <sub>3</sub> ).....	66
2.3.6	Preparation of PdL <sub>2</sub> (L = PMeBu <sup>t</sup> <sub>2</sub> ).....	67
2.3.7	Preparation of PdCl <sub>2</sub> [PMeBu <sup>t</sup> <sub>2</sub> ] <sub>2</sub> .....	67

2.3.8	Preparation of PdCl <sub>2</sub> [PCy <sub>3</sub> ] <sub>2</sub> .....	68
2.3.9	Preparation of <i>trans</i> -PdPh[PCy <sub>3</sub> ] <sub>2</sub> Br.....	69
2.3.10	Preparation of Pd[COD]Br <sub>2</sub> .....	70
2.3.11	Attempted Preparation of Pd(PBu <sup>t</sup> <sub>3</sub> ) <sub>2</sub> Br <sub>2</sub> .....	71
2.4	<i>In Situ</i> generation of PdL <sub>n</sub> .....	72
2.4.1	<i>In Situ</i> Generation of PdL <sub>n</sub> from Pd(η <sup>3</sup> -C <sub>3</sub> H <sub>5</sub> )(η <sup>5</sup> -C <sub>5</sub> H <sub>5</sub> ).....	72
2.4.1.1	L = PCy <sub>3</sub> .....	73
2.4.1.2	L = PMeBu <sup>t</sup> <sub>2</sub> .....	73
2.4.1.3	L = PBu <sup>t</sup> <sub>3</sub> .....	73
2.4.1.4	L = PPh <sub>3</sub> .....	74
2.4.1.5	L = PMe <sub>3</sub> .....	74
2.4.1.6	Independent Oxidation of L (L = PPh <sub>3</sub> , PCy <sub>3</sub> ).....	75
2.4.2	<i>In Situ</i> Generation of PdL <sub>2</sub> from Pd(η <sup>3</sup> -1-Ph-C <sub>3</sub> H <sub>4</sub> )(η <sup>5</sup> -C <sub>5</sub> H <sub>5</sub> ).....	75
2.4.2.1	L = PCy <sub>3</sub> .....	75
2.4.2.2	L = PMeBu <sup>t</sup> <sub>2</sub> .....	76
2.4.2.3	L = PPh <sub>3</sub> .....	76
2.5	Thermodynamic Parameters for Dissociation of PdL <sub>3</sub> .....	76
2.5.1	L = PCy <sub>3</sub> .....	76
2.5.2	L = PMeBu <sup>t</sup> <sub>2</sub> .....	77
2.5.3	L = PBu <sup>t</sup> <sub>3</sub> .....	77
2.6	Generation of Heteroleptic Systems PdLL'.....	77
2.6.1	PCy <sub>3</sub> / PBu <sup>t</sup> <sub>3</sub> .....	77
2.6.2	PMeBu <sup>t</sup> <sub>2</sub> / PBu <sup>t</sup> <sub>3</sub> .....	79



2.6.3	PCy <sub>3</sub> /PMeBu <sup>t</sup> <sub>2</sub> .....	79
2.6.4	PCy <sub>3</sub> /PPh <sub>3</sub> .....	80
2.7	Investigative Experiments Involving Oxidative Addition.....	80
2.7.1	Oxidative Addition with Isolated PdL <sub>2</sub> .....	81
2.7.1.1	Oxidative Addition with Pd(PCy <sub>3</sub> ) <sub>2</sub> and Pd(PMeBu <sup>t</sup> <sub>2</sub> ) <sub>2</sub> .....	81
2.7.1.2	Attempted Oxidative Addition with Pd(PBu <sup>t</sup> <sub>3</sub> ) <sub>2</sub> .....	81
2.7.2	Oxidative Addition with <i>In Situ</i> Generated PdL <sub>2</sub> .....	82
2.8	Kinetic Study of Oxidative Addition.....	83
2.8.1	Oxidative Addition of PhBr to Pd(PCy <sub>3</sub> ) <sub>2</sub> .....	83
2.8.1.1	In the Presence of TOPB.....	83
2.8.1.2	In the Presence of Additional PCy <sub>3</sub> .....	84
2.9	Studies of Transmetalation by GC.....	84
2.10	Attempted Preparation of [TOP[[PhBF <sub>3</sub> ]].....	85
2.10.1	Preparation In Water.....	85
2.10.2	Anhydrous Preparation.....	86
2.11	Reduction of Pd(II) Compounds.....	86
2.12	References.....	88
CHAPTER 3. Results and Discussion.....		90
3.1	<i>In Situ</i> Generation of PdL <sub>n</sub> from Pd(η <sup>3</sup> -C <sub>3</sub> H <sub>5</sub> )(η <sup>5</sup> -C <sub>5</sub> H <sub>5</sub> ).....	90
3.1.1	Displacement Reactions of Pd(η <sup>3</sup> -C <sub>3</sub> H <sub>5</sub> )(η <sup>5</sup> -C <sub>5</sub> H <sub>5</sub> ) Complexes.....	91
3.1.2	Generation of PdL <sub>2</sub> (L= PCy <sub>3</sub> , P MeBu <sup>t</sup> <sub>2</sub> , PBu <sup>t</sup> <sub>3</sub> ).....	99
3.1.2.1	L = PCy <sub>3</sub> .....	99
3.1.2.2	L = PMeBu <sup>t</sup> <sub>2</sub> .....	108

3.1.2.3	L = PBu <sup>t</sup> <sub>3</sub> .....	112
3.1.3	Generation of PdL <sub>n</sub> (L = PMe <sub>3</sub> , PPh <sub>3</sub> ) where n >2.....	115
3.1.3.1	L = PMe <sub>3</sub> .....	118
3.1.3.2	L = PPh <sub>3</sub> .....	122
3.2	Generation of PdL <sub>2</sub> from Pd(η <sup>3</sup> -1-Ph-C <sub>3</sub> H <sub>4</sub> )(η <sup>5</sup> -C <sub>5</sub> H <sub>5</sub> ).....	129
3.2.1	L = PCy <sub>3</sub> .....	131
3.2.2	L = PMeBu <sup>t</sup> <sub>2</sub> .....	143
3.2.3	L = PPh <sub>3</sub> .....	146
3.3	Homoleptic Compounds PdL <sub>3</sub> ; Equilibria between PdL <sub>2</sub> and PdL <sub>3</sub> .....	151
3.4	Syntheses of the 2:1 Heteroleptic Compounds PdLL'; Identification of Corresponding 3:1 Compounds.....	156
3.5	Investigative Experiments In Oxidative Addition.....	172
3.5.1	Oxidative Addition with Isolated PdL <sub>2</sub> .....	172
3.5.2	Oxidative Addition with <i>In Situ</i> Generated PdL <sub>2</sub> .....	181
3.6	Kinetic Analyses of Oxidative Addition of PhBr to Pd(PCy <sub>3</sub> ) <sub>2</sub> .....	183
3.6.1	Assessment of the Effect of Added Halide as TOPB.....	187
3.6.2	Oxidative Addition in the Presence of Additional PCy <sub>3</sub> .....	188
3.6.3	Mechanistic Interpretation of Kinetic Data for Oxidative Addition.....	190
3.7	Studies Initiated to Examine Transmetallation.....	206
3.7.1	Attempted GC study.....	206
3.7.2	Study and Attempted Preparation of [TOP][PhBF <sub>3</sub> ].....	208
3.8	Preparation and Reduction Experiments Involving PdL <sub>2</sub> Cl <sub>2</sub> .....	212
3.8.1	Spectroscopic Characteristics of <i>trans</i> -Pd(PMeBu <sup>t</sup> <sub>2</sub> ) <sub>2</sub> Cl <sub>2</sub> .....	213

3.8.2	Reduction Experiments with PdL <sub>2</sub> Cl <sub>2</sub> (L = PCy <sub>3</sub> , P <sup>t</sup> MeBu <sub>2</sub> ).....	216
3.9	References.....	222
CHAPTER 4. Summary and Conclusions.....		228
4.1	References.....	233
APPENDIX I.....		234
A.1.	Rate Law Derivations.....	234
A.1.1	Derivation of Rate Expressions for the Oxidative Addition of ArX to PdL <sub>2</sub> in the Absence of Excess Phosphine.....	234
A.1.1.1	Rate Expressions Assuming a Rapid K <sub>2</sub> .....	235
A.1.1.2	Rate Expressions Assuming Non-rapid K <sub>2</sub> .....	236
A.1.2	Derivation of Rate Expressions for the Oxidative Addition of ArX to PdL <sub>2</sub> in the Presence of One Equivalent of L.....	239
A.1.2.1	Rate Expressions for Rapid K <sub>2</sub> and K <sub>1</sub> .....	240
A.1.2.2	Rate Expressions for Rapid K <sub>2</sub> and Non-rapid K <sub>1</sub> .....	242
A.1.2.3	Rate Expressions for Non-rapid K <sub>2</sub> and Rapid K <sub>1</sub> .....	243
A.1.2.4	Rate Expressions for Non-rapid K <sub>2</sub> and K <sub>1</sub> .....	245
A.1.3	Rate Expression Derivations in Terms of [Pd] <sub>T</sub> for Large [L].....	248
A.1.3.1	Rate Expressions for Rapid K <sub>1</sub> and Non-rapid K <sub>2</sub> at Large [L].....	249
A.1.3.2	Rate Expressions for Non-rapid K <sub>1</sub> and K <sub>2</sub> at Large [L].....	250
A.1.4	Kinetic Data for Oxidative Addition of PhBr to Pd(PCy <sub>3</sub> ) <sub>2</sub> .....	251
A. 1.4.1	ln[Pd(PCy <sub>3</sub> ) <sub>2</sub> ] as a Function of Time Without TOPB.....	251
A.1.4.2	ln[Pd(PCy <sub>3</sub> ) <sub>2</sub> ] as a Function of Time With TOPB.....	254
A. 1.4.3	[Pd(PCy <sub>3</sub> ) <sub>2</sub> PhBr] as a Function of Time in the Presence of Added PCy <sub>3</sub> .....	257

## LIST OF TABLES

- Table 1. Summary of experiments involving *in situ* generation of PdL<sub>n</sub> from Pd( $\eta^3$ -C<sub>3</sub>H<sub>5</sub>)( $\eta^5$ -C<sub>5</sub>H<sub>5</sub>) with PPh<sub>3</sub>.
- Table 2. Summary of attempted oxidative addition experiments with Pd(PCy<sub>3</sub>)<sub>2</sub> and Pd(PMeBu<sup>t</sup><sub>2</sub>)<sub>2</sub>.
- Table 3. Summary of oxidative addition experiments with Pd(PBu<sup>t</sup><sub>2</sub>)<sub>2</sub>.
- Table 4. Summary of oxidative addition reactions with *in situ* generated PdL<sub>2</sub>.
- Table 5. Summary of reduction experiments with PdCl<sub>2</sub>(PMeBu<sup>t</sup><sub>2</sub>)<sub>2</sub>.
- Table 6. Summary of reduction experiments with PdCl<sub>2</sub>(PCy<sub>3</sub>)<sub>2</sub>.
- Table 7. Relevant species described by Werner *et al.*
- Table 8. <sup>1</sup>H NMR assignment for 1-(2-methylallyl)cyclopentadiene.
- Table 9. Simulated <sup>1</sup>H NMR chemical shifts for allyl-cyclopentadiene isomers.
- Table 10. <sup>1</sup>H and <sup>13</sup>C NMR assignment for Pd<sub>2</sub>(PPh<sub>3</sub>)<sub>2</sub>( $\mu$ -C<sub>3</sub>H<sub>5</sub>)( $\mu$ -C<sub>5</sub>H<sub>5</sub>) in toluene-d<sub>8</sub>.
- Table 11. <sup>1</sup>H and <sup>13</sup>C NMR data for Pd( $\eta^1$ -CH<sub>2</sub>CH=CHPh)( $\eta^5$ -C<sub>5</sub>H<sub>5</sub>)(PCy<sub>3</sub>) in toluene-d<sub>8</sub>.
- Table 12. Simulated chemical shifts for reductive elimination products derived from 5-(3-phenylallyl)cyclopentadiene.
- Table 13. Simulated chemical shifts for alternative reductive elimination products derived from 5-(1-phenylallyl)cyclopentadiene.
- Table 14. Summary of <sup>1</sup>H NMR data for Pd( $\eta^1$ -CH<sub>2</sub>CH=CHPh)( $\eta^5$ -C<sub>5</sub>H<sub>5</sub>)(PBu<sup>t</sup><sub>2</sub>Me).
- Table 15. <sup>1</sup>H NMR Assignment for Pd( $\eta^1$ -CH<sub>2</sub>CH=CHPh)( $\eta^5$ -C<sub>5</sub>H<sub>5</sub>)(PPh<sub>3</sub>).<sup>a</sup>
- Table 16. <sup>31</sup>P NMR data for homoleptic and heteroleptic PdL<sub>n</sub> (n = 2,3) species (L = PCy<sub>3</sub>, PBu<sup>t</sup><sub>3</sub>, PMeBu<sup>t</sup><sub>2</sub>) at 25 °C in toluene-d<sub>8</sub>.
- Table 17. Attempted oxidative addition reactions involving PdL<sub>2</sub> (L = PCy<sub>3</sub>, PMeBu<sup>t</sup><sub>2</sub>) at 21 °C.

- Table 18. Attempted oxidative addition experiments involving  $\text{Pd}(\text{P}^t\text{Bu}_3)_2$ .
- Table 19. Oxidative addition experiments performed with *in situ*  $\text{PdL}_2$ .
- Table 20. Summary of rate expression derivations for oxidative addition of  $\text{Pd}(\text{PCy}_3)_2$  in the absence of additional  $\text{PCy}_3$ .
- Table 21. Possible rate expressions describing oxidative addition of PhBr to  $\text{Pd}(\text{PCy}_3)_2$  under pseudo first order conditions.
- Table 22. Percentage of product produced by each pathway at varied  $[\text{ArX}]$  for the oxidative addition reaction of PhBr to  $\text{Pd}(\text{PCy}_3)_2$ .
- Table 23. Summary of rate law possibilities for oxidative addition of PhBr to  $\text{Pd}(\text{PCy}_3)_2$  in the presence of excess  $\text{PCy}_3$ .
- Table 24. Possible rate equations for oxidative addition of  $\text{Pd}(\text{PCy}_3)_2$  in the presence of excess  $\text{PCy}_3$ .
- Table 25. Possible rate equations at large values of  $[\text{L}]$  for oxidative addition of  $\text{Pd}(\text{PCy}_3)_2$  in the presence of excess  $\text{PCy}_3$ .
- Table 26. Summary of GC experiments in toluene.
- Table 27. Summary of reduction experiments with  $\text{PdCl}_2(\text{PCy}_3)_2$ .
- Table 28. Summary of reduction experiments with  $\text{PdCl}_2(\text{P}^t\text{MeBu}_2)_2$ .

## LIST OF FIGURES

- Figure 1. Generally accepted catalytic cycle for SM cross-coupling reactions.
- Figure 2. Examples of relevant phosphines for SM cross-coupling reactions.
- Figure 3.  $n,n'$ -Z-dba ( $n,n'$ -Z = 4,4'-OMe, 3,5,3',5'-OMe, 4,4'-<sup>t</sup>Bu, 3,3'-NO<sub>2</sub>, 4,4'-CF<sub>3</sub>).
- Figure 4. Buchwald ligands for SM cross-coupling.
- Figure 5. Representation of the interaction involved in **4**•Pd(dba).
- Figure 6. 1,6-diene stabilized monophosphine catalyst systems.
- Figure 7. Alternate precursor Pd( $\eta^3$ -1-Ph-C<sub>3</sub>H<sub>4</sub>)( $\eta^5$ -C<sub>5</sub>H<sub>5</sub>).
- Figure 8. The  $\eta^1$ -allyl complex Pd( $\eta^3$ -2-R-C<sub>3</sub>H<sub>4</sub>)( $\eta^5$ -C<sub>5</sub>H<sub>5</sub>) isolated as a primary intermediate (I) (L = P(OEt)<sub>3</sub>, P(OMe)<sub>3</sub>, P(OPh)<sub>3</sub>).
- Figure 9. Simultaneous  $\pi$ - $\sigma$  isomerization of the primary intermediate (I) (R = Me, Bu<sup>t</sup>, L = PPr<sup>i</sup><sub>3</sub>, PCy<sub>3</sub>, PBu<sup>t</sup>Ph<sub>2</sub>, PCy<sub>2</sub>Ph, PBu<sup>i</sup><sub>3</sub>).
- Figure 10. Stacked plots of <sup>31</sup>P NMR spectra (163.0 MHz) for reaction of Pd( $\eta^3$ -C<sub>3</sub>H<sub>5</sub>)( $\eta^5$ -C<sub>5</sub>H<sub>5</sub>) with two equivalents PCy<sub>3</sub> in toluene-d<sub>8</sub> at 25 °C.
- Figure 11. Stacked plots of <sup>1</sup>H NMR spectra ( $\delta$  3.8 – 7.2; 600 MHz) for the reaction of Pd( $\eta^3$ -C<sub>3</sub>H<sub>5</sub>)( $\eta^5$ -C<sub>5</sub>H<sub>5</sub>) with two equivalents of PCy<sub>3</sub> in toluene-d<sub>8</sub> at 25 °C.
- Figure 12. Stacked plots of <sup>1</sup>H NMR spectra ( $\delta$  2.0 – 4.0; 600 MHz) for the reaction of Pd( $\eta^3$ -C<sub>3</sub>H<sub>5</sub>)( $\eta^5$ -C<sub>5</sub>H<sub>5</sub>) with two equivalents of PCy<sub>3</sub> in toluene-d<sub>8</sub> at 25 °C.
- Figure 13. Stacked plots of <sup>31</sup>P NMR spectra (163.0 MHz) for reaction of Pd( $\eta^3$ -C<sub>3</sub>H<sub>5</sub>)( $\eta^5$ -C<sub>5</sub>H<sub>5</sub>) with two equivalents PCy<sub>3</sub> in toluene-d<sub>8</sub> at 65 °C.
- Figure 14. Stacked plots of <sup>31</sup>P NMR spectra (163.0 MHz) for reaction of Pd( $\eta^3$ -C<sub>3</sub>H<sub>5</sub>)( $\eta^5$ -C<sub>5</sub>H<sub>5</sub>) with two equivalents of PMeBu<sup>t</sup><sub>2</sub> in benzene-d<sub>6</sub> at 25 °C.
- Figure 15. <sup>1</sup>H NMR spectrum (400 MHz) for reaction of Pd( $\eta^3$ -C<sub>3</sub>H<sub>5</sub>)( $\eta^5$ -C<sub>5</sub>H<sub>5</sub>) with two equivalents of PMeBu<sup>t</sup><sub>2</sub> 3 h after mixing at 25 °C in benzene-d<sub>6</sub>.

- Figure 16. Stacked plots of  $^{31}\text{P}$  NMR spectra (163.0 MHz) for reaction of  $\text{Pd}(\eta^3\text{-C}_3\text{H}_5)(\eta^5\text{-C}_5\text{H}_5)$  with two equivalents  $\text{PMeBu}_2^t$  in toluene- $\text{d}_8$  at 77 °C.
- Figure 17. a)  $^{31}\text{P}$  NMR spectrum (163.0 MHz) of the reaction of  $\text{Pd}(\eta^3\text{-C}_3\text{H}_5)(\eta^5\text{-C}_5\text{H}_5)$  with two equivalents  $\text{PBU}_3^t$  in toluene- $\text{d}_8$  at 77°C 25 minutes after mixing b)  $^1\text{H}$  NMR spectrum (300 MHz) at 25°C 120 minutes after mixing.
- Figure 18.  $^{31}\text{P}$  NMR spectra of  $\text{Pd}(\eta^3\text{-C}_3\text{H}_5)(\eta^5\text{-C}_5\text{H}_5)$  and two equivalents  $\text{PMe}_3$ , 35 minutes after mixing in toluene- $\text{d}_8$  at 25 °C (202.3 MHz) and 2 °C (242.9 MHz).
- Figure 19.  $^1\text{H}$  NMR spectrum (500 MHz) of reaction of  $\text{Pd}(\eta^3\text{-C}_3\text{H}_5)(\eta^5\text{-C}_5\text{H}_5)$  and two equivalents of  $\text{PMe}_3$  in toluene- $\text{d}_8$  35 minutes after mixing at 25 °C.
- Figure 20.  $^{31}\text{P}$  NMR spectrum (242 MHz) of reaction of  $\text{Pd}(\eta^3\text{-C}_3\text{H}_5)(\eta^5\text{-C}_5\text{H}_5)$  and two equivalents of  $\text{PMe}_3$  in toluene- $\text{d}_8$  at 20 minutes after mixing at -55 °C.
- Figure 21.  $^1\text{H}$  NMR spectrum (600 MHz) of reaction of  $\text{Pd}(\eta^3\text{-C}_3\text{H}_5)(\eta^5\text{-C}_5\text{H}_5)$  and two equivalents of  $\text{PMe}_3$  in toluene- $\text{d}_8$  25 minutes after mixing at -55 °C.
- Figure 22.  $^{31}\text{P}$  NMR spectrum (242 MHz) of reaction of  $\text{Pd}(\eta^3\text{-C}_3\text{H}_5)(\eta^5\text{-C}_5\text{H}_5)$  with one equivalent of  $\text{PPh}_3$  in toluene- $\text{d}_8$  at 25 °C 17 minutes after mixing.
- Figure 23.  $^1\text{H}$  NMR spectrum (600 MHz) of reaction of  $\text{Pd}(\eta^3\text{-C}_3\text{H}_5)(\eta^5\text{-C}_5\text{H}_5)$  with one equivalent of  $\text{PPh}_3$  in toluene- $\text{d}_8$  at 25 °C 10 minutes after mixing.
- Figure 24.  $^{31}\text{P}$  NMR spectrum (163.0 MHz) of reaction of  $\text{Pd}(\eta^3\text{-C}_3\text{H}_5)(\eta^5\text{-C}_5\text{H}_5)$  with two equivalents of  $\text{PPh}_3$  in toluene- $\text{d}_8$  at 25 °C 22 minutes after mixing.
- Figure 25.  $^{31}\text{P}$  NMR spectrum (163.0 MHz) of reaction of  $\text{Pd}(\eta^3\text{-C}_3\text{H}_5)(\eta^5\text{-C}_5\text{H}_5)$  with two equivalents of  $\text{PPh}_3$  in toluene- $\text{d}_8$  at 80 °C.
- Figure 26.  $^{31}\text{P}$  NMR spectrum (242.9 MHz) for reaction of  $\text{Pd}(\eta^3\text{-1-Ph-C}_3\text{H}_4)(\eta^5\text{-C}_5\text{H}_5)$  with two equivalents of  $\text{PCy}_3$  20 minutes after mixing at 25 °C in toluene- $\text{d}_8$ .
- Figure 27.  $^{31}\text{P}$  NMR spectrum (242.9 MHz) for reaction of  $\text{Pd}(\eta^3\text{-1-Ph-C}_3\text{H}_4)(\eta^5\text{-C}_5\text{H}_5)$  with two equivalents of  $\text{PCy}_3$  in toluene- $\text{d}_8$  at 25 °C 45 h after mixing.

- Figure 28.  $^1\text{H}$  NMR spectrum (600 MHz) for reaction of  $\text{Pd}(\eta^3\text{-1-Ph-C}_3\text{H}_4)(\eta^5\text{-C}_5\text{H}_5)$  with two equivalents of  $\text{PCy}_3$  at 25 °C in toluene- $\text{d}_8$  at 20 minutes after mixing.
- Figure 29.  $^1\text{H}$  NMR spectrum (600 MHz) for reaction of  $\text{Pd}(\eta^3\text{-1-Ph-C}_3\text{H}_4)(\eta^5\text{-C}_5\text{H}_5)$  with two equivalents of  $\text{PCy}_3$  in toluene- $\text{d}_8$  at 25 °C at 45 hours after mixing.
- Figure 30. Stacked plots of  $^{31}\text{P}$  NMR spectra (161.9 MHz) for reaction of  $\text{Pd}(\eta^3\text{-1-Ph-C}_3\text{H}_4)(\eta^5\text{-C}_5\text{H}_5)$  with two equivalents  $\text{PCy}_3$  in toluene- $\text{d}_8$  at 50 °C.
- Figure 31.  $^{31}\text{P}$ - $^{31}\text{P}$  correlation spectrum (242.9 MHz) for reaction of  $\text{Pd}(\eta^3\text{-1-Ph-C}_3\text{H}_4)(\eta^5\text{-C}_5\text{H}_5)$  with two equivalents  $\text{PCy}_3$  in toluene- $\text{d}_8$  at 50 °C (spectrum obtained upon cooling to 25 °C).
- Figure 32. Postulated *anti* and *syn* isomers of  $\text{Pd}(\eta^3\text{-1-Ph-C}_3\text{H}_4)(\eta^5\text{-C}_5\text{H}_5)(\text{PCy}_3)_2$ .
- Figure 33.  $^{31}\text{P}$  NMR spectrum (163.0 MHz) for reaction of  $\text{Pd}(\eta^3\text{-1-Ph-C}_3\text{H}_4)(\eta^5\text{-C}_5\text{H}_5)$  is reacted with two equivalents of  $\text{PCy}_3$  in toluene- $\text{d}_8$  at 77 °C 12 minutes after mixing.
- Figure 34.  $^{31}\text{P}$  NMR spectrum (163.0 MHz) for reaction of  $\text{Pd}(\eta^3\text{-1-Ph-C}_3\text{H}_4)(\eta^5\text{-C}_5\text{H}_5)$  with two equivalents of  $\text{PMeBu}^t_2$  in toluene- $\text{d}_8$  at 25 °C one hour after mixing.
- Figure 35.  $^1\text{H}$  NMR spectrum (600 MHz) of  $\text{Pd}(\eta^3\text{-1-Ph-C}_3\text{H}_4)(\eta^5\text{-C}_5\text{H}_5)$  with two equivalents of  $\text{PMeBu}^t_2$  in toluene- $\text{d}_8$  ten minutes after mixing at 25 °C.
- Figure 36.  $^{31}\text{P}$  NMR spectrum (242.9 MHz) for reaction of  $\text{Pd}(\eta^3\text{-1-Ph-C}_3\text{H}_4)(\eta^5\text{-C}_5\text{H}_5)$  with two equivalents of  $\text{PMeBu}^t_2$  after 51 hours at 25 °C, followed by heating to 50 °C.
- Figure 37.  $^1\text{H}$  NMR spectrum (600 MHz) for reaction of  $\text{Pd}(\eta^3\text{-1-Ph-C}_3\text{H}_4)(\eta^5\text{-C}_5\text{H}_5)$  with two equivalents of  $\text{PPh}_3$  in toluene- $\text{d}_8$  7.5 minutes after mixing at 25 °C).
- Figure 38.  $^{31}\text{P}$  NMR spectra (242.9 MHz) for reaction of  $\text{Pd}(\eta^3\text{-1-Ph-C}_3\text{H}_4)(\eta^5\text{-C}_5\text{H}_5)$  with two equivalents of  $\text{PPh}_3$  in toluene- $\text{d}_8$  at 25 °C.



- Figure 39.  $^{31}\text{P}$ - $^{31}\text{P}$  correlation spectrum (242.9 MHz) of  $\text{Pd}(\eta^3\text{-1-Ph-C}_3\text{H}_4)(\eta^5\text{-C}_5\text{H}_5)$  and two equivalents  $\text{PPh}_3$  in toluene- $\text{d}_8$  at 25 °C.
- Figure 40.  $^1\text{H}$  NMR spectrum (600 MHz) for reaction of  $\text{Pd}(\eta^3\text{-1-Ph-C}_3\text{H}_4)(\eta^5\text{-C}_5\text{H}_5)$  with two equivalents of  $\text{PPh}_3$  in toluene- $\text{d}_8$  35 minutes after mixing at 25 °C.
- Figure 41. Stacked plots of low temperature  $^{31}\text{P}$  inverse gated NMR spectra (242.9 MHz) for reaction of  $\text{Pd}(\text{PCy}_3)_2$  with one equivalent of  $\text{PCy}_3$ .
- Figure 42. Plot of  $\ln K_D$  as a function of  $1/T$  for the dissociation of  $\text{Pd}(\text{PCy}_3)_3$ .
- Figure 43. Plot of  $\ln K_D$  as a function of  $1/T$  for the dissociation of  $\text{Pd}(\text{PMeBu}^t_2)_3$ .
- Figure 44.  $^{31}\text{P}$  NMR spectrum (121.5 MHz) of the reaction of  $\text{Pd}(\eta^3\text{-C}_3\text{H}_5)(\eta^5\text{-C}_5\text{H}_5)$  with one equivalent  $\text{PCy}_3$  and one equivalent of  $\text{PBu}^t_3$  in toluene- $\text{d}_8$  at 77 °C (after cooling to 25 °C).
- Figure 45.  $^{31}\text{P}$ - $^{31}\text{P}$  correlation spectrum (242.9 MHz) of equimolar quantities of  $\text{Pd}(\text{PBu}^t_3)_2$  and  $\text{Pd}(\text{PCy}_3)_2$  in toluene- $\text{d}_8$  at 25 °C.
- Figure 46.  $^{31}\text{P}$ - $^{31}\text{P}$  correlation spectrum (242.9 MHz) of equimolar amounts of  $\text{Pd}(\text{PBu}^t_3)_2$  with  $\text{Pd}(\text{PMeBu}^t_2)_2$  in toluene- $\text{d}_8$  at 25 °C.
- Figure 47.  $^{31}\text{P}$  NMR spectrum (121.5 MHz) of reaction of  $\text{Pd}(\eta^3\text{-C}_3\text{H}_5)(\eta^5\text{-C}_5\text{H}_5)$  with one equivalent each of  $\text{PCy}_3$  and  $\text{PPh}_3$  after cooling to 21 °C.
- Figure 48. a)  $^{31}\text{P}$  NMR spectrum (242.9 MHz) at 25 °C of a solution containing equimolar quantities of  $\text{Pd}(\text{PCy}_3)_2$  and  $\text{Pd}(\text{PMeBu}^t_2)_2$  b) Representation of postulated AB quartet.
- Figure 49.  $^{31}\text{P}$ - $^{31}\text{P}$  correlation spectrum (242.9 MHz) of  $\text{Pd}(\text{PMeBu}^t_2)_2$  and  $\text{Pd}(\text{PCy}_3)_2$  at 25 °C.
- Figure 50. Stacked plots of variable temperature  $^{31}\text{P}$  NMR spectra (242.9 MHz) of the reaction of  $\text{Pd}(\text{PCy}_3)_2$  with one equivalent of  $\text{PMeBu}^t_2$  in toluene- $\text{d}_8$ .
- Figure 51.  $^{31}\text{P}$  NMR spectra (242.9 MHz) of the reaction of  $\text{Pd}(\text{PCy}_3)_2$  with two equivalents of  $\text{PMeBu}^t_2$  at -88 °C.
- Figure 52.  $^{31}\text{P}$ - $^{31}\text{P}$  correlation spectrum (242.9 MHz) of a solution containing  $\text{Pd}(\text{PCy}_3)_2$  and two equivalents  $\text{PMeBu}^t_2$  in toluene- $\text{d}_8$  at -88 °C.
- Figure 53.  $^{31}\text{P}$  NMR spectrum (163.0 MHz) for reaction of equimolar quantities of  $\text{Pd}(\text{PCy}_3)_2$  and bromobenzene in benzene- $\text{d}_6$  at 25 °C.

- Figure 54.  $^1\text{H}$  NMR spectrum (400 MHz) for reaction of equimolar quantities of  $\text{Pd}(\text{PCy}_3)_2$  and bromobenzene in benzene- $\text{d}_6$  at 25 °C two hours after mixing.
- Figure 55.  $^1\text{H}$  NMR spectrum (300 MHz) for reaction of  $\text{Pd}(\text{PCy}_3)_2$  and three equivalents (1-bromo)ethylbenzene in benzene- $\text{d}_6$  two hours after mixing at 21 °C.
- Figure 56.  $^{31}\text{P}$  NMR spectrum (163.0 MHz) for reaction of  $\text{Pd}(\text{PCy}_3)_2$  and three equivalents (1-bromo)ethylbenzene 2.5 hours after mixing at 21 °C.
- Figure 57.  $^{31}\text{P}$  NMR spectrum (163.0 MHz) for reaction of  $\text{Pd}(\text{PMeBu}^t_2)_2$  with one equivalent bromobenzene in benzene- $\text{d}_6$  at 25 °C.
- Figure 58.  $^1\text{H}$  NMR spectrum (400 MHz) for reaction of  $\text{Pd}(\text{PMeBu}^t_2)_2$  with one equivalent bromobenzene at 25 °C.
- Figure 59.  $^{31}\text{P}$  NMR spectrum (163.0 MHz) for attempted reaction of  $\text{Pd}(\text{PBu}^t_3)_2$  with one equivalent bromobenzene at 60 °C 20 minutes after mixing.
- Figure 60.  $^{31}\text{P}$  NMR spectrum (242.9 MHz) for reaction of  $\text{Pd}(\text{PBu}^t_3)_2$  with bromobenzene in toluene- $\text{d}_8$ /THF at 60 °C.
- Figure 61. Tetrabutylammonium bromide (TBAB) and tetraoctylphosphonium bromide (TOPB).
- Figure 62. Concentration of  $\text{Pd}(\text{PCy}_3)_2$  as a function of time for the oxidative addition of PhBr (0.483 M) to  $\text{Pd}(\text{PCy}_3)_2$  ( $[\text{Pd}(\text{PCy}_3)_2]_0 = 0.0232$  M) at 25 °C in toluene- $\text{d}_8$ .
- Figure 63.  $\ln[\text{Pd}(\text{PCy}_3)_2]$  as a function of time for oxidative addition of PhBr (0.483 M) to  $\text{Pd}(\text{PCy}_3)_2$  ( $[\text{Pd}(\text{PCy}_3)_2]_0 = 0.0232$  M) at 25 °C in toluene- $\text{d}_8$ .
- Figure 64.  $k_{\text{obs}}$  as a function of time for the oxidative addition of PhBr to  $\text{Pd}(\text{PCy}_3)_2$  at 25 °C in toluene- $\text{d}_8$ .
- Figure 65.  $k_{\text{obs}}$  as a function of time for the oxidative addition of PhBr to  $\text{Pd}(\text{PCy}_3)_2$  in the presence of TOPB.
- Figure 66. Plot of  $[\text{Pd}(\text{PCy}_3)_2(\text{Ph})(\text{Br})]$  as a function of time for oxidative addition of PhBr (0.272 M) to  $\text{Pd}(\text{PCy}_3)_2$  ( $[\text{Pd}(\text{PCy}_3)_2]_0 = 0.021$  M) a) in the presence of one equivalent of  $\text{PCy}_3$  ( $[\text{PCy}_3] = 0.021$  M) b) in the absence of one equivalent of  $\text{PCy}_3$ .

- Figure 67.  $k_{\text{obs}}$  as a function of time for the oxidative addition of PhBr to  $\text{Pd}(\text{PCy}_3)_2$  in the presence of one equivalent of  $\text{PCy}_3$ .
- Figure 68. Percentage of produced by pathway for oxidative addition of PhBr to  $\text{Pd}(\text{PCy}_3)_2$  ( $[\text{PhBr}] = 0.693 \text{ M}$ ).
- Figure 69.  $^1\text{H}$  NMR spectrum (400 MHz) of colourless oil in  $\text{CDCl}_3$  obtained as product in the attempted preparation of  $[\text{TOP}][\text{PhBF}_3]$ .
- Figure 70.  $^1\text{H}$  NMR spectrum (400 MHz) in  $\text{CDCl}_3$  for attempted preparation of  $[\text{TOP}][\text{PhBF}_3]$  from anhydrous MeOH.
- Figure 71. a)  $^{31}\text{P}$  NMR spectra (163.0 MHz) of  $\text{Pd}(\text{PMeBu}^t_2)_2\text{Cl}_2$  in  $\text{TCE-d}_2$  at 25 °C and b) at 77 °C.
- Figure 72.  $^{13}\text{C}$  NMR spectrum (125.7 MHz) of  $\text{Pd}(\text{PMeBu}^t_2)_2\text{Cl}_2$  in  $\text{CDCl}_3$  at 25 °C.
- Figure 73.  $^{13}\text{C}$  NMR spectrum (100.6 MHz) of  $\text{Pd}(\text{PMeBu}^t_2)_2\text{Cl}_2$  ( $\text{TCE-d}_2$  at 77 °C).
- Figure 74.  $^{31}\text{P}$  NMR spectrum (242.9 MHz) of the attempted reduction of  $\text{Pd}(\text{PMeBu}^t_2)_2\text{Cl}_2$  in the presence of  $\text{PhB}(\text{OH})_2$ , toluene,  $\text{H}_2\text{O}$  and  $\text{K}_2\text{CO}_3$ , heated to 80 °C prior to acquisition.
- Figure 75. a)  $^{31}\text{P}$  NMR spectrum (242.9 MHz) of the attempted reduction of  $\text{Pd}(\text{PMeBu}^t_2)_2\text{Cl}_2$  in the presence of toluene,  $\text{H}_2\text{O}$  and  $\text{K}_2\text{CO}_3$  (2 eq.) b) in the presence of toluene,  $\text{H}_2\text{O}$  and  $\text{K}_2\text{CO}_3$  (4 eq.) heated to 80 °C prior to acquisition.
- Figure 76.  $^{31}\text{P}$  NMR spectrum (242.9 MHz,  $\text{CD}_2\text{Cl}_2$ ) of residue of the reaction of  $\text{Pd}(\text{COD})\text{Br}_2$  and two eq.  $\text{PBU}^t_3$  at 5 °C for 1 h.
- Figure 77.  $\ln[\text{Pd}(\text{PCy}_3)_2]$  as a function of time for oxidative addition of PhBr (0.234 M) to  $\text{Pd}(\text{PCy}_3)_2$  ( $[\text{Pd}(\text{PCy}_3)_2]_0 = 0.0232 \text{ M}$ ) at 25 °C in toluene- $\text{d}_8$ .
- Figure 78.  $\ln[\text{Pd}(\text{PCy}_3)_2]$  as a function of time for oxidative addition of PhBr (0.263 M) to  $\text{Pd}(\text{PCy}_3)_2$  ( $[\text{Pd}(\text{PCy}_3)_2]_0 = 0.0232 \text{ M}$ ) at 25 °C in toluene- $\text{d}_8$ .
- Figure 79.  $\ln[\text{Pd}(\text{PCy}_3)_2]$  as a function of time for oxidative addition of PhBr (0.483 M) to  $\text{Pd}(\text{PCy}_3)_2$  ( $[\text{Pd}(\text{PCy}_3)_2]_0 = 0.0232 \text{ M}$ ) at 25 °C in toluene- $\text{d}_8$ .

- Figure 80.  $\ln[\text{Pd}(\text{PCy}_3)_2]$  as a function of time for oxidative addition of PhBr (0.688 M) to  $\text{Pd}(\text{PCy}_3)_2$  ( $[\text{Pd}(\text{PCy}_3)_2]_0 = 0.0226 \text{ M}$ ) at 25 °C in toluene- $d_8$ .
- Figure 81.  $\ln[\text{Pd}(\text{PCy}_3)_2]$  as a function of time for oxidative addition of PhBr (0.693 M) to  $\text{Pd}(\text{PCy}_3)_2$  ( $[\text{Pd}(\text{PCy}_3)_2]_0 = 0.0326 \text{ M}$ ) at 25 °C in toluene- $d_8$ .
- Figure 82.  $\ln[\text{Pd}(\text{PCy}_3)_2]$  as a function of time for oxidative addition of PhBr (1.16 M) to  $\text{Pd}(\text{PCy}_3)_2$  ( $[\text{Pd}(\text{PCy}_3)_2]_0 = 0.0232 \text{ M}$ ) at 25 °C in toluene- $d_8$ .
- Figure 83.  $\ln[\text{Pd}(\text{PCy}_3)_2]$  as a function of time for oxidative addition of PhBr (0.234 M) to  $\text{Pd}(\text{PCy}_3)_2$  in the presence of TOPB ( $[\text{Pd}(\text{PCy}_3)_2]_0 = 0.0232 \text{ M}$ ,  $[\text{TOPB}] = 0.0231 \text{ M}$ ) at 25 °C in toluene- $d_8$ .
- Figure 84.  $\ln[\text{Pd}(\text{PCy}_3)_2]$  as a function of time for oxidative addition of PhBr (0.263 M) to  $\text{Pd}(\text{PCy}_3)_2$  in the presence of TOPB ( $[\text{Pd}(\text{PCy}_3)_2]_0 = 0.0232 \text{ M}$ ,  $[\text{TOPB}] = 0.0231 \text{ M}$ ) at 25 °C in toluene- $d_8$ .
- Figure 85.  $\ln[\text{Pd}(\text{PCy}_3)_2]$  as a function of time for oxidative addition of PhBr (0.483 M) to  $\text{Pd}(\text{PCy}_3)_2$  in the presence of TOPB ( $[\text{Pd}(\text{PCy}_3)_2]_0 = 0.0232 \text{ M}$ ,  $[\text{TOPB}] = 0.0231 \text{ M}$ ) at 25 °C in toluene- $d_8$ .
- Figure 86.  $\ln[\text{Pd}(\text{PCy}_3)_2]$  as a function of time for oxidative addition of PhBr (0.688 M) to  $\text{Pd}(\text{PCy}_3)_2$  in the presence of TOPB ( $[\text{Pd}(\text{PCy}_3)_2]_0 = 0.0226 \text{ M}$ ,  $[\text{TOPB}] = 0.0231 \text{ M}$ ) at 25 °C in toluene- $d_8$ .
- Figure 87.  $\ln[\text{Pd}(\text{PCy}_3)_2]$  as a function of time for oxidative addition of PhBr (1.16 M) to  $\text{Pd}(\text{PCy}_3)_2$  in the presence of TOPB ( $[\text{Pd}(\text{PCy}_3)_2]_0 = 0.0232 \text{ M}$ ,  $[\text{TOPB}] = 0.0231 \text{ M}$ ) at 25 °C in toluene- $d_8$ .
- Figure 88.  $\ln[\text{Pd}(\text{PCy}_3)_2]$  as a function of time for oxidative addition of PhBr (1.39 M) to  $\text{Pd}(\text{PCy}_3)_2$  in the presence of TOPB ( $[\text{Pd}(\text{PCy}_3)_2]_0 = 0.0235 \text{ M}$ ,  $[\text{TOPB}] = 0.0231 \text{ M}$ ) at 25 °C in toluene- $d_8$ .
- Figure 89. Concentration of  $\text{Pd}(\text{PCy}_3)_2(\text{Ph})(\text{Br})$  as a function of time for the oxidative addition of PhBr (0.272 M) to  $\text{Pd}(\text{PCy}_3)_2$  in the presence of added  $\text{PCy}_3$  ( $[\text{Pd}(\text{PCy}_3)_2]_0 = 0.0213 \text{ M}$ ,  $[\text{PCy}_3]_0 = 0.0214 \text{ M}$ ) at 25 °C in toluene- $d_8$  (Trial 1).
- Figure 90. Concentration of  $\text{Pd}(\text{PCy}_3)_2(\text{Ph})(\text{Br})$  as a function of time for the oxidative addition of PhBr (0.272 M) to  $\text{Pd}(\text{PCy}_3)_2$  in the presence of added  $\text{PCy}_3$  ( $[\text{Pd}(\text{PCy}_3)_2]_0 = 0.0213 \text{ M}$ ,  $[\text{PCy}_3]_0 = 0.0214 \text{ M}$ ) at 25 °C in toluene- $d_8$  (Trial 2).

- Figure 91. Concentration of  $\text{Pd}(\text{PCy}_3)_2(\text{Ph})(\text{Br})$  as a function of time for the oxidative addition of PhBr (0.476 M) to  $\text{Pd}(\text{PCy}_3)_2$  in the presence of added  $\text{PCy}_3$  ( $[\text{Pd}(\text{PCy}_3)_2]_0 = 0.0214 \text{ M}$ ,  $[\text{PCy}_3]_0 = 0.0214 \text{ M}$ ) at 25 °C in toluene- $\text{d}_8$  (Trial 1).
- Figure 92. Concentration of  $\text{Pd}(\text{PCy}_3)_2(\text{Ph})(\text{Br})$  as a function of time for the oxidative addition of PhBr (0.476 M) to  $\text{Pd}(\text{PCy}_3)_2$  in the presence of added  $\text{PCy}_3$  ( $[\text{Pd}(\text{PCy}_3)_2]_0 = 0.0214 \text{ M}$ ,  $[\text{PCy}_3]_0 = 0.0214 \text{ M}$ ) at 25 °C in toluene- $\text{d}_8$  (Trial 2).
- Figure 93. Concentration of  $\text{Pd}(\text{PCy}_3)_2(\text{Ph})(\text{Br})$  as a function of time for the oxidative addition of PhBr (0.680 M) to  $\text{Pd}(\text{PCy}_3)_2$  in the presence of added  $\text{PCy}_3$  ( $[\text{Pd}(\text{PCy}_3)_2]_0 = 0.0219 \text{ M}$ ,  $[\text{PCy}_3]_0 = 0.0214 \text{ M}$ ) at 25 °C in toluene- $\text{d}_8$  (Trial 1).
- Figure 94. Concentration of  $\text{Pd}(\text{PCy}_3)_2(\text{Ph})(\text{Br})$  as a function of time for the oxidative addition of PhBr (0.680 M) to  $\text{Pd}(\text{PCy}_3)_2$  in the presence of added  $\text{PCy}_3$  ( $[\text{Pd}(\text{PCy}_3)_2]_0 = 0.0219 \text{ M}$ ,  $[\text{PCy}_3]_0 = 0.0214 \text{ M}$ ) at 25 °C in toluene- $\text{d}_8$  (Trial 2).
- Figure 95. Concentration of  $\text{Pd}(\text{PCy}_3)_2(\text{Ph})(\text{Br})$  as a function of time for the oxidative addition of PhBr (0.816 M) to  $\text{Pd}(\text{PCy}_3)_2$  in the presence of added  $\text{PCy}_3$  ( $[\text{Pd}(\text{PCy}_3)_2]_0 = 0.0214 \text{ M}$ ,  $[\text{PCy}_3]_0 = 0.0214 \text{ M}$ ) at 25 °C in toluene- $\text{d}_8$  (Trial 1).
- Figure 96. Concentration of  $\text{Pd}(\text{PCy}_3)_2(\text{Ph})(\text{Br})$  as a function of time for the oxidative addition of PhBr (0.816 M) to  $\text{Pd}(\text{PCy}_3)_2$  in the presence of added  $\text{PCy}_3$  ( $[\text{Pd}(\text{PCy}_3)_2]_0 = 0.0214 \text{ M}$ ,  $[\text{PCy}_3]_0 = 0.0214 \text{ M}$ ) at 25 °C in toluene- $\text{d}_8$  (Trial 2).
- Figure 97. Concentration of  $\text{Pd}(\text{PCy}_3)_2(\text{Ph})(\text{Br})$  as a function of time for the oxidative addition of PhBr (1.09 M) to  $\text{Pd}(\text{PCy}_3)_2$  in the presence of added  $\text{PCy}_3$  ( $[\text{Pd}(\text{PCy}_3)_2]_0 = 0.0212 \text{ M}$ ,  $[\text{PCy}_3]_0 = 0.0214 \text{ M}$ ) at 25 °C in toluene- $\text{d}_8$  (Trial 1).
- Figure 98. Concentration of  $\text{Pd}(\text{PCy}_3)_2(\text{Ph})(\text{Br})$  as a function of time for the oxidative addition of PhBr (1.09 M) to  $\text{Pd}(\text{PCy}_3)_2$  in the presence of added  $\text{PCy}_3$  ( $[\text{Pd}(\text{PCy}_3)_2]_0 = 0.0219 \text{ M}$ ,  $[\text{PCy}_3]_0 = 0.0214 \text{ M}$ ) at 25 °C in toluene- $\text{d}_8$  (Trial 2).
- Figure 99. Concentration of  $\text{Pd}(\text{PCy}_3)_2(\text{Ph})(\text{Br})$  as a function of time for the oxidative addition of PhBr (1.09 M) to  $\text{Pd}(\text{PCy}_3)_2$  in the presence of added  $\text{PCy}_3$  ( $[\text{Pd}(\text{PCy}_3)_2]_0 = 0.0214 \text{ M}$ ,  $[\text{PCy}_3]_0 = 0.0214 \text{ M}$ ) at 25 °C in toluene- $\text{d}_8$  (Trial 3).

## LIST OF SCHEMES

- Scheme 1. General catalyzed carbon-carbon cross-coupling reaction.
- Scheme 2. Carbon-carbon bond formation by RMgX and RLi.
- Scheme 3. Ni catalyzed cross-coupling with Grignard reagents at  $sp^2$  carbons.
- Scheme 4. Pathway for Ni catalysis proposed by Kumada *et al.*
- Scheme 5. Generalized Stille carbon-carbon cross-coupling reaction.
- Scheme 6. Generalized SM carbon-carbon cross-coupling reaction.
- Scheme 7. Oxidative addition of PhI to  $Pd(PPh_3)_2$ .
- Scheme 8. Proposed mechanism for oxidative addition of  $Pd(PPh_3)_2$ .
- Scheme 9. Limiting mechanistic scenarios proposed for oxidative addition.
- Scheme 10. Isolation and isomerization of *cis* oxidative addition product.
- Scheme 11. Isomerization of *cis*- $Pd(PPh_3)_2(C_6Cl_2F_2)I$ .
- Scheme 12. Pathways for transmetallation in the SM reaction.
- Scheme 13. Isomerization and reductive elimination for *cis/trans*- $Pd(Me)_2L_2$ .
- Scheme 14. Concerted reductive elimination for diarylpalladium(II) complexes.
- Scheme 15. Dissociation equilibria associated with  $Pd(PPh_3)_4$  in solution.
- Scheme 16. Monoligation of Pd(0) by dba in the presence of  $PPh_3$ .
- Scheme 17. Equilibrium between dba ligated Pd(0) and  $Pd(PPh_3)_2$ .
- Scheme 18. Inhibition of oxidative addition as a result of alkene coordination.
- Scheme 19. Equilibrium releasing  $Pd(PPh_3)_2$  from *n,n'*-Z-dba complex.
- Scheme 20. SM cross-coupling of electron rich and hindered aryl chlorides.
- Scheme 21. Generation of active catalysts from  $Pd_2(\mu-Br)_2(PR_3)_2$ .
- Scheme 22. Room temperature SM cross-coupling of hindered aryl chlorides.

- Scheme 23. Isolation of monomeric T-shaped arylpalladium(II) complexes.
- Scheme 24. SM cross-coupling with Buchwald System using ligand **5**.
- Scheme 25. Beller ligand systems for SM cross-coupling of aryl chlorides.
- Scheme 26. Reduction of Pd(OAc)<sub>2</sub> in the presence of PPh<sub>3</sub> in DMF.
- Scheme 27. Reduction of Pd(OAc)<sub>2</sub> in the presence of PBU<sup>n</sup><sub>3</sub>.
- Scheme 28. Electrochemical reduction of PdCl<sub>2</sub>(PPh<sub>3</sub>)<sub>2</sub>.
- Scheme 29. Electrochemical reduction of PdBr<sub>2</sub>(PPh<sub>3</sub>)<sub>2</sub>.
- Scheme 30. Generation of [Pd(η<sup>3</sup>-C<sub>3</sub>H<sub>5</sub>)<sub>2</sub>] and Pd(η<sup>3</sup>-C<sub>3</sub>H<sub>5</sub>)(η<sup>5</sup>-C<sub>5</sub>H<sub>5</sub>).
- Scheme 31. Pathway for reaction of Pd(η<sup>3</sup>-C<sub>3</sub>H<sub>5</sub>)(η<sup>5</sup>-C<sub>5</sub>H<sub>5</sub>) with phosphines.
- Scheme 32. Isolation of Pd(PR<sub>3</sub>)<sub>2</sub> from Pd(η<sup>3</sup>-C<sub>3</sub>H<sub>5</sub>)(η<sup>5</sup>-C<sub>5</sub>H<sub>5</sub>).
- Scheme 33. Preparation of PdL<sub>2</sub> from Pd(η<sup>3</sup>-C<sub>3</sub>H<sub>5</sub>)(η<sup>5</sup>-C<sub>5</sub>H<sub>5</sub>) (PR<sub>3</sub> = PCy<sub>3</sub>, PPhBu<sup>t</sup><sub>2</sub>, PBU<sup>t</sup><sub>3</sub>).
- Scheme 34. Initial mechanism proposed for ligand displacement of Pd(η<sup>3</sup>-C<sub>3</sub>H<sub>5</sub>)(η<sup>5</sup>-C<sub>5</sub>H<sub>5</sub>) by P(OR)<sub>3</sub> (R = Ph).
- Scheme 35. Reaction sequence in the formation of PdL<sub>2</sub> from Pd(η<sup>3</sup>-C<sub>3</sub>H<sub>5</sub>)(η<sup>5</sup>-C<sub>5</sub>H<sub>5</sub>).
- Scheme 36. Anticipated mechanism of reductive elimination from Pd(η<sup>1</sup>-CH<sub>2</sub>CH=CHPh)(η<sup>5</sup>-C<sub>5</sub>H<sub>5</sub>)(PCy<sub>3</sub>).
- Scheme 37. Dissociation equilibrium for Pd(PCy<sub>3</sub>)<sub>3</sub>.
- Scheme 38. Generation of heteroleptic 2:1 compounds from Pd(η<sup>3</sup>-C<sub>3</sub>H<sub>5</sub>)(η<sup>5</sup>-C<sub>5</sub>H<sub>5</sub>).
- Scheme 39. Oxidative addition reaction involving PdL<sub>2</sub>.
- Scheme 40. Generalized representation of *in situ* oxidative addition reaction.
- Scheme 41. Oxidative addition of Pd(PCy<sub>3</sub>)<sub>2</sub> and bromobenzene.
- Scheme 42. Possible mechanistic pathways for the oxidative addition of PdL<sub>2</sub> to PhBr (L = PCy<sub>3</sub>).

- Scheme 43. Possible mechanistic pathways for the oxidative addition of  $\text{PdL}_2$  to  $\text{PhBr}$  in the presence of excess  $\text{PCy}_3$ .
- Scheme 44. Mechanism proposed for alkali induced reduction of  $\text{Pd}(\text{PPh}_3)_2\text{Cl}_2$ .
- Scheme 45. Pathways proposed for rate law derivation for the oxidative addition of  $\text{ArX}$  to  $\text{PdL}_2$  in the absence of additional  $\text{L}$ .
- Scheme 46. Pathways proposed for rate law derivation for the oxidative addition of  $\text{ArX}$  to  $\text{PdL}_2$  in the presence of additional  $\text{L}$ .



## LIST OF SYMBOLS AND ABBREVIATIONS

acac	acetylacetonato
Allyl	propenyl
Ar	aryl group
Å	Ångström
$^{11}\text{B}$ NMR	boron NMR
br.	broad
Bu <sup>n</sup>	n-butyl
Bu <sup>t</sup>	tert-butyl
°C	degrees Celsius
Cp	cyclopentadienyl ( $\eta^5\text{-C}_5\text{H}_5$ )
Cy	cyclohexyl
$^{13}\text{C}$ NMR	carbon NMR
COSY	correlation spectroscopy
$\delta$	chemical shift in ppm
d	doublet
dba	dibenzylideneacetone
DFT	density functional theory
DMF	dimethylformamide
dppb	1,1'-bis(diphenylphosphino)butane
dppe	1,1'-bis(diphenylphosphino)ethane
dppf	1,1'-bis(diphenylphosphino)ferrocene
dppm	1,1'-bis(diphenylphosphino)methane

Et	ethyl
GC	gas chromatography
g	grams
$\eta$	hapticity
h	hour
$\Delta H$	enthalpy change
$\Delta H^\ddagger$	enthalpy of activation
$^1\text{H}$ NMR	proton NMR
Hz	hertz
HMBC	heteronuclear multiple bond coherence
HSQC	heteronuclear single quantum coherence
$J$	coupling constant
L	litres
m	multiplet
$m$	meta
M	moles/litre
Me	methyl
MeOH	methanol
mg	milligrams
MHz	megahertz
min	minute
mL	millilitres
mol	moles

mmol	mmol
$\mu\text{L}$	microlitres
NMR	nuclear magnetic resonance
<i>o</i>	ortho
OAc	acetate
OTf	triflate
<i>p</i>	para
Ph	phenyl
$^{31}\text{P}$ NMR	phosphorus NMR
ppm	parts per million
$\text{Pr}^i$	isopropyl
R	alkyl group
s	singlet
$\Delta\text{S}$	entropy change
$\Delta\text{S}^\ddagger$	entropy of activation
t	triplet
TCE	1,1,2,2-tetrachloroethane- $\text{d}_2$
THF	tetrahydrofuran
vt	virtual triplet

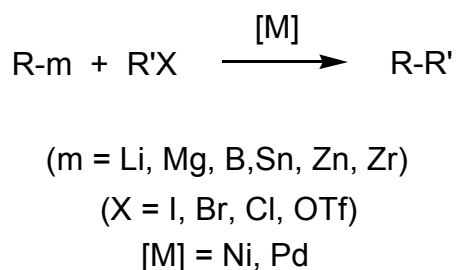
# Chapter 1

## Introduction

It is widely accepted that the development of cross-coupling reactions has revolutionized methodologies for the formation of carbon-carbon bonds, and have thereby profoundly changed the strategies for the construction of many types of complex organic molecules. Modern cross-coupling reactions now encompass a field of research that continues to expand at an astounding rate, thus requiring many frequent and thorough reviews.<sup>1</sup>

It is the catalytically performed cross-coupling of organometallic reagents with organic electrophiles that now constitutes one of the main classes of chemical reactions for the formation of carbon-carbon bonds. More recently, catalytic cross-coupling has evolved to include other bond forming reactions (e.g. C-N, C-O), inciting novel areas of research.<sup>2</sup>

Catalyzed cross-coupling reactions are perhaps best defined as an assisted exchange, as shown in Scheme 1.

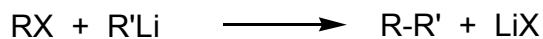
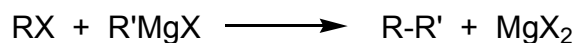


Scheme 1. Generalized catalytic carbon-carbon cross-coupling reaction.

Here R-m is the organometallic, nucleophilic component of the system, and R'X is an organic electrophile. Given the wide variety of possible R-m species, many processes have developed over many years of research. However, the Suzuki-Miyaura (SM) reaction (m = B) has become by far the most widely utilized cross-coupling methodology for the formation of carbon-carbon bonds.<sup>1d,e,l,o</sup> Consequently, the SM reaction has been the focus of overwhelmingly extensive research, producing varied and seemingly infinite literature reports. A concise description of the historical development of the SM reaction is warranted in order to fully appreciate both its mechanistic features and limitations.

### 1.1 Historical Development of Cross-coupling Reactions

Modern cross-coupling reactions have their origins in the pioneering efforts of Grignard, whose work initiated the utilization of organometallic reagents in organic synthesis. Carbon-carbon bond formation historically has involved the use of organic halides RX with alkyl-magnesium or alkyl-lithium reagents, producing the coupled species R-R' (Scheme 2).<sup>3</sup> The use of such electropositive metals creates a highly polar M-C bond, effectively producing a strong nucleophilic and basic carbanion.



(R = alkyl, R' = aryl, X = halogen)

Scheme 2. Carbon-carbon bond formation by means of RMgX and RLi.

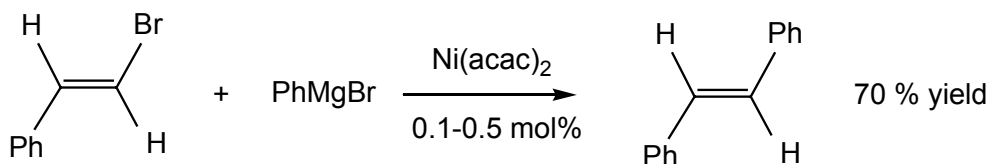
However, the scope of these reagents is quite limited in terms of their broader utility in organic synthesis. As strong bases and nucleophiles, organometallic compounds of Mg and Li are extremely reactive and highly intolerant of acidic and electrophilic functional groups. Complications thus result when reactions are performed with unprotected functional groups such as OH and C=O.<sup>4</sup> While methyl, primary alkyl, allyl and benzyl halides can undergo coupling with organic Li and Mg reagents, coupling is difficult when performed with hindered organic halides RX and reactions involving organic halides with unsaturated sp<sup>2</sup> and sp carbons are unsuccessful.<sup>3</sup> Cross-coupling reactions with these organoalkali reagents are thus plagued by a variety of undesirable side reactions, severely limiting their broader application to organic synthesis.<sup>3</sup>

### 1.1.1 “First Generation” Palladium Catalyzed Cross-coupling

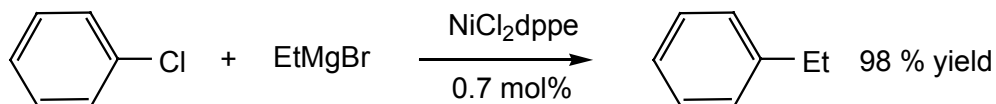
The genesis of modern palladium-catalyzed cross-coupling occurred as a result of the combined research efforts to overcome the limitations associated with organoalkali and organoalkali earth reagents. Until the early 1970's, cross-coupling had remained generally limited to the above mentioned reactions involving Li and Mg.<sup>3</sup> Over three decades, research has involved a wide variety of other organometallic compounds and the “modern” cross-coupling processes that have resulted are to a great extent performed catalytically. An extremely significant advance towards universally applicable cross-coupling involved the discovery that Ni complexes can catalyze the cross-coupling of Grignard reagents at sp<sup>2</sup> carbons.<sup>5</sup> Reported independently in 1972, Corriu and Masse,

as well as Kumada *et al.* demonstrated the utility of group 10 transition metals in surmounting the original difficulties of RLi and RMgX nucleophilic substitution at  $sp^2$  carbon atoms (Scheme 3).<sup>5,6</sup>

### Corriu and Masse

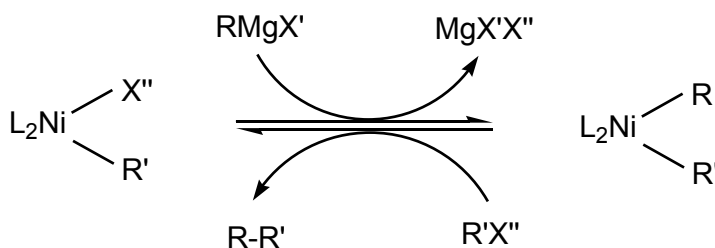


### Kumada *et al.*



Scheme 3. Ni catalyzed cross-coupling of Grignard reagents at  $sp^2$  carbons.<sup>5</sup>

The proposed reaction pathway put forth by Kumada *et al.* for the cross-coupling has been considered a basis for transition metal catalyzed coupling processes (Scheme 4).<sup>1p</sup>



Scheme 4. Pathway for Ni catalysis proposed by Kumada *et al.*

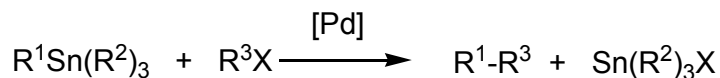
The development of palladium catalyzed cross-coupling, beginning around 1975, was predominantly influenced by the successes achieved with the aforementioned nickel catalysts.<sup>3</sup> Many contributors adopted the use of palladium as an alternate method to overcome some of the restrictions associated with nickel catalysis. For example, Ni catalysts were found to be ineffective for the equivalent coupling with RLi reagents, but Murahashi *et al.* achieved some successful coupling by utilizing Pd rather than Ni.<sup>1e,6,7</sup> Further work by Negishi *et al.* indicated that the use of Pd allowed for the replacement of Mg with other less electropositive metals (e.g. Al, Zn, Zr), leading to the development of what has been called the “first generation” Pd catalyzed cross-coupling reactions.<sup>3,8</sup> In addition, these studies demonstrated the more general applicability of palladium as an effective cross-coupling catalyst, facilitating the coupling of a greater range of substrates with fewer side reactions than had been observed with Ni.<sup>3</sup> These significant discoveries thus revealed the potential of palladium as a powerful and versatile metal for catalyzed cross-coupling.

### 1.1.2 “Second Generation”

In subsequent work, the spectrum of suitable coupling partners for palladium-catalyzed cross-coupling was widened to encompass more convenient, organometallic reagents. The first examples of palladium-catalyzed cross-coupling with organotin reagents were reported in 1977 by Kosugi *et al.*<sup>9</sup> Stille, for whom the cross-coupling process is now named (Scheme 5), also



reported palladium assisted coupling of organotin reagents in 1978<sup>10</sup> and provided an in depth examination of its mechanistic features.<sup>11</sup>



R<sup>1</sup> = vinyl, aryl, alkynyl, allyl

R<sup>2</sup> = butyl, methyl

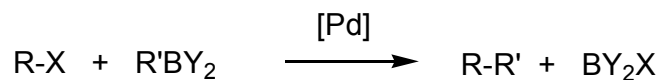
X = I, Br, OTf

Scheme 5. Generalized Stille carbon-carbon cross-coupling reaction.<sup>10</sup>

The Stille reaction remains an important method for the formation of new carbon-carbon bonds, particularly because of the versatility of organotin reagents.<sup>10</sup> Organotins are both air and moisture stable, leading to their convenient preparation and storage.<sup>1e</sup> Furthermore, protecting group strategies are almost never required as organotins are quite tolerant of many functional groups.<sup>1e</sup> Despite these advantages, Stille coupling possesses a key shortcoming, severely prohibiting its widespread applicability: the toxicity of organotin reagents. This unfortunate disadvantage has meant that other equally versatile, but innocuous organometallic coupling partners are required for truly general applicability to industrially significant organic synthesis.

## 1.2 The Suzuki-Miyaura (SM) Reaction

The development of the SM reaction represents a momentous achievement in the evolution of palladium catalyzed cross-coupling methodologies. Of its predecessors, it has found the greatest success in terms of its applications to organic synthesis. Developed by Suzuki and Miyaura beginning in 1979, the process involves the coupling of an organic electrophile with an environmentally benign, non-toxic organoboron reagent acting as the organometallic coupling partner (Scheme 6).<sup>1e,12</sup>



R = aryl, vinyl, allyl, benzyl

R' = alkyl, aryl, vinyl

X = I, Br, OTf

Y = OH, OR

Scheme 6. Generalized SM carbon-carbon cross-coupling reaction.

Most often, SM coupling is utilized to react an aryl halide ArX (X = Cl, Br, I, OTf) catalytically with an *in situ* generated arylborate [Ar'BY'Y<sub>2</sub>] (Y' = F, OH, OR) to form the coupled product Ar-Ar', although extensions to the coupling of alkyl halides have also been explored.<sup>13</sup>

The synthetic utility of the SM reaction has been widespread to say the least, and many well-summarized and comprehensive treatments of its applicability exist.<sup>11,12,14</sup> As such, a description of the synthetic applicability of the

process will be set aside in this work, favoring instead an examination of the current body of work on its mechanistic features.

### 1.2.1 Mechanistic Features of the SM Reaction

The mechanistic features associated with the SM reaction are common to many palladium catalyzed cross-coupling reactions. The most widely accepted catalytic cycle (Figure 1) typically involves oxidative addition of ArX, a commonly used substrate, to the catalytically active species, a bisphosphinepalladium(0) complex  $\text{PdL}_2$  (L = tertiary phosphines), followed by transmetallation and reductive elimination steps.<sup>1</sup> Transmetallation requires that the organoborane (e.g. organoboronic acid, organoboronate, organotrifluoroborate salt) utilized be tetracoordinate, thus allowing the organic group on boron to be sufficiently carbanionic for transfer to Pd.<sup>11</sup>

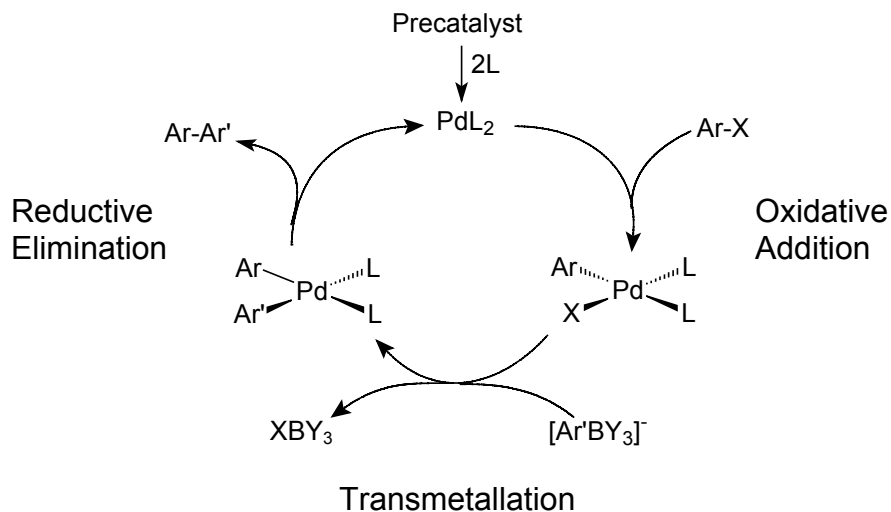
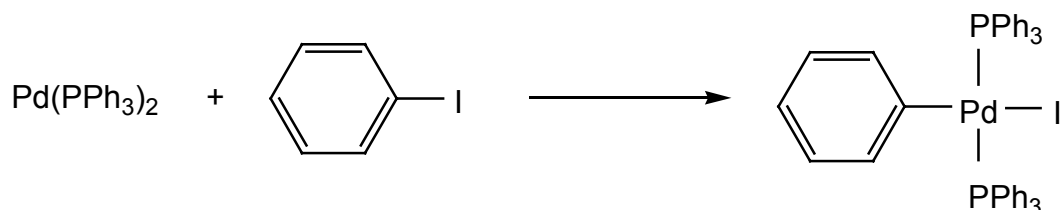


Figure 1. Generally accepted catalytic cycle for SM cross-coupling reactions.

### 1.2.1.1 Oxidative Addition

Oxidative addition to Pd(0) is common to many catalytic processes and has therefore received substantial attention in the literature. A number of reviews summarize the important work that has examined oxidative addition as it relates to catalysis.<sup>10,15</sup> Mechanistically, oxidative addition is generally believed to be the rate limiting step in the SM catalytic cycle<sup>1b,f,m</sup> and many attempts have therefore been made to maximize the rates of oxidative addition of various classes of organic substrates by varying the phosphine ligands.<sup>1</sup>

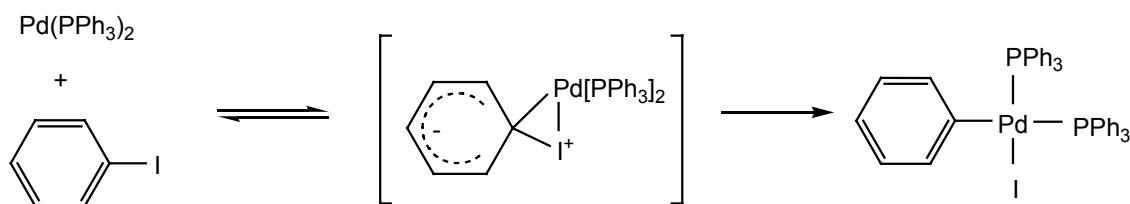
Some of the earliest research on oxidative addition to Pd(0) was conducted by Fitton *et al.*, who observed the addition of aryl halides to Pd(PPh<sub>3</sub>)<sub>2</sub> (Scheme 7).<sup>16</sup>



Scheme 7. Oxidative addition of PhI to Pd(PPh<sub>3</sub>)<sub>2</sub>.

The relative reactivity of aryl halides was found to be PhI > PhBr > PhCl. While iodobenzene can undergo oxidative addition at room temperature, bromobenzene was found to require heating to 80°C and chlorobenzene was found to be unreactive, even at 135°C. Of note, aryl chlorides activated with electron withdrawing groups (e.g. NO<sub>2</sub>, CN) were found to be reactive, implying that the mechanism for oxidative addition might be similar to that of nucleophilic aromatic displacement.<sup>16</sup>

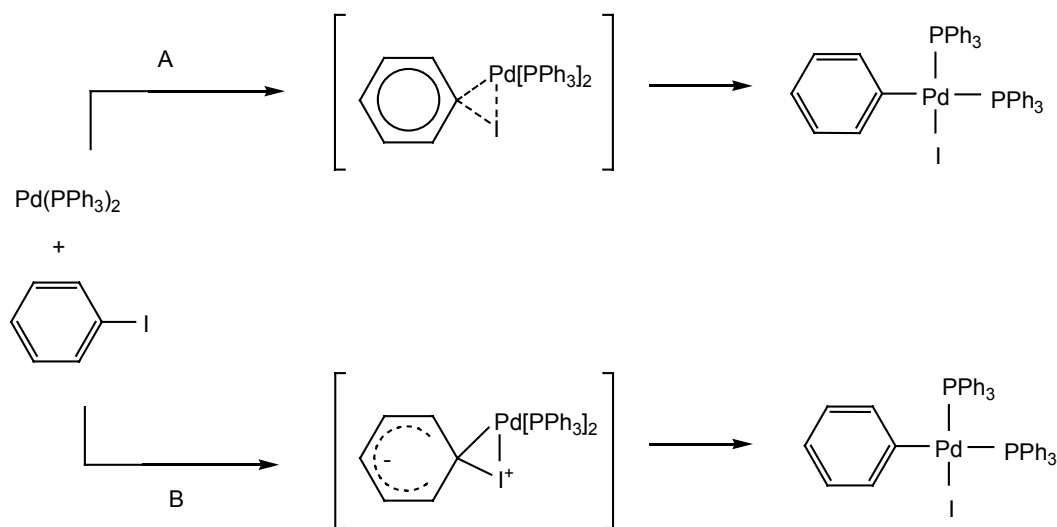
Fauvarque *et al.* initiated further studies of oxidative addition to palladium systems in the early 1980s.<sup>17</sup> The authors discovered that the reaction of  $\text{Pd}(\text{PPh}_3)_4$  and  $\text{PhI}$  is first order with respect to both  $[\text{PhI}]$  and  $[\text{Pd}]$ , while inversely proportional to  $[\text{PPh}_3]$ , due to the dissociation of  $\text{Pd}(\text{PPh}_3)_3$  to give the reactive  $\text{Pd}(\text{PPh}_3)_2$ . Furthermore, activation parameters were determined to be  $\Delta H^\ddagger = +77 \text{ kJ/mol}$  and  $\Delta S^\ddagger = +13 \text{ J/mol}\cdot\text{K}$ , supporting oxidative addition of  $\text{ArX}$  to  $\text{Pd}(\text{PPh}_3)_2$ . Studies of oxidative addition with a variety of substituted aryl iodides revealed a Hammett relationship of  $\rho = +2$ , indicating that addition is assisted by the presence of electron withdrawing groups on the aryl ring. It was therefore suggested that the mechanism for oxidative addition of  $\text{Pd}(\text{PPh}_3)_2$  to  $\text{PhI}$  is similar to that of nucleophilic aromatic substitution (Scheme 8), as was earlier put forward by Fitton *et al.*<sup>16</sup>



Scheme 8. Proposed mechanism for oxidative addition of  $\text{Pd}(\text{PPh}_3)_2$ .<sup>17</sup>

It was also suggested that  $\text{I}$ , being “softer” than both  $\text{Br}$  and  $\text{Cl}$ , is a better ligand for palladium and facilitates the addition. The proposed mechanism is therefore consistent with the observed relative reactivity of  $\text{ArX}$  where  $\text{ArI} > \text{ArBr} > \text{ArCl}$ .

Pflüger and Amatore have also contributed significantly to the determination of the mechanism of oxidative addition to aryl halides.<sup>18</sup> The authors view the mechanism of oxidative addition as one of two limiting processes, where one possible route is concerted with a three centered, neutral transition state (A), while the other involves oxidative addition by means of ionic intermediates or transition state (B), as suggested by Fauvarque<sup>17</sup> and Fitton<sup>16</sup> (Scheme 9).<sup>18</sup>

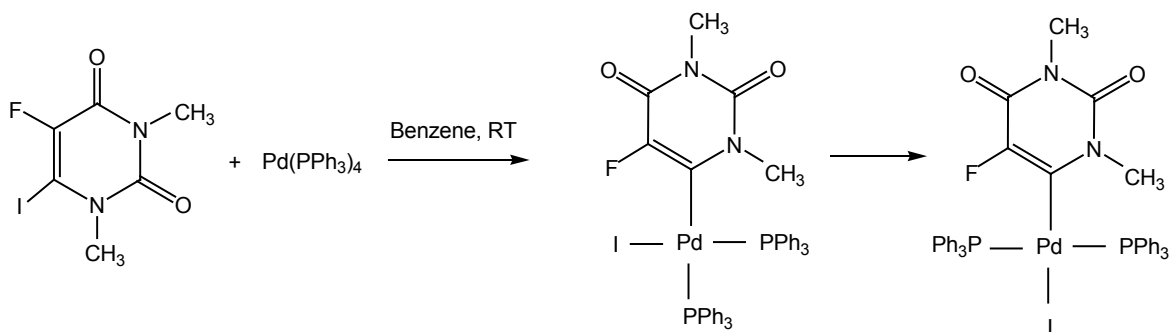


Scheme 9. Limiting mechanistic scenarios proposed for oxidative addition.<sup>18</sup>

Pflüger and Amatore found that oxidative addition of Pd(PPh<sub>3</sub>)<sub>4</sub> with a variety of substituted aryl iodides in toluene revealed a Hammett correlation of  $\rho = + 2.3$ , quite similar to the value obtained by Fauvarque in THF (+ 2). In addition, solvent variation from THF to toluene had no significant effect on observed activation parameters ( $\Delta H^\ddagger = + 75$  kJ/mol and  $\Delta S^\ddagger = + 7$  J/mol·K in toluene).

It was therefore concluded that the mechanism of oxidative addition to aryl iodides cannot involve a transition state with any significant ionic character, as changes in solvent polarity would affect the observed activation parameters for a charged transition state. Pflüger and Amatore therefore supported a concerted mechanism for oxidative addition with a three centered, neutral transition state (A), rather than one similar to nucleophilic aromatic substitution.<sup>15a</sup>

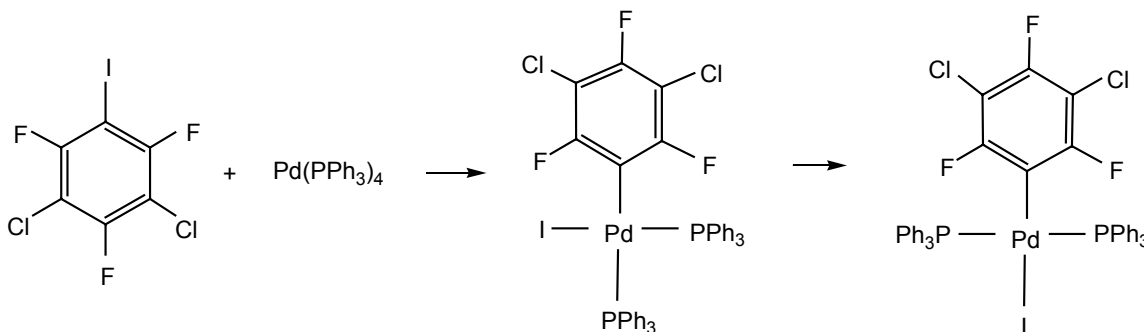
The geometry of the oxidative addition product in the above mentioned mechanism is worth noting.<sup>15a,19</sup> Generally, the isolated products of oxidative addition reactions are *trans* complexes,<sup>20</sup> while that described above in the three-centered mechanism yields a Pd complex with *cis* geometry. Interestingly, the first *cis*-phosphine palladium(II) complex was isolated by Fuchikami *et al.*<sup>21</sup>. Their work revealed that the reaction of 1,3-dimethyl-5-fluoro-6-iodouracil with Pd(PPh<sub>3</sub>)<sub>4</sub> yields a *cis*-product, which isomerizes to the *trans* product according to first order kinetics ( $k_{\text{obs}} = 2.78 \times 10^{-5} \text{ s}^{-1}$ ) (Scheme 10). This result supports the validity of the above mentioned mechanistic pathways, since a *cis* isomer can be formed and subsequently converted the more thermodynamically stable *trans* isomer.



Scheme 10. Isolation and isomerization of *cis* oxidative addition product.<sup>21</sup>

Furthermore, the addition of phosphine to the Fuchikami system was found to decrease the rate of isomerization ( $5.28 \times 10^{-6} \text{ s}^{-1}$ ), implying that the isomerization proceeds by initial dissociation of a phosphine from the *cis* complex.<sup>19,21</sup>

Further work has since been performed on the isomerization of *cis* to *trans* arylpalladium(II) species. Espinet *et al.* observed that oxidative addition of 3,5-dichlorotrifluorophenyl iodide with  $\text{Pd}(\text{PPh}_3)_4$  results in a *cis* product (Scheme 11).<sup>19</sup>



Scheme 11. Isomerization of *cis*- $\text{Pd}(\text{PPh}_3)_2(\text{C}_6\text{Cl}_2\text{F}_2)\text{I}$ .<sup>19</sup>

The slow transformation from the *cis* to the *trans* isomer allowed for the kinetic determination of the mechanism of isomerization.<sup>19</sup> The authors discovered that not one, but four concurrent pathways exist for the isomerization, implying that a substantial degree of complexity generally exists for the *cis* to *trans* isomerization involving  $\text{PdRXL}_2$  species. Although it is the *trans* product that is obtained when performing oxidative addition on a stoichiometric scale, it has been emphasized



that in a catalytic system, the isomerization from *cis* to *trans* may itself be slower than subsequent transmetallation.<sup>15a,22</sup>

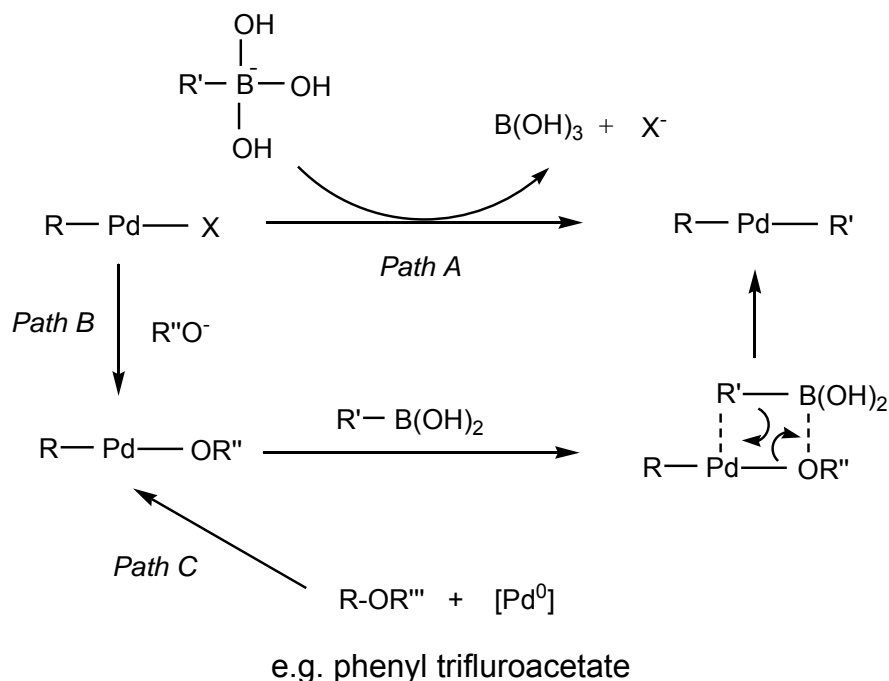
### 1.2.1.2 Transmetallation

While considerable research has been devoted to oxidative addition reactions, much less has been focused on the process of transmetallation.<sup>23</sup> It has been noted that this deficiency is likely because the mechanism of transmetallation depends upon organometallic reagent in question, as well as the reaction conditions used for the coupling process.<sup>12</sup> Generally, transmetallation occurs under SM conditions as a result of the differing electronegativities of palladium and boron.<sup>1i</sup> Under the conditions for SM coupling, boron is more electropositive than palladium, resulting in the transfer of the R group to the more electronegative Pd.

However, organoboronic acids contain a C-B bond that is itself too weakly nucleophilic to undergo transmetallation.<sup>1e,o</sup> A base-assisted transmetallation is therefore customary when performing cross-coupling with organoboronic acids. Added base results in the quaternization of boron, which enhances the nucleophilicity of the organic group on boron, and facilitates transfer of R to Pd.<sup>23</sup> Typically added bases include Na<sub>2</sub>CO<sub>3</sub>, K<sub>2</sub>CO<sub>3</sub>, NaOH, and K<sub>3</sub>PO<sub>4</sub> (1.5-2 equivalents) in either aqueous solution or in suspension.<sup>1d</sup>

Several pathways have been suggested by Miyaura for transmetallation in the SM reaction (Scheme 12).<sup>1d,23</sup> Firstly, the proposed path A involves transmetallation with R'B(OH)<sub>3</sub><sup>-</sup>, which exists in equilibrium with RB(OH)<sub>2</sub> under

basic aqueous conditions. A second route, path B involves exchange of  $X^-$  for the base  $R''O^-$  ( $R'' = H, \text{alkyl, acetyl}$ ) on  $PdRL_2X$ , producing a complex which undergoes transmetallation with  $R'B(OH)_2$ . A third path (path C) has also been proposed where the substrate (e.g. phenyl trifluoroacetate) oxidatively adds to directly produce a complex that can then transmetallation without base, as is the case in path B.



Scheme 12. Pathways for transmetallation in the SM reaction.<sup>23</sup>

In some instances, one path might dominate another<sup>1d,23,24</sup> and it has also been indicated that transmetallation is a function of the organoboron reagents used.<sup>1d,12</sup>

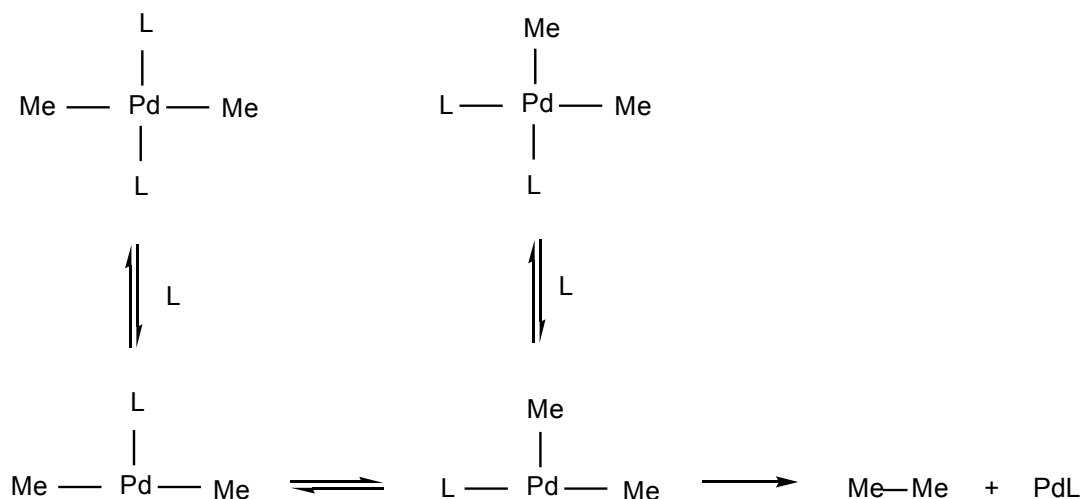
It is also worth noting that the transmetallation is not typically favored should coupling be with an alkyl halide that possesses a  $\beta$ -hydrogen. Generally,

$\beta$ -hydride elimination of the oxidative addition product will occur rather than the desired transmetalation.<sup>13c,d</sup>

### 1.2.1.3 Reductive Elimination

Reductive elimination is a catalytic step by no means exclusive to SM cross-coupling reactions. As was the case with oxidative addition, reductive elimination is crucial to many other palladium catalyzed cross-coupling reactions. Given its significance as the step responsible for carbon-carbon bond formation and release of the active PdL<sub>2</sub>, one might anticipate that reductive elimination of diorganopalladium(II) complexes has been well studied. However, reductive elimination has historically been the focus of much less research when compared to its reverse process, oxidative addition to Pd(0).<sup>25</sup>

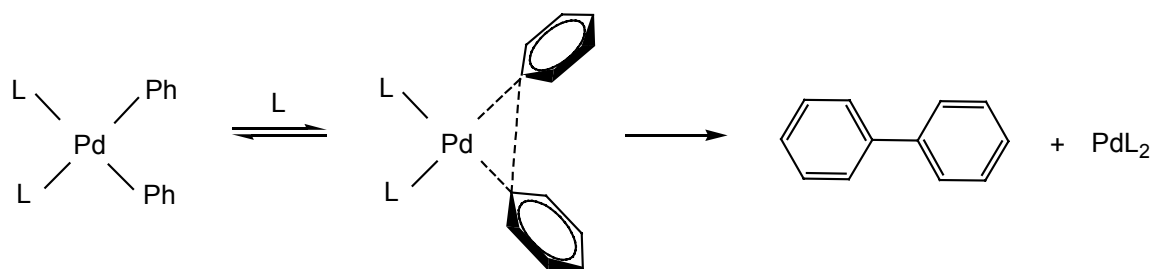
Studies involving dialkylpalladium(II) complexes revealed some of the mechanistic requirements for reductive elimination.<sup>26</sup> Stille and Gillie have shown that the reductive elimination of *cis*-Pd(Me)<sub>2</sub>L<sub>2</sub> (L = PPh<sub>3</sub>, PPh<sub>2</sub>CH<sub>3</sub>) in coordinating solvents is inhibited by the addition of excess L. Furthermore, *trans*-Pd(Me)<sub>2</sub>L<sub>2</sub> was noted to isomerize to the *cis* complex prior to undergoing reductive elimination (Scheme 13).



Scheme 13. Isomerization and reductive elimination for *cis/trans*-Pd(Me)<sub>2</sub>L<sub>2</sub>.<sup>26</sup>

The equivalent chelating complex Pd(dppe)(Me)<sub>2</sub> was found to eliminate much more slowly than its monodentate counterparts. These observations imply that reductive elimination in these dialkyl complexes requires a *cis* geometry and dissociation of L.<sup>26</sup>

However, a different mechanism for reductive elimination has been observed for diarylpalladium(II) complexes and such species are of greater relevance to the SM reaction.<sup>12</sup> Diarylpalladium(II) species must be *cis* complexes, but require no prior dissociation of phosphine in order to undergo reductive elimination. Rather, they proceed through a concerted elimination directly from the four-coordinate *cis*-palladium(II) complex (Scheme 14).<sup>12,25a,27</sup>



Scheme 14. Concerted reductive elimination for diarylpalladium(II) complexes.<sup>27</sup>

Moreover, it has been noted the order of reactivity in diorganopalladium(II) complexes is diaryl- > (alkyl)aryl- > dimethyl, which implies that the  $\pi$  system of the aromatic ring in some way assists the reductive formation of the new carbon-carbon bond.<sup>12,27</sup> Stille has suggested that the relative ease of reductive elimination involving an  $sp^2$  carbon compared to an  $sp^3$  carbon originates from its greater s character.<sup>28</sup> An  $sp^2$  hybrid orbital is therefore less directional and can more easily participate in multicentred bonding in the transition state of reductive elimination.<sup>28</sup>

In a recent review, Hartwig has put forward a detailed summary of the generally accepted steric and electronic factors affecting reductive elimination in carbon and carbon-heteroatom bond forming reactions.<sup>29</sup> It is now generally accepted that bulky ligands encourage reductive elimination. Additionally, electron rich auxiliary ligands are found to slow reductive elimination and subsequent formation of Pd(0) compared to those ligands that are electron poor.<sup>28-30</sup> It has also been noted that the reductive elimination process is facile when the ligands to be eliminated are themselves electron donating, and more difficult when they are electron withdrawing.<sup>28-31</sup> Thus, groups that electronically

increase the strength of the M-C bond decrease the driving force for reductive elimination.<sup>29</sup>

### **1.2.2 Common Conditions for SM Reactions**

A wide variability exists for the conditions appropriate for successful SM cross-coupling. Generally speaking, high temperatures in high boiling solvents and long reaction times are utilized to obtain good yields. Attempts to further improve coupling efficiencies have predominantly involved varying the nature of the phosphines L, although the variation of precatalyst systems, bases, solvents, additives and other ligands has proven successful with certain substrates. There is therefore substantial variance among effective SM protocols, which continues to stimulate the development of a universally applicable catalytic system for effective SM cross-coupling.

#### **1.2.2.1 Generally Used Precatalyst**

Many palladium compounds have been successfully used to catalyze SM coupling. Pd(II) salts have been considered a particularly convenient source to introduce Pd into the SM catalytic cycle. The most frequently used are Pd(OAc)<sub>2</sub> and PdCl<sub>2</sub>(PPh<sub>3</sub>)<sub>2</sub>, although Pd(II) precursors such as PdCl<sub>2</sub> have also found uses in SM coupling.<sup>11</sup> Typically, phosphines are assumed to cause the reduction of Pd(II) precursors to Pd(0).<sup>11</sup> Pd(0) complexes are also commonly used as SM cross-coupling precatalysts. Pd(PPh<sub>3</sub>)<sub>4</sub> is an effective source of Pd(0) and is perhaps the most common catalyst used<sup>11</sup>, although its air sensitivity

is often considered a nuisance. A convenient, air stable alternative to  $\text{Pd}(\text{PPh}_3)_4$  is  $\text{Pd}(\text{dba})_2$  (dba = *trans, trans*-dibenzylideneacetone).<sup>32</sup> When recrystallized, the composition of this complex is  $\text{Pd}_2(\text{dba})_3 \cdot \text{CHCl}_3$ . Both  $\text{Pd}(\text{dba})_2$  and  $\text{Pd}_2(\text{dba})_3$  have found utility in the context of SM cross-coupling.

A far greater variability exists in the choice of ligand for a given SM cross-coupling reaction. New ligands are regularly designed in order to achieve high catalyst efficiency and broaden the scope of the coupling process.<sup>11</sup> Historically, phosphines have been the ligands of choice for SM cross-coupling (Figure 2). The most widely used is triphenylphosphine ( $\text{PPh}_3$ ), although a variety of phosphines have been applied to the SM process with the rationale that properties inherent to the phosphine bring about a certain coupling outcome. More recently, bulky, highly donating ligands ( $\text{L} = \text{PCy}_3, \text{PMeBu}^t_2, \text{PBu}^t_3$ )<sup>33</sup> have become catalytically significant for coupling with  $\text{ArCl}$ .<sup>1a,b,g,h</sup> (see below). Generally, electron rich ligands are understood to assist oxidative addition, while bulky phosphines, as well as bidentate phosphines, are thought to assist in reductive elimination.<sup>29</sup>

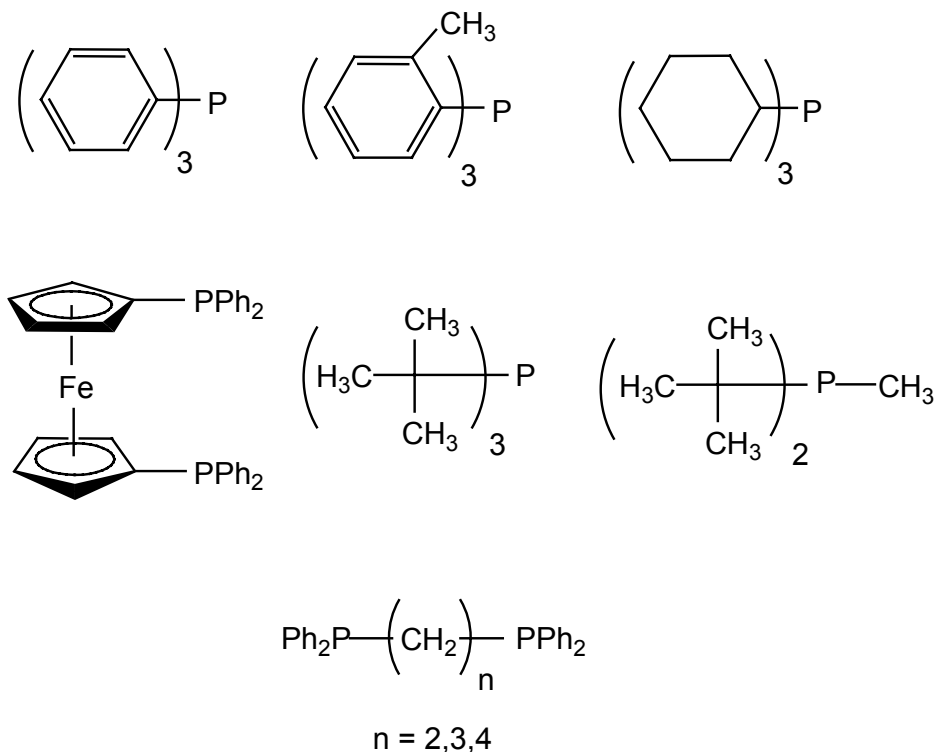


Figure 2. Examples of relevant phosphines for SM cross-coupling reactions.

Non-phosphorus containing ligands such as N-heterocyclic carbenes<sup>34</sup> are becoming increasingly relevant to SM cross-coupling. However, a proper treatment of the development and relevance of all of these ligands far exceeds the scope of this work.

### 1.2.2.2 Organoboron Reagents

The commonly chosen organometallic reagents (R-m) for SM coupling are organoboronic acids  $\text{RB}(\text{OH})_2$ . While these compounds avoid many of the difficulties associated with their organometallic predecessors  $\text{RMgX}$ ,  $\text{RLi}$  and  $\text{RSnR}'_3$ , they are not without their own disadvantages.<sup>35</sup> Their shelf life is limited



due to reactions with  $O_2$  and  $H_2O$ .<sup>35a,b</sup> Furthermore, boronic acids can cyclize and trimerize, losing  $H_2O$  to form boroxines.<sup>35c</sup> As a result, an excess of the boron reagent is often needed to ensure the stoichiometric requirements of a particular coupling are met. In addition, the purification of organoboronic acids is particularly difficult and often meets with minimal success.<sup>35d</sup>

Boronate esters ( $RB(OR)_2$ ) are a useful substitute for organoboronic acids in many SM reactions.<sup>35f</sup> However, it has been noted that while they are more easily purified than their parent organoboronic acids, their use lacks in atom economy.<sup>35d,36</sup>

Organotrifluoroborate salts ( $K[RBF_3]$ ) have recently become an attractive alternative to other available organoboron reagents in SM coupling reactions. They are both air and moisture stable and resolve the above mentioned difficulties associated with organoboronic acids and boronate esters. It has been previously assumed that organotrifluoroborate salts are more effective transmetallation partners than trivalent organoboranes, as they are added to a coupling reaction as a tetravalent species and are thus believed to be “primed” for the SM transmetallation step.<sup>35a</sup> However, experimental evidence has led to the suggestion that the species undergoing transmetallation is in fact a hydroxyl derivative of the type  $RBF_2(OH)$  or  $RBF(OH)_2$ , generated *in situ* from the organotrifluoroborate salt in the presence of water.<sup>35a,e</sup> In fact, coupling product yields in some instances are low to non-existent when performed with an organotrifluoroborate salt in the absence of water.<sup>35e</sup>

### 1.2.2.3 Aryl Electrophiles

The standard electrophiles for palladium catalyzed cross-coupling reactions, including the SM reaction, are aryl iodides, bromides and triflates.<sup>1e</sup> Aryl iodides are most reactive for oxidative addition, while aryl bromides and triflates possess similar, albeit reduced, reactivities.<sup>1e</sup>

The broad applicability of the SM reaction has been limited by the poor reactivity of aryl chlorides.<sup>37</sup> Aryl chlorides are highly desirable substrates for SM cross-coupling reactions, as they provide a greater diversity of coupling partners and a lower cost than aryl bromides, iodides and triflates.<sup>37</sup> The reduced reactivity of aryl chlorides in palladium-catalyzed coupling has been attributed to the higher C-X bond strength in aryl chlorides (C-Cl 96 kcal/mol), as compared to bromides (C-Br 81 kcal/mol) and iodides (65 kcal/mol). As a result, aryl chlorides experience more difficulty undergoing the initial oxidative addition step in the catalytic cycle. This difficulty can be circumvented by the presence of an electron-withdrawing group on the aromatic ring of the aryl chloride.<sup>38</sup> While this activates the aryl chloride for oxidative addition, the range of possible substrates is thus restricted. However, in the late 1990's extensive research performed by both Fu and Buchwald indicated that effective SM coupling can be achieved with both electron neutral or electron rich aryl chlorides (i.e. deactivated substrates).<sup>37</sup> The key to success with these demanding substrates was found to lie in the choice of ligand for catalysis. While the more conventionally employed phosphines (e.g. PPh<sub>3</sub>) are ineffective for aryl chlorides, electron-rich, bulky phosphines (e.g. PCy<sub>3</sub>, P<sup>t</sup>Bu<sub>2</sub>Me, P<sup>i</sup>Bu<sub>3</sub>) were found to meet the criteria

necessary for oxidative addition of deactivated aryl chlorides.<sup>37</sup> This discovery has incited extensive research towards the design of many new ligand systems to effect catalysis of aryl chlorides.<sup>37</sup>

### 1.3 Challenges to “Textbook” SM Catalysis

As mentioned previously (Section 1.1.2), the SM reaction often requires high temperatures and long reaction times to obtain good product yields, and attempts to improve reaction efficiencies have involved varying the nature of the phosphines L (sterically demanding phosphines often seem to be best) and the L:Pd ratios, as well as the solvent, the temperature, the role of added anions and cations, and the nature of Y (Scheme 6).<sup>1</sup> There are thus an oppressive number of reaction variables to achieve optimum SM cross-coupling. Surprisingly, it has been said, with respect to palladium catalyzed cross-coupling reactions, that “relatively few fundamental principles are involved, the understanding of which will bring order out of this apparent chaos, and make the area both approachable and usable”.<sup>39</sup> While SM catalysis has proven to be consistently useful, it has come to light in recent years that the principles involved in this area of catalysis are by no means simple. Moreover, frequent developments and studies in SM catalysis reveal the possibility of new catalytic species and mechanistic pathways for product formation. As a result, many questions regarding mechanistic details and the nature of catalytic intermediates remain to be answered.

Interestingly, a possibly central variable that has not generally been considered is the extent to which the putative catalytic species, PdL<sub>2</sub>, is actually

present in solution. The following examination of the wide variety of commonly used precatalyst systems demonstrates that there is very little evidence to show that the presumed active species  $\text{PdL}_2$  is generated *in situ* in SM cross-coupling catalysis.

### 1.3.1 Consequences Associated with Choice of Precatalyst

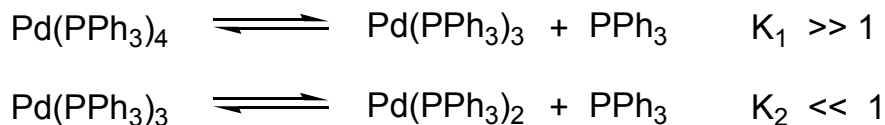
Because of their delicate, unpredictable nature, “preformed”  $\text{PdL}_2$  complexes, the presumed active catalysts in SM cross-coupling, are rarely used directly as catalysts in SM cross-coupling reactions. Bisphosphinepalladium(0) compounds are not only air sensitive, but are also prone to form clusters containing Pd-Pd bonds and to expand their coordination spheres to form species of the type  $\text{PdL}_2\text{L}'$  or  $\text{PdL}_2\text{L}'_2$  ( $\text{L}' = \text{CO}$ , alkenes, alkynes, small phosphines).<sup>2</sup> Consequently, the more readily accessible precatalysts, such as  $\text{Pd}(\text{PPh}_3)_4$ <sup>33b,40d,h,i</sup> are utilized. Interestingly, the use of a particular precatalyst system can often introduce synthetic and mechanistic consequences unique to the system in question, as described below.

#### 1.3.1.1 $\text{Pd}(\text{PPh}_3)_4$

$\text{Pd}(\text{PPh}_3)_4$  is understood to be an 18 electron complex which in solution dissociates to produce the tris-substituted 16 electron species  $\text{Pd}(\text{PPh}_3)_3$ .<sup>33b,41</sup>

However, the truly active species in oxidative addition was later identified as the 14 electron complex  $\text{Pd}(\text{PPh}_3)_2$ .<sup>17</sup> The low concentration of this active species is

governed by a disadvantageous equilibrium that favors Pd(PPh<sub>3</sub>)<sub>3</sub> as the major species in solution (Scheme 15).



Scheme 15. Dissociation equilibria associated with Pd(PPh<sub>3</sub>)<sub>4</sub> in solution.<sup>17</sup>

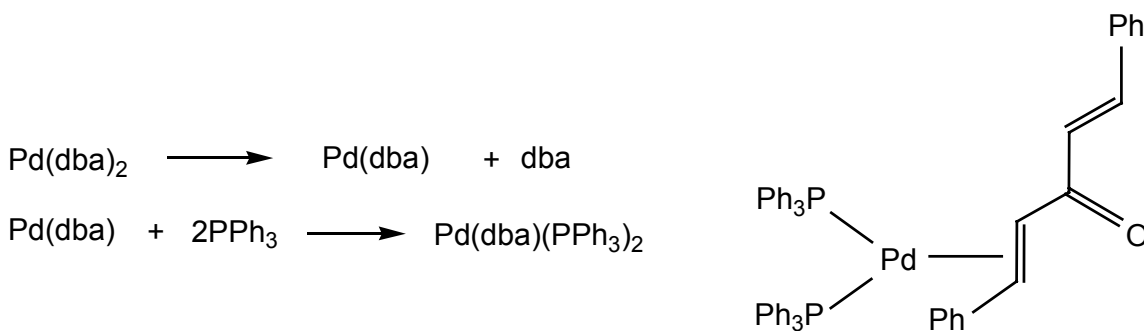
This behaviour is not limited to Pd(0) species ligated by PPh<sub>3</sub>. Other phosphines also participate in similar equilibria and low ligated species where n = 2 and n = 3 are possible. However, the preference for low coordination number appears to relate not to basicity, but rather to the steric hindrance associated with the phosphine in question: PMe<sub>3</sub> ~ PMe<sub>2</sub>Ph ~ PMePh<sub>2</sub> < PPh<sub>3</sub> < P<sup>i</sup>Pr<sub>3</sub> < PCy<sub>3</sub>.<sup>41</sup> As a result, complexes of the type PdL<sub>2</sub> are isolable with phosphines possessing particularly large cone angles (P<sup>t</sup>Bu<sub>3</sub> and PCy<sub>3</sub>). The degree of coordinative unsaturation thus depends on the steric bulk of the phosphine in question. As a result, a complex of higher substitution, and possibly of lower reactivity for oxidative addition, may be the dominant species in solution rather than the desired coordinatively unsaturated, catalytically active species.

### 1.3.1.2 Pd(dba)<sub>2</sub>/Pd<sub>2</sub>(dba)<sub>3</sub>

As mentioned above, palladium(0) complexes of dba have often been used as alternate catalyst precursors in SM cross-coupling reactions.<sup>11</sup> For a given SM cross-coupling protocol, the desired phosphine is added to solutions of

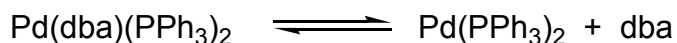
$\text{Pd}(\text{dba})_2$  or  $\text{Pd}_2(\text{dba})_3$  ( $\text{dba} = \textit{trans, trans}$ -dibenzylideneacetone).<sup>32</sup> With  $\text{dba}$  containing precursors, it had been thought that the true  $\text{Pd}(0)$  catalyst,  $\text{PdL}_2$ , is generated *in situ*, thus eliminating the need for the more air sensitive  $\text{Pd}(\text{PPh}_3)_4$ .<sup>42</sup> Furthermore, the addition and quantity of the phosphine used in this case is more easily controlled, which is particularly advantageous when utilizing expensive phosphines.<sup>42</sup>

It has been generally assumed that  $\text{dba}$  is completely displaced from  $\text{Pd}(\text{dba})_2$  or, if not, that it does not impede oxidative addition. While catalyst preparation from  $\text{Pd}(\text{dba})_2 + 2\text{L}$  has generally been thought to generate  $\text{PdL}_2$  *in situ*,<sup>43</sup>  $\text{Pd}(\text{dba})_2 + 4\text{L}$  has been assumed to generate  $\text{PdL}_4$ .<sup>43</sup> In studying these systems, Amatore *et al.* showed that the assumed “innocent”  $\text{dba}$  ligand in fact affects the nature of the catalyst species generated in solution. Their work demonstrated that  $\text{Pd}(\text{dba})_2 + 2\text{PPh}_3$  is not, as anticipated, a direct source of  $\text{PdL}_2$ . Their  $^{31}\text{P}$  NMR experiments indicate that monoligation through  $\text{dba}$  double bond occurs when  $\text{Pd}(\text{dba})_2$  is combined with two equivalents of  $\text{PPh}_3$  (Scheme 16).<sup>43</sup>



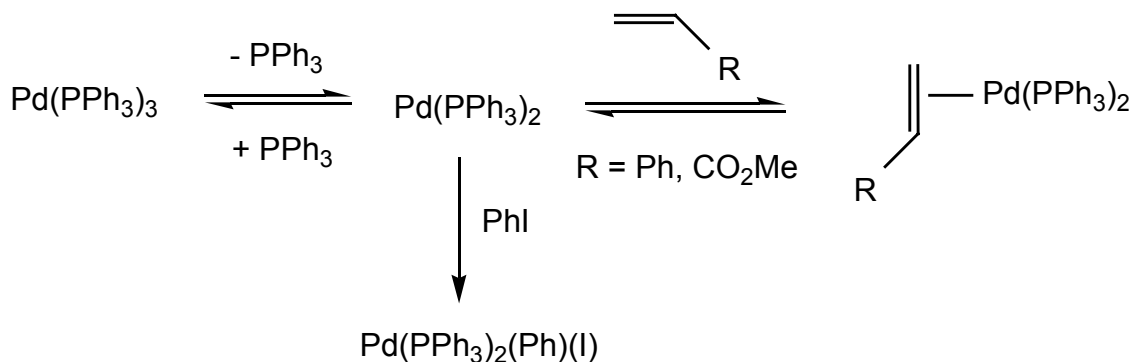
Scheme 16. Monoligation of  $\text{Pd}(0)$  by  $\text{dba}$  in the presence of  $\text{PPh}_3$ .<sup>43</sup>

A similar observation was made for mixtures of Pd(dba)<sub>2</sub> + L-L (L-L = dppm, dppe, dppb, dppf)<sup>43</sup> which generates Pd(dba)(L-L). Essentially, these monoligated species are unreactive and release dba in an equilibrium that influences the concentration of the species that are capable of undergoing oxidative addition (Scheme 17).<sup>43</sup>



Scheme 17. Equilibrium between dba ligated Pd(0) and Pd(PPh<sub>3</sub>)<sub>2</sub>.<sup>43</sup>

There is therefore ample evidence showing that alkenes possessing electron withdrawing groups, including dba, bind very strongly to Pd(0) and are not always fully displaced by tertiary phosphines.<sup>42,43,44</sup> As ligands, dba and other alkenes can thus inhibit many oxidative addition reactions.<sup>42,43,44</sup> Amatore *et al.* found that in DMF, oxidative addition of PhI to Pd(PPh<sub>3</sub>)<sub>4</sub> can be slowed in the presence of styrene and methyl acrylate by the formation of unreactive (olefin)Pd(PPh<sub>3</sub>)<sub>2</sub>, thus decreasing the amount of Pd(PPh<sub>3</sub>)<sub>2</sub> available for oxidative addition (Scheme 18).<sup>44b</sup>



Scheme 18. Inhibition of oxidative addition as a result of alkene coordination.<sup>44b</sup>

A similar effect is observed when oxidative addition of PhI to Pd(PPh<sub>3</sub>)<sub>4</sub> is performed in the presence of terminal alkynes such as phenylacetylene and ethylpropiolate, producing complexes of the type [(η<sup>2</sup>-RC≡CH)Pd<sup>0</sup>(PPh<sub>3</sub>)<sub>2</sub>] (R = Ph, EtO<sub>2</sub>).<sup>44c</sup>

Lee *et al.* discovered that the variation of the electronic character of dba in a Pd(0) precatalyst has an impact upon the observed SM cross-coupling of 4-chlorotoluene and phenylboronic acid.<sup>44d</sup> It was anticipated that the strength of the η<sup>2</sup> coordination of the alkene to Pd(0) would depend on the π-accepting ability of the dba derivative Pd<sub>2</sub>(n,n'-Z-dba)<sub>3</sub> (n,n'-Z = 4,4'-OMe, 3,5,3',5'-OMe, 4,4'-<sup>t</sup>Bu, 3,3'-NO<sub>2</sub>, 4,4'-CF<sub>3</sub>) (Figure 3). It was proposed that electron withdrawing groups would strengthen alkene coordination due to increased backbonding, thus diminishing the availability of active catalyst PdL<sub>2</sub>. Conversely, electron donating groups (OMe) would diminish backbonding, thus weakening alkene coordination



and increasing the concentration of the bisphosphine species. As expected, tuning the electronic character of dba in this way resulted in a 86% conversion when R = 3,5,3',5'-OMe, compared with a 77% conversion with unsubstituted Pd<sub>2</sub>(dba)<sub>3</sub>. Additionally, the catalysis efficiency was found to be significantly reduced (20% conversion) when R = 3,3'-NO<sub>2</sub>.

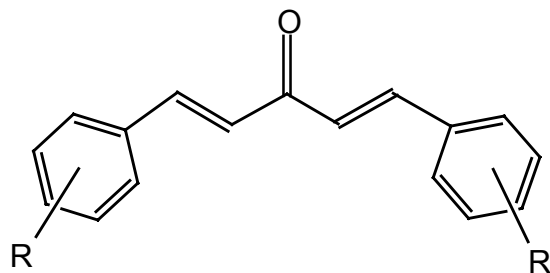
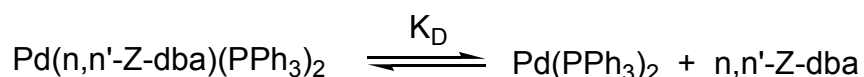


Figure 3. n,n'-Z-dba (n,n'-Z = 4,4'-OMe, 3,5,3',5'-OMe, 4,4'-<sup>t</sup>Bu, 3,3'-NO<sub>2</sub>, 4,4'-CF<sub>3</sub>).<sup>44d</sup>

Jutand *et al.* confirmed that the abovementioned effects on SM coupling are the result of inhibition of oxidative addition.<sup>44e</sup> As with their work involving Pd(dba)<sub>2</sub>/PPh<sub>3</sub> systems, it was found that the addition of two or four equivalents of PPh<sub>3</sub> to Pd<sub>2</sub>(n,n'-Z-dba)<sub>3</sub> (n,n'-Z = 4,4'-F, 4,4'-OMe, 3,3',4,4',5,5'-OMe) or Pd(n,n'-Z-dba)<sub>2</sub> (n,n'-Z = 4,4'-Br, 4,4'-Cl, 4,4'-CH<sub>3</sub>, 3,3',5,5'-OMe) resulted in the formation Pd(n,n'-Z-dba)(PPh<sub>3</sub>)<sub>2</sub>, which is unreactive towards oxidative addition and in equilibrium with Pd(PPh<sub>3</sub>)<sub>2</sub> and free n,n'-Z-dba (Scheme 19).<sup>44e</sup>



Scheme 19. Equilibrium releasing Pd(PPh<sub>3</sub>)<sub>2</sub> from n,n'-Z-dba complex.<sup>44e</sup>

The authors found that as the electron donating properties of *n,n'*-Z-dba were increased, the value of the  $K_D$  for the equilibrium releasing  $\text{Pd}(\text{PPh}_3)_2$  increased, thus enhancing the rate of oxidative addition with PhI.

It has therefore been well established that dba, among other alkenes, are not merely “innocent” spectator ligands. The aforementioned work indicates that the use of dba containing precursors can have a serious impact on the efficiency of SM cross-coupling catalysis.

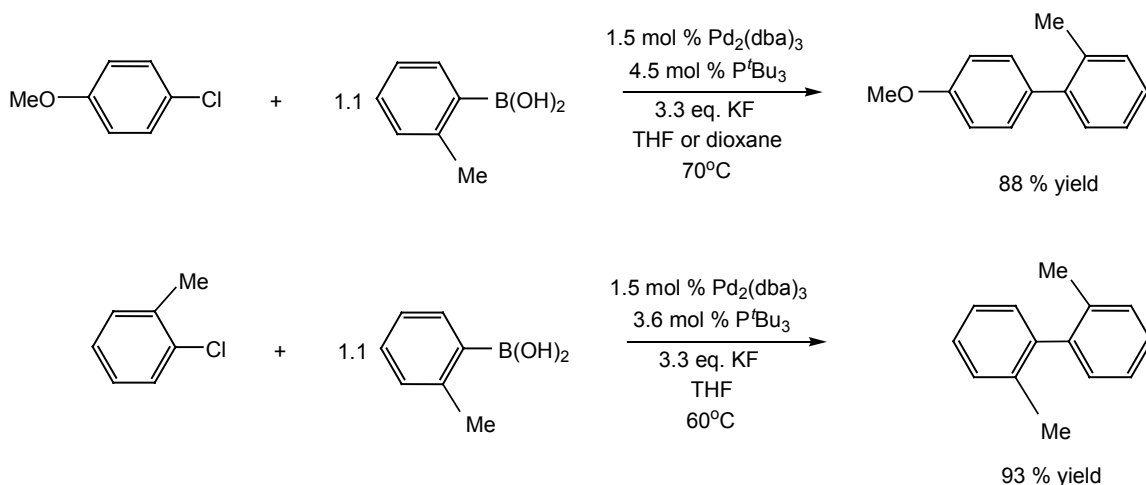
### 1.3.1.3 Monophosphine Complexes

The vast efforts to achieve SM coupling with difficult substrates (i.e. aryl chlorides) have yielded a variety of very efficient catalyst systems based upon bulky, electron rich phosphines.<sup>1n</sup> The success of many of these systems has been attributed to the generation of highly reactive monophosphine species, Pd-L, whose existence is likely a direct result of the ability of the involved phosphine to stabilize the coordinatively unsaturated complex or destabilize the 2:1 complex.<sup>1m,45</sup>

As mentioned above, a number of kinetic studies have been reported for the oxidative addition of aryl halides to palladium(0) compounds  $\text{Pd}(\text{PPh}_3)_2$ ,<sup>7</sup> and evidence for the intermediacy of this 2:1 compound has been deduced although, with some other phosphines, inhibition by added L has been interpreted in terms of 1:1 species PdL being kinetically preferred.<sup>1m,45</sup> The significance of 12

electron Pd-L species as the truly active catalytic species with such phosphines has challenged previous notions regarding the role of PdL<sub>2</sub> as SM catalysts.

There is ample experimental evidence which points to the existence of Pd-L as the catalyst species in cross-coupling reactions. Such a system was reported by Fu *et al.*, who showed that a highly active SM catalyst system can be obtained by using a precatalyst mixture consisting of Pd<sub>2</sub>(dba)<sub>3</sub> and P<sup>t</sup>Bu<sub>3</sub>. This system successfully couples a variety of aryl chlorides, and more notably was the first to allow for coupling of electron rich aryl chlorides.<sup>45h,i</sup> Further studies revealed that the Pd<sub>2</sub>(dba)<sub>3</sub>/P<sup>t</sup>Bu<sub>3</sub> system can effect coupling of both electron rich and sterically hindered aryl chlorides (Scheme 20).<sup>45i</sup>

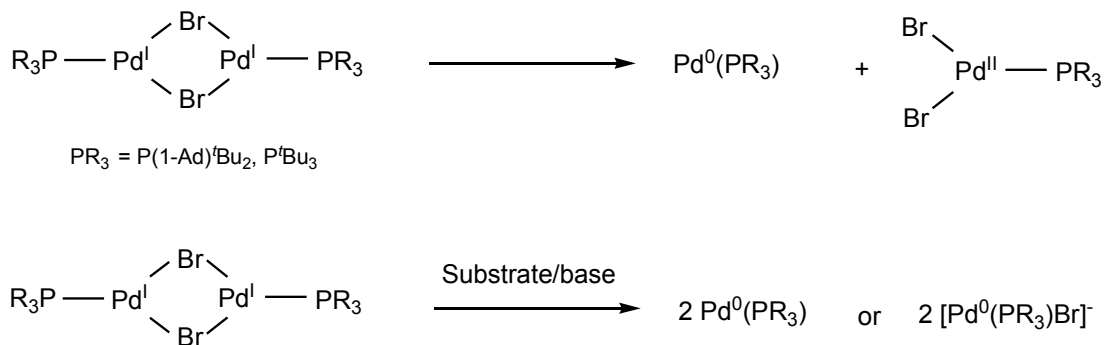


Scheme 20. SM cross-coupling of electron rich and hindered aryl chlorides.

The existence of a monophosphine catalyst was suggested as a rationale for the noted optimum Pd:P<sup>t</sup>Bu<sub>3</sub> ratio for catalysis. It was found that high catalyst activity required this ratio to be in the range of 1:1 – 1:1.5. Once the ratio was elevated

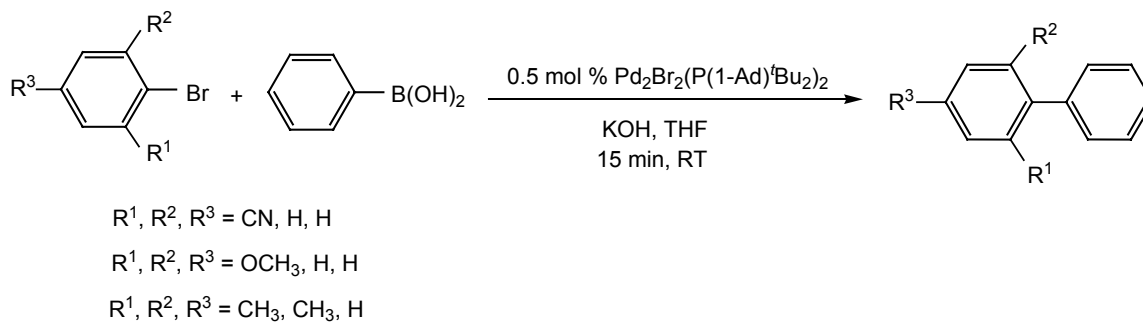
to 1:2, the catalyst activity was greatly diminished.  $^{31}\text{P}$  NMR spectroscopy revealed that for systems at each of the above ratios, the only detectable species was  $\text{Pd}(\text{P}^t\text{Bu}_3)_2$ . The authors inferred that half of palladium present in the system must be exist as the unreactive  $\text{Pd}(\text{P}^t\text{Bu}_3)_2$ , which the other half remained unligated. It was thus concluded that the active catalyst must be monoligated  $\text{Pd}-\text{P}^t\text{Bu}_3$ . Moreover, it was found that  $\text{Pd}_2(\text{dba})_3$  was a superior precursor to  $\text{Pd}(\text{OAc})_2$ . It is possible that the presence of dba in the catalyst system allows for some stabilization of  $\text{Pd}-\text{P}^t\text{Bu}_3$  by means of coordination through the dba alkene moiety.

Others have provided further experimental evidence for the significance of monophosphine palladium(0) complexes as active catalytic species for SM cross-coupling. Hartwig *et al.* discovered that the dimeric species  $\text{Pd}_2(\mu\text{-Br})_2(\text{PR}_3)_2$  ( $\text{PR}_3 = \text{P}(1\text{-Ad})\text{Bu}^t_2, \text{P}^t\text{Bu}_3$ ) could be utilized as a catalyst precursor to affect the cross-coupling of hindered aryl bromides with phenylboronic acid.<sup>45k</sup> The catalytically active species are believed to be the result of either the cleavage of the dimer, yielding monoligated  $\text{Pd}(\text{PR}_3)$ , or by reduction in the presence of substrate and base to produce  $\text{Pd}(\text{PR}_3)$  or  $[\text{Pd}(\text{PR}_3)\text{Br}]^-$  (Scheme 21).



Scheme 21. Generation of active catalysts from  $\text{Pd}_2(\mu\text{-Br})_2(\text{PR}_3)_2$

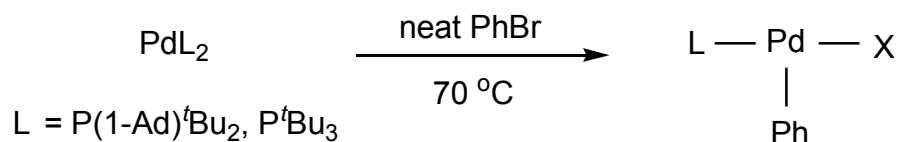
The resulting system was capable of successfully coupling *o*-substituted aryl bromides (92-96% yield) and 2-bromo-*m*-xylene (84% yield) at room temperature in 15 minutes (Scheme 22).



Scheme 22: Room temperature SM cross-coupling of hindered aryl chlorides.

Hartwig *et al.* have also successfully isolated monomeric, arylpalladium(II) complexes of the type  $\text{Pd}(\text{PR}_3)(\text{Ph})(\text{X})$ , lending credence to the possibility of monophosphine bound intermediates in SM catalysis. ( $\text{PR}_3 = (1\text{-AdP}^t\text{Bu}_2, \text{P}^t\text{Bu}_3$ ,

X = Br, I).<sup>1m,45k</sup> It was observed that Pd(PBu<sup>t</sup><sub>3</sub>)PhBr and Pd(1-AdPBu<sup>t</sup><sub>2</sub>)PhBr could be isolated in neat PhBr from PdL<sub>2</sub> at 70 °C (Scheme 23).



Scheme 23. Isolation of monomeric, T-shaped arylpalladium(II) complexes.<sup>45k</sup>

The resulting complexes represented the first examples of T-shaped, monomeric arylpalladium(II) complexes that lack coordinated solvent. In fact, IR and computational data indicate that the complexes possess a weak agostic interaction between Pd and the C-H present in the phosphine ligand.<sup>45k</sup> Such interactions may very well be present in other monophosphine intermediates that participate in catalysis.

Buchwald *et al.* have also provided a great deal of experimental evidence supporting the existence of monophosphine Pd-L species and their significance in SM catalysis.<sup>45d,e,m</sup> Their highly reactive catalyst systems have been a result of the utilization of ligands that enhance the stability of monoligated Pd-L.<sup>45d,e,m</sup> A variety of dialkylphosphanylbiaryl ligands were developed to provide the ideal electronic and steric environments necessary to facilitate oxidative addition and reductive elimination (Figure 4).

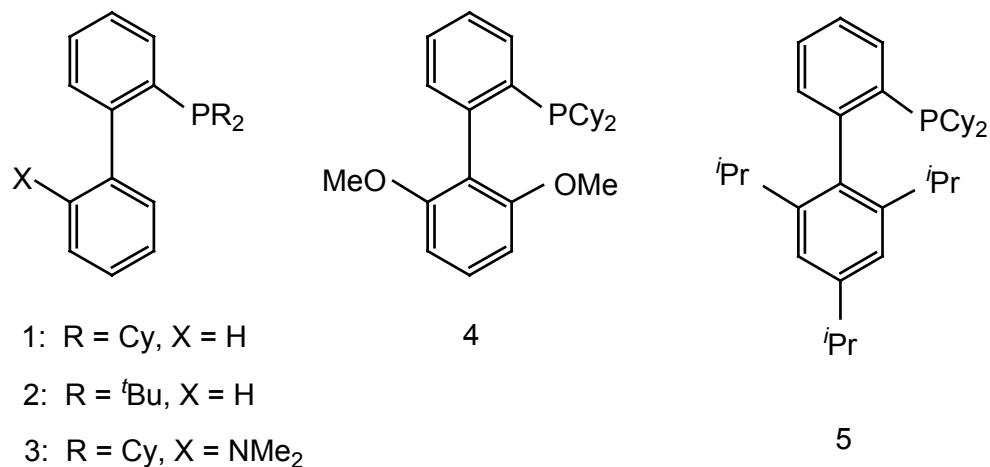
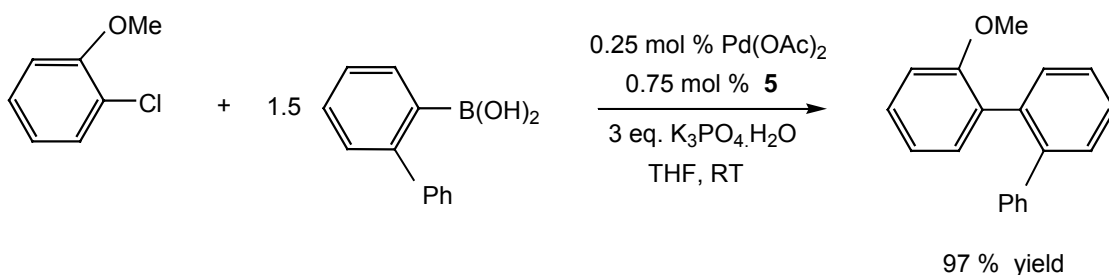


Figure 4. Buchwald ligands for SM cross-coupling.<sup>45d,e,m</sup>

When applied to SM cross-coupling, extremely efficient protocols have been achieved, including the successful coupling of aryl chlorides at room temperature. Furthermore, one can achieve room temperature cross-coupling in good yield involving hindered, as well as an electron rich, aryl chlorides (Scheme 24).



Scheme 24: SM cross-coupling with Buchwald system using ligand **5**.

The authors believe the overall success of the catalyst systems lies in a  $\pi$  interaction between Pd(0) and the biaryl ligand moiety.<sup>45d</sup> Supporting this

supposition, crystallographic analysis of isolated  $4 \cdot \text{Pd}(\text{dba})$  demonstrated a Pd-C(*ipso*) interaction between biaryl ligand.<sup>45d</sup> Computational analysis indicated that the Pd-C(*ipso*) distance in this complex is 2.378 Å, contrasting with the observed Pd-C(*ortho*) distances of 2.696 Å and 2.788 Å.<sup>45e</sup> This shorter distance implies an  $\eta^1$ -interaction between Pd(0) and the biaryl ligand (Figure 5).

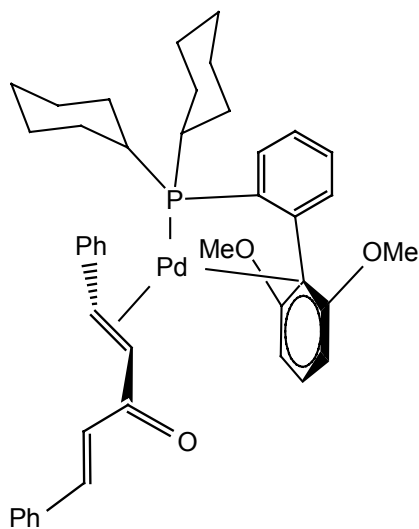


Figure 5. Representation of the interaction involved in  $4 \cdot \text{Pd}(\text{dba})$ .<sup>50d</sup>

Such an interaction thus stabilizes the highly reactive monophosphine Pd-L. However, DFT calculations of  $4 \cdot \text{Pd}$  indicate an  $\eta^1$ -Pd arene interaction with an aryl *ortho* carbon, rather than the *ipso* carbon.<sup>45m</sup> Furthermore, these interactions exist in both the active catalyst and the oxidative addition products, but remain absent in the associated transition state structures, indicating that the Pd-arene  $\pi$  interaction serves to stabilize the metal when it is not participating in catalytically relevant steps.<sup>45m</sup> Additionally, the isolation and crystallographic analysis of  $\text{PdL}_2$  indicates that it lacks the abovementioned  $\eta^1$ -arene interaction,



and its large size likely means that oxidative addition is prohibitive. The result is an encouraged dissociation of L, shifting the  $\text{PdL}_2/\text{Pd-L}$  equilibrium towards the stabilized and more highly reactive monoligated species.<sup>45e</sup> Regardless of the type of arene interaction (*ortho* or *ipso* carbon), it is clear in the Buchwald systems that the hitherto “accepted” cross-coupling catalyst  $\text{PdL}_2$  in fact plays a minor role as compared to monoligated PdL species.

While the Buchwald systems depend on the intrinsic nature of the phosphine to stabilize Pd-L, Beller *et al.* have also succeeded in producing stabilized monophosphine catalyst systems. However, in their work the catalytically active species are stabilized by virtue of a coordinated 1,6-diene. (Figure 6).<sup>46</sup> The resulting catalysts effectively couple aryl chlorides with phenylboronic acid (Scheme 25).

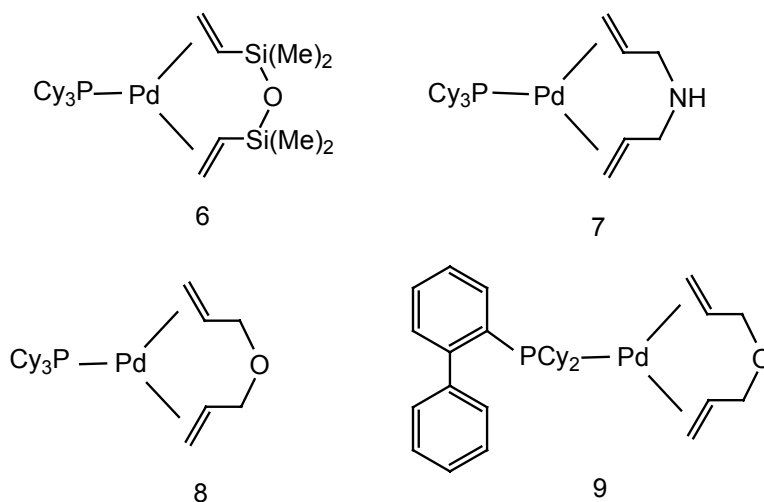
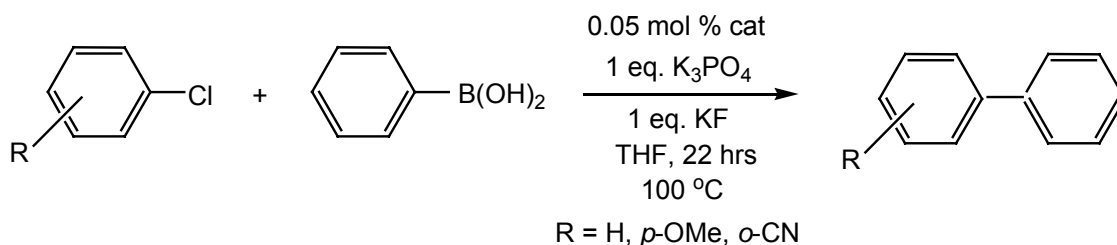


Figure 6. 1,6-diene stabilized monophosphine catalyst systems.<sup>46</sup>



Scheme 25. Beller ligand systems for SM cross-coupling of aryl chlorides.<sup>46</sup>

Improved product yield and turnover number were observed with complex **8**, as compared to cross-coupling caused by 1:1 Pd<sub>2</sub>(dba)<sub>2</sub>/PCy<sub>3</sub>, 1:1 Pd(OAc)<sub>2</sub>/PCy<sub>3</sub>, and 1:2 Pd(OAc)<sub>2</sub>/PCy<sub>3</sub>. Furthermore, as the acceptor ability of the coordinated diene increased, a decrease in the catalyst reactivity was observed in the order of **8** > **7** > **6**, implying that the lability of the diene was linked to the enhanced reactivity of the catalyst system. Thus the successful cross-coupling observed in these systems is attributed to the release of the diene to produce the anticipated catalytically active Pd-L.<sup>46</sup> The most efficient of the coordinated diene systems was **9**, based on the Buchwald di-cyclohexyl-*o*-biphenyl ligand. It is likely in the case of this phosphine that Pd-L stabilization results from both the coordinated diene as well as the Pd(0) η<sup>1</sup>-arene interaction described by Buchwald.<sup>45d,e,m</sup>

While the above represents substantial experimental evidence indicating the importance and potential of Pd-L species as catalysts in cross-coupling reactions, theoretical work has also been performed to assess the importance of these low coordination complexes. Norrby *et al.* studied the reaction of PhI to Pd(0) through DFT calculations in an effort to determine the stability of Pd(0)

complexes containing one to three ligands.<sup>45n</sup> Their work led them to conclude that oxidative addition is in fact most favorable when Pd(0) is linearly bound by PhI and one ligand only, lending support to the catalytic significance of Pd-L species. Additionally, calculations indicated that anionic palladium (0) complexes are more likely to be monophosphine complexes of the type  $[\text{Pd}(\text{PPh}_3)\text{X}]$ , rather than anionic complexes  $[\text{Pd}(\text{PPh}_3)_2\text{X}^-]$  suggested by Amatore *et al.*<sup>45n</sup>

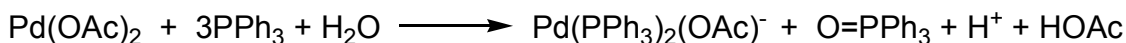
Overwhelming evidence thus points to the existence and significance of coordinatively unsaturated, 12 electron species of the type Pd-L. It seems that the choice of ligand has a profound impact on the nature of the Pd species that acts as active catalyst. Through efforts to attain more efficient cross-coupling reactions with a broader scope of substrates (namely aryl chlorides), the Pd-L species, rather than  $\text{PdL}_2$ , has become forerunner as “active catalyst” in the many SM cross-coupling protocols.

#### 1.3.1.4 $\text{Pd}(\text{OAc})_2 + n\text{PPh}_3$

Catalyst solutions for SM cross-coupling are also generated by adding a phosphine to a suspension or solution of  $\text{Pd}(\text{OAc})_2$ , the assumption being that the palladium(II) salts are reduced to palladium(0) compounds.<sup>1</sup> However, for most of the phosphines used in SM catalysts, there is little evidence that reduction is achieved either rapidly or completely.

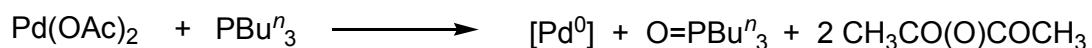
Some studies exist that describe the reduction  $\text{Pd}(\text{OAc})_2$  when it is treated with  $\text{PPh}_3$ .<sup>47</sup> Amatore *et al.* discovered that in these systems the anticipated  $\text{Pd}(\text{PPh}_3)_2$  is not the species generated.<sup>47a</sup> In fact, the acetate anions introduced

through the Pd(II) precursor are significant in the process, producing an anionic palladium(0) species (Scheme 26). Similar results were observed when Pd(OCOCF<sub>3</sub>)<sub>2</sub> was treated with PPh<sub>3</sub> in DMF.<sup>47b</sup>



Scheme 26. Reduction of Pd(OAc)<sub>2</sub> in the presence of PPh<sub>3</sub> in DMF.<sup>47b</sup>

Additionally, other phosphines are capable of causing the reduction of Pd(II). Mandai *et al.* have observed that catalytically active but unidentified Pd(0) complexes can be generated *in situ* from Pd(OAc)<sub>2</sub> and PBu<sup>n</sup><sub>3</sub> in a 1:1 ratio in THF or benzene (Scheme 27).<sup>48</sup>



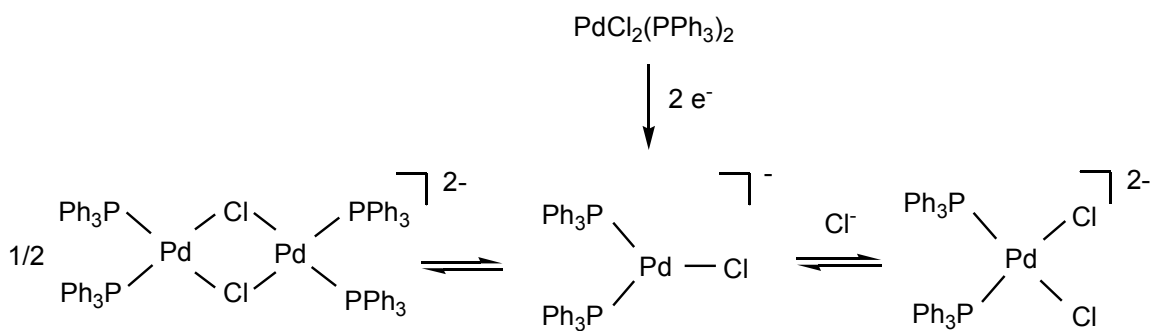
Scheme 27. Reduction of Pd(OAc)<sub>2</sub> in the presence of PBu<sup>n</sup><sub>3</sub>.<sup>48</sup>

Likewise, reactions of Pd(OAc)<sub>2</sub> with PBu<sup>n</sup><sub>3</sub>, PMe<sub>2</sub>Ph and PMePh<sub>2</sub> give similar species in DMF at 60 °C.<sup>48</sup> Thus reduction to palladium(0) does occur in some instances although the species produced have not always been identified. Interestingly, under the particular conditions of the latter study, reduction is inhibited by bulky substituents on phosphorus<sup>47a</sup> such that reduction of Pd(OAc)<sub>2</sub> by monodentate phosphines becomes disfavored when the phosphine cone angle is ~130°; this corresponds approximately to the size of PEt<sub>3</sub>,<sup>49</sup> and thus reduction of Pd(OAc)<sub>2</sub> by the bulkier phosphines normally used in Suzuki coupling reactions<sup>1</sup> is problematic. Reduction to Pd(0) from Pd(OAc)<sub>2</sub> is

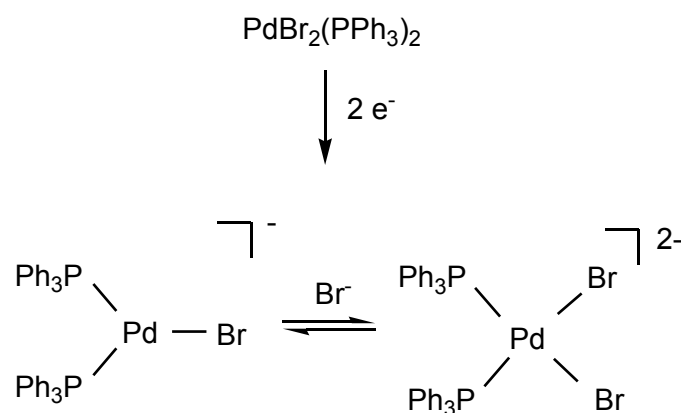
therefore dependent upon the phosphine in question. Furthermore, anionic species of the type  $\text{PdL}_2(\text{OAc}^-)$ , rather than the anticipated  $\text{PdL}_2$ , may be generated as a result of the chosen precursor  $\text{Pd}(\text{OAc})_2$ .

### 1.3.1.5 $\text{PdCl}_2(\text{PPh}_3)_2$

Palladium (II) complexes of the type  $\text{Pd}(\text{PPh}_3)_2\text{Cl}_2$  have often been used as catalyst precursors as an alternative to  $\text{Pd}(\text{PPh}_3)_4$ .<sup>50d</sup> They are often considered improved catalyst precursors as they are anticipated to quantitatively generate  $\text{Pd}(\text{PPh}_3)_2$ . However, work by Amatore *et al.* indicates that this is not the case.<sup>51</sup> Reduction of  $\text{PdCl}_2(\text{PPh}_3)_2$  yields not  $\text{Pd}(\text{PPh}_3)_2$  but several anionic Pd complexes in equilibrium (Scheme 28).<sup>51</sup> Reduction of  $\text{Pd}(\text{PPh}_3)_2\text{Br}_2$  results in two equilibrating anionic species (Scheme 29).



Scheme 28. Electrochemical reduction of  $\text{PdCl}_2(\text{PPh}_3)_2$ .<sup>51</sup>



Scheme 29. Electrochemical reduction of  $\text{PdBr}_2(\text{PPh}_3)_2$ .<sup>51</sup>

Anionic species of the types  $[\text{PdX}(\text{PPh}_3)_2]^-$ ,  $[\text{Pd}(\mu\text{-X})(\text{PPh}_3)_2]^{2-}$  and  $[\text{PdX}_2(\text{PPh}_3)_2]^{2-}$  (X = Cl, Br) are thus formed in the presence of halide ions,<sup>47a,50,51</sup> and these have been thought to undergo oxidative addition more rapidly than does the neutral tris-phosphine compound  $\text{Pd}(\text{PPh}_3)_3$ .

#### 1.4 Research Objectives

The prevailing theme revealed in this complicated and often confusing area of literature is that SM catalyst reactivity and subsequent efficiency is not only a function of chosen ligand, but can also be a result of the chosen precursor to the active Pd(0) catalyst. The question arises then, if one particular palladium(II)-phosphine cross-coupling catalyst system is found to be more effective than another, does the difference arise because one phosphine is intrinsically superior, as is often assumed? Or does the difference arise because more of the palladium(II) precursor is reduced in the one case than in the other?

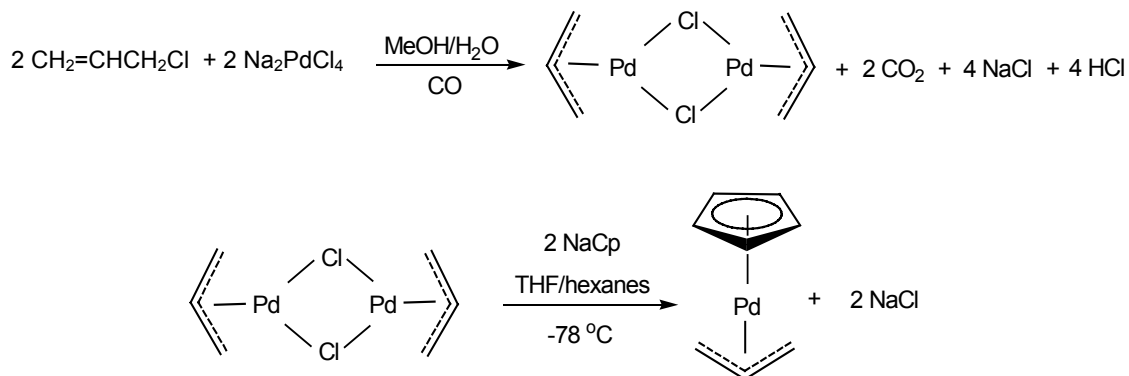
Furthermore, in situations where reduction by the phosphine L is far from complete such that the ratio of L:Pd(0)  $\gg 1$ , might the major catalytic species in solution be predominantly of the type PdL<sub>3,4</sub>, depending on the steric requirements of L? In addition, does a particular phosphine favour a more highly coordinatively unsaturated active species Pd-L, over the generally accepted PdL<sub>2</sub> catalyst? The importance of and difficulties in identifying the true catalyst(s) in the plethora of processes investigated has been recognized,<sup>1n</sup> although it may be an exaggeration to suggest that the “literature has grown into a morass, with an endless list of hypothesized or claimed true catalytic species”.<sup>1n</sup>

However, as mentioned above, high temperatures and long reaction times are often required to obtain good yields in SM cross-coupling. If one hypothesizes that somewhat extreme conditions may be necessary in order for a particular palladium(0) catalyst species to be formed in significant concentrations, then an efficient method to produce PdL<sub>2</sub> unambiguously would permit an accurate assessment of the relative merits of various phosphines in the overall catalytic cycle. It might also result in the realization of much milder reaction conditions for cross-coupling reactions involving otherwise poorly reducible palladium(II) precatalysts.

#### **1.4.1 Optimization of PdL<sub>2</sub> Generation**

In order to assess the true relevance of compounds of the type PdL<sub>1,2,3</sub> in cross-coupling protocols, this work initiates a study in which compounds of the specific stoichiometry PdL<sub>2</sub> are generated quantitatively and unambiguously. The

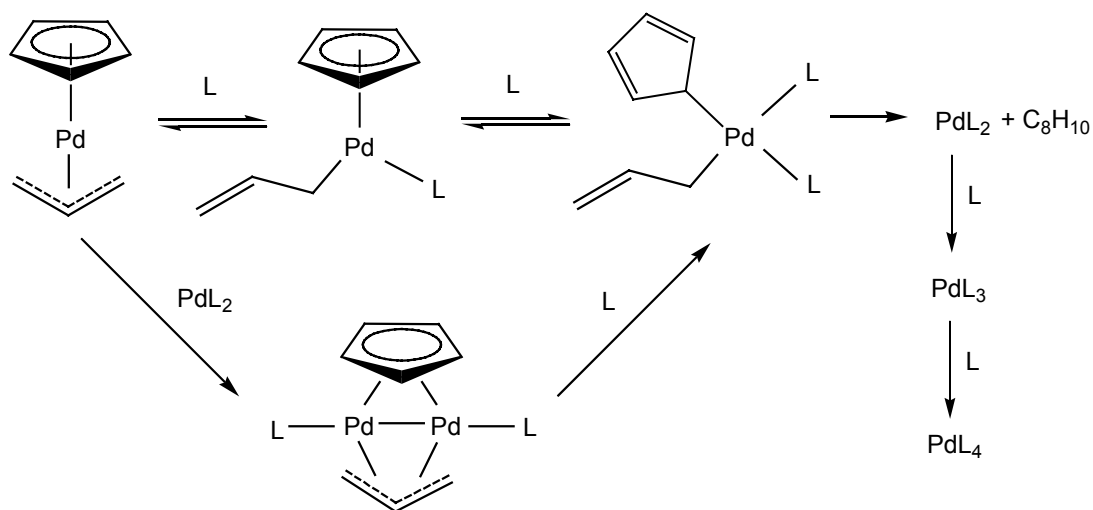
method chosen utilizes  $\text{Pd}(\eta^3\text{-C}_3\text{H}_5)(\eta^5\text{-C}_5\text{H}_5)^{52}$ , which can be prepared according to the method of Otsuka from  $[\text{PdCl}(\eta^3\text{-C}_3\text{H}_5)]_2^{52}$  (Scheme 30).



Scheme 30. Generation of  $[\text{PdCl}(\eta^3\text{-C}_3\text{H}_5)]_2$  and  $\text{Pd}(\eta^3\text{-C}_3\text{H}_5)(\eta^5\text{-C}_5\text{H}_5)^{52}$

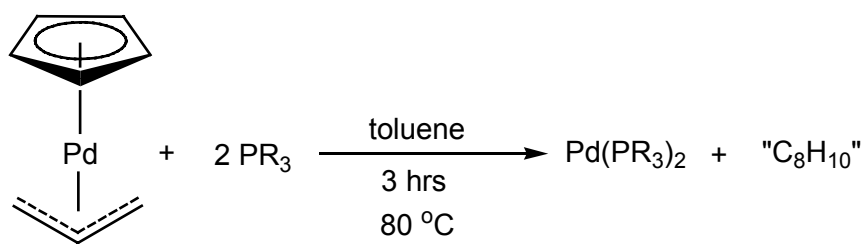
Upon heating in the absence of potential ligands,  $\text{Pd}(\eta^3\text{-C}_3\text{H}_5)(\eta^5\text{-C}_5\text{H}_5)^{52}$  reductively eliminates  $\text{C}_5\text{H}_5\text{-C}_3\text{H}_5$  to deposit palladium metal.<sup>53</sup> There is a fairly complex chemical behaviour associated with  $\text{Pd}(\eta^3\text{-C}_3\text{H}_5)(\eta^5\text{-C}_5\text{H}_5)$ , as it is known to react with phosphines L to produce  $\eta^1$  intermediates depending upon the nature of L.<sup>54</sup> Furthermore, precedence exists for the generation of intermediate dinuclear species of the type  $\text{Pd}_2\text{L}_2(\mu\text{-Cp})(\mu\text{-allyl})$ .<sup>54</sup> Reductive elimination of  $\text{C}_5\text{H}_5\text{-C}_3\text{H}_5$  produces the anticipated palladium(0) complexes of the types  $\text{PdL}_n$  ( $n = 2\text{-}4$ ).<sup>33c,45a,55</sup> The system has been studied at great length by Werner *et al.*<sup>54</sup> and the accepted pathway to  $\text{PdL}_2$  by this route is shown in Scheme 31.





Scheme 31. Pathway for reaction of  $\text{Pd}(\eta^3\text{-C}_3\text{H}_5)(\eta^5\text{-C}_5\text{H}_5)$  with phosphine.<sup>54</sup>

$\text{Pd}(\eta^3\text{-C}_3\text{H}_5)(\eta^5\text{-C}_5\text{H}_5)$  has been used previously as described above to generate palladium(0) cross-coupling catalysts.<sup>33c,45a,53</sup> Bisphosphinepalladium(0) complexes in this work are isolated from  $\text{Pd}(\eta^3\text{-C}_3\text{H}_5)(\eta^5\text{-C}_5\text{H}_5)$  (Scheme 32).<sup>52</sup>



Scheme 32. Isolation of  $\text{Pd}(\text{PR}_3)_2$  from  $\text{Pd}(\eta^3\text{-C}_3\text{H}_5)(\eta^5\text{-C}_5\text{H}_5)$ .<sup>52</sup>

However, a description of the minimum reaction conditions required to obtain compounds of the type  $\text{PdL}_2$  has not been provided in the literature. The goal of this work is to determine the optimum conditions under which the

catalytically very important<sup>1a,b,g,h</sup> compounds PdL<sub>2</sub> (L = PCy<sub>3</sub>, PMeBu<sup>t</sup><sub>2</sub>, PBu<sup>t</sup><sub>3</sub>)<sup>33</sup> are generated from Pd(η<sup>3</sup>-C<sub>3</sub>H<sub>5</sub>)(η<sup>5</sup>-C<sub>5</sub>H<sub>5</sub>) cleanly (i.e. without the presence of the aforementioned intermediates) and essentially quantitatively. It is anticipated that the minimum temperature and maximum time required to generate these species from Pd(η<sup>3</sup>-C<sub>3</sub>H<sub>5</sub>)(η<sup>5</sup>-C<sub>5</sub>H<sub>5</sub>) is often exceeded in literature examples.

In addition, the feasibility of PdL<sub>2</sub> generation from Pd(η<sup>3</sup>-1-Ph-C<sub>3</sub>H<sub>4</sub>)(η<sup>5</sup>-C<sub>5</sub>H<sub>5</sub>)<sup>56</sup> will be assessed (Figure 7). This precursor is conveniently generated from [PdCl(η<sup>3</sup>-1-Ph-C<sub>3</sub>H<sub>4</sub>)]<sub>2</sub><sup>57</sup> and provides a substantial advantage to the Pd(η<sup>3</sup>-C<sub>3</sub>H<sub>5</sub>)(η<sup>5</sup>-C<sub>5</sub>H<sub>5</sub>) route to PdL<sub>2</sub>, as Pd(η<sup>3</sup>-1-Ph-C<sub>3</sub>H<sub>4</sub>)(η<sup>5</sup>-C<sub>5</sub>H<sub>5</sub>) is less volatile and more thermally stable than Pd(η<sup>3</sup>-C<sub>3</sub>H<sub>5</sub>)(η<sup>5</sup>-C<sub>5</sub>H<sub>5</sub>). The reactivity of Pd(η<sup>3</sup>-1-Ph-C<sub>3</sub>H<sub>4</sub>)(η<sup>5</sup>-C<sub>5</sub>H<sub>5</sub>) with a variety of L and the related route to PdL<sub>2</sub> will be described.

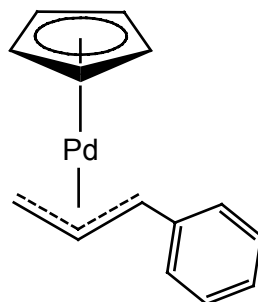


Figure 7. Alternate precursor Pd(η<sup>3</sup>-1-Ph-C<sub>3</sub>H<sub>4</sub>)(η<sup>5</sup>-C<sub>5</sub>H<sub>5</sub>).<sup>56</sup>

#### 1.4.2 Assessment of the Relevance of Species of the Type PdL<sub>1,2,3</sub>

As noted above, should reduction of a chosen Pd(II) precursor by a phosphine be incomplete, such that the ratio of L: Pd(0) >>1, one can predict that the major catalytic species in solution could be predominantly of the type PdL<sub>3,4</sub>.

One must therefore be cognizant of situations in which these more highly substituted species are present, as they can conceivably affect the oxidative addition step. The conditions under which 3:1 compounds  $\text{PdL}_3$  ( $\text{L} = \text{PCy}_3$ ,  $\text{PMeBu}^t_2$ ) may exist in equilibrium with the isolated 2:1 species  $\text{PdL}_2$  will be defined in this work, as well as the thermodynamic parameters for the dissociation of  $\text{PdL}_3$  by variable temperature  $^{31}\text{P}$  NMR spectroscopy. These parameters will allow the assessment of the concentration and subsequent relevance of catalytically inactive species, such as  $\text{PdL}_3$ .

### 1.4.3 Kinetics of Oxidative Addition with $\text{Pd}(\text{PCy}_3)_2$

As mentioned previously, the extent to which the “innocent” anions (e.g.  $\text{OAc}^-$ ,  $\text{Cl}^-$ ,  $\text{Br}^-$ ), introduced via precatalysts, may coordinate to species of the type  $\text{PdL}_2$  is not generally known. However, many probably do and can be expected to influence the rates of oxidative addition. In any case, the mechanism shown in Figure 1 and referred to recently as the “consensus” or “text book” mechanism,<sup>50h</sup> probably does not apply when anions are present. This work initiates a kinetic study of the oxidative addition of  $\text{PhBr}$  to  $\text{Pd}(\text{PCy}_3)_2$  in toluene and assesses the effect of added bromide, as the toluene soluble tetraoctylphosphonium bromide salt (TOPB). In addition, the effect of added  $\text{PCy}_3$  on oxidative addition is also assessed.

#### 1.4.4 Studies in Transmetallation and Reduction of Pd(II)

It was noted above that few research efforts have been focused on the process of transmetallation in the context of catalyzed coupling reactions. A minor objective of this work was to initiate new methods to study the process of transmetallation and establish a simple, efficient protocol using gas chromatography. The product of oxidative addition of Pd(PCy<sub>3</sub>)<sub>2</sub> and bromobenzene, *trans*-Pd(PCy<sub>3</sub>)<sub>2</sub>(Ph)(Br), was chosen as the palladium species, while the organotrifluoroborate salt K[PhBF<sub>3</sub>] was selected as the boron containing reagent for examination. It is anticipated that GC analysis will allow a simple method with which to assess the effects of a wide variety of reaction conditions (temperature, solvent, base) on the transmetallation of *trans*-Pd(PCy<sub>3</sub>)<sub>2</sub>(Ph)(Br) and K[PhBF<sub>3</sub>]. Furthermore, it is anticipated that GC analysis will allow for a facile kinetic study of transmetallation between the chosen reagents.

It was also of interest to initiate transmetallation studies by means of multinuclear NMR spectroscopy. As kinetic studies of this kind require an easily monitored internal standard for integration purposes, it was desirable to utilize a borate salt as a coupling partner whose cation also possessed an easily monitored, NMR active nucleus. Tetraoctylphosphonium phenyltrifluoroborate, [TOP][PhBF<sub>3</sub>] is thus an ideal coupling partner for such studies, as TOP<sup>+</sup> can serve as internal standard for kinetic analysis by <sup>31</sup>P NMR, while also increasing the solubility of the borate salts in organic solvents. This phosphonium salt has not been reported in the literature and its preparation will be attempted by the

method of counter ion exchange using tetraoctylphosphonium bromide and  $K[PhBF_3]$ .

While significant work has addressed the nature of species resulting from the reduction of Pd(II) precursors to active Pd(0) species, few efforts have been made to examine the mode of reduction in the greater context of an actual SM reaction protocol. Given the wide variety of conditions for successful SM coupling, any meaningful study of the reduction of Pd(II) precatalysts should be performed in the presence of several different reaction components, including base and solvents appropriate for coupling. In this work, an assessment of the effect of the boron containing reagent ( $PhB(OH)_2$  and  $K[PhBF_3]$ ) on reduction of  $PdL_2Cl_2$  ( $L = Cy_3, PMeBu^t_2$ ) is undertaken. In the instance where  $PhB(OH)_2$  is used, the effect of added aqueous base ( $K_2CO_3$ ) will also be assessed.

## 1.5 References

1. For recent reviews, see (a) Littke, A. F.; Fu, G. C. *Angew. Chem., Int. Ed.* **2002**, *41*, 4177. (b) Kotha, S.; Lahiri, K.; Kashinath *Tetrahedron* **2002**, *58*, 9633. (c) *Handbook of Organopalladium Chemistry for Organic Synthesis*; Negishi, E., de Meijere, Eds.; Wiley: New York and Chichester, U.K., 2002. (d) Miyaura, N. *Top. Curr. Chem.* **2002**, *219*, 11. (e) Beletskaya, I. P.; Cheprakov, A. V. In *Comprehensive Coordination Chemistry II*; McCleverty, J. A.; Meyer, T. J., Eds.; Elsevier: Oxford, U.K., 2004; Vol. 9, 305-368. (f) Hassan, J.; Sévignon, M.; Gozzi, C.; Schulz, E.; Lemaire, M. *Chem. Rev.* **2002**, *102*, 1359. (g) Farina, V. *Adv. Synth. Catal.* **2004**, *346*, 1553. (h) Bellina, F.; Carpita, A.; Rossi, R. *Synthesis* **2004**, 2419. (i) Tsuji, J. *Palladium Reagents and Catalysts*; 2<sup>nd</sup> ed.; Wiley, New York, 2004. (j) Cepanec, I. *Synthesis of Biaryls*; Elsevier: Amsterdam, 2004. (k) Zapf, A.; Beller, M. *Chem. Commun.* **2005**, 431. (l) Miyaura, N., *Metal Catalyzed Cross-Coupling Reactions*; 2<sup>nd</sup> ed'n., de Meijere, A., Diederich, F., Eds.; John Wiley & Sons: New York, 2004, pp. 41-123. (m) Christmann, U.; Vilar, R. *Angew. Chem., Int. Ed.* **2005**, *44*, 366, and references therein. (n) Phan, N. T. S.; Van Der Sluys, M.; Jones, C. W. *Adv. Synth. Catal.* **2006**, *348*, 609. (o) Echavarren, A. M.; Cardenas, D. J. *Metal Catalyzed Cross-Coupling Reactions*; 2<sup>nd</sup> ed'n., de Meijere, A., Diederich, F., Eds.; John Wiley & Sons: New York, 2004, pp. 1-31. (p) Tamao, K.; Miyaura, N. *Top. Curr. Chem.* **2002**, *219*, 1.

2. (a) Jiang, L.; Buchwald, S. L. *Metal Catalyzed Cross-Coupling Reactions*; 2<sup>nd</sup> ed'n., de Meijere, A., Diederich, F., Eds.; John Wiley & Sons: New York, 2004, pp. 699-756. (b) Hartwig, J. F.; *Handbook of Organopalladium Chemistry for Organic Synthesis*; Negishi, E., de Meijere, Eds.; Wiley: New York and Chichester, U.K., **2002**, 1051-1096. (c) Muci, A. R., Buchwald, S. L. *Top. Curr. Chem.* **2002**, 219, 133. (d) Baranano, D.; Mann, G.; Hartwig, J. F. *Curr. Org. Chem.* **1997**, 1, 287-305.
3. Negishi, E. *J. Organomet. Chem.* **2002**, 653, 34.
4. Carey, F. A.; Sundberg, C. *Advanced Organic Chemistry Part B: Reactions and Synthesis*. 3<sup>rd</sup> Ed. Plenum Press: New York and London, **1990**.
5. (a) Corriu, R. J. P.; Masse, J. P. *J. Chem. Soc., Chem. Comm.*, **1972**, 144. (b) Tamao, K.; Sumitani, K.; Kumada, M. *J. Am. Chem. Soc.* **1972**, 94, 4374.
6. Murahashi, S. *J. Organomet. Chem.* **2002**, 653, 27.
7. Yamamura, M.; Moritani, I.; Murahashi, S. *J. Organomet. Chem.* **1975**, 91, C39.
8. (a) Baba, S.; Negishi, E. *J. Chem. Soc., Chem. Comm.* **1976**, 596b. (b) Okukado, N.; King, A. O.; Negishi, E. *J. Org. Chem.* **1977**, 42, 1821. (c) Van Horn, D. E.; Negishi, E. *J. Am. Chem. Soc.* **1977**, 3168.

9. (a) Kosugi, M.; Shimizu, Y.; Migita, T. *J. Organomet. Chem.* **1977**, 129, C36. (b) Kosugi, M.; Shimizu, Y.; Migita, T. *Chem. Lett.* **1977**, 1423. (c) Kosugi, M.; Sasazawa, K.; Shimizu, Y.; Migita, T. *Chem. Lett.* **1977**, 301.
10. Milstein, D.; Stille, J. K. *J. Am. Chem. Soc.* **1978**, 100, 3636.
11. Stille, J. K. *Angew. Chem. Int. Ed.* **1986**, 25, 508.
12. Miyaura, N.; Suzuki, A. *Chem. Rev.* **1995**, 95, 2457.
13. (a) Chemler, S. R.; Trauner, D.; Danishefsky, S. J. *Angew. Chem. Int. Ed.* **2001**, 40, 4544. (b) Cárdenas, D. J. *Angew. Chem. Int. Ed.* **2003**, 44, 384. (c) Frisch, A. C.; Beller, M. *Angew. Chem. Int. Ed.* **2005**, 44, 674. (d) Cárdenas, D. J. *Angew. Chem. Int. Ed.* **1999**, 38, 3018.
14. (a) Suzuki, A. *J. Organomet. Chem.* **1999**, 576, 147. (b) Bellina, F.; Carpita, A.; Rossi, R. *Synthesis*, **2004**, 2419.
15. (a) Knowles, J. P.; Whiting, A. *Org. Biomol. Chem.* **2007**, 5, 31. (b) Espinet, P.; Echavarren, A. M. *Angew. Chem. Int. Ed.* **2004**, 43, 4704.
16. Fitton, P.; Rick, E. A. *J. Organomet. Chem.* **1971**, 28, 287.
17. Fauvarque, J-F.; Pflüger, F.; Troupel, M. *J. Organomet. Chem.* **1981**, 208, 419.
18. Pflüger, F.; Amatore, C. *Organometallics* **1990**, 9, 2276.
19. Casado, A. L.; Espinet, P. *Organometallics* **1998**, 17, 954.
20. Fitton, P.; Johnson, M. P.; McKeon, J. E. *Chem. Comm.* **1968**, 6.
21. Urata, H.; Tanaka, M.; Fuchikami, T. *Chem. Lett.* **1987**, 751.
22. Beller, M.; Riermeier, T. H. *Eur. J. Inorg. Chem.* **1998**, 29.
23. Miyaura, N. *J. Organomet. Chem.* **2002**, 653, 54.



24. Matos, K.; Soderquist, J. A. *J. Org. Chem.* **1998**, *63*, 461.
25. (a) Yamamoto, A. *Organotransition Metal Chemistry Fundamental Concepts and Applications*. John Wiley and Sons, New York: 1986. (b) Crabtree, R. H. *The Organometallic Chemistry of the Transition Metals*. John Wiley and Sons, New York: 1988.
26. Gillie, A.; Stille, J. K. *J. Am. Chem. Soc.* **1980**, *102*, 4933.
27. Ozawa, F.; Yamamoto, A. *Nippon Kagaku Kaishi*, **1987**, *5*, 773.
28. Tatsumi, K.; Hoffmann, R.; Yamamoto, A.; Stille, J. K. *Bull. Chem. Soc. Jpn.* **1981**, *54*, 1857.
29. Hartwig, J. F. *Inorg. Chem.* **2007**, *46*, 1936.
30. Low, J. J.; Goddard, W. A., III. *J. Am. Chem. Soc.* **1986**, *108*, 6115.
31. Low, J. J.; Goddard, W. A., III. *J. Am. Chem. Soc.* **1984**, *106*, 6928.
32. (a) Takahashi, Y.; Ito, T.; Sakai, S.; Ishii, Y. *J. Chem. Soc. D.* **1970**, 1065. (b) Ukai, T.; Kawazura, H.; Ishii, Y.; Bonnet, J. J.; Ibers, J. A. *J. Organomet. Chem.* **1974**, *65*, 253. (c) Ito, T.; Hasegawa, S.; Takahashi, Y.; Ishii, Y. *J. Organomet. Chem.* **1974**, *73*, 401. (d) Ishii, Y.; Hasegawa, S.; Kimura, S.; Itoh, K. *J. Organomet. Chem.* **1974**, *73*, 411. (e) Rettig, M. F.; Maitlis, P. NM. *Inorg. Synth.* **1990**, *28*, 110.
33. (a) Immirzi, A.; Musco, A. *J. C. S. Chem. Comm.* **1974**, 400. (b) Mann, B. E.; Musco, A. *J. C. S. Dalton* **1975**, 1673. (c) Otsuka, S.; Yoshida, T.; Nakatsu, K. *J. Am. Chem. Soc.* **1976**, *98*, 5850. (d) Yoshida, T.; Otsuka, S. *Inorg. Synth.* **1990**, *28*, 113. (e) Krause, J.; Bonrath, W.; Porschke, K. R. *Organometallics* **1992**, *11*, 1158. (f) Tanaka, M. *Acta Cryst. C* **1992**, *48*,

739. (g) Kirchoff, J. H.; Netherton, M. R.; Hills, I. D.; Fu, G. C. *J. Am. Chem. Soc.* **2002**, *124*, 13662.
34. Glorius, F. *Top. Organomet. Chem.* 2007, *21*, 1.
35. (a) Stefani, V.; Cella, R.; Vieira, A. S. *Tetrahedron*, **2007**, *63*, 3623. (b) Darses, S.; Genet, J-P. *Eur. J. Inor. Chem.* **2003**, 4313. (c) Molander, G. A.; Ellis, N. *Acc. Chem. Res.* **2007**, *40*, 275. (d) Molander, G. A.; Figueroa, R. *AldrichimicaActa*, **2005**, *38*, 49. (e) Batey, R. A.; Quach, T. D. *Tet. Lett.* **2001**, *42*, 9099. (f) Wong, K.; Chien, Y.; Liao, Y.; Lin, C.; Chou, M.; Leung, M. *J. Org. Chem.* **2002**, *67*, 1041.
36. Trost, B. M. *Science*, **1991**, *254*, 1471.
37. Littke, A. F.; Fu, G. C. *Angew. Chem. Int. Ed.* **2002**, *41*, 4176.
38. Grushin, V. V.; Alper, H. *Chem. Rev.* **1994**, *94*, 1047.
39. Hegedus, L. S. *Organopalladium Chemistry in Organometallics in Synthesis: a Manual.*, 2<sup>nd</sup> ed., Schlosser, M. ed. John Wiley and Sons, New York, 2002, 1123-1217.
40. For background references information on Pd(0) chemistry in general, see (a) Kudo, K.; Hidai, M.; Uchida, Y. *J. Organomet. Chem.* **1971**, *33*, 393. (b) Kudo, K.; Sato, M.; Hadai, M.; Uchida, Y. *Bull. Chem. Soc. Jap.* **1973**, *46*, 2820. (c) Minematsu, H.; Nonaka, Y.; Takahashi, S.; Hagihara, N. *J. Organomet. Chem.* **1973**, *59*, 395. (d) Mednikov, E. G.; Eremenko, N. K. *Izv. Akad. Nauk SSSR*, **1984**, 2781. (e) Otsuka, S.; Yoshida, T.; Nakatsu, K. *J. Am. Chem. Soc.* **1976**, *98*, 5850. (f) Yoshida, T.; Otsuka, S. *J. Am. Chem. Soc.* **1977**, *99*, 2134. (g) Ozawa, F.; Ito, T.; Nakamura, Y.;

- Yamamoto, A. *J. Organomet. Chem.* **1979**, 168, 375. (h) Negishi, E-I.; Takahashi, T.; Akiyoshi, K. *J. Chem. Soc., Chem. Commun.* **1986**, 1338. (i) Urata, H.; Suzuki, H.; Moro-oka, Y.; Ikawa, T. *J. Organomet. Chem.* **1989**, 364, 235. (j) Krause, J.; Bonrath, W.; Porschke, K. R. *Organometallics* **1992**, 11, 1158. 739. (k) Amatore, C.; Jutand, A.; Meyer, G. *Inorg. Chim. Acta* **1998**, 273, 76. (l) Kuran, W.; Musco, A. *Inorg. Chim. Acta* **1975**, 12, 187.
41. Musco, A.; Kuran, W.; Silvani, A.; Anker, M. W. *J. Chem. Soc., Chem. Comm.* **1973**, 938.
42. Amatore, C.; Jutand, A. *J. Organomet. Chem.* **1999**, 576, 254.
43. a) Amatore, C.; Jutand, A.; Khalil, F.; M'Barki, M. A.; Mottier, L. *Organometallics*, **1993**, 12, 3168. b) Amatore, C.; Broeker, G.; Jutand, A.; Khalil, F. *J. Am. Chem. Soc.*, **1997**, 119, 5176.
44. (a) Jutand, A.; Hii, K. K.; Thornton-Pett, M.; Brown, J. M. *Organometallics* **1999**, 18, 5367. (b) Amatore, C.; Carré, E.; Jutand, A.; Medjour, Y. *Organometallics* **2002**, 21, 4540. (c) Amatore, C.; Bensalem, S.; Ghalem, S.; Jutand, A.; Medjour, Y. *Eur. J. Org. Chem.* **2004**, 366. (d) Fairlamb, I. J. S.; Kapdi, A. R.; Lee, A. F. *Org. Lett.* **2004**, 6, 4435. (e) Macé, Y.; Kapdi, A. R.; Fairlamb, I. J. S.; Jutand, A. *Organometallics* **2006**, 25, 1795. (f) Amatore, C.; Jutand, A. *Coord. Chem. Rev.* **1998**, 178-180, 511. (g) Shekhar, S.; Ryberg, P.; Hartwig, J. F.; Mathew, J. S.; Blackmond, D. G.; Strieter, E. R.; Buchwald, S. L. *J. Am. Chem. Soc.* **2006**, 128, 3584. (h) Paul, F.; Patt, J.; Hartwig, J. F. *Organometallics* **1995**, 14, 3030.

45. (a) Galardon, E.; Ramdeehul, S.; Brown, J. M.; Cowley, A.; Hii, K. K.; Jutand, A. *Angew. Chem., Int. Ed.* **2002**, *41*, 1760. (b) Barrios-Landeros, F.; Hartwig, J. H. *J. Am. Chem. Soc.* **2005**, *127*, 6944. (c) Stambuli, J. P.; Buhl, M.; Hartwig, J. F. *J. Am. Chem. Soc.* **2002**, *124*, 9346. (d) Walker, S. D.; Barder, T. E.; Martinelli, J. R.; Buchwald, S. L. *Angew. Chem., Int. Ed.* **2004**, *43*, 1871. (e) Barder, T. E.; Walker, S. D.; Martinelli, J. R.; Buchwald, S. L. *J. Am. Chem. Soc.* **2005**, *127*, 4685. (f) Chang, Y.-C.; Lee, J.-C.; Hong, F.-E. *Organometallics* **2005**, *24*, 5686. (g) Hartwig, J. F.; Paul, F. *J. Am. Chem. Soc.* **1995**, *117*, 5373. (h) Littke, A. F.; Fu, G. C. *Angew. Chem., Int. Ed.* **1998**, *37*, 3387. (i) Littke, A. F.; Dai, C.; Fu, G. C. *J. Am. Chem. Soc.* **2000**, *122*, 4020. (j) Littke, A. F.; Fu, G. C. *J. Am. Chem. Soc.* **2001**, *123*, 6989. (k) Stambuli, J. P.; Kuwano, R.; Hartwig, J. F. *Angew. Chem., Int. Ed.* **2002**, *41*, 4746. (l) Prashad, M.; Mak, X. Y.; Liu, Y.; Repič, O. *J. Org. Chem.* **2003**, *68*, 1163. (m) Barder, T. E.; Biscoe, M. R.; Buchwald, S. L. *Organometallics* **2007**, *26*, 2183-2192. For a recent theoretical treatment, see (n) Ahlquist, M.; Fristrup, P.; Tanner, D.; Norrby, P.-O. *Organometallics* **2006**, *25*, 2066.
46. Beller, M.; Zapf, A.; Andreu, M. C. *Chem. Comm.* **2000**, 2475-2476.
47. (a) Amatore, C.; Carré, E.; Jutand, A.; M'Barki, M. A. *Organometallics*, **1995**, *14*, 1818. (b) Amatore, C.; Jutand, A.; Lemaître, F.; Richard, J. L.; Kozuch, S.; Shaik, S. *J. Organomet. Chem.* **2004**, *689*, 3728.
48. Mandai, T.; Matsumoto, T.; Tsuji, J. *Tet. Lett.* **1993**, *34*, 2513.
49. Tolman, C. A. *Chem. Rev.* **1977**, *77*, 313.

50. (a) Amatore, C.; Carré, E.; Jutand, A.; M'Barki, M. A.; Meyer, G. *Organometallics* **1995**, *14*, 5605. (b) Amatore, C.; Jutand, A.; Lemaître, F.; Ricard, J. L.; Kozuch, S.; Shaik, S. *J. Organomet. Chem.* **2004**, *689*, 3728. (c) Amatore, C.; Jutand, A.; Suarez, A. *J. Am. Chem. Soc.* **1993**, *115*, 9531. (d) Amatore, C.; Jutand, A. *Acc. Chem. Res.* **2000**, *33*, 314. (e) Jutand, A. *Appl. Organomet. Chem.* **2004**, *18*, 574. (f) Kozuch, S.; Shaik, S.; Jutand, A.; Amatore, C. *Chem. Eur. J.* **2004**, *10*, 3072. (g) Goossen, L. J.; Koley, D.; Hermann, H. L.; Thiel, W. *Organometallics* **2005**, *24*, 2398. (h) Kozuch, S.; Amatore, C.; Jutand, A.; Shaik, S. *Organometallics* **2005**, *24*, 2319.
51. Amatore, C.; Azzabi, M.; Jutand, A. *J. Am. Chem. Soc.* **1991**, *113*, 8375
52. Tatsuno, Y.; Yoshida, T.; Otsuka, S. *Inorg. Synth.* **1990**, *28*, 342.
53. (a) Liang, C.; Soltani-Ahmadi, H.; Fischer, R. A.; Muhler, M. *Chem. Comm.* **2005**, 282. (b) Niklewski, A.; Strunskus, T.; Witte, G.; Wöll, C. *Chem. Mater.* **2005**, *17*, 861. (c) Xia, W.; Schlüter, O. F.-K.; Liang, C.; van den Berg, M. W.E.; Guraya, M.; Muhler, M. *Catal. Today* **2005**, *102-103*, 34.
54. (a) Werner, H.; Kühn, A.; Tune, D. *J. Chem. Ber.* **1977**, *110*, 1763. (b) Kühn, A.; Werner, H. *J. Organomet. Chem.* **1979**, *179*, 421. (c) Werner, H.; Kühn, A.; Burschka, C. *Chem. Ber.* **1980**, *113*, 2291. (d) Werner, H. *Angew. Chem. Int. Ed.* **1977**, *16*, 1.
55. a) Matsumoto, M.; Yoshioka, H.; Nakatsu, K.; Yoshida, T.; Otsuka, S. *J. Am. Chem. Soc.* **1974**, *96*, 3322. (b) Yoshida, T.; Otsuka, S. *Inorg. Synth.*

**1990**, 28, 113. (c) Kirchoff, J. H.; Netherton, M. R.; Hills, I. D.; Fu, G. C. *J. Am. Chem. Soc.* **2002**, 124, 13662. (d) Leoni, P. *Organometallics* **1993**, 12, 2432. (e) Stauffer, S. R.; Beare, N. A.; Stambuli, J. P.; Hartwig, J. H. *J. Am. Chem. Soc.* **2001**, 123, 4641. (f) Matsumoto, T.; Kasai, T.; Tatsumi, K. *Chem. Lett.* **2002**, 346.

56. Murrall, N. W.; Welch, A. J. *J. Organomet. Chem.* **1986**, 301, 109.

57. Auburn, P. R.; Mackenzie, P. B.; Bosnich, B. *J. Am. Chem. Soc.* **1985**, 107, 2033.

## Chapter 2

### Experimental

#### 2.1 Physical Methods

When indicated, syntheses were carried out under a dry, deoxygenated argon atmosphere using standard Schlenk line techniques. Argon was deoxygenated by passage through a heated column of BASF copper catalyst, and then dried by passing through a column of 4 Å molecular sieves. Handling and storage of air-sensitive organometallic compounds were done in an MBraun Labmaster glove box. Solvents (anhydrous THF, hexanes and toluene) were stored in 18 L containers packaged under nitrogen; they were dried by passage through columns of activated alumina (Innovative Technology Solvent Purification System) and stored over 4 Å molecular sieves. Methanol (MeOH) was dried over magnesium and iodine under argon .

NMR spectra were recorded using Bruker AV 300 ( $^{31}\text{P}$ : 121.5 MHz,  $^{13}\text{C}$ : 75.4 MHz), AV 400 ( $^{31}\text{P}$ : 163.0 MHz,  $^{13}\text{C}$ : 100.6 MHz), AV 500 ( $^{31}\text{P}$ : 202.3 MHz,  $^{13}\text{C}$ : 125.7 MHz) and AV 600 ( $^{31}\text{P}$ : 242.9 MHz,  $^{13}\text{C}$ : 150.9 MHz) spectrometers.  $^{31}\text{P}$  NMR spectra were referenced with respect to external 85%  $\text{H}_3\text{PO}_4$ , while  $^1\text{H}$  and  $^{13}\text{C}$  NMR spectra were referenced to TMS via the residual protons signals of the deuterated solvents. All chemical shifts are reported on the  $\delta$  (ppm) scale with positive values referring to chemical shifts downfield from 0 ppm.

GC analysis was conducted on a Varian 3900 GC equipped with a CP-8400 autosampler, a CP-1177 injector, an FID detector and a Varian WCOT Fused Silica column (CP-Sil 8CB, 25 m x 0.32 mm ID, DF = 0.52).

## 2.2 Chemical Supplies

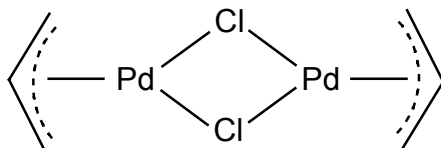
All supplies were purchased from Aldrich and used without further purification, with the following exceptions. Bromobenzene (PhBr) was distilled from sodium under argon and stored over 4 Å molecular sieves prior to use. Allyl chloride, (1-bromo)ethylbenzene and chlorobenzene were degassed and stored over 4 Å molecular sieves prior to use. Toluene-d<sub>8</sub>, benzene-d<sub>6</sub> and 1,1,2,2-tetrachloroethane-d<sub>2</sub> (TCE) (Cambridge Isotope Laboratories, Inc. or CDN Isotopes) were degassed under vacuum and dried by passage through a small column of activated alumina before being stored over 4 Å molecular sieves. PdCl<sub>2</sub> was obtained on loan courtesy of Johnson Matthey. The phosphines PCy<sub>3</sub>, PMeBu<sup>t</sup><sub>2</sub> and PBu<sup>t</sup><sub>3</sub> were obtained from Strem, while PMe<sub>3</sub> was obtained from Aldrich, and all were used without further purification. Potassium phenyltrifluoroborate (K[C<sub>6</sub>H<sub>5</sub>BF<sub>3</sub>]) and phenylboronic acid (PhB(OH)<sub>2</sub>) were dried at 25 °C under vacuum for 16 hours. Tetraoctylphosphonium bromide (TOPB) and tetrabutylammonium bromide (TBAB) were dried for 16 hours under vacuum at 45 °C and 110 °C respectively prior to use. PPh<sub>3</sub> was recrystallized from dry and deoxygenated MeOH. Sodium cyclopentadienide (NaCp) was prepared according to methods reported in the literature by Panda *et al.*<sup>1</sup>



## 2.3 Preparation of Palladium Compounds

### 2.3.1 Preparation of $[\text{PdCl}(\eta^3\text{-C}_3\text{H}_5)]_2$

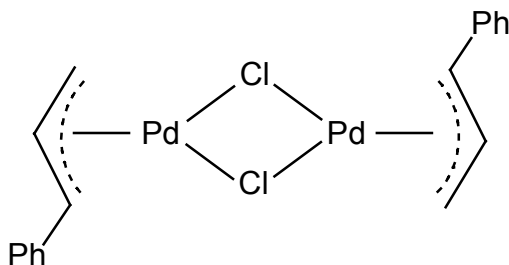
The following compound was prepared based on the method described by Tatsuno *et al.*<sup>2</sup>



$\text{PdCl}_2$  (2.19 g, 12.5 mmol) and  $\text{NaCl}$  (1.52 g, 26.0 mmol) were placed in a one neck 100 mL round bottom flask and dissolved in a mixture of distilled water (5 mL) and  $\text{MeOH}$  (35 mL). The resulting red-brown solution was allowed to stir for 16 hours at 25 °C. 3-chloro-1-propene (3.4 mL, 42 mmol) was then added by needle to the stirring palladium solution.  $\text{CO}_{(g)}$  was bubbled through the solution through a syringe at an approximate rate of 4  $\text{cm}^3/\text{s}$ . Within 15 minutes the red-brown solution became yellow, and the  $\text{CO}_{(g)}$  flow was continued for one hour. The yellow water/ $\text{MeOH}$  solution was then added to distilled water (100 mL) and extracted with three 20 mL portions of  $\text{CHCl}_3$ . The  $\text{CHCl}_3$  extracts were collected and washed with three 20 mL portions of distilled water. The  $\text{CHCl}_3$  layer was then dried with  $\text{MgSO}_4$  and  $\text{CHCl}_3$  was then removed under vacuum to yield a yellow powder. Yield: 1.80 g, 79 %.  $^1\text{H}$  NMR ( $\text{CDCl}_3$ , 400 MHz):  $\delta$  3.03 (d,  $J$  = 12.1 Hz, 2H), 4.10 (d,  $J$  = 6.7 Hz, 2H), 5.45 (tt,  $J$  = 6.6 Hz, 12.1 Hz, 1H).  $^{13}\text{C}$  NMR ( $\text{CDCl}_3$ , 100.6 MHz):  $\delta$  62.9 ( $\text{CH}_2$ ), 111.1 (CH). Lit.<sup>2</sup>  $^1\text{H}$  NMR ( $\text{CDCl}_3$ )  $\delta$  3.03 (d,  $J$  = 12.0 Hz, anti  $\text{CH}_2$ ), 4.10 (d,  $J$  = 7.1 Hz, syn  $\text{CH}_2$ ), 5.48 (CH, t).

### 2.3.2 Preparation of $[\text{PdCl}(\eta^3\text{-1-Ph-C}_3\text{H}_4)]_2$

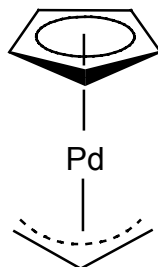
The following compound was prepared according to the method described by Auburn *et al.*<sup>3</sup>



A solution of cinnamyl chloride ( $\text{PhCH}=\text{CHCH}_2\text{Cl}$ ) (1.6 mL, 9.6 mmol) in 95 % ethanol (6 mL) was added to a stirring solution of  $\text{PdCl}_2$  (0.5 g, 3 mmol) and  $\text{LiCl}$  (0.5 g, 12 mmol) in warm distilled water (0.7 mL).  $\text{CO}_{(\text{g})}$  was bubbled through the resulting solution at 25 °C and, within 15 minutes, an oily orange solid was formed. After three hours the  $\text{CO}_{(\text{g})}$  flow was stopped and the solution was allowed to stir under an atmosphere of carbon monoxide for 20 hours. The resulting product was filtered and washed with MeOH (5 mL) and ether (5 mL). The product was then recrystallized from chloroform and ether, yielding an orange crystalline solid. Yield: 0.641 g, 88 %.  $^1\text{H NMR}$  ( $\text{CDCl}_3$ , 400 MHz):  $\delta$  3.04 (d,  $J = 12.1$  Hz, 1H), 3.97 (d,  $J = 6.8$  Hz, 1H), 4.63 (d,  $J = 11.4$  Hz, 1H), 5.80 (ddd,  $J = 6.5$  Hz, 11.6 Hz, 11.9 Hz, 1H), 7.27 (t,  $J = 7.8$  Hz, 2H), 7.35 (t,  $J = 7.3$  Hz, 1H), 7.50 (d,  $J = 7.3$  Hz, 2H).  $^{13}\text{C NMR}$  ( $\text{CDCl}_3$ , 150.9 MHz):  $\delta$  59.6 ( $\text{CH}_2$ ), 82.0 ( $\text{CH}(\text{Ph})$ ), 106.1 (CH), 128.1 ( $p\text{-CH}$ ), 128.7 ( $o\text{-CH}$ ), 129.2 ( $m\text{-CH}$ ), 137.2 (C). Lit:<sup>3</sup>  $^1\text{H NMR}$  ( $\text{dms}\text{-d}_6$ )  $\delta$  3.83 (d,  $J = 10$  Hz, 2H), 5.13 (d,  $J = 12$  Hz, 1H), 6.40 (dt,  $J = 12$  Hz, 10 Hz, 1H), 7.0-7.8 (m, 5H)

### 2.3.3 Preparation of $\text{Pd}(\eta^3\text{-C}_3\text{H}_5)(\eta^5\text{-C}_5\text{H}_5)$

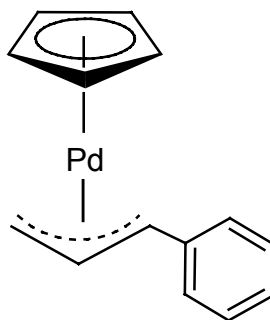
The following compound was prepared according to the method described by Tatsuno *et al.*<sup>2</sup>



A one-neck, 50 mL round bottom flask was charged with  $[\text{PdCl}(\eta^3\text{-C}_3\text{H}_5)]_2$  (1.1 g, 2.7 mmol) and a stir bar and placed under Ar. Dry THF (10 mL) and hexanes (10 mL) were then added via syringe, producing a clear yellow solution that was then cooled to  $-20^\circ\text{C}$  in an isopropanol/dry ice bath. A THF solution (1.1 M) of NaCp (0.93 g, 11 mmol) was then added dropwise over 1.5 hours to the stirring  $[\text{PdCl}(\eta^3\text{-C}_3\text{H}_5)]_2$  solution. The resulting red solution was warmed to approximately  $0^\circ\text{C}$  and the solvent was evaporated under vacuum. The obtained dark red solid was extracted with two 10 mL portions of hexanes. The red extract was filtered and the solvent was removed under vacuum to obtain a red crystalline solid that was then stored under nitrogen at  $-30^\circ\text{C}$ . Yield: 0.91 g, 80 %.  $^1\text{H NMR}$  ( $\text{C}_6\text{D}_6$ , 600 MHz):  $\delta$  2.09 (d,  $J = 10.8$  Hz, 2H), 3.40 (d,  $J = 5.9$  Hz, 2H), 4.58 (tt,  $J = 6.0$  Hz, 10.8 Hz 1H), 5.84 (s, 5H). Lit:<sup>4</sup>  $^1\text{H NMR}$  ( $\text{C}_6\text{D}_6$ ,  $25^\circ\text{C}$ )  $\delta$  2.07 (d), 3.38 (d), 4.52 (tt), 5.73 (s).

### 2.3.4 Preparation of Pd( $\eta^3$ -1-Ph-C<sub>3</sub>H<sub>4</sub>)( $\eta^5$ -C<sub>5</sub>H<sub>5</sub>)

The following compound was prepared according to the method described by Murrall *et al.*<sup>5</sup>



NaCp (0.402 g, 4.56 mmol) in THF (30 mL) was added by cannula to a solution of [PdCl( $\eta^3$ -1-Ph-C<sub>3</sub>H<sub>4</sub>)<sub>2</sub>] (0.508 g, 0.981 mmol) in THF (15 mL). The orange solution immediately turned red, and after 15 minutes of stirring the solvent was removed under vacuum. The non-volatile, deep red solid was extracted with two 20 mL portions of hexanes, filtered, and the filtrate was reduced under vacuum, producing a deep red solid. The solid was recrystallized from a minimum of hexanes. Yield: 0.22 g, 78 %. <sup>1</sup>H NMR (C<sub>7</sub>D<sub>8</sub>, 400 MHz):  $\delta$  2.16 (d, J = 10.6 Hz, 1H), 3.36 (d, J = 6.1 Hz, 1H), 3.83 (d, 9.9 Hz, 1H), 5.13 (ddd, J = 6.3 Hz, 10.1 Hz, 11.1 Hz, 1H), 5.63 (s, 5H),  $\delta$  7.00 (t, J = Hz, 2H), 7.10 (t, J = Hz, 1H), 7.25 (d, J = Hz, 2H). <sup>13</sup>C NMR (C<sub>7</sub>D<sub>8</sub>, 100.6 MHz):  $\delta$  42.8 (CH<sub>2</sub>), 68.3 (CH(Ph)), 92.1 (CH), 95.2 (C<sub>5</sub>H<sub>5</sub>), 126.7 (*p*-CH), 126.9 (*o*-CH), 137.44 (*m*-CH), 148.8 (C). Lit:<sup>5</sup> <sup>1</sup>H NMR (dms<sub>o</sub>-d<sub>6</sub>) 2.35 (d, J = 10.5 Hz, 1H), 3.60 (d, 1H, J = 6.06 Hz), 4.14 (d, 1H, 9.79 Hz), 5.55 (m, 1H), 5.56 (s, 5H),  $\delta$  7.17-7.58 (Ph). Lit:<sup>6</sup> <sup>13</sup>C NMR (C<sub>7</sub>D<sub>8</sub>, 100.6 MHz):  $\delta$  42.8, (CH<sub>2</sub>) 68.3 (CH(Ph)), 92.1 (CH), 95.2 (C<sub>5</sub>H<sub>5</sub>), 126.7 (*p*-CH), 126.9 (*o*-CH), 137.44 (*m*-CH), 148.8 (C).

### 2.3.5 Preparation of PdL<sub>2</sub> (L = PCy<sub>3</sub>, PBu<sup>t</sup><sub>3</sub>)

The following complexes were prepared according to the method described by Yoshida and Otsuka.<sup>7</sup>

A 150 mL Schlenk flask under inert atmosphere was charged with PCy<sub>3</sub> (0.803 g, 2.86 mmol), Pd( $\eta^3$ -C<sub>3</sub>H<sub>5</sub>)( $\eta^5$ -C<sub>5</sub>H<sub>5</sub>) (0.273 g, 1.28 mmol), a stir bar, and dry toluene (12 mL). The red solution was then stirred in an oil bath at 80 °C for three hours. The solvent was removed under vacuum and the brown residue was washed with two 10 mL portions of dry, deoxygenated MeOH. The residue was then recrystallized from dry, hot toluene (5 mL) and MeOH (5 mL) and stored for 16 hours at -10 °C. The mother liquor was removed by syringe, and the remaining beige crystalline solid was washed with MeOH (5 mL), dried under vacuum and stored under nitrogen. Yield: 0.854 g, 73 %. <sup>1</sup>H NMR (C<sub>6</sub>D<sub>6</sub>, 400 MHz):  $\delta$  1.21 – 2.22 (m, H<sub>Cy</sub>). <sup>31</sup>P NMR (C<sub>6</sub>D<sub>6</sub>, 163.0 MHz):  $\delta$  39.31 (s). Lit<sup>5</sup>: <sup>1</sup>H NMR (C<sub>6</sub>D<sub>6</sub>):  $\delta$  0.70 – 2.60 (m) Lit<sup>8</sup>: <sup>31</sup>P NMR (C<sub>6</sub>D<sub>6</sub>, 121.9 MHz):  $\delta$  39.4 (s).

Pd(PBu<sup>t</sup><sub>3</sub>)<sub>2</sub> was also prepared according to the method described above. However, PBu<sup>t</sup><sub>3</sub> (0.56 mL, 2.3 mmol) was added by means of a heated syringe (m.p. 30 °C) to a Schlenk tube containing (Pd( $\eta^3$ -C<sub>3</sub>H<sub>5</sub>)( $\eta^5$ -C<sub>5</sub>H<sub>5</sub>)) (0.21 g, 0.98 mmol) in toluene (15 mL). After heating and removal of the solvent, the residue was washed with three 10 mL portions of MeOH prior to recrystallization. Yield: 0.17 g, 34 %. <sup>1</sup>H NMR (C<sub>6</sub>D<sub>6</sub>, 400 MHz):  $\delta$  1.53 (vt, J = 6.0 Hz, CCH<sub>3</sub>). <sup>31</sup>P NMR (C<sub>6</sub>D<sub>6</sub>, 163.0 MHz):  $\delta$  85.1 (s). Lit:<sup>9</sup> <sup>1</sup>H NMR (C<sub>6</sub>D<sub>6</sub>):  $\delta$  1.53 (t, J = 5.7 Hz), <sup>31</sup>P NMR (C<sub>6</sub>D<sub>6</sub>):  $\delta$  85.2 (s).

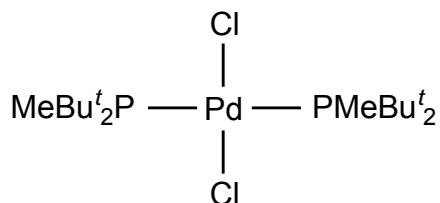
### 2.3.6 Preparation of PdL<sub>2</sub> (L = P<sup>t</sup>MeBu<sub>2</sub>)

The preparation of Pd(P<sup>t</sup>MeBu<sub>2</sub>)<sub>2</sub> was based on the method for Pd(PCy<sub>3</sub>)<sub>2</sub> and Pd(PBu<sup>t</sup>)<sub>3</sub> described by Yoshida and Otsuka.<sup>7</sup>

A 150 mL Schlenk flask under inert atmosphere was charged with Pd(η<sup>3</sup>-C<sub>3</sub>H<sub>5</sub>)(η<sup>5</sup>-C<sub>5</sub>H<sub>5</sub>) (0.20 g, 0.94 mmol), a stir bar, and dry toluene (10 mL). P<sup>t</sup>MeBu<sub>2</sub>Me (0.24 mL, 1.8 mmol) was added to the Schlenk flask by syringe. The red solution was stirred in an oil bath at 80 °C for three hours. The solvent was then removed under vacuum, producing a dark brown solid. Crude yield: 0.26 g, 67 %. <sup>1</sup>H NMR (C<sub>7</sub>D<sub>8</sub>, 600 MHz): δ 1.04 (bs, 3H), 1.27 (vt, 18H, J = 6.0 Hz). <sup>31</sup>P NMR (C<sub>7</sub>D<sub>8</sub>, 242.9 MHz): δ 41.9 (s). Lit.<sup>10</sup> <sup>1</sup>H NMR (C<sub>6</sub>D<sub>6</sub>): δ 1.28, δ 1.07 <sup>31</sup>P NMR (C<sub>6</sub>D<sub>6</sub>): δ 41.0 (s).

### 2.3.7 Preparation of PdCl<sub>2</sub>[P<sup>t</sup>MeBu<sub>2</sub>]<sub>2</sub>

PdCl<sub>2</sub>[P<sup>t</sup>MeBu<sub>2</sub>]<sub>2</sub> was prepared according to the method described by Mann *et al.*<sup>11</sup>

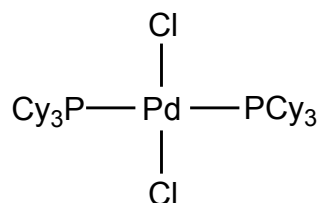


Under inert atmosphere, P<sup>t</sup>MeBu<sub>2</sub> (1.25 mL, 6.43 mmol) was dissolved in dry, deoxygenated MeOH (5 mL). This solution was then added over five minutes to a warmed (approx. 40 °C) MeOH solution (15 mL) of PdCl<sub>2</sub> (0.569 g, 3.20 mmol) and NaCl (0.409 g, 6.99 mmol). The resulting yellow solution was stirred for one hour and then reduced under vacuum to yield an orange solid.

The product was recrystallized from a minimum of CH<sub>2</sub>Cl<sub>2</sub> and MeOH, producing an orange crystalline solid. Yield: 0.94 g, 59 %. <sup>1</sup>H NMR (CDCl<sub>3</sub>, 600 MHz, 298 K): δ 1.35 (br. s, 3H), 1.45, (vt, 18H, J = 6.6 Hz). <sup>13</sup>C NMR (CDCl<sub>3</sub>, 125.7 MHz, 298 K): δ 2.43 (bs, P-CH<sub>3</sub> syn-syn or syn-anti), 3.63 (bs, P-CH<sub>3</sub> syn-syn or syn-anti), 29.7 (bt, C-CH<sub>3</sub>), 35.6 (t, P-C, J = 8.7 Hz). <sup>13</sup>C NMR (100.6 MHz, TCE, 350 K): δ 3.32 (t, J = 11.7 Hz, P-CH<sub>3</sub>), 29.7 (t, J = 2.3 Hz, CH<sub>3</sub>), 35.8 (t, J = 8.3 Hz, P-C). <sup>31</sup>P NMR (TCE, 163.0 MHz, 298 K): δ 28.4 (s P-CH<sub>3</sub> syn-syn or syn-anti), 30.9 (s, syn-syn or syn-anti). <sup>31</sup>P NMR (163.0 MHz, TCE, 350 K): δ 30.5 (br. s, P-CH<sub>3</sub>). Lit:<sup>11</sup> <sup>1</sup>H NMR (CH<sub>2</sub>Cl<sub>2</sub>) δ 1.42 (Bu<sup>t</sup>) δ 1.25 (Me).

### 2.3.8 Preparation of PdCl<sub>2</sub>[PCy<sub>3</sub>]<sub>2</sub>

PdCl<sub>2</sub>[PCy<sub>3</sub>]<sub>2</sub> was prepared by the method described by Grushin *et al.*<sup>8</sup>

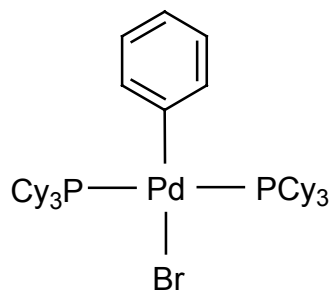


PdCl<sub>2</sub> (0.222 g, 1.25 mmol) and NaCl (0.161 g, 2.75 mmol) were dissolved in distilled water (12.5 mL) to produce a brown solution that was then deoxygenated by means of bubbling with Ar. The palladium containing solution was then added by syringe to a warmed solution (approx. 40 °C) of PCy<sub>3</sub> (0.92 g, 3.3 mmol) in similarly deoxygenated EtOH (60 mL). A pale yellow precipitate was immediately produced and the solution was then stirred at 21 °C for a further 45 minutes. The resulting yellow solid was collected by filtration, washed with 10

mL distilled water, 10 mL EtOH and 10 mL ether, and allowed to dry. Yield: 0.807 g, 87 %.  $^1\text{H}$  NMR ( $\text{CDCl}_3$ , 400 MHz):  $\delta$  1.17 – 2.60 (m,  $\text{H}_{\text{Cy}}$ ).  $^{31}\text{P}$  NMR ( $\text{CDCl}_3$ , 163.0 MHz):  $\delta$  26.2 (s). Lit.<sup>8</sup>  $^1\text{H}$  NMR ( $\text{CDCl}_3$ )  $\delta$  1.0 – 2.7 (m)  $^{31}\text{P}$  NMR ( $\text{CDCl}_3$ )  $\delta$  25.4 (s).

### 2.3.9 Preparation of *trans*-PdPh[PCy<sub>3</sub>]<sub>2</sub>Br

This compound was prepared according to the method described by Stambuli *et al.*<sup>12</sup>



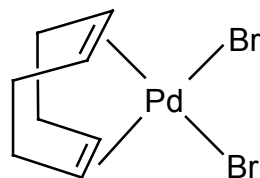
Under an inert atmosphere, a 100 mL Schlenk flask was charged with Pd(PCy<sub>3</sub>)<sub>2</sub> (0.2 g, 0.3 mmol), a stir bar and toluene (5 mL). PhBr (0.055 mL, 0.523 mmol) was added and the resulting orange solution was stirred at 21 °C for 24 hours. The solution was then reduced under vacuum to produce an orange residue. A minimum of cold ether was added by syringe, resulting in the precipitation of a beige solid. The solution stored at 0 °C for 16 hours, followed by filtration and washing with cold ether (5 mL). The beige solid was collected and dried under vacuum. Yield: 0.2 g, 81%.  $^1\text{H}$  NMR ( $\text{C}_7\text{D}_8$ , 600 MHz):  $\delta$  1.12 – 2.27 (m,  $\text{H}_{\text{Cy}}$ ),  $\delta$  6.85 - 7.56 (m, Ph).  $^{31}\text{P}$  NMR ( $\text{C}_7\text{D}_8$ , 242.9 MHz):  $\delta$  20.3 (s). Lit.<sup>12</sup>  $^1\text{H}$  NMR ( $\text{C}_6\text{D}_6$ , 500 MHz):  $\delta$  1.11-1.22 (br. s, 18H), 1.59-1.76 (m, 30H),



2.07-2.09 (m, 12H), 2.29 (br. s, 6H), 6.87 (t, J = 7.0 Hz, 1H), 6.87 (t, J = 7.0 Hz, 2H), 7.59 (d, J = 7.0 Hz, 2H).  $^{31}\text{P}$  NMR  $\text{C}_6\text{D}_6$ , 202 MHz):  $\delta$  20.6.

### 2.3.10 Preparation of $\text{Pd}[\text{COD}]\text{Br}_2$

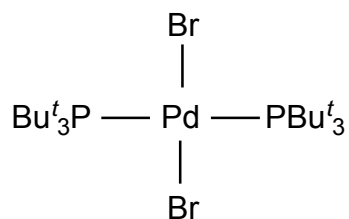
This compound was prepared according to the method described by Drew *et al.*<sup>13</sup>



A NaBr solution (2.33 g, 22.6 mmol) in distilled water (3.5 mL) was added to a solution of  $\text{PdCl}_2$  (1.0 g, 5.6 mmol) in warm, concentrated HCl (2.5 mL). The resulting solution was heated to 55 °C for 5 minutes, followed by addition of absolute ethanol (25 mL). The red solution was then filtered and the collected NaCl was washed with three 5 mL portions of 75 % EtOH/water. 1,5-cyclooctadiene (1.5 mL, 12 mmol) was added to the combined filtrate and washings, immediately producing an orange precipitate. The orange product was collected by filtration and washed with two 25 mL portions of distilled water followed by two 50 mL portions of ether. Yield: 1.95g, 91%.  $^1\text{H}$  NMR ( $\text{CDCl}_3$ , 400 MHz):  $\delta$  2.82 (br. d, 4H,  $\text{CH}_2$ ),  $\delta$  6.38 (br t. CH).  $^{13}\text{C}$  NMR ( $\text{CDCl}_3$ , 100.6 MHz):  $\delta$  31.1 (C=C), 116.6 ( $\text{CH}_2$ ). Lit.<sup>13</sup>  $^1\text{H}$  NMR ( $\text{CDCl}_3$ ):  $\delta$  2.60 ( $\text{CH}_2$ ),  $\delta$  6.42 (CH).

### 2.3.11 Attempted Preparation of Pd(PBu<sup>t</sup><sub>3</sub>)<sub>2</sub>Br<sub>2</sub>

Several attempts were made to isolate Pd(PBu<sup>t</sup><sub>3</sub>)<sub>2</sub>Br<sub>2</sub>, based on the method described by Goel and Montemayor.<sup>14</sup>



In a first attempt, a 150 mL Schlenk tube under inert atmosphere was charged with dried Pd[COD]Br<sub>2</sub> (0.374 g, 0.998 mmol), CH<sub>2</sub>Cl<sub>2</sub> (25 mL) and a stir bar. The resulting orange solution was stirred for 10 minutes, followed by addition of PBu<sup>t</sup><sub>3</sub> (0.49 mL, 2.0 mmol) by heated syringe. The solution changed from orange to dark amber and finally to a green-black colour. The solution was allowed to stir at room temperature for 16 hours. The solvent was then reduced under vacuum to yield an intractable, tar-like brown residue with apparent amounts of Pd black. There was no indication (namely a virtual triplet in the <sup>1</sup>H NMR) that the desired compound had been isolated.

In a second attempt, a 15 mL Schlenk tube under inert atmosphere was charged with dried Pd[COD]Br<sub>2</sub> (0.011 g, 0.029 mmol), CH<sub>2</sub>Cl<sub>2</sub> (1.5 mL) and a stir bar. The resulting orange solution was allowed to stir in an ice bath at 5 °C for approximately 15 minutes. PBu<sup>t</sup><sub>3</sub> (0.05 mL, 0.20 mmol) was then added to a second 15 mL Schlenk tube containing CH<sub>2</sub>Cl<sub>2</sub> (2 mL). 0.1 mL the PBu<sup>t</sup><sub>3</sub> solution was then added to the Pd[COD]Br<sub>2</sub> solution, and after 10 minutes the orange solution became green-black in colour. Three additional portions of the PBu<sup>t</sup><sub>3</sub>

solution (0.15 mL, 0.12 mL, 0.15 mL) were added over the course of an hour, for a total of 0.52 mL (0.053 mmol). The solution was then allowed to warm to 21 °C.  $^1\text{H}$  NMR and  $^{31}\text{P}$  NMR spectra were then obtained of the green-black solution in  $\text{CD}_2\text{Cl}_2$ .  $^{31}\text{P}$  NMR spectra indicated that  $\text{Pd}(\text{PBU}^t_3)_2$  and  $\text{PBU}^t_3$  were the major species present.

In a third attempt, a 150 mL Schlenk tube under inert atmosphere was charged with dried  $\text{Pd}[\text{COD}]\text{Br}_2$  (0.010 g, 0.027 mmol), hexanes (50 mL) and a stir bar. The resulting orange solution was allowed to stir in an ice bath at 5 °C for approximately 15 minutes.  $\text{PBU}^t_3$  (0.13 mL, 0.53 mmol) was then added to a second 100 mL Schlenk tube containing hexanes (25 mL). The  $\text{PBU}^t_3$  solution was then added to the  $\text{Pd}[\text{COD}]\text{Br}_2$  solution in 3 mL increments over the course of 90 minutes, with no observable colour change.  $\text{CH}_2\text{Cl}_2$  (25 mL) was then added to orange hexanes solution and the solution then turned green-black. The solution was warmed to 21 °C, reduced under vacuum and  $^1\text{H}$  and  $^{31}\text{P}$  NMR spectra were obtained.

## 2.4 *In Situ* Generation of $\text{PdL}_n$

### 2.4.1 *In Situ* Generation of $\text{PdL}_n$ from $\text{Pd}(\eta^3\text{-C}_3\text{H}_5)(\eta^5\text{-C}_5\text{H}_5)$

The following describes the *in situ*, NMR monitored generation of  $\text{PdL}_n$  developed from the method described by Yoshida and Otsuka.<sup>7</sup>

#### 2.4.1.1 L = PCy<sub>3</sub>

In a typical reaction, PCy<sub>3</sub> (12 mg, 0.043 mmol) was dissolved in 0.3 mL C<sub>6</sub>D<sub>6</sub> under inert atmosphere, placed in an NMR tube and sealed with a Teflon cap. A similarly prepared solution of Pd( $\eta^3$ -C<sub>3</sub>H<sub>5</sub>)( $\eta^5$ -C<sub>5</sub>H<sub>5</sub>) (4.5 mg, 0.021 mmol) in 0.18 mL C<sub>6</sub>D<sub>6</sub> was added to the PCy<sub>3</sub> solution by syringe and a <sup>31</sup>P NMR spectrum of the solution was run every 10 min for 2 h at 25 °C. This experiment was repeated to obtain corresponding <sup>1</sup>H NMR spectra. Similar experiments (<sup>1</sup>H and <sup>31</sup>P NMR) were carried out for various periods of time, at 65 °C and 77 °C in toluene-d<sub>8</sub>. In these instances the PCy<sub>3</sub> solution was warmed to prior to addition of Pd( $\eta^3$ -C<sub>3</sub>H<sub>5</sub>)( $\eta^5$ -C<sub>5</sub>H<sub>5</sub>).

#### 2.4.1.2 L = PMeBu<sup>t</sup><sub>2</sub>

The same procedure was followed as in 2.4.1.1, except that PMeBu<sup>t</sup><sub>2</sub> (7.3  $\mu$ L, 0.038 mmol) was added by microlitre syringe to a sealed NMR tube containing C<sub>6</sub>D<sub>6</sub> or C<sub>7</sub>D<sub>8</sub>. Similar <sup>1</sup>H and <sup>31</sup>P NMR experiments were performed at both 25 °C and 77 °C.

#### 2.4.1.3 L = PBu<sup>t</sup><sub>3</sub>

The same general procedure was followed as in 2.4.1.1, except that PBu<sup>t</sup><sub>3</sub> (0.1 mL, 0.4 mmol) was added by a heated syringe to a Schlenk containing toluene-d<sub>8</sub> (2 mL). The resulting PBu<sup>t</sup><sub>3</sub> solution (0.20 M) was added (0.28 mL, 0.06 mmol) to a sealed NMR tube containing 0.05 mL toluene-d<sub>8</sub>, prior to addition of Pd( $\eta^3$ -C<sub>3</sub>H<sub>5</sub>)( $\eta^5$ -C<sub>5</sub>H<sub>5</sub>) (5.95 mg, 0.028 mmol) in 0.2 mL toluene-d<sub>8</sub>.

Additionally, experiments with a Pd:PBu<sup>t</sup><sub>3</sub> ratio of 1:1 were conducted in this manner. <sup>1</sup>H and <sup>31</sup>P NMR experiments were performed at both 25 °C and 77 °C.

#### 2.4.1.4 L = PPh<sub>3</sub>

The same procedure was followed as in 2.4.1.1., except that multiple experiments were conducted at various Pd:PPh<sub>3</sub> ratios and temperatures in exclusively toluene-d<sub>8</sub>. Spectra (<sup>1</sup>H, <sup>31</sup>P) at 25 °C were obtained immediately after mixing. These conditions are summarized in Table 1.

Table 1. Summary of experiments involving *in situ* generation of PdL<sub>n</sub> from Pd(η<sup>3</sup>-C<sub>3</sub>H<sub>5</sub>)(η<sup>5</sup>-C<sub>5</sub>H<sub>5</sub>) with PPh<sub>3</sub>.

Entry	Pd(η <sup>3</sup> -C <sub>3</sub> H <sub>5</sub> )(η <sup>5</sup> -C <sub>5</sub> H <sub>5</sub> ):PPh <sub>3</sub>	Temperature/°C
1	1:1	25°C
2	1:2	25°C
3	1:2	80°C <sup>a</sup>
4	1:4	25°C

a) heated for 150 min, spectrum obtained at 80 °C.

#### 2.4.1.5 L = PMe<sub>3</sub>

The same general procedure was followed as in 2.4.1.2. However, NMR experiments were conducted at 25 °C, 2°C or -55 °C in exclusively toluene-d<sub>8</sub>. Prior to mixing at low temperature, reagents were kept cold in an ice or N<sub>2(l)</sub> bath.

#### 2.4.1.6 Independent Oxidation of L (L = PPh<sub>3</sub>, PCy<sub>3</sub>, PMeBu<sup>t</sup><sub>2</sub>)

In order to determine the <sup>31</sup>P NMR chemical shifts of the related oxide of the phosphines used in NMR experiments, approximately 20 mg of PCy<sub>3</sub> was placed in a vial and left open to air for 24 h. The solid was then dissolved in 0.5 mL of toluene-d<sub>8</sub> and a <sup>31</sup>P NMR spectrum was obtained of the solution. This procedure was repeated with PPh<sub>3</sub> and PMeBu<sup>t</sup><sub>2</sub> in benzene-d<sub>6</sub> and toluene-d<sub>8</sub> respectively, however, the vial was in these cases left open to air for several days. <sup>31</sup>P NMR (C<sub>7</sub>D<sub>8</sub>, 242 MHz): δ 9.9 PCy<sub>3</sub>, δ 47.2 O=PCy<sub>3</sub>. Lit: δ 10.27 PCy<sub>3</sub> (C<sub>6</sub>D<sub>6</sub>),<sup>15</sup> O=PCy<sub>3</sub> δ 47.3<sup>16</sup> <sup>31</sup>P NMR (C<sub>7</sub>D<sub>8</sub>, 162 MHz): δ -5.1 PPh<sub>3</sub>, δ 24.8 O=PPh<sub>3</sub>. Lit: δ -4.93 PPh<sub>3</sub> (C<sub>6</sub>D<sub>6</sub>),<sup>15</sup> δ 25.4, O=PPh<sub>3</sub>.<sup>17</sup> <sup>31</sup>P NMR (C<sub>7</sub>D<sub>8</sub>, 242 MHz): δ 61.7 O=PMeBu<sup>t</sup><sub>2</sub> Lit: δ 60.0 O=PMeBu<sup>t</sup><sub>2</sub> (CCl<sub>4</sub>).<sup>11</sup>

#### 2.4.2 In Situ Generation of PdL<sub>2</sub> from Pd(η<sup>3</sup>-1-Ph-C<sub>3</sub>H<sub>4</sub>)(η<sup>5</sup>-C<sub>5</sub>H<sub>5</sub>)

##### 2.4.2.1 L = PCy<sub>3</sub>

In a typical reaction, 0.3 mL of a toluene-d<sub>8</sub> solution of PCy<sub>3</sub> (34 mg, 0.12 mmol) were placed in an NMR tube under inert atmosphere and sealed with a rubber septum. 0.3 mL of a toluene-d<sub>8</sub> solution of Pd(η<sup>3</sup>-1-Ph-C<sub>3</sub>H<sub>4</sub>)(η<sup>5</sup>-C<sub>5</sub>H<sub>5</sub>) (17 mg, 0.06 mmol) were then injected into the NMR tube and <sup>1</sup>H and <sup>31</sup>P NMR spectra of the solution were obtained every 10 minutes for 2 hrs at 25 °C. Similar experiments (<sup>1</sup>H and <sup>31</sup>P NMR) were carried out at 80 °C, with the PCy<sub>3</sub> solution heated prior to addition of Pd(η<sup>3</sup>-1-Ph-C<sub>3</sub>H<sub>4</sub>)(η<sup>5</sup>-C<sub>5</sub>H<sub>5</sub>).

#### 2.4.2.2 L = P<sup>t</sup>MeBu<sub>2</sub>

The same procedure was used as in 2.4.2.1, except that P<sup>t</sup>MeBu<sub>2</sub> (22 μL, 0.12 mmol) was added by microlitre syringe to the sealed NMR tube prior to injection of Pd(η<sup>3</sup>-1-Ph-C<sub>3</sub>H<sub>4</sub>)(η<sup>5</sup>-C<sub>5</sub>H<sub>5</sub>). <sup>31</sup>P and <sup>1</sup>H NMR spectra were obtained at 25 °C over two hours, as well as 24 hours after mixing.

#### 2.4.2.3 L = PPh<sub>3</sub>

The same procedure was followed as in 2.4.2.1. Successive <sup>1</sup>H and <sup>31</sup>P NMR spectra were obtained at 25 °C for two hours, followed by <sup>31</sup>P-<sup>31</sup>P correlation and <sup>13</sup>C spectra.

### 2.5 Thermodynamic Parameters for Dissociation of PdL<sub>3</sub>

#### 2.5.1 L = PCy<sub>3</sub>

In a typical experiment, 0.5 mL of a 0.018 M solution of Pd(PCy<sub>3</sub>)<sub>2</sub> (6.1 mg, 9.8 × 10<sup>-3</sup> mmol) in toluene-d<sub>8</sub> was added to 0.1 mL of a 0.09 M solution of PCy<sub>3</sub> (2.5 mg, 9.0 × 10<sup>-3</sup> mmol) in toluene-d<sub>8</sub>. The resulting solution was diluted with an additional 0.2 mL toluene, a glass capillary containing a toluene-d<sub>8</sub> solution of TOPB (0.046 M, 3.0 × 10<sup>-3</sup> mmol) was added ([Pd(PCy<sub>3</sub>)<sub>2</sub>]<sub>0</sub> = [PCy<sub>3</sub>] = 0.011 M) and <sup>31</sup>P inverse-gated NMR spectra were obtained between -85 and -68 °C with d<sub>1</sub> = 45 s.

### 2.5.2 L = P<sup>t</sup>MeBu<sup>t</sup><sub>2</sub>

Pd( $\eta^3$ -C<sub>3</sub>H<sub>5</sub>)( $\eta^5$ -C<sub>5</sub>H<sub>5</sub>) (0.020 g, 0.094 mmol) were dissolved in 5 mL toluene in a Schlenk tube with a stir bar. P<sup>t</sup>MeBu<sup>t</sup><sub>2</sub> (37  $\mu$ L, 0.19 mmol) were added and the solution was heated to 80 °C for three hours. The brown solution was reduced under vacuum, and the residue was dissolved in 1 mL toluene-d<sub>8</sub>. 0.6 mL of this solution was transferred to an NMR tube that contained a sealed glass capillary standard (TOPB in toluene, 3.30 x 10<sup>-3</sup> mmol). An inverse-gated <sup>31</sup>P NMR spectrum was obtained followed by injection of P<sup>t</sup>MeBu<sup>t</sup><sub>2</sub> (19  $\mu$ L, 0.095 mmol). Inverse-gated <sup>31</sup>P NMR spectra were then obtained from at variable temperatures (-73 °C to -88 °C) with d<sub>1</sub> = 45 s.

### 2.5.3 L = P<sup>t</sup>Bu<sup>t</sup><sub>3</sub>

The procedure was followed according to 2.6.1, except that P<sup>t</sup>Bu<sup>t</sup><sub>3</sub> (10  $\mu$ L, 0.041 mmol) was added by means of a heated microsyringe to a sealed NMR tube containing Pd(P<sup>t</sup>Bu<sup>t</sup><sub>3</sub>)<sub>2</sub> (4.65 mg, 0.0230 mmol) in 0.6 mL toluene-d<sub>8</sub>.

## 2.6 Generation of Heteroleptic Systems PdLL'

### 2.6.1 PCy<sub>3</sub>/ P<sup>t</sup>Bu<sup>t</sup><sub>3</sub>

In a typical experiment, 0.18 mL of a 0.2 M solution of P<sup>t</sup>Bu<sup>t</sup><sub>3</sub> (7.3 mg, 0.036 mmol) in toluene-d<sub>8</sub> was injected into a sealed NMR tube containing 0.25 mL of a 0.14 M solution of PCy<sub>3</sub> (10 mg, 0.036 mmol) in toluene-d<sub>8</sub>. The NMR



tube was heated to 77 °C and 0.25 mL of a 0.14 M solution of Pd( $\eta^3$ -C<sub>3</sub>H<sub>5</sub>)( $\eta^5$ -C<sub>5</sub>H<sub>5</sub>) (7.6 mg, 0.036 mmol) in toluene-d<sub>8</sub> was injected. After 1 hour of heating, a <sup>31</sup>P NMR spectrum was obtained.

A similar spectrum, as well as a <sup>31</sup>P-<sup>31</sup>P correlation spectrum, was obtained at 21 °C by reacting 500  $\mu$ L of a 0.021 M toluene solution of Pd(PCy<sub>3</sub>)<sub>2</sub> (7.0 mg, 0.011 mmol) with Pd(PBu<sup>t</sup><sub>3</sub>)<sub>2</sub> (7.3 mg, 0.014 mmol), followed by dilution with 0.2 mL toluene-d<sub>8</sub>.

Complementary experiments were performed varying the ratio of PBu<sup>t</sup><sub>3</sub>:PCy<sub>3</sub> (1:2 and 2:1). In the instance where the phosphine ratio was 1:2, 0.11 mL of a 0.20 M solution of PBu<sup>t</sup><sub>3</sub> (4.48 mg, 0.0217 mmol) in toluene-d<sub>8</sub> was injected into a sealed NMR tube containing 0.3 mL of a 0.142 M solution of PCy<sub>3</sub> (11.9 mg, 0.04254 mmol) in toluene-d<sub>8</sub>. 0.15 mL of a 0.141 M solution of Pd( $\eta^3$ -C<sub>3</sub>H<sub>5</sub>)( $\eta^5$ -C<sub>5</sub>H<sub>5</sub>) in toluene-d<sub>8</sub> (4.48 mg, 0.0211 mmol) were then injected into the NMR tube, and introduced into the spectrometer at 77 °C. After 15 minutes, successive <sup>31</sup>P NMR spectra were obtained in intervals of ten minutes for 2 hours. In the case where the phosphine ratio was 2:1, 0.14 mL of a 0.20 M solution of PBu<sup>t</sup><sub>3</sub> (5.58 mg, 0.0276 mmol) in toluene-d<sub>8</sub> was injected into a sealed NMR tube containing 0.25 mL of a 0.057 M solution of PCy<sub>3</sub> (3.99 mg, 0.0143 mmol) in toluene-d<sub>8</sub>. 0.15 mL of a 0.141 M solution of Pd( $\eta^3$ -C<sub>3</sub>H<sub>5</sub>)( $\eta^5$ -C<sub>5</sub>H<sub>5</sub>) in toluene-d<sub>8</sub> (3.0 mg, 0.014 mmol) were then injected into the NMR tube and introduced into the spectrometer at 77 °C. After 15 minutes, successive <sup>31</sup>P NMR spectra were obtained in intervals of ten minutes for 2 hours.

### 2.6.2 **PMeBu<sup>t</sup><sub>2</sub>/ PBu<sup>t</sup><sub>3</sub>**

Pd(PMeBu<sup>t</sup><sub>2</sub>)<sub>2</sub> (71 mg, 0.17 mmol) and Pd(PBu<sup>t</sup><sub>3</sub>)<sub>2</sub> (89 mg, 0.17 mmol) were dissolved in 0.65 mL toluene-d<sub>8</sub>. The solution was transferred to a sealed NMR tube and a <sup>31</sup>P NMR spectrum, as well as a <sup>31</sup>P-<sup>31</sup>P correlation spectrum was obtained.

### 2.6.3 **PCy<sub>3</sub>/ PMeBu<sup>t</sup><sub>2</sub>**

Under inert atmosphere, 0.25 mL of a PCy<sub>3</sub> solution in toluene-d<sub>8</sub> (0.143, 0.0357 mmol) was placed in a NMR tube and sealed with a Teflon cap. PMeBu<sup>t</sup><sub>2</sub> (4.5 μL, 0.023 mmol, 0.65 eq.) was added to the NMR tube, followed by 0.25 mL of a Pd(η<sup>3</sup>-C<sub>3</sub>H<sub>5</sub>)(η<sup>5</sup>-C<sub>5</sub>H<sub>5</sub>) solution in toluene-d<sub>8</sub> (0.141 M, 0.0353 mmol). The NMR tube was introduced into the spectrometer at 77 °C and after 30 minutes, successive <sup>31</sup>P NMR spectra were obtained at ten minute intervals for 2.5 hours.

Additional experiments were performed by combining a solution of Pd(PMeBu<sup>t</sup><sub>2</sub>)<sub>2</sub> (4.4 mg, 0.010 mmol, 0.021 M) in 0.5 mL benzene-d<sub>6</sub> with 0.5 mL of a 0.022 M benzene-d<sub>6</sub> solution of Pd(PCy<sub>3</sub>)<sub>2</sub> (7.2 mg, 0.011 mmol). An aliquot of 0.6 mL of the resulting solution was diluted further with 0.1 mL benzene-d<sub>6</sub>, placed in an NMR tube and a <sup>31</sup>P NMR spectrum was obtained.

In complementary <sup>31</sup>P NMR experiments, 500 μL of a 0.03 M solution of Pd(PCy<sub>3</sub>)<sub>2</sub> (10 mg, 0.015 mmol) in toluene-d<sub>8</sub> in an NMR tube and diluted with an additional 0.2 mL toluene-d<sub>8</sub> was treated with 3 μL of PMeBu<sup>t</sup><sub>2</sub> (2.5 mg, 0.015 mmol) and <sup>31</sup>P NMR spectra were obtained in the temperature range 25 °C to -

93 °C. Similarly, Pd(PCy<sub>3</sub>)<sub>2</sub> (27 mg, 0.04 mmol) in 700 μL toluene-d<sub>8</sub> in a sealed NMR tube was treated with 16 μL PMeBu<sup>t</sup><sub>2</sub> (13 mg, 0.082 mmol) and a <sup>31</sup>P-<sup>31</sup>P NMR correlation spectrum was obtained at -93 °C.

#### 2.6.4 PCy<sub>3</sub>/PPh<sub>3</sub>

Under inert atmosphere, 0.2 mL of a PCy<sub>3</sub> solution in toluene-d<sub>8</sub> (0.142 M, 0.0284 mmol) and 0.21 mL PPh<sub>3</sub> solution in toluene-d<sub>8</sub> (0.134 M, 0.0281 mmol) were placed in an NMR tube and sealed with a rubber septum. 0.2 mL of a Pd(η<sup>3</sup>-C<sub>3</sub>H<sub>5</sub>)(η<sup>5</sup>-C<sub>5</sub>H<sub>5</sub>) solution in toluene-d<sub>8</sub> (0.140 M, 0.0280 mmol) was then injected into the NMR tube and the tube was introduced into the spectrometer at 77 °C. Thirty minutes after injection of Pd(η<sup>3</sup>-C<sub>3</sub>H<sub>5</sub>)(η<sup>5</sup>-C<sub>5</sub>H<sub>5</sub>), successive <sup>31</sup>P NMR spectra were obtained at 10 minute intervals for 2.5 hours.

### 2.7 Investigative Experiments Involving Oxidative Addition

Several experiments were performed to qualitatively monitor the formation of products and associated reaction conditions for oxidative addition reactions involving PdL<sub>n</sub> (n = 2 for L = PCy<sub>3</sub>, PMeBu<sup>t</sup><sub>2</sub>, PBu<sup>t</sup><sub>3</sub>). These were conducted on pre-generated PdL<sub>2</sub>, as well as *in situ* generated PdL<sub>2</sub> from Pd(η<sup>3</sup>-C<sub>3</sub>H<sub>5</sub>)(η<sup>5</sup>-C<sub>5</sub>H<sub>5</sub>).

## 2.7.1 Oxidative Addition with Isolated PdL<sub>2</sub>

### 2.7.1.1 Oxidative addition with Pd(PCy<sub>3</sub>)<sub>2</sub> and Pd(PMeBu<sup>t</sup>)<sub>2</sub>

Under inert atmosphere, 0.5 mL of a 0.031 M Pd(PCy<sub>3</sub>)<sub>2</sub> solution in toluene-d<sub>8</sub> (0.0103 g, 0.0154 mmol) was placed in a NMR tube and sealed with a rubber septum. Bromobenzene (15 μL, 0.14 mmol) was injected into the tube and successive <sup>31</sup>P NMR spectra were obtained at 25 °C for intervals of 1.5 minutes for 10 minutes.

Similar experiments were performed as above with other substrates (chlorobenzene, allyl chloride, (1-bromoethyl)benzene)) to examine their reactivity with Pd(PCy<sub>3</sub>)<sub>2</sub>. Furthermore, oxidative addition experiments were performed with Pd(PMeBu<sup>t</sup>)<sub>2</sub> and bromobenzene. These results are described in Table 2.

Table 2. Summary of attempted oxidative addition experiments with Pd(PCy<sub>3</sub>)<sub>2</sub> and Pd(PMeBu<sup>t</sup>)<sub>2</sub>.

Entry	PdL <sub>2</sub>	Substrate	Pd:Substrate	Solvent	Time /h
1	Pd(PCy <sub>3</sub> ) <sub>2</sub>	C <sub>6</sub> H <sub>5</sub> CH(CH <sub>3</sub> )Br	1:3	C <sub>6</sub> D <sub>6</sub>	2
2	Pd(PCy <sub>3</sub> ) <sub>2</sub>	CH <sub>2</sub> CHCH <sub>2</sub> Cl	1:0.4	C <sub>6</sub> D <sub>6</sub>	3
3	Pd(PCy <sub>3</sub> ) <sub>2</sub>	C <sub>6</sub> H <sub>5</sub> Cl	1:11	C <sub>7</sub> D <sub>8</sub>	1
4	Pd(PCy <sub>3</sub> ) <sub>2</sub>	C <sub>6</sub> H <sub>5</sub> Br	1:1	C <sub>6</sub> D <sub>6</sub>	2
5	Pd(PCy <sub>3</sub> ) <sub>2</sub>	C <sub>6</sub> H <sub>5</sub> Br	1:10	C <sub>7</sub> D <sub>8</sub>	0.2
6	Pd(PMeBu <sup>t</sup> ) <sub>2</sub>	C <sub>6</sub> H <sub>5</sub> Br	1:1	C <sub>7</sub> D <sub>8</sub>	3

### 2.7.1.2 Attempted Oxidative Addition with Pd(PBu<sup>t</sup>)<sub>3</sub>)<sub>2</sub>

Under inert atmosphere, Pd(PBu<sup>t</sup>)<sub>3</sub>)<sub>2</sub> (0.0211 g, 0.0413 mmol) was dissolved in 0.5 mL toluene-d<sub>8</sub>, placed in an NMR tube and sealed with a

septum. Bromobenzene (0.04 mL, 0.4 mmol) were added to the NMR tube by syringe and subsequent  $^{31}\text{P}$  NMR spectra were obtained at 25 °C at 10 minute intervals for 2.5 hours. Similar experiments were performed in this manner, with some variation in reaction conditions, described in Table 3.

Table 3. Summary of oxidative addition experiments with  $\text{Pd}(\text{P}^t\text{Bu}_3)_2$

Entry	$\text{Pd}(\text{P}^t\text{Bu}_3)_2\text{:PhBr}$	Solvent	Time /h	Temperature/°C
1	1:1	$\text{C}_7\text{D}_8$	1	25
2	1:1	$\text{C}_6\text{D}_6$	0.33	60
3	1:10	$\text{C}_7\text{D}_8$	2.5	25
4	1:10	1:1.5 $\text{C}_7\text{D}_8/\text{THF}$	2.5	25
5	1:10	1:1.5 $\text{C}_7\text{D}_8/1,4\text{-dioxane}$	3	25
6	1:10	1:1.5 $\text{C}_7\text{D}_8/\text{THF}$	1	60
7	1:10	1,4-dioxane	2.75	25
8	1:10	THF	3	25

### 2.7.2 Oxidative Addition with *In Situ* Generated $\text{PdL}_2$

Under inert atmosphere,  $\text{Pd}(\eta^3\text{-C}_3\text{H}_5)(\eta^5\text{-C}_5\text{H}_5)$  (0.0079 g, 0.037 mmol) was placed in an NMR tube with  $\text{PCy}_3$  (0.0196 g, 0.0698 mmol) and 0.5 mL toluene. The tube was sealed with a septum and heated at 100 °C for 1 hour. After cooling to 21 °C,  $\text{PhBr}$  (75  $\mu\text{L}$ , 0.71 mmol) was injected into the tube and successive  $^{31}\text{P}$  NMR spectra were obtained at 25 °C at 10 minute intervals for three hours.

In addition, experiments were performed in which the *in situ* generation of  $\text{Pd}(\text{PCy}_3)_2$  and  $\text{Pd}(\text{P}^t\text{MeBu}_2)_2$  was done in the presence of TBAB (in THF) or TOPB (in toluene). These experiments are summarized in Table 4.

Table 4. Summary of oxidative addition reactions with *in situ* generated PdL<sub>2</sub>.

Entry	L	<i>In Situ</i> Conditions	Pd:PhBr	Halide	Solvent
1	PCy <sub>3</sub>	60 °C, 180 min	1:10	TBAB	THF
2 <sup>a</sup>	PCy <sub>3</sub>	75 °C, 180 min	1:10	TOPB	C <sub>7</sub> D <sub>8</sub>
3	PMeBu <sub>2</sub> <sup>t</sup>	60 °C, 60 min	1:10	TBAB	THF
4 <sup>a</sup>	PMeBu <sub>2</sub> <sup>t</sup>	75 °C, 150 min	1:10	TOPB	C <sub>7</sub> D <sub>8</sub>

a) halide source added after heating, prior to PhBr

## 2.8 Kinetic Study of Oxidative Addition

### 2.8.1 Oxidative Addition of PhBr to Pd(PCy<sub>3</sub>)<sub>2</sub>

In a typical experiment, 500 μL of a 0.03 M solution of Pd(PCy<sub>3</sub>)<sub>2</sub> (10 mg, 0.015 mmol) in toluene were added to a vial containing 180 μL of toluene, and the solution was transferred to an NMR tube containing a sealed glass capillary of TOPB in toluene (0.045 M, 2.7 x 10<sup>-3</sup> mmol). The appropriate amount of PhBr was then injected, in this case 20 μL (0.27 M, ratio of PhBr:Pd 13:1). The time was noted and <sup>31</sup>P inverse gated spectra were obtained at 94 s intervals for greater than 2 t<sub>1/2</sub>. These experiments were repeated at several PhBr concentrations of 0.47 M, 0.68 M, 0.82 M and 1.08 M (ratios of PhBr:Pd 22:1, 32:1, 38:1 and 51:1 respectively), varying the amount of toluene added such that the total sample volume was consistently 700 μL.

#### 2.8.1.1 In the Presence of TOPB

To assess the effects of bromide ion, added as TOPB, 0.5 mL of a 0.03 M solution of Pd(PCy<sub>3</sub>)<sub>2</sub> (10 mg, 0.015 mmol) was added to an NMR tube

containing 0.15 mL of a 0.1 M solution of TOPB (8.456 mg, 0.015 mmol) in toluene. A volume of bromobenzene was injected by microsyringe into the NMR tube so that the ratio of PhBr:Pd(PCy<sub>3</sub>)<sub>2</sub> was varied in each experiment, from 10:1 to 50:1 (0.23 - 1.2 M PhBr). The sample was then introduced into the NMR probe preset at the desired temperature (25 °C) and the probe was tuned utilizing a separate sample of toluene-d<sub>8</sub>. The time of PhBr injection was recorded and a <sup>31</sup>P inverse-gated spectrum was run at 94 s intervals. The total experimental run time for each experiment was greater than 2 t<sub>1/2</sub>.

### **2.8.1.2 In the Presence of Additional PCy<sub>3</sub>**

To assess the effects of added PCy<sub>3</sub>, the above experiments were repeated in the presence of one equivalent of PCy<sub>3</sub>. In these instances, 500 μL of a 0.03 M solution of Pd(PCy<sub>3</sub>)<sub>2</sub> (10 mg, 0.015 mmol) in toluene were added to a solution containing 34 μL of a 0.44 M toluene solution of PCy<sub>3</sub> (4.2 mg, 0.015 mmol). To ensure that the initial concentration ratio of Pd(PCy<sub>3</sub>)<sub>2</sub> to PCy<sub>3</sub> was 1:1, an appropriate amount of toluene was added prior to injection of PhBr (thus 146 μL toluene were used for 20 μL PhBr).

## **2.9 Studies of Transmetalation by GC**

Under inert atmosphere, *trans*-Pd(PCy<sub>3</sub>)<sub>2</sub>(Ph)(Br) (0.0105 g, 0.0121 mmol) and K[C<sub>6</sub>H<sub>5</sub>BF<sub>3</sub>] (0.0024 g, 0.012 mmol) were placed in a vial and both dissolved in toluene (1 mL). The vial was sealed with a septum cap and heated in a water bath at 50 °C for ten minutes. An aliquot (1 μL) was injected into the GC injection

port (300 °C), introducing the sample to the column oven with gradient temperature programming (100 °C to 260 °C over 10 minutes). After 19 hours at 21 °C, a second aliquot (1 µL) of the sample was introduced into the GC at the same conditions. This experiment was repeated in a 5:1 toluene/THF mixture.

In complementary experiments, *trans*-Pd(PCy<sub>3</sub>)<sub>2</sub>(Ph)(Br) (0.0106 g, 0.0121 mmol) and K[C<sub>6</sub>H<sub>5</sub>BF<sub>3</sub>] (0.0022 g, 0.012 mmol) were dissolved in 1 mL toluene and heated at 80 °C for 2 hours, prior to an aliquot (1 µL) being injected into GC at the above mentioned conditions. After the sample had been heated at 80 °C for an additional hour, a second aliquot (1 µL) was injected.

## **2.10 Attempted Preparation of [TOP][C<sub>6</sub>H<sub>5</sub>BF<sub>3</sub>]**

### **2.10.1 Preparation in Water**

In a 150 mL Erlenmeyer flask, a solution of TOPB (0.672 g, 1.19 mmol) in CH<sub>2</sub>Cl<sub>2</sub> (10 mL) was added to a solution of K[C<sub>6</sub>H<sub>5</sub>BF<sub>3</sub>] (0.229 g, 1.24 mmol) in distilled water (10 mL). The resulting biphasic solution was allowed to stir for 1.5 hours. The CH<sub>2</sub>Cl<sub>2</sub> layer was then washed with three 10 mL portions of distilled water. The water layer was extracted with three 10 mL portions of CH<sub>2</sub>Cl<sub>2</sub>. The respective layers were combined and the CH<sub>2</sub>Cl<sub>2</sub> solution was dried with MgSO<sub>4</sub>. The resulting water and CH<sub>2</sub>Cl<sub>2</sub> layers were allowed to evaporate, yielding a white solid (0.107 g) and a viscous, colourless oil (0.616 g) respectively. <sup>1</sup>H NMR spectroscopy of the oil indicated side product formation.



### 2.10.2 Anhydrous Preparation

Under inert atmosphere, a 150 mL Schlenk flask was charged with TOPB (0.67 g, 1.2 mmol),  $K[C_6H_5BF_3]$  (0.23 g, 1.2 mmol) and a stir bar. The Schlenk flask was then warmed until the mixture became viscous and it then was allowed to stir for 3 hours at room temperature. MeOH (20 mL) was then added by syringe, and the solution was allowed to stir for an additional hour. The solvent was removed under vacuum, yielding a viscous, colourless oil with a suspended white residue. The product was extracted with  $CDCl_3$  (1 mL) and a  $^1H$  NMR spectrum indicated side product formation.

### 2.11 Attempted Reduction of Pd(II) Compounds

In a typical experiment, a 15 mL Schlenk tube under inert atmosphere was charged with  $PdCl_2[PMeBu^t_2]_2$  (0.0250 g, 0.0502 mmol),  $K[C_6H_5BF_3]$  (0.0184 g, 0.0999 mmol) and a stir bar. Toluene (5 mL) was added by syringe and the solution was allowed to stir for 22 hours at 21 °C. The solvent was then removed under vacuum, the residue was taken up in toluene- $d_8$  and a  $^{31}P$  NMR spectrum was obtained.

Many complementary experiments were performed as mentioned above, with a number of variations. Similar experiments were also performed with  $PdCl_2[PCy_3]_2$ . Experiments were also repeated at either 65 °C or 80 °C. The solvent system was also varied to a 5:1 mixture of toluene/water (deoxygenated), or 5:1 DMF/water. Finally, experiments were repeated with 2 eq. of  $PhB(OH)_2$

and  $K_2CO_3$ , instead of  $K[PhBF_3]$ . All of these variations are summarized in Table 5 and 6.

Table 5. Summary of reduction experiments with  $PdCl_2(PMeBu^t_2)_2$ .

Entry	Pd(II) Complex	Boron Reagent	Solvent	Base	Temperature/°C
1	$PdCl_2(PMeBu^t_2)_2$	$K[C_6H_5BF_3]$	toluene	-	25
2	$PdCl_2(PMeBu^t_2)_2$	$K[C_6H_5BF_3]$	toluene/ $H_2O$	-	25
3	$PdCl_2(PMeBu^t_2)_2$	$K[C_6H_5BF_3]$	toluene	-	80
4	$PdCl_2(PMeBu^t_2)_2$	$K[C_6H_5BF_3]$	toluene/ $H_2O$	-	80
5	$PdCl_2(PMeBu^t_2)_2$	$C_6H_5B(OH)_2$	toluene	$K_2CO_3$	25
6	$PdCl_2(PMeBu^t_2)_2$	$C_6H_5B(OH)_2$	toluene/ $H_2O$	$K_2CO_3$	25
7	$PdCl_2(PMeBu^t_2)_2$	$C_6H_5B(OH)_2$	toluene	$K_2CO_3$	80
8	$PdCl_2(PMeBu^t_2)_2$	$C_6H_5B(OH)_2$	toluene/ $H_2O$	$K_2CO_3$	80
9	$PdCl_2(PMeBu^t_2)_2$	-	toluene/ $H_2O$	-	80
10	$PdCl_2(PMeBu^t_2)_2$	-	toluene/ $H_2O$	$K_2CO_3$	80
11 <sup>a</sup>	$PdCl_2(PMeBu^t_2)_2$	-	toluene/ $H_2O$	$K_2CO_3$	80

a) 4 eq. of  $K_2CO_3$  used

Table 6. Summary of reduction experiments with  $PdCl_2(PCy_3)_2$ .

Entry	Pd(II) Complex	Boron Reagent	Solvent	Base	Temperature/°C
1	$PdCl_2(PCy_3)_2$	$K[C_6H_5BF_3]$	toluene	-	25
2	$PdCl_2(PCy_3)_2$	$K[C_6H_5BF_3]$	toluene/ $H_2O$	-	25
3	$PdCl_2(PCy_3)_2$	$K[C_6H_5BF_3]$	toluene	-	65
4	$PdCl_2(PCy_3)_2$	$K[C_6H_5BF_3]$	toluene/ $H_2O$	-	65
5	$PdCl_2(PCy_3)_2$	$K[C_6H_5BF_3]$	DMF	-	25
6	$PdCl_2(PCy_3)_2$	$K[C_6H_5BF_3]$	DMF/ $H_2O$	-	25
7	$PdCl_2(PCy_3)_2$	$K[C_6H_5BF_3]$	DMF	-	65
8	$PdCl_2(PCy_3)_2$	$K[C_6H_5BF_3]$	DMF/ $H_2O$	-	65

## 2. 12 References

1. Panda, T. K.; Gamer, M. T.; Roesky, P. W. *Organometallics*, **2003**, *22*, 877.
2. Tatsuno, Y.; Yoshida, T.; Otsuka, S. *Inorg. Synth.* **1990**, *28*, 342.
3. Auburn, P. R.; Mackenzie, P. B.; Bosnich, B. *J. Am. Chem. Soc.* **1985**, *107*, 2033.
4. Parker, G.; Werner, H. *Helv. Chim. Acta.* **1973**, *46*, 2819.
5. Murrall, N. W.; Welch, A. J. *J. Organomet. Chem.* **1986**, *301*, 109.
6. Pleixtats, R.; Parella, T.; Pajuelo, F.; Moreno-Manás, M.; Malet, R. *Magn. Res. Chem.* **1997**, *35*, 227.
7. Yoshida, T.; Otsuka, S. *Inorg. Synth.* **1990**, *28*, 113.
8. Grushin, V. V.; Bensimon, C.; Alper, H. *Inorg. Chem.* **1994**, *33*, 4804.
9. Dai, C.; Fu, G. C. *J. Am. Chem. Soc.* **2001**, *123*, 2719.
10. Kirchoff, J. H.; Netherton, M.R.; Hills, I.D.; Fu, G.C. *J. Am. Chem. Soc.* **2002**, *124*, 13662.
11. Mann, B. E.; Shaw, B. L.; Slade, R. M. *J. Chem. Soc. A: Inorg. Phys. Theor.* **1971**, 2976.
12. Stambuli, J. P.; Incarvito, C. D.; Bühl, M.; Hartwig, J. F. *J. Am. Chem. Soc.* **2004**, *126*, 1184.
13. Drew, D.; Doyle, J. R. *Inorg. Synth.* **1972**, *13*, 47.
14. Goel, R. G.; Montemayor, R. G. *Inorg. Chem.* **1977**, *16*, 2183.
15. Potyen, M.C.; Rothwell, I. P. *J. Chem. Soc. Chem. Comm.* **1995**, 849.

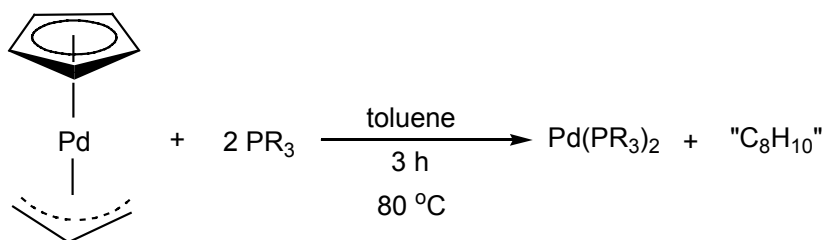
16. Van Gaal, H.L.M.; Van den Bekerom, F. L.A. *J. Organomet. Chem.* **1977**, *134*, 237.
17. Grice, D.; Harvey, P.J.; Jenkins, I.D.; Gallagher, M.J.; Ranasinghe, M.G. *Tet. Lett.* **1996**, *37*, 1087.

## Chapter 3

### Results and Discussion

#### 3.1 *In Situ* Generation of PdL<sub>n</sub> from Pd( $\eta^3$ -C<sub>3</sub>H<sub>5</sub>)( $\eta^5$ -C<sub>5</sub>H<sub>5</sub>)

The primary goal of this research was to determine the optimum conditions under which PdL<sub>2</sub> (L = PCy<sub>3</sub>, PMeBu<sup>t</sup><sub>2</sub>, PBu<sup>t</sup><sub>3</sub>) is generated cleanly and quantitatively. The synthetic preparation described by Otsuka *et al.*<sup>1</sup> for these phosphines was chosen as a starting point from which to begin optimization studies of PdL<sub>2</sub> formation (Scheme 33). A series of both <sup>1</sup>H and <sup>31</sup>P NMR monitoring experiments was performed in which one or two equivalents of different phosphines (L = PCy<sub>3</sub>, PMeBu<sup>t</sup><sub>2</sub>, PBu<sup>t</sup><sub>3</sub>) were mixed with a toluene-d<sub>8</sub> solution of Pd( $\eta^3$ -C<sub>3</sub>H<sub>5</sub>)( $\eta^5$ -C<sub>5</sub>H<sub>5</sub>). These experiments were performed at both room temperature and elevated temperature (60 – 80 °C) to assess the conditions for PdL<sub>2</sub> generation. Additionally, these experiments were repeated with PMe<sub>3</sub> and PPh<sub>3</sub> with the goal of observing PdL<sub>n</sub> (n = 2 - 4) formation.



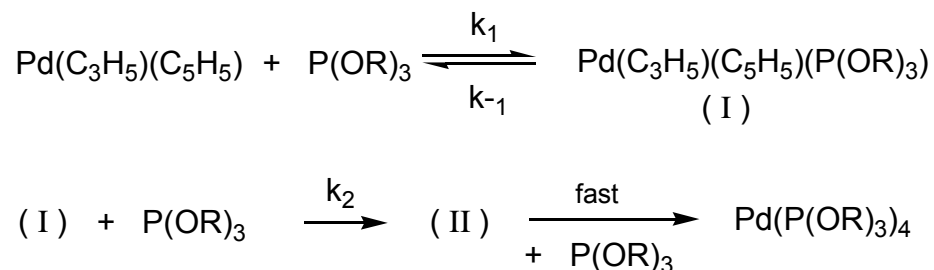
Scheme 33. Preparation of PdL<sub>2</sub> from Pd( $\eta^3$ -C<sub>3</sub>H<sub>5</sub>)( $\eta^5$ -C<sub>5</sub>H<sub>5</sub>) (PR<sub>3</sub> = PCy<sub>3</sub>, PPhBu<sup>t</sup><sub>2</sub>, PBu<sup>t</sup><sub>3</sub>).<sup>1</sup>

At the time that this procedure for the synthesis of PdL<sub>2</sub> was reported, ligand displacement reactions of Pd( $\eta^3$ -2-R-C<sub>3</sub>H<sub>4</sub>)( $\eta^5$ -C<sub>5</sub>H<sub>5</sub>) (R = H, Me, Bu<sup>t</sup>) with

phosphines  $\text{PR}_3$  ( $\text{R} = \text{Ph}, \text{Pr}^i, \text{Me}, \text{Ph}_2\text{Me}, \text{PhMe}_2, \text{Bu}^n$ ) and phosphites  $\text{P}(\text{OR})_3$  ( $\text{R} = \text{Me}, \text{Et}, \text{Ph}, o\text{-tol}$ ) were the subject of several reports by Werner *et al.*<sup>2</sup> These studies revealed that a significant degree of complexity exists in the displacement reactions of  $\text{Pd}(\eta^3\text{-2-R-C}_3\text{H}_4)(\eta^5\text{-C}_5\text{H}_5)$ . As a result, some of the previously reported work was herein reexamined in order to better understand these systems in the context of clean and quantitative  $\text{PdL}_2$  generation monitored by NMR spectroscopy. Furthermore, much of the work of Werner *et al.* focused on reactions of  $\text{Pd}(\eta^3\text{-2-RC}_3\text{H}_4)(\eta^5\text{-C}_5\text{H}_5)$  when  $\text{R} = \text{Me}$ , leaving an incomplete assessment of the systems involving the more reactive  $\text{Pd}(\eta^3\text{-C}_3\text{H}_5)(\eta^5\text{-C}_5\text{H}_5)$ .<sup>29,3</sup> A summary of the relevant findings revealed by previous work in the area is thus beneficial prior to the examination of the current results.

### 3.1.1. Displacement Reactions of $\text{Pd}(\eta^3\text{-C}_3\text{H}_5)(\eta^5\text{-C}_5\text{H}_5)$ Complexes

In their initial work, Werner *et al.* studied the kinetics of ligand displacement reactions of  $\text{Pd}(\eta^3\text{-2-R-C}_3\text{H}_4)(\eta^5\text{-C}_5\text{H}_5)$  ( $\text{R} = \text{H}$ ) with phosphite  $\text{P}(\text{OR})_3$  ( $\text{R} = \text{Ph}$ ) and determined that displacement proceeds according to a second order rate law.<sup>1i</sup> This led to a mechanistic proposal in which the first step of ligand displacement is the reversible formation of an intermediate species (I), from nucleophilic attack of  $\text{P}(\text{OR})_3$  (Scheme 34).<sup>1i</sup> A secondary, unidentified intermediate (II) was proposed, eventually resulting in the formation of  $\text{Pd}(\text{P}(\text{OPh})_3)_4$ .



Scheme 34. Initial mechanism proposed for ligand displacement of  $\text{Pd}(\eta^3\text{-C}_3\text{H}_5)(\eta^5\text{-C}_5\text{H}_5)$  by  $\text{P}(\text{OR})_3$  ( $\text{R} = \text{Ph}$ ).<sup>11</sup>

Further NMR investigations showed that the reaction of  $\text{Pd}(\eta^3\text{-2-R-C}_3\text{H}_4)(\eta^5\text{-C}_5\text{H}_5)$  ( $\text{R} = \text{CH}_3$ ) with phosphites  $\text{P}(\text{OR})_3$  ( $\text{R} = \text{Et, Me Ph}$ ) at low temperature yields a  $\eta^1$ -allyl complex as primary intermediate (I) (Figure 8).<sup>29</sup> Several of these complexes were successfully isolated at  $-6\text{ }^\circ\text{C}$  and characterized by  $^1\text{H}$  NMR. The  $^1\text{H}$  NMR data for  $\text{Pd}(\eta^1\text{-2-CH}_3\text{-C}_3\text{H}_4)(\eta^5\text{-C}_5\text{H}_5)(\text{P}(\text{OMe})_3)$ ,<sup>29</sup> along with that of other significant intermediate species, are summarized in Table 7.

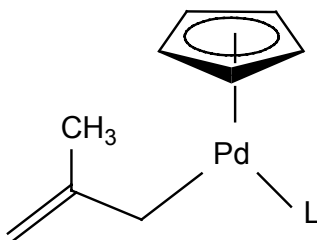
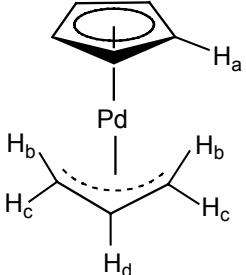
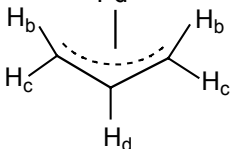
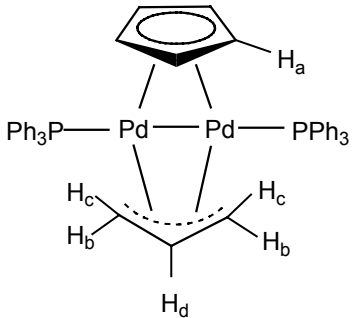
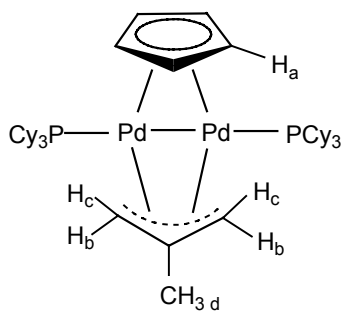
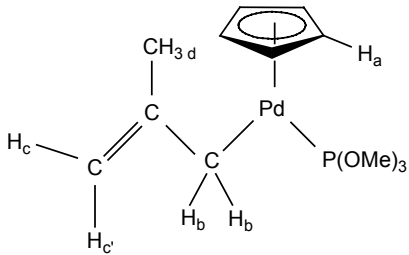


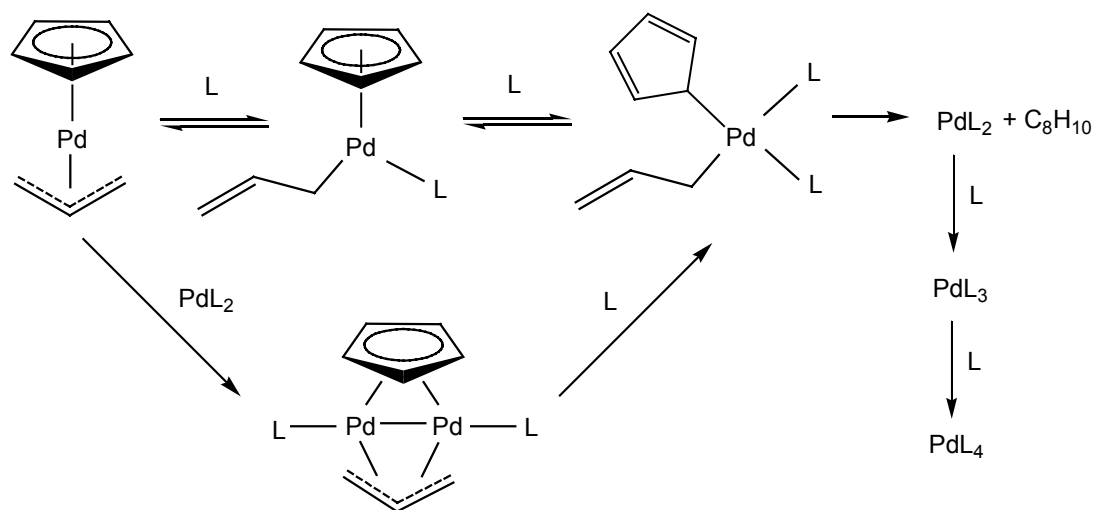
Figure 8. The  $\eta^1$ -allyl complex  $\text{Pd}(\eta^3\text{-2-R-C}_3\text{H}_4)(\eta^5\text{-C}_5\text{H}_5)$  isolated as primary intermediate (I) ( $\text{L} = \text{P}(\text{OEt})_3, \text{P}(\text{OMe})_3, \text{P}(\text{OPh})_3$ ).<sup>29</sup>

Table 7. Relevant Species described by Werner *et al.*<sup>2</sup>

Species	$\delta$ <sup>1</sup> H NMR	Notes	Reference
	H <sub>a</sub> 5.73 (s) H <sub>b</sub> 2.07 (d) H <sub>c</sub> 3.38 (d) H <sub>d</sub> 4.52 (tt)	C <sub>6</sub> D <sub>6</sub> 25 °C	2g
	H <sub>a</sub> 5.80 (s) H <sub>b</sub> 2.09 (d) H <sub>c</sub> 3.42 (d) H <sub>d</sub> 4.60 (tt)	C <sub>7</sub> D <sub>8</sub> 25 °C	this work
	Ph not given H <sub>a</sub> 5.42 (t, $J_{PH} = 1.5$ Hz) H <sub>b</sub> 2.18 (q, $J_{PH}, J_{HH} = 8$ Hz) H <sub>c</sub> 0.8 (d, $J_{HH} = 12$ Hz) H <sub>d</sub> 2.85 (m)	CD <sub>2</sub> Cl <sub>2</sub>	2a
	Cy not given H <sub>a</sub> 5.95 (t, $J_{PH} = 1.5$ Hz) H <sub>b</sub> 3.05 (t, $J_{PH} = 5.5$ Hz) H <sub>c</sub> 2.1 (br.s) H <sub>d</sub> 1.47 (t, $J_{PH} = 3$ Hz)	C <sub>6</sub> D <sub>6</sub>	2b
	H <sub>a</sub> 5.62 (d, $J_{PH} = 1.7$ Hz) H <sub>b</sub> 2.70 (br.d, $J_{PH} = 6.5$ Hz) H <sub>c,c'</sub> 4.97, 4.54 (m) H <sub>d</sub> 1.95 (s)	C <sub>7</sub> D <sub>8</sub> -6 °C	2g



Through their continued efforts to isolate  $\eta^1$ -allyl intermediates, equimolar quantities of  $\text{Pd}(\eta^3\text{-2-R-C}_3\text{H}_4)(\eta^5\text{-C}_5\text{H}_5)$  ( $\text{R} = \text{CH}_3$ ) and  $\text{L}$  ( $\text{L} = \text{PPh}_3, \text{P(OPh)}_3, \text{P(OMe)}_3$ ) were combined at room temperature, producing unanticipated dinuclear metal complexes of the type  $\text{Pd}_2\text{L}_2(\mu\text{-2-R-C}_3\text{H}_4)(\mu\text{-C}_5\text{H}_5)$ .<sup>2a,b,d,f,j</sup> Further investigations resulted in the overall proposed mechanism shown in Scheme 35.<sup>2d,e</sup>



Scheme 35. Reaction sequence in the formation of  $\text{PdL}_2$  from  $\text{Pd}(\eta^3\text{-C}_3\text{H}_5)(\eta^5\text{-C}_5\text{H}_5)$ .<sup>2d,e</sup>

One must remain cognizant of many of the above mentioned findings during the analysis of the systems described in this work. Firstly, one must anticipate the existence of a  $\eta^1$ -allyl species,  $\text{Pd}(\eta^1\text{-CH}_2\text{CH=CH}_2)(\eta^5\text{-C}_5\text{H}_5)(\text{L})$ , as a primary intermediate in the formation of  $\text{PdL}_2$ . At the temperatures utilized in this work (mainly 25 °C to 80 °C) such an intermediate may undergo rapid equilibration with  $\text{Pd}(\eta^3\text{-C}_3\text{H}_5)(\eta^5\text{-C}_5\text{H}_5)$  and  $\text{L}$ , producing a dynamic NMR spectrum that may demonstrate a series of time-averaged resonances.

Further complicating these systems, the later work of Werner *et al.* showed that reactions of  $\text{Pd}(\eta^3\text{-2-R-C}_3\text{H}_4)(\eta^5\text{-C}_5\text{H}_5)$  ( $\text{R} = \text{Me, Bu}^t$ ) with phosphines  $\text{L}$  ( $\text{L} = \text{PPr}^i_3, \text{PCy}_3, \text{P}^t\text{BuPh}_2, \text{PCy}_2\text{Ph, P}^i\text{Bu}_3$ ) can produce a primary intermediate that is in fact a mixture of two isomers, involving a simultaneous  $\pi\text{-}\sigma$  shift of each of the organic ligands (Figure 9).<sup>2c,h</sup> The constant for the isomerization equilibrium was calculated to be  $K_{\text{eq}} = 1.39$  for the reaction of  $\text{Pd}(\eta^3\text{-2-CH}_3\text{-C}_3\text{H}_4)(\eta^5\text{-C}_5\text{H}_5)$  with  $\text{PCy}_2\text{Ph}$  at 292 K, indicating a slight prevalence of  $\eta^1\text{-allyl-}\eta^5\text{-Cp}$  isomer at ambient temperature.<sup>2h</sup> The value for  $K_{\text{eq}}$  was found to increase to 2.33 at 333 K<sup>2h</sup>, thus setting a precedent for the currently observed systems (at 25 °C - 80 °C). Should this type of isomerization exist for the primary intermediate, one must again anticipate a dynamic NMR spectrum, depending upon the rate of exchange between the isomers. Should the rate of exchange be slow compared to that of the NMR timescale, one would expect to see distinct resonances for both  $\eta^1\text{-allyl-}\eta^5\text{-Cp}$  and  $\eta^3\text{-allyl-}\eta^1\text{-Cp}$  isomers. However, as the work of Werner suggests,<sup>2c</sup> the rate of isomerization at room temperature may be comparable to that of the NMR timescale, producing broadened resonances which represent an average of the resonances expected for each of the species in a static (low temperature) spectrum. In either case, the possibility of simultaneously isomerizing  $\eta^1\text{-allyl-}\eta^5\text{-Cp}$  and  $\eta^3\text{-allyl-}\eta^1\text{-Cp}$  isomers must be anticipated, adding a degree of complexity to the obtained NMR data in the currently examined systems.

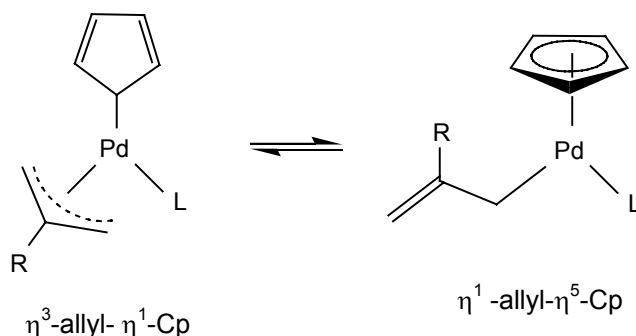


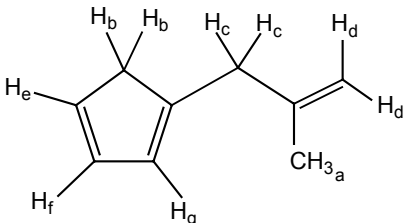
Figure 9. Simultaneous  $\pi$ - $\sigma$  isomerization of the primary intermediate (I) (R = Me, Bu<sup>t</sup>, L = PPr'<sub>3</sub>, PCy<sub>3</sub>, PBu<sup>t</sup>Ph<sub>2</sub>, PCy<sub>2</sub>Ph, PBu'<sub>3</sub>).<sup>2c,h</sup>

These are not the only instances in which resonance broadening may be observed in the obtained NMR spectra. Studies of the solution stoichiometry of Pd(PCy<sub>3</sub>)<sub>2</sub> in the presence of additional PCy<sub>3</sub> indicate that the complex can undergo rapid phosphine exchange at room temperature, producing broadened <sup>31</sup>P NMR resonances.<sup>4</sup> This behaviour is confirmed in this work and the current study indicates similar behaviour for Pd(PMeBu<sup>t</sup><sub>2</sub>)<sub>2</sub> (Section 3.3). In addition, Pd(PPh<sub>3</sub>)<sub>4</sub> has been shown to undergo exchange and also dissociate in solution, existing predominantly as Pd(PPh<sub>3</sub>)<sub>3</sub>, which in turn can dissociate to form Pd(PPh<sub>3</sub>)<sub>2</sub>.<sup>4,5,6</sup> Rapid phosphine exchange has also been noted for Pd(PMe<sub>3</sub>)<sub>4</sub> in the presence of free PMe<sub>3</sub>. Such ligand exchange and the resulting broadening of any observed <sup>31</sup>P NMR resonances must therefore be anticipated during the examination of these systems.

One must also consider the reductive elimination product "C<sub>8</sub>H<sub>10</sub>" in the currently examined systems. Previous work with Pd( $\eta^3$ -2-R-C<sub>3</sub>H<sub>4</sub>)( $\eta^5$ -C<sub>5</sub>H<sub>5</sub>) (R = CH<sub>3</sub>) indicated that the reductive elimination product (methylallyl-cyclopentadiene) isomerizes by 1,5-hydride shift, producing several isomeric side

products.<sup>29</sup> Parker and Werner thus synthesized and characterized 1-(2-methylallyl)cyclopentadiene to serve as a model compound for these products.<sup>29</sup> The <sup>1</sup>H NMR data are summarized in Table 8, as a means of comparison to the work described herein.

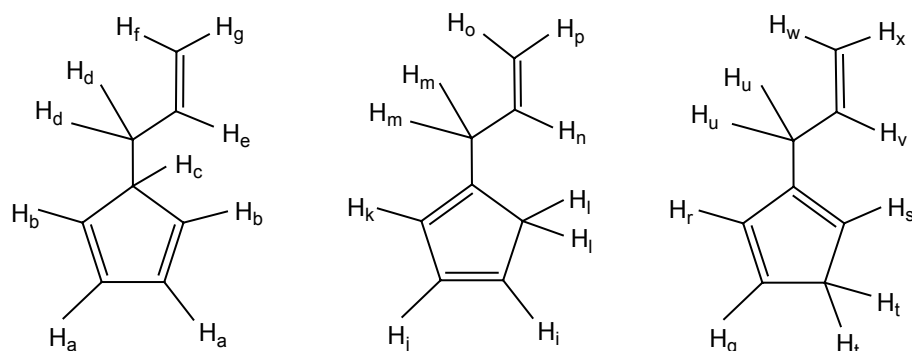
Table 8. <sup>1</sup>H NMR assignment for 1-(2-methylallyl)cyclopentadiene in CDCl<sub>3</sub>.<sup>29</sup>

Structure	δ
	H <sub>a</sub> 1.7 H <sub>b</sub> 2.77 H <sub>c</sub> 3.09 H <sub>d</sub> 4.7 H <sub>e,f,g</sub> 6.6 - 6.1

It is anticipated that similar products (allyl-cyclopentadiene and related isomers) will emerge in the current systems, potentially obscuring many regions of the <sup>1</sup>H NMR spectrum. In order to better identify the reductive elimination species, the approximate <sup>1</sup>H NMR chemical shifts of 5-allylcyclopentadiene (isomer A) and related isomers (isomers B and C) were simulated and summarized in Table 9.<sup>7,8</sup> The <sup>1</sup>H NMR chemical shifts of these potential reductive elimination products were calculated using the method summarized by Silverstein *et al.*,<sup>7</sup> which utilizes tabulated substituent constants for a variety of R groups (*gem*, *trans* and *cis* groups) to calculate the approximate chemical shift of an olefinic proton. A more thorough simulation of the <sup>1</sup>H NMR spectrum of each of these products was performed using ACD Labs <sup>1</sup>H NMR Predictor software,<sup>8</sup> which utilizes a

database of approximately 200,000 experimentally obtained  $^1\text{H}$  NMR spectra upon which to estimate the chemical shifts of an entered chemical structure.

Table 9. Simulated  $^1\text{H}$  NMR chemical shifts for allyl-cyclopentadiene isomers.<sup>7,8</sup>



Isomer A		Isomer B		Isomer C	
	$\delta$		$\delta$		$\delta$
H <sub>a</sub>	6.3	H <sub>h</sub>	6.0	H <sub>q</sub>	6.2
H <sub>b</sub>	6.3	H <sub>i</sub>	6.0	H <sub>r</sub>	6.4
H <sub>c</sub>	3.0	H <sub>j</sub>	6.3	H <sub>s</sub>	6.1
H <sub>d</sub>	2.1	H <sub>k</sub>	2.9	H <sub>t</sub>	3.0
H <sub>e</sub>	5.8	H <sub>l</sub>	3.0	H <sub>u</sub>	2.9
H <sub>f</sub>	4.9	H <sub>m</sub>	5.8	H <sub>v</sub>	5.9
H <sub>g</sub>	5.2	H <sub>n</sub>	5.1	H <sub>w</sub>	5.1
		H <sub>o</sub>	5.0	H <sub>x</sub>	5.2

Additional complexity in the NMR monitoring of these systems arises from the choice of phosphine (e.g.  $\text{PCy}_3$ ), as its resonances can obscure portions of the  $^1\text{H}$  NMR spectrum. This is particularly relevant when attempting to assign the  $^1\text{H}$  resonances of dinuclear species, which are shifted upfield significantly from  $\text{Pd}(\eta^3\text{-C}_3\text{H}_5)(\eta^5\text{-C}_5\text{H}_5)$ .<sup>2a,b,d,f,j</sup> Emerging  $^1\text{H}$  resonances associated with the isomeric reductive elimination products also result in many overlapping  $^1\text{H}$  NMR signals.

The research efforts described in this work, driven by the desire for the optimization of the conditions for PdL<sub>2</sub> generation, are far from exhaustive in providing a clear picture of these complex systems. An analysis of these systems was performed using several phosphines (PCy<sub>3</sub>, PMeBu<sup>t</sup><sub>2</sub>, PBu<sup>t</sup><sub>3</sub>, PPh<sub>3</sub>, PMe<sub>3</sub>) noting the likely intermediates (when possible) and the ideal conditions in which one can cleanly and completely generate PdL<sub>2</sub>. Chemical shifts of representative η<sup>1</sup>-allyl and dinuclear species described in the literature are used as the best possible precedent to identify likely species in the presently examined systems (Table 7).

### 3.1.2 Generation of PdL<sub>2</sub> (L= PCy<sub>3</sub>, P MeBu<sup>t</sup><sub>2</sub>, PBu<sup>t</sup><sub>3</sub>)

Conversion of Pd(η<sup>3</sup>-C<sub>3</sub>H<sub>5</sub>)(η<sup>5</sup>-C<sub>5</sub>H<sub>5</sub>) to the 2:1 compounds was expected to proceed as described above in Scheme 35.<sup>2</sup> The following describes the results of each NMR monitoring experiment according to each phosphine used.

#### 3.1.2.1 L = PCy<sub>3</sub>

Reactions of Pd(η<sup>3</sup>-C<sub>3</sub>H<sub>5</sub>)(η<sup>5</sup>-C<sub>5</sub>H<sub>5</sub>) with two equivalents of PCy<sub>3</sub> (δ 10.0) at 25 °C (Figure 10) were monitored by <sup>31</sup>P NMR spectroscopy and found to proceed slowly to produce a species exhibiting a <sup>31</sup>P resonance at δ 27.8, attributable to the corresponding dinuclear species.<sup>2</sup> In addition, an extremely broad resonance at δ 54.6 was present, barely visible in the baseline, possibly representing an η<sup>1</sup>-allyl intermediate, such as that seen above in Table 7.<sup>2c</sup>

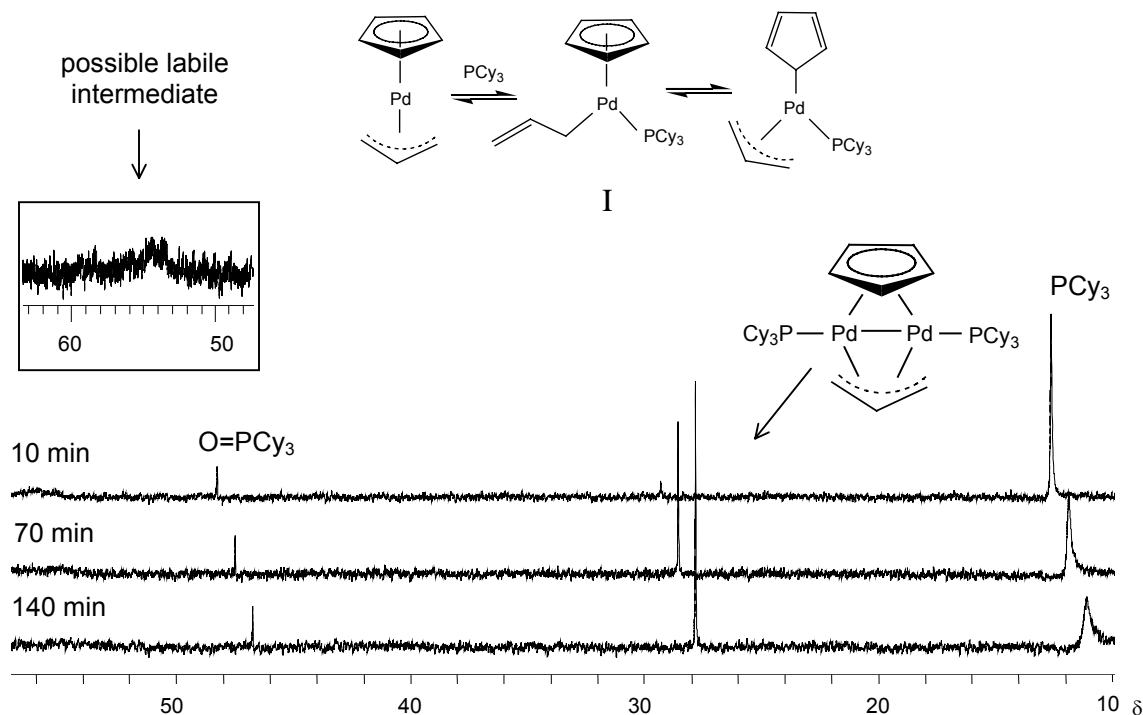


Figure 10. Stacked plots of  $^{31}\text{P}$  NMR spectra (163.0 MHz) for reaction of  $\text{Pd}(\eta^3\text{-C}_3\text{H}_5)(\eta^5\text{-C}_5\text{H}_5)$  with two equivalents  $\text{PCy}_3$  in toluene- $d_8$  at 25 °C.

This resonance was thought to be broadened due to the equilibration of the starting material  $\text{Pd}(\eta^3\text{-C}_3\text{H}_5)(\eta^5\text{-C}_5\text{H}_5)$  and the anticipated primary intermediate I (Figure 10). This broadening may also be explained by the possible isomerization of the primary intermediate I between  $\eta^1\text{-allyl-}\eta^5\text{-Cp}$  and  $\eta^3\text{-allyl-}\eta^1\text{-Cp}$  coordination (Figure 10).<sup>2c,h</sup> In either case, the rate of exchange is likely comparable to the NMR timescale, producing broadened resonances. The slow disappearance of this broad peak occurred over the course of four hours. The resonance at  $\delta$  54.6 in the currently studied system is similar to that observed in systems such as  $\text{Pd}(\eta^3\text{-2-Me-C}_3\text{H}_4)(\eta^5\text{-C}_5\text{H}_5)/\text{PPr}^i_3$  ( $\delta$  59.6)<sup>2c</sup> and  $\text{Pd}(\eta^3\text{-2-Bu}^t$

$\text{C}_3\text{H}_4)(\eta^5\text{-C}_5\text{H}_5)/\text{PPr}^i_3$  ( $\delta$  51.2).<sup>2c</sup> However, while the  $\text{Pd}(\eta^3\text{-2-Me-C}_3\text{H}_4)(\eta^5\text{-C}_5\text{H}_5)/\text{PPr}^i_3$  system was shown to involve rapidly equilibrating  $\eta^1\text{-allyl-}\eta^5\text{-Cp}$  and  $\eta^3\text{-allyl-}\eta^1\text{-Cp}$  species, that derived from the  $\text{Pd}(\eta^3\text{-2-Bu}^t\text{-C}_3\text{H}_4)(\eta^5\text{-C}_5\text{H}_5)/\text{PPr}^i_3$  system was found to be exclusively an  $\eta^3\text{-allyl-}\eta^1\text{-Cp}$  species. The exact nature of the species observed in this system at  $\delta$  54.6 thus remains unconfirmed by experiments conducted at 25 °C.

No  $^{31}\text{P}$  NMR resonance was observed at  $\delta$  39.4 ( $\text{Pd}(\text{PCy}_3)_2$ )<sup>9</sup> in the  $^{31}\text{P}$  NMR monitoring of the  $\text{Pd}(\eta^3\text{-C}_3\text{H}_5)(\eta^5\text{-C}_5\text{H}_5)/\text{PCy}_3$  system, although after two hours a broad resonance at this chemical shift was seen. After approximately five hours, the dinuclear species appears to be the major component in solution ( $\delta$  27.8).<sup>2</sup> Additionally, the signal observed at  $\delta$  47.6 is due to  $\text{O}=\text{PCy}_3$ , confirmed by literature<sup>10</sup> as well as an independent oxidation of a sample of  $\text{PCy}_3$  (Section 2.4.1.6).

Several significant features were observed in the associated  $^1\text{H}$  NMR spectra obtained over the course of the reaction (Figure 11 and 12). The Cp resonance ( $\text{H}_a$ ,  $\delta$  5.81) for the starting material,  $\text{Pd}(\eta^3\text{-C}_3\text{H}_5)(\eta^5\text{-C}_5\text{H}_5)$ , was replaced by a broadened resonance at  $\delta$  5.84 labeled I (see Figure 11). This broadened resonance initially increased and subsequently diminished in intensity over the course of the reaction, consistent with the formation of a fluxional primary intermediate species and likely corresponds to the intermediate species with  $^{31}\text{P}$  NMR  $\delta$  54.6 (see above). As reported previously for other phosphines,<sup>2c</sup> and mentioned above,  $\text{Pd}(\eta^3\text{-C}_3\text{H}_5)(\eta^5\text{-C}_5\text{H}_5)$  may react with  $\text{PCy}_3$  to



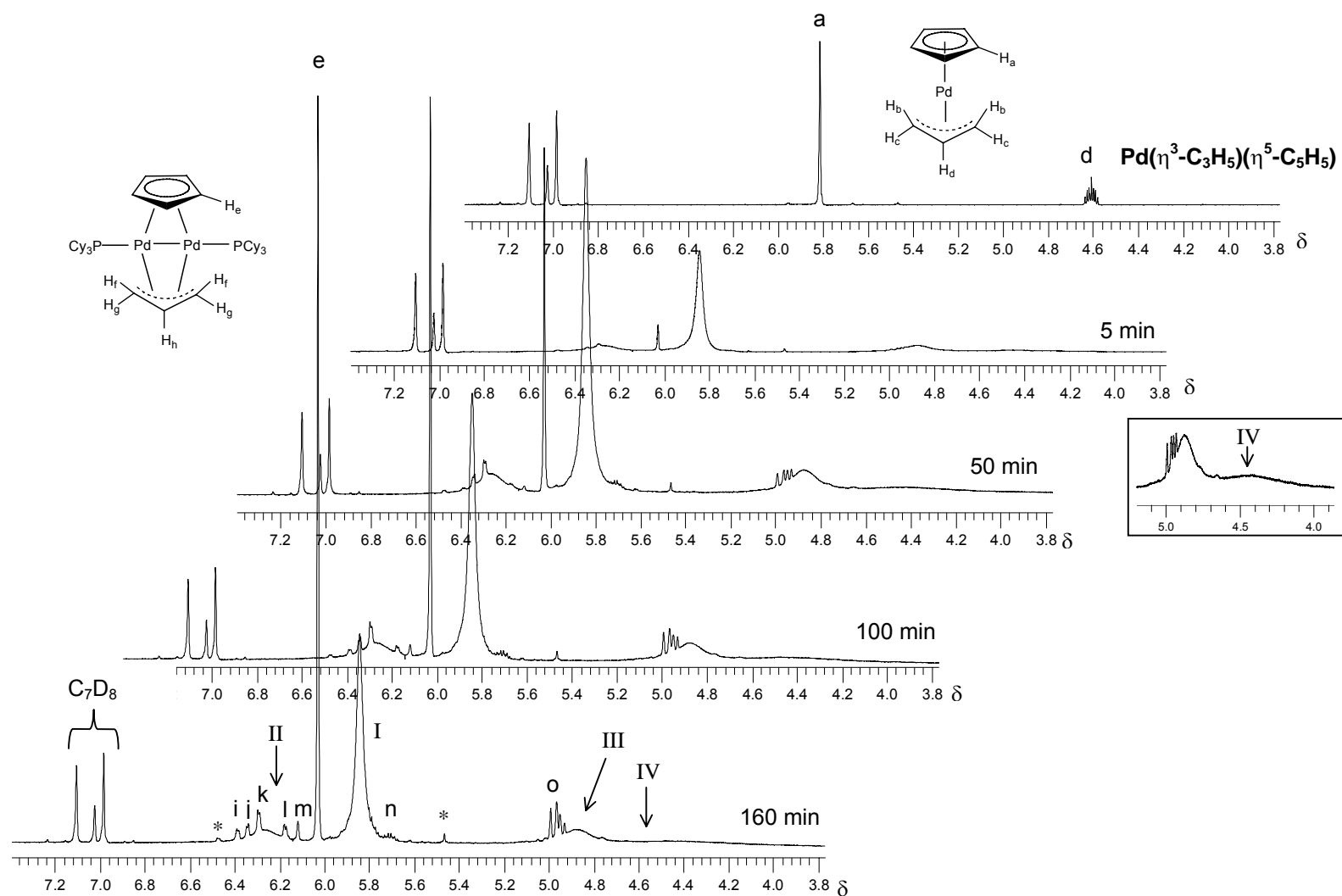


Figure 11. Stacked plots of  $^1\text{H}$  NMR spectra ( $\delta$  3.8 – 7.2; 600 MHz) for the reaction of  $\text{Pd}(\eta^3\text{-C}_3\text{H}_5)(\eta^5\text{-C}_5\text{H}_5)$  with two equivalents of  $\text{PCy}_3$  in toluene- $d_8$  at 25  $^\circ\text{C}$  (\* indicated unidentified resonances).

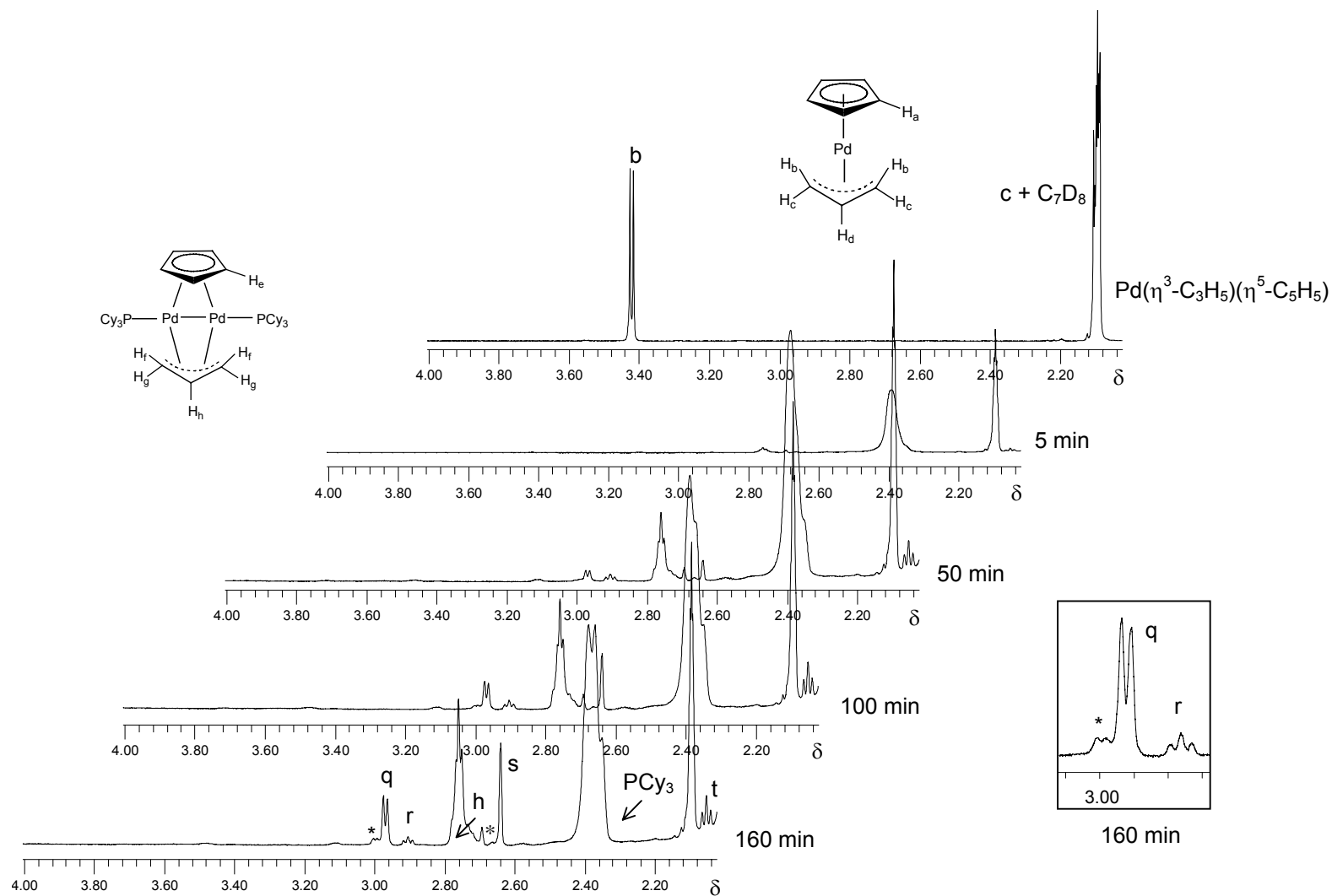


Figure 12. Stacked plots of  $^1\text{H}$  NMR spectra ( $\delta$  2.0 – 4.0; 600 MHz) for the reaction of  $\text{Pd}(\eta^3\text{-C}_3\text{H}_5)(\eta^5\text{-C}_5\text{H}_5)$  with two equivalents of  $\text{PCy}_3$  in  $\text{toluene-d}_8$  at  $25^\circ\text{C}$  (\* indicates unidentified resonances).

reversibly produce a primary intermediate species and this rapid equilibration between  $\text{Pd}(\eta^3\text{-C}_3\text{H}_5)(\eta^5\text{-C}_5\text{H}_5)$  and  $\text{PCy}_3$  and primary intermediate produces broadened, time averaged resonances in the  $^1\text{H}$  NMR spectrum. Additionally, the observed broadening could be due to the simultaneous isomerization of the primary intermediate between  $\eta^1\text{-allyl-}\eta^5\text{-Cp}$  and  $\eta^3\text{-allyl-}\eta^1\text{-Cp}$  coordination modes, producing time-averaged  $^1\text{H}$  NMR resonances of the individual  $\eta^1\text{-allyl-}\eta^5\text{-Cp}$  and  $\eta^3\text{-allyl-}\eta^1\text{-Cp}$  intermediates (Figure 10).<sup>2c,h</sup>

Several other broadened resonances in the  $^1\text{H}$  NMR spectra support the existence of rapidly equilibrating or fluxional species. Two of these broad resonances were observed at  $\delta$  6.26 (II) and 4.86 (III), while the third, barely visible, appeared in the region around  $\delta$  4.43 (IV). Given the broadening observed, it is not possible to provide a definitive assignment of the intermediate species at 25 °C. However, it can be said that the resonances present are not consistent with a static, stable  $\eta^1\text{-allyl}$  intermediate (see Table 7 above). The broadened resonances labeled III and IV could possibly be the terminal  $\text{CH}_2=$  protons of a rapidly equilibrating  $\eta^1\text{-allyl}$  species ( $\delta$  4.97, 4.54 in Table 7). However, the additional broadened resonance at  $\delta$  6.26 (II), possibly a time averaged Cp resonance, supports the possibility of a rapidly isomerizing primary intermediate where both  $\eta^1\text{-allyl-}\eta^3\text{-Cp}$  and  $\eta^3\text{-allyl-}\eta^1\text{-Cp}$  isomers were present. Previously reported work indicates that equimolar quantities of  $\text{Pd}(\eta^3\text{-2-Me-C}_3\text{H}_4)(\eta^5\text{-C}_5\text{H}_5)$  and  $\text{PCy}_3$  produce such an intermediate species.<sup>2c,h</sup> The reported NMR data in toluene- $d_8$  at  $-60$  °C showed a Cp resonance at  $\delta$  5.66 for the isomer with  $\eta^1\text{-allyl-}\eta^3\text{-Cp}$  coordination, and a second Cp resonance at  $\delta$

6.60 for the  $\eta^3$ -allyl- $\eta^1$ -Cp isomer.<sup>2c</sup> The additional broadened resonance at  $\delta$  6.26 (II) observed in the current system may represent the  $\eta^1$ -Cp resonance of a  $\eta^3$ -allyl- $\eta^1$ -Cp isomer, rapidly equilibrating with  $\eta^1$ -allyl- $\eta^3$ -Cp, possibly at  $\delta$  5.84. One might anticipate, however, coalescence of these Cp resonances at room temperature, as was reported for the  $\text{Pd}(\eta^3\text{-2-Me-C}_3\text{H}_4)(\eta^5\text{-C}_5\text{H}_5)/(\text{PCy}_3)$  system. A low temperature examination of the current system was not performed and would be required to assign the above mentioned resonances with certainty.

A sharp Cp singlet appeared at  $\delta$  6.03 (Figure 11), which increased in intensity over the course of the reaction. In a separate experiment, this resonance showed a correlation by HSQC to a  $^{13}\text{C}$  resonance at  $\delta$  89.4. These  $^1\text{H}$  and  $^{13}\text{C}$  resonances are typical of a coordinated  $\eta^5\text{-C}_5\text{H}_5$  ligand ( $\text{H}_e$ ) in a dinuclear species  $\text{Pd}_2(\text{PCy}_3)_2(\mu\text{-C}_3\text{H}_5)(\mu\text{-C}_5\text{H}_5)$  (Figure 11).<sup>2b</sup>

The resonances of the allyl protons of the dinuclear species cannot be assigned with certainty, due to overlap with both  $\text{PCy}_3$  and reductive elimination products (Figure 12). It was anticipated that the allyl protons f, g, and h would each exhibit a complex multiplet pattern resulting from coupling to adjacent protons, as well as coupling to phosphorus, as has been observed in the literature (see Table 7).<sup>2a,b,d,f,j</sup> The resonance observed at  $\delta$  2.76 (labeled h) possibly represents the central allyl proton, showing a COSY correlation to a resonance at  $\delta$  1.10, perhaps representative of  $\text{H}_f$ . However, precedent dinuclear species suggest that protons f and g should appear further downfield ( $\delta$  2.10 and 3.05 respectively).<sup>2a,b,d,f,j</sup> In addition, the resonance  $\delta$  2.76 appeared to overlap with a second resonance, possibly from  $\text{PCy}_3$ . A  $\text{PCy}_3$  resonance in this region

would be expected to show COSY correlation to other PCy<sub>3</sub> resonances, such as those in the region of  $\delta$  1.10. The PCy<sub>3</sub> protons appear to shift downfield from free PCy<sub>3</sub> ( $\delta$  1.10 – 1.19) upon coordination to palladium, as can be seen by the strong resonance that appeared at  $\delta$  2.40. As a result, the resonances in the anticipated allyl region for the dinuclear species cannot be assigned with certainty from the current NMR spectra.

One can identify several small yet distinct resonances that emerged over the reaction (Figure 11 and 12), consistent with the formation of reductive elimination products, C<sub>5</sub>H<sub>5</sub>-C<sub>3</sub>H<sub>5</sub>, formed as a mixture of isomers.<sup>2d,g</sup> Those labeled i ( $\delta$  6.39), j ( $\delta$  6.34), k ( $\delta$  6.29), l ( $\delta$  6.18) and m ( $\delta$  6.12) correspond to the cyclopentadiene protons of these products as seen in Table 9. The presence of more than two signals in this region suggests that the initial reductive elimination product, 5-allylcyclopentadiene (isomer A), has isomerized over the course of the reaction, producing 1-allylcyclopentadiene and 2-allylcyclopentadiene (isomer B and C respectively). Regions of the spectra labeled n ( $\delta$  5.68-5.75) and o ( $\delta$  4.93-5.00) correspond to vinyl protons CH=CH<sub>2</sub> and CH=CH<sub>2</sub> respectively (Figure 11). Several signals of similar intensity in the region  $\delta$  2.00-3.00 (q,r,s,t) are consistent with methylene protons CH<sub>2</sub>CH=CH<sub>2</sub> as well as the methylene protons of the cyclopentadiene ring.

The reaction of Pd( $\eta^3$ -C<sub>3</sub>H<sub>5</sub>)( $\eta^5$ -C<sub>5</sub>H<sub>5</sub>) with two equivalents of PCy<sub>3</sub> thus suggests the existence of an intermediate species ( $\eta^1$ -allyl- $\eta^5$ -Cp and possibly isomerizing to  $\eta^3$ -allyl- $\eta^1$ -Cp), as well as a dominant dinuclear species Pd<sub>2</sub>(PCy<sub>3</sub>)<sub>2</sub>( $\mu$ -C<sub>3</sub>H<sub>5</sub>)( $\mu$ -C<sub>5</sub>H<sub>5</sub>) at 25 °C. Consequently, the described Pd( $\eta^3$ -

$C_3H_5(\eta^5-C_5H_5)/PCy_3$  system at 25 °C does not represent optimal conditions for the efficient generation of the desired  $Pd(PCy_3)_2$ . The same system was subsequently monitored at 65 °C and 77 °C in order to assess the generation of  $Pd(PCy_3)_2$  at elevated temperatures.

At 65 °C, the dinuclear species  $Pd_2(PCy_3)_2(\mu-C_3H_5)(\mu-C_5H_5)$  is slowly consumed to produce the anticipated 2:1 product  $Pd(PCy_3)_2$  ( $\delta$  39.4) (Figure 13).

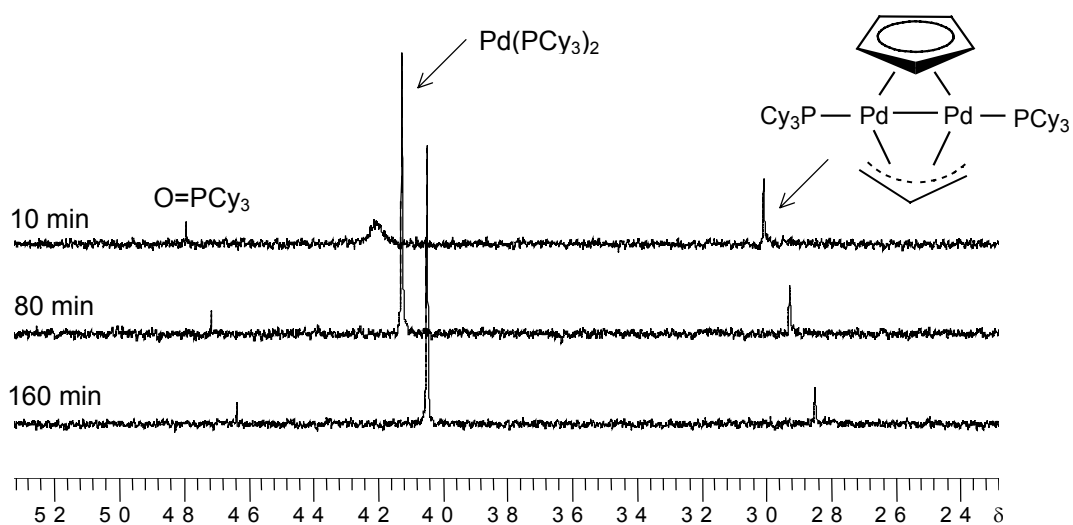


Figure 13. Stacked plots of  $^{31}P$  NMR spectra (163.0 MHz) for reaction of  $Pd(\eta^3-C_3H_5)(\eta^5-C_5H_5)$  with two equivalents  $PCy_3$  in toluene- $d_8$  at 65 °C.

The initial resonance for  $Pd(PCy_3)_2$  observed at 10 min is quite broad, likely a result of rapid exchange with unreacted  $PCy_3$ , which is not observed at  $\delta$  10.0. However, within 20 min of mixing, the  $Pd(PCy_3)_2$  resonance was observed to sharpen, suggesting that all free  $PCy_3$  had reacted to produce both  $Pd(PCy_3)_2$  and  $Pd_2(PCy_3)_2(\mu-C_3H_5)(\mu-C_5H_5)$ . Such experiments were repeated at 77 °C and indicated the reproducible and quantitative generation of  $Pd(PCy_3)_2$  ( $\delta$  39.5)

within 1 h. In addition, the resonances for the reductive elimination products were observed in the corresponding  $^1\text{H}$  NMR spectra.

Werner *et al.* indicate that bulky phosphines like  $\text{PCy}_3$  require heating in order to generate the dinuclear palladium species.<sup>2</sup> However, the above mentioned NMR data suggest that the dinuclear species can in fact be formed at room temperature. Heating is required in order to convert the dinuclear species quantitatively to  $\text{Pd}(\text{PCy}_3)_2$ .

### 3.1.2.2 L = $\text{PMeBu}^t_2$

Reactions of  $\text{Pd}(\eta^3\text{-C}_3\text{H}_5)(\eta^5\text{-C}_5\text{H}_5)$  with two equivalents of  $\text{PMeBu}^t_2$  at 25 °C were anticipated to produce similar intermediates as seen with  $\text{PCy}_3$ . Successive NMR spectra indicated the formation of a species exhibiting a  $^{31}\text{P}$  resonance at  $\delta$  35.4, which was identified as the dinuclear species  $\text{Pd}(\text{PMeBu}^t_2)_2(\mu\text{-C}_3\text{H}_5)(\mu\text{-C}_5\text{H}_5)$  (Figure 14)<sup>2</sup>. In addition, an extremely broad resonance at  $\delta$  61.0 was observed, which was attributed to an  $\eta^1$ -allyl intermediate<sup>2g</sup> or a rapidly isomerizing  $\eta^3$ -allyl-  $\eta^1$ -Cp and  $\eta^1$ -allyl-  $\eta^5$ -Cp isomers, as mentioned above.<sup>2c,h</sup>

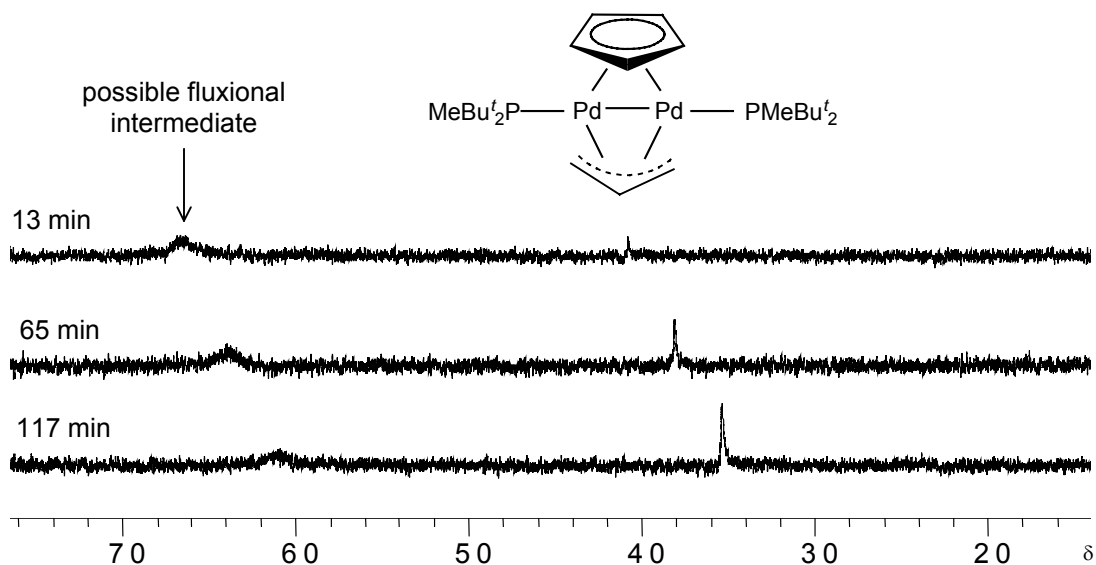


Figure 14. Stacked plots of  $^{31}\text{P}$  NMR spectra (163.0 MHz) for reaction of  $\text{Pd}(\eta^3\text{-C}_3\text{H}_5)(\eta^5\text{-C}_5\text{H}_5)$  with two equivalents of  $\text{PMeBu}^t_2$  in benzene- $\text{d}_6$  at 25 °C.

Over the course of the experiment at 25 °C, no  $^{31}\text{P}$  resonance was observed at  $\delta$  41.0, the chemical shift of the 2:1 compound  $\text{Pd}(\text{PMeBu}^t_2)_2$ .<sup>11</sup> In addition, no resonance was observed consistent with reports of free  $\text{PMeBu}^t_2$  ( $\delta$  11.4 in  $\text{C}_6\text{D}_6$ ).<sup>12</sup> This report was confirmed by an independently run  $^{31}\text{P}$  NMR spectrum of  $\text{PMeBu}^t_2$  in  $\text{C}_6\text{D}_6$  ( $\delta$  11.5).

A  $^1\text{H}$  NMR spectrum obtained three hours after mixing at 25 °C (Figure 15) showed unreacted starting material ( $\text{Pd}(\eta^3\text{-C}_3\text{H}_5)(\eta^5\text{-C}_5\text{H}_5)$ ) at  $\delta$  5.86 ( $\text{H}_a$ ),  $\delta$  4.59 ( $\text{H}_d$ ),  $\delta$  3.42 ( $\text{H}_c$ ) and  $\delta$  2.11 ( $\text{H}_b$ ) and in addition, a new species emerged with a  $^1\text{H}$  NMR resonance at  $\delta$  6.02 ( $\text{H}_e$ ), consistent with what was expected for the coordinated  $\mu\text{-C}_5\text{H}_5$  ring of a dinuclear species (Figure 15).<sup>2b,b,d,f,j</sup>



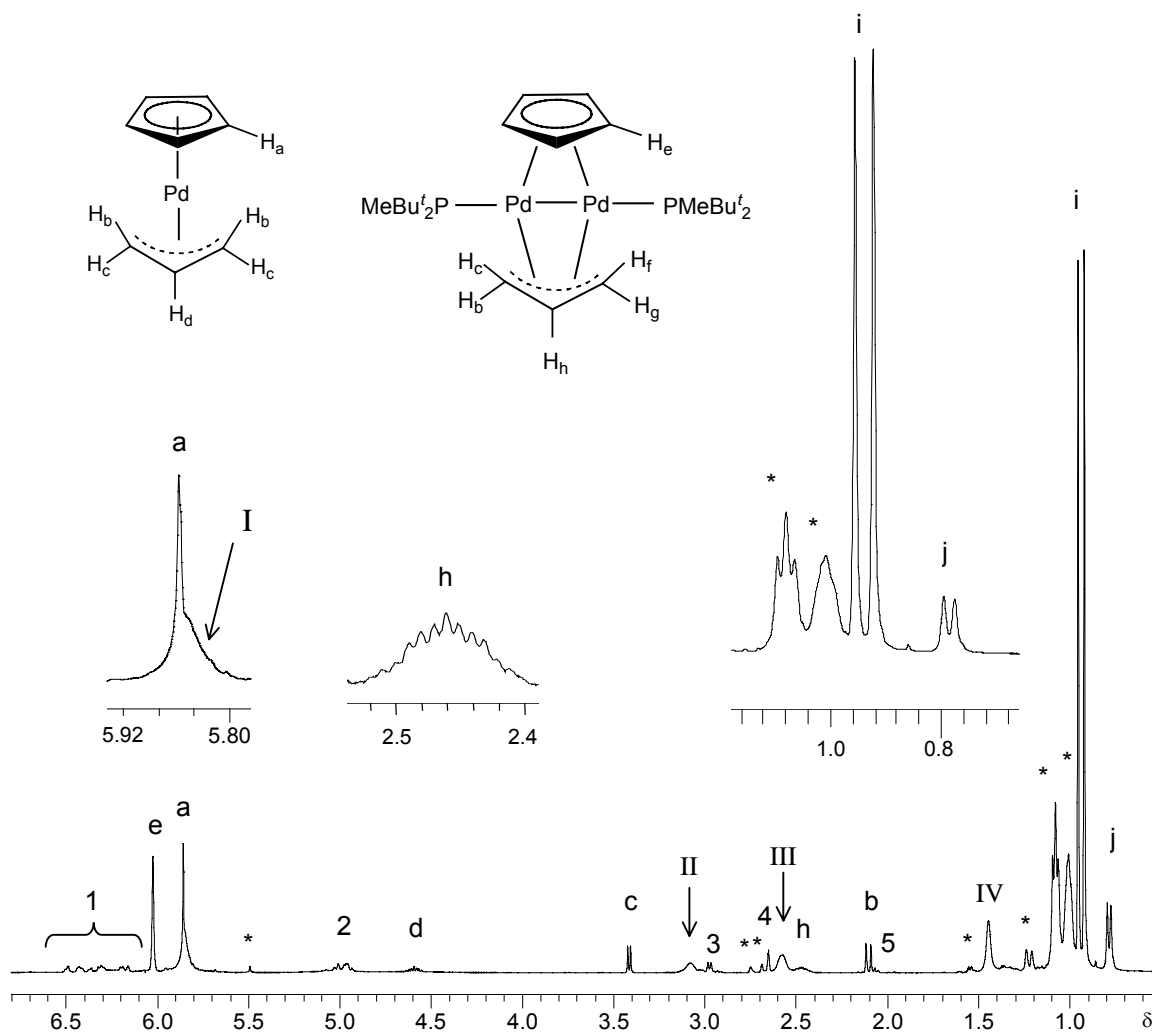


Figure 15.  $^1\text{H}$  NMR spectrum (400 MHz) for reaction of  $\text{Pd}(\eta^3\text{-C}_3\text{H}_5)(\eta^5\text{-C}_5\text{H}_5)$  with two equivalents of  $\text{PMeBu}^t_2$  3 h after mixing at 25 °C in benzene- $d_6$  (\* indicates unidentified resonances).

Interestingly, a broad resonance at  $\delta$  5.85 (labeled I) was observed underneath the Cp resonance  $\text{H}_a$ . It is possible that this broad resonance, likely corresponding to a coordinated Cp group, appeared for the same reasons discussed in the  $\text{PCy}_3$  system above. The reversible reaction of  $\text{Pd}(\eta^3\text{-C}_3\text{H}_5)(\eta^5\text{-C}_5\text{H}_5)$  and  $\text{PMeBu}^t_2$  may form a primary intermediate species, which in turn may

be rapidly isomerizing between  $\eta^1$ -allyl- $\eta^5$ -Cp and  $\eta^3$ -allyl- $\eta^1$ -Cp coordination modes. This dynamic system may be undergoing exchange at a rate comparable to that of the NMR timescale, producing  $^1\text{H}$  resonances which reflect an average of the resonances that would be anticipated for each individual Pd containing species. Several other broadened resonances (labeled II, III and IV) remain unidentified.

The multiplet observed at  $\delta$  2.46 ( $\text{H}_h$ ) is consistent in its splitting pattern the central allyl CH proton of a dinuclear species, appearing upfield from the corresponding CH resonance at  $\delta$  4.59 for  $\text{Pd}(\eta^3\text{-C}_3\text{H}_5)(\eta^5\text{-C}_5\text{H}_5)$  (Table 7).<sup>2a</sup> The remaining allyl protons cannot be assigned with certainty, although the small unidentified doublet at  $\delta$  1.22 may be that of  $\text{H}_f$  or  $\text{H}_g$ . In addition, the resonances of the anticipated reductive elimination products  $\text{C}_5\text{H}_5\text{-C}_3\text{H}_5$  are also observed in the  $^1\text{H}$  spectrum, labeled regions 1-5.

Although the resonances observed at  $\delta$  1.08 and  $\delta$  1.00 have the appearance of virtual triplets, they could not be attributed to alkyl groups of  $\text{Pd}_2(\text{PMeBu}^t_2)_2(\mu\text{-C}_3\text{H}_5)(\mu\text{-C}_5\text{H}_5)$ , as their relative integrations are not consistent with  $\text{Bu}^t$  and Me groups (1:2:1). In addition, two large doublets appeared at  $\delta$  0.94 and  $\delta$  0.79 (relative integrations 18:3), labeled i and j respectively and were observed to diminish in intensity over the course of the reaction. These resonances did not correspond to free  $\text{PMeBu}^t_2$  ( $\text{Bu}^t$   $\delta$  1.04, Me  $\delta$  0.83),<sup>12</sup> nor did they correspond to  $\text{Pd}(\text{PMeBu}^t_2)_2$  ( $\text{Bu}^t$   $\delta$  1.28, Me  $\delta$  1.07).<sup>11</sup> This suggests that resonances i and j are associated with a  $\text{PMeBu}^t_2$  bound to a primary intermediate ( $\eta^1$ -allyl- $\eta^5$ -Cp, or perhaps  $\eta^1$ -Cp- $\eta^3$ -allyl).

At 77 °C, the disappearance of the dinuclear species ( $\delta$  35.4) was observed with the concurrent, quantitative formation of the anticipated 2:1 product  $\text{Pd}(\text{PMeBu}^t_2)_2$  ( $\delta$  41.0) in less than one hour (Figure 16).<sup>11</sup> As was seen with reactions involving  $\text{PCy}_3$ , the anticipated resonances for the reductive

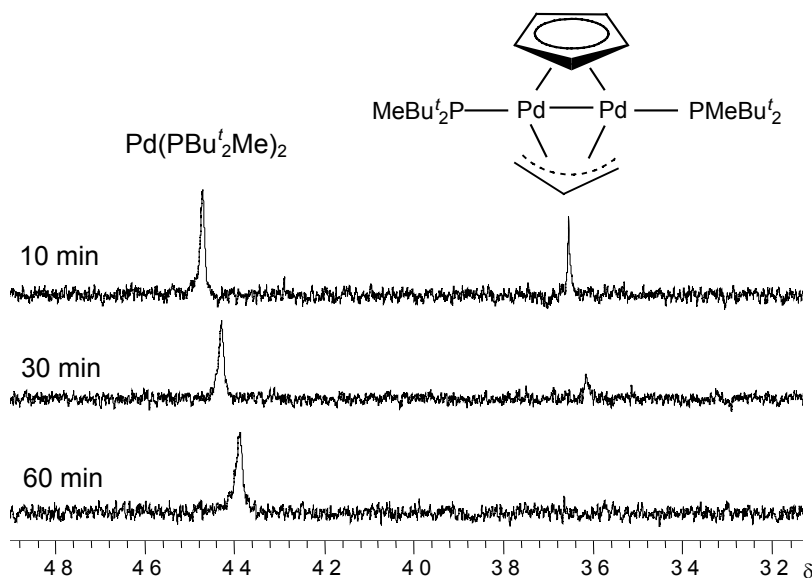


Figure 16. Stacked plots of  $^{31}\text{P}$  NMR spectra (163.0 MHz) for reaction of  $\text{Pd}(\eta^3\text{-C}_3\text{H}_5)(\eta^5\text{-C}_5\text{H}_5)$  with two equivalents  $\text{PMeBu}^t_2$  in toluene- $\text{d}_8$  at 77 °C.

elimination products  $\text{C}_5\text{H}_5\text{-C}_3\text{H}_5$  were also observed in the  $^1\text{H}$  NMR spectra while, for the  $\text{PMeBu}^t_2$  system, broad resonances at  $\delta$  1.26 and 1.03 appeared and are attributed to the  $\text{Bu}^t$  and Me groups, respectively, of  $\text{Pd}(\text{PMeBu}^t_2)_2$ .<sup>11</sup>

### 3.1.2.3 L = $\text{PBu}^t_3$

In contrast, it was found that  $\text{PBu}^t_3$  generated neither primary intermediates ( $\eta^1\text{-allyl-}\eta^5\text{-Cp}$ ,  $\eta^3\text{-allyl-}\eta^1\text{-Cp}$ ) nor dinuclear intermediate species at 25 °C in toluene- $\text{d}_8$ , as has been noted elsewhere.<sup>2e</sup> Only  $\text{Pd}(\text{PBu}^t_3)_2$  was formed in a reaction which was complete within one hour at 25 °C. The  $^{31}\text{P}$  and

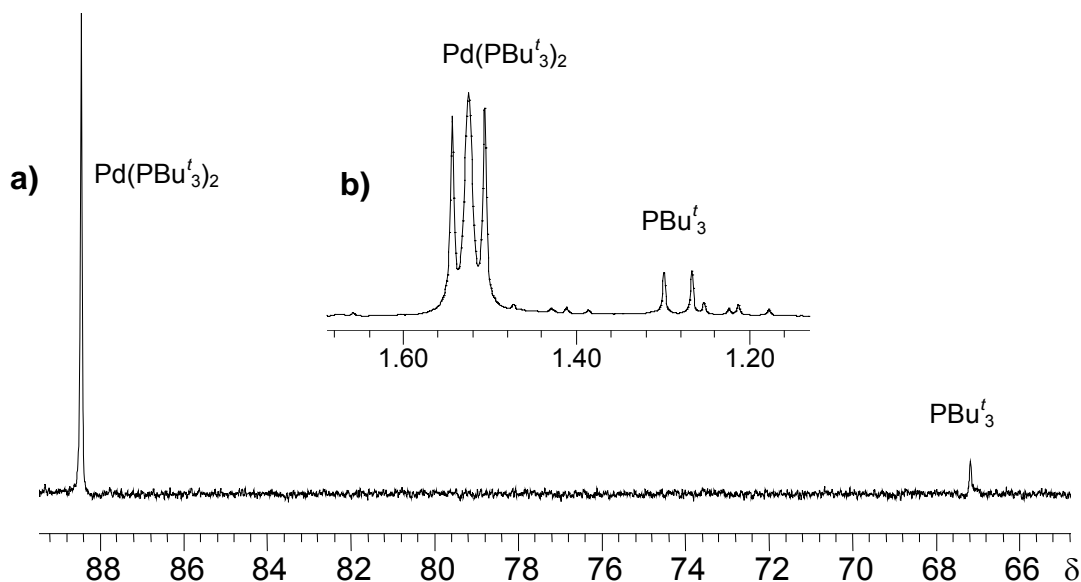


Figure 17. a)  $^{31}\text{P}$  NMR spectrum (163.0 MHz) of the reaction of  $\text{Pd}(\eta^3\text{-C}_3\text{H}_5)(\eta^5\text{-C}_5\text{H}_5)$  with two equivalents  $\text{PBu}^t_3$  in toluene- $d_8$  at  $77^\circ\text{C}$  25 minutes after mixing b)  $^1\text{H}$  NMR spectrum (300 MHz) at  $25^\circ\text{C}$  120 minutes after mixing.

$^1\text{H}$  NMR spectra ( $25^\circ\text{C}$ ) exhibited resonances at  $\delta$  86.0 and at  $\delta$  1.49 (vt) respectively, consistent with the formation of the anticipated 2:1 product  $\text{Pd}(\text{PBu}^t_3)_2$  (Figure 17).<sup>13</sup> Furthermore,  $\text{Pd}(\text{PBu}^t_3)_2$  was formed quantitatively in about 30 minutes at  $77^\circ\text{C}$ .

It seems likely in this system that a primary intermediate species ( $\eta^1$ -allyl- $\eta^5$ -Cp) species is initially formed from  $\text{Pd}(\eta^3\text{-C}_3\text{H}_5)(\eta^5\text{-C}_5\text{H}_5)$ , but that the steric bulk of the  $\text{PBu}^t_3$  ligand induces rapid reductive elimination of  $\text{C}_5\text{H}_5\text{-C}_3\text{H}_5$ . The anticipated resonances of the latter were observed in the  $^1\text{H}$  NMR spectra of the reaction mixtures at both  $25$  and  $77^\circ\text{C}$ .

In summary, variable temperature  $^1\text{H}$  and  $^{31}\text{P}$  NMR experiments have permitted the evaluation of the optimum condition in which to produce  $\text{PdL}_2$  from  $\text{Pd}(\eta^3\text{-C}_3\text{H}_5)(\eta^5\text{-C}_5\text{H}_5)$  with L (L =  $\text{PCy}_3$ ,  $\text{PMeBu}^t_2$  and  $\text{PBu}^t_3$ ). While both  $\text{PCy}_3$

and  $\text{PMeBu}_2^t$  require heating at 77 °C for 1 h to form their respective bisphosphine complexes,  $\text{PBU}_3^t$  requires only 30 min at this temperature to quantitatively form  $\text{Pd}(\text{PBU}_3^t)_2$ .

One can compare this now optimized method to the alternate methods that have been previously reported for the generation of  $\text{PdL}_2$  ( $\text{L} = \text{PCy}_3$ ,  $\text{PMeBu}_2^t$ ,  $\text{PBU}_3^t$ ). The formation of these complexes has generally involved the reduction of Pd(II) precursors by a variety of means. However, the method described by Otsuka,<sup>1</sup> optimized herein, represents the only method that has been successfully used for each of the phosphines described. Furthermore, the method of Otsuka represents the only successful preparation for  $\text{Pd}(\text{PMeBu}_2^t)_2$ .<sup>11,14</sup>

The alternative methods for the preparation of  $\text{Pd}(\text{PCy}_3)_2$  have been performed at a variety of temperatures and reaction times.  $\text{Pd}(\text{PCy}_3)_2$  has been successfully prepared by reaction of  $\text{PdCl}_2(\text{PCy}_3)_2$ ,  $\text{PCy}_3$ , KOH and 18-crown-6 in refluxing toluene (20 h) (85-90% yield).<sup>9</sup> The preparation of  $\text{Pd}(\text{PCy}_3)_2$  has also been described at room temperature from the reaction  $[\eta^3\text{-Me-C}_3\text{H}_4\text{PdCl}]_2$ , NaOMe and  $\text{PCy}_3$  for 24 h at room temperature (80%).<sup>15</sup> In comparison, the current method represents a significant improvement on the described alternative methods, as it provides significantly shorter reaction times to obtain  $\text{Pd}(\text{PCy}_3)_2$ .

Several alternative methods for the preparation of  $\text{Pd}(\text{PBU}_3^t)_2$  have also been reported in the literature. The isolation of  $\text{Pd}(\text{PBU}_3^t)_2$  has been performed by the reaction of  $\text{Pd}(\text{dba})_2$  and excess  $\text{PBU}_3^t$  at room temperature for 15 h (65 % yield).<sup>16</sup> A similar preparation has been reported from  $\text{Pd}_2(\text{dba})_3$  and two

equivalents of  $\text{PBU}^t_3$  in DMF for 3 h at room temperature (83% yield).<sup>13</sup> Both require significantly longer reaction times at room temperature than does the method optimized herein (1 h at 25 °C). A further method for the preparation of  $\text{Pd}(\text{PBU}^t_3)_2$  is that reported by Goel *et al.*, which involves the reaction of  $\text{PdCl}_2(\text{NCPH})_2$  and two equivalents of  $\text{PBU}^t_3$  with sodium naphthalenide in 1 h in THF at room temperature (70 % yield).<sup>17</sup> Although this method involves a comparable reaction time and temperature to the method described herein, it utilizes additional and relatively inconvenient reducing agent (sodium naphthalenide). The currently optimized method of Otsuka<sup>1</sup> thus represents an general, efficient and mild method for the quantitative generation of  $\text{PdL}_2$  (L =  $\text{PBU}^t_3$ ,  $\text{PCy}_3$ ,  $\text{PMeBu}^t_2$ ).

### 3.1.3 Generation of $\text{PdL}_n$ (L = $\text{PMe}_3$ , $\text{PPh}_3$ ) where $n > 2$

As the method described above was successfully optimized for the clean and quantitative formation of  $\text{PdL}_2$  (L =  $\text{PCy}_3$ ,  $\text{PBU}^t_3$ ,  $\text{PMeBu}^t_2$ ), it was also desirable to evaluate the process for less sterically demanding phosphines, such as  $\text{PPh}_3$  and  $\text{PMe}_3$  (cone angles 118 ° and 145 ° respectively).<sup>18</sup> Such phosphines tend to result in palladium complexes  $\text{PdL}_n$  with higher coordination number ( $n = 3,4$ ) as a result of the reduced steric bulk of the phosphine.<sup>19</sup> Although the reaction of  $\text{Pd}(\eta^3\text{-C}_3\text{H}_5)(\eta^5\text{-C}_5\text{H}_5)$  with these phosphines has been studied by Werner *et al.*, it has not been utilized for the synthesis and isolation of palladium(0) complexes of  $\text{PPh}_3$  and  $\text{PMe}_3$ .<sup>2</sup> Rather, the reported preparation of  $\text{Pd}(\text{PMe}_3)_4$  involves the reaction of  $[\text{PdCl}(\eta^3\text{-2-Me-C}_3\text{H}_4)]_2$  and  $\text{PMe}_3$ .<sup>15</sup>

$\text{Pd}(\text{PPh}_3)_4$  has also been successfully obtained by numerous means, the most widely utilized being the reaction of  $\text{PdCl}_2$  with  $\text{PPh}_3$  and  $\text{N}_2\text{H}_4 \cdot \text{H}_2\text{O}$  in dmsO.<sup>20</sup> Complexes of lower coordination number, both  $\text{Pd}(\text{PPh}_3)_3$  and  $\text{Pd}(\text{PPh}_3)_2$ , have also been isolated and are discussed below.<sup>15,21</sup> It thus worth considering the current body of work regarding the nature of these complexes prior to examining the systems herein.

There have been very few studies of the nature, lability and structure of homoleptic  $\text{Pd}(0)$  complexes of  $\text{PMe}_3$ . While the tetrakis substituted complex  $\text{Pd}(\text{PMe}_3)_4$  has been reported and characterized by elemental analysis and NMR ( $^{31}\text{P}$ ,  $^1\text{H}$ ,  $^{13}\text{C}$ ),<sup>4,15</sup> complexes of lower coordination number, namely  $\text{Pd}(\text{PMe}_3)_3$  and  $\text{Pd}(\text{PMe}_3)_2$  have not been isolated. The solution stoichiometry of  $\text{Pd}(\text{PMe}_3)_4$  has been previously studied by low temperature  $^{31}\text{P}$  NMR spectroscopy.<sup>4</sup> It was reported that a sample containing  $\text{Pd}(\text{PMe}_3)_4$  produced no new  $^{31}\text{P}$  resonances upon cooling to  $-60$  °C, indicating that  $\text{Pd}(\text{PMe}_3)_4$  does not dissociate in solution to form  $\text{Pd}(\text{PMe}_3)_3$ .<sup>4</sup> In addition, the cooling of samples containing both  $\text{Pd}(\text{PMe}_3)_4$  and excess  $\text{PMe}_3$  to  $-60$  °C revealed the decoalescence of the exchange averaged  $^{31}\text{P}$  resonance for  $\text{Pd}(\text{PMe}_3)_4$  and  $\text{PMe}_3$ , indicating that phosphine exchange is rapid on the NMR timescale at room temperature.<sup>4</sup>

Several studies have been performed to characterize  $\text{Pd}(0)$  complexes of  $\text{PPh}_3$ . Crystallographic work indicates that  $\text{Pd}(\text{PPh}_3)_4$  is tetrahedral in geometry.<sup>22</sup> In contrast to  $\text{Pd}(\text{PMe}_3)_4$ ,  $\text{Pd}(\text{PPh}_3)_4$  is known to dissociate in solution, producing almost exclusively  $\text{Pd}(\text{PPh}_3)_3$ , as indicated by low temperature  $^{31}\text{P}$  NMR studies and cryoscopic molecule weight measurements.<sup>4,23</sup>

$\text{Pd}(\text{PPh}_3)_3$  has itself been isolated from the reaction of [2-methylallyl] $\text{Pd}(\text{PPh}_3)_2\text{BF}_4$ ,  $\text{PPh}_3$  and benzylamine and has been found to possess trigonal planar geometry.<sup>15,24</sup> In solution,  $\text{Pd}(\text{PPh}_3)_3$  dissociates minimally to form  $\text{Pd}(\text{PPh}_3)_2$  ( $K_D \ll 1$ ).<sup>4,5,6,15,25</sup> Although several reports<sup>26</sup> have been made of the *in situ* preparation and use of  $\text{Pd}(\text{PPh}_3)_2$  only Urata *et al.* have attempted to characterize  $\text{Pd}(\text{PPh}_3)_2$ , isolated by reaction of  $[(\eta^3\text{-C}_3\text{H}_5)\text{Pd}(\text{PPh}_3)_2][\text{PF}_6]$  with  $\text{Ph}_2\text{MeSiLi}$ .<sup>21</sup> In their work IR,  $^1\text{H}$ ,  $^{13}\text{C}$  and  $^{31}\text{P}$  NMR ( $^{31}\text{P}$   $\delta$  31.0) and elemental analysis all suggest the isolation of  $\text{Pd}(\text{PPh}_3)_2$ . Their low temperature  $^{31}\text{P}$  NMR studies also indicated that while ligand exchange (resonance broadening as a result of  $\text{PPh}_3$  dissociation and coordination) occurs for  $\text{Pd}(\text{PPh}_3)_3$  even at  $-80$  °C.<sup>21</sup> However, no such broadening is observed for  $\text{Pd}(\text{PPh}_3)_2$  at  $-40$  °C,<sup>21</sup> implying no equilibration of  $\text{Pd}(\text{PPh}_3)_2$  to  $(\text{Pd}(\text{PPh}_3) + \text{PPh}_3)$ .

Given what is known of Pd(0) complexes of  $\text{PMe}_3$  and  $\text{PPh}_3$ , the current work aims to evaluate the effective generation of  $\text{PdL}_n$  ( $\text{L} = \text{PMe}_3, \text{PPh}_3, n = 2,3,4$ ) from  $\text{Pd}(\eta^3\text{-C}_3\text{H}_5)(\eta^5\text{-C}_5\text{H}_5)$ . As described above for  $\text{PCy}_3$ ,  $\text{P}^t\text{Bu}_3$  and  $\text{P}^t\text{MeBu}_2$ , the reactions of  $\text{Pd}(\eta^3\text{-C}_3\text{H}_5)(\eta^5\text{-C}_5\text{H}_5)$  with  $\text{PMe}_3$  or  $\text{PPh}_3$  were monitored by  $^{31}\text{P}$  and  $^1\text{H}$  NMR at various temperatures in an effort to determine the nature of the species formed, as well as the optimum conditions for  $\text{PdL}_n$  formation ( $n = 2,3,4$ ). It was anticipated that intermediate species, such as the  $\eta^1$ -allyl- $\eta^5$ -Cp or  $\eta^3$ -allyl- $\eta^1$ -Cp type intermediates, as well as dinuclear species, as described above (Section 3.1.1 and 3.1.2) may also be present in the currently studied systems ( $\text{PPh}_3$  and  $\text{PMe}_3$ ).



### 3.1.3.1 L = PMe<sub>3</sub>

When Pd( $\eta^3$ -C<sub>3</sub>H<sub>5</sub>)( $\eta^5$ -C<sub>5</sub>H<sub>5</sub>) was reacted with two equivalents of PMe<sub>3</sub> at 25 °C, an immediate colour change from red to green-yellow was observed. Within 3 hours, traces of palladium metal were observed. A <sup>31</sup>P spectrum obtained 35 minutes after mixing showed a broadened resonance at  $\delta$  -32.3. This resonance is consistent with that reported for Pd(PMe<sub>3</sub>)<sub>4</sub> ( $\delta$  -34.8 ppm) (Figure 18).<sup>4</sup>

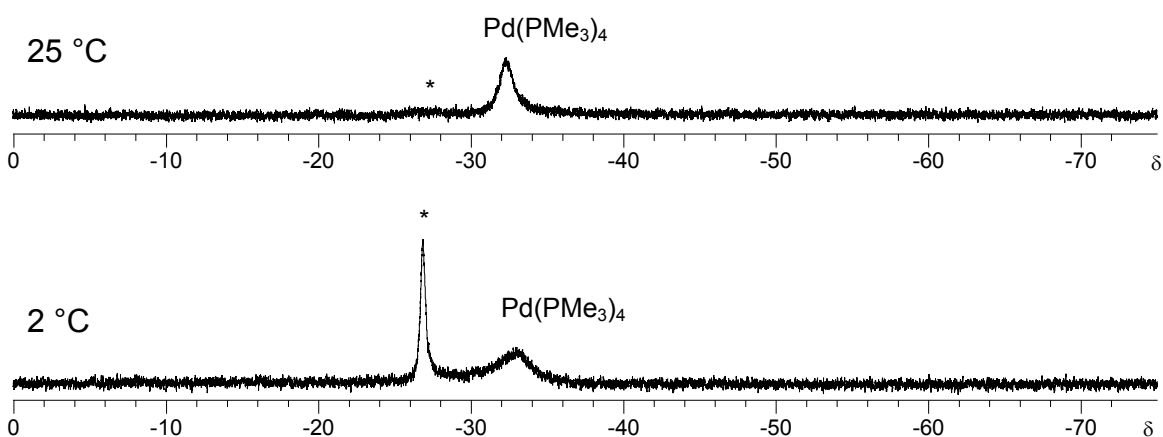


Figure 18. <sup>31</sup>P NMR spectra of Pd( $\eta^3$ -C<sub>3</sub>H<sub>5</sub>)( $\eta^5$ -C<sub>5</sub>H<sub>5</sub>) and two equivalents PMe<sub>3</sub>, 35 minutes after mixing in toluene-d<sub>8</sub> at 25 °C (202.3 MHz) and 2 °C (242.9 MHz) (\* indicates unidentified resonances).

An additional broad resonance was observed at  $\delta$  -26.5, but the resonance for free PMe<sub>3</sub> was absent from the spectrum ( $\delta$  -62).<sup>27</sup> When this reaction was repeated at 2 °C, in an effort to reduce broadening, the resonance at  $\delta$  -26.5 was sharper, while that at  $\delta$  -32.3 remained broad, compared to the experiment at 25 °C (Figure 18). As neither Pd(PMe<sub>3</sub>)<sub>3</sub> nor Pd(PMe<sub>3</sub>)<sub>2</sub> have been previously reported, the resonance at  $\delta$  -26.5 cannot be assigned as either of these species with any certainty. It was also possible that this resonance might

result from an intermediate species ( $\eta^1$ -allyl- $\eta^5$ -Cp,  $\eta^3$ -allyl- $\eta^1$ -Cp, or dinuclear species  $\text{Pd}(\mu\text{-C}_3\text{H}_5)(\mu\text{-C}_5\text{H}_5)(\text{PMe}_3)_2$ ) prior to formation of  $\text{Pd}(\text{PMe}_3)_4$ . A corresponding  $^1\text{H}$  NMR spectrum was thus consulted to gain insight as to the nature of the resonance observed at  $\delta -26.5$  (Figure 19).

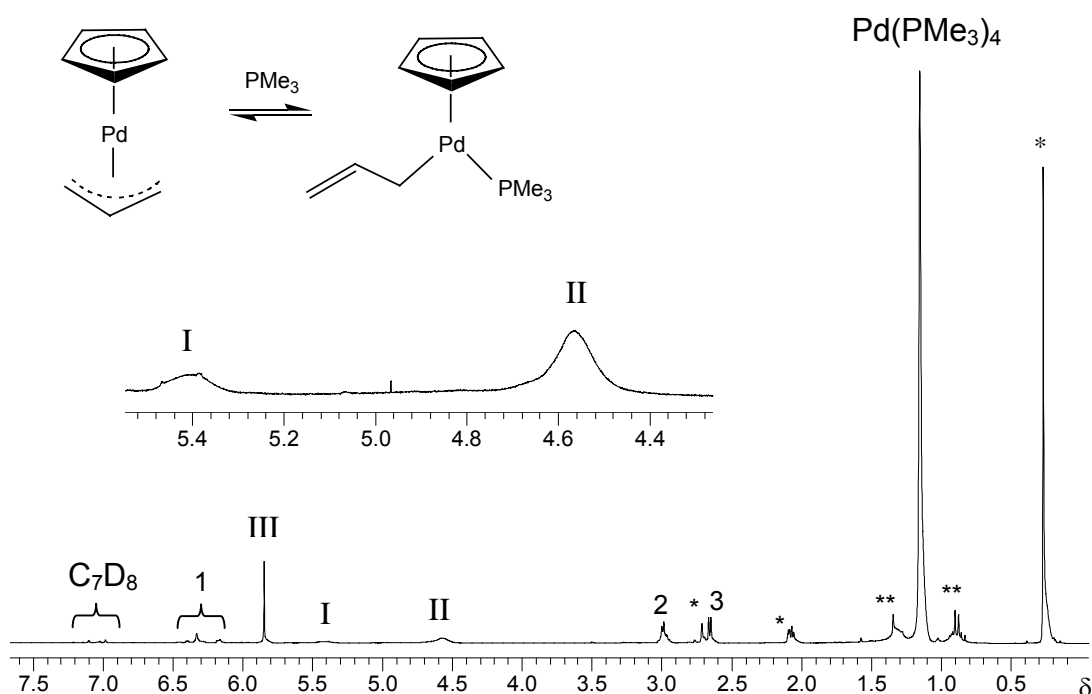


Figure 19.  $^1\text{H}$  NMR spectrum (500 MHz) of reaction of  $\text{Pd}(\eta^3\text{-C}_3\text{H}_5)(\eta^5\text{-C}_5\text{H}_5)$  and two equivalents of  $\text{PMe}_3$  in toluene- $\text{d}_8$  35 minutes after mixing at 25 °C (\* and roman numerals indicate unidentified peaks, \*\* indicates impurity).

The  $^1\text{H}$  NMR spectrum also suggested the presence of  $\text{Pd}(\text{PMe}_3)_4$ , seen at  $\delta$  1.16 at 25 °C, which is consistent with the literature ( $\delta$  1.16).<sup>15</sup> A sharp resonance indicative of an  $\eta^5\text{-C}_5\text{H}_5$  species was observed at  $\delta$  5.84 (III), similar in chemical shift to the broad Cp resonance of the primary intermediate observed in the  $\text{Pd}(\eta^3\text{-C}_3\text{H}_5)(\eta^5\text{-C}_5\text{H}_5)/\text{PCy}_3$  system. This resonance remains present in the  $^1\text{H}$  NMR spectrum two hours after mixing. In addition, broad  $^1\text{H}$  NMR

resonances were observed in the region of  $\sim \delta$  5.4 and  $\delta$  4.4 (labeled I and II). These resonances remained broad for two hours, while the singlet at  $\delta$  5.84 remained sharp. This suggests a  $\eta^1$ -allyl- $\eta^5$ -Cp intermediate (Figure 19), perhaps in equilibrium  $\text{Pd}(\eta^3\text{-C}_3\text{H}_5)(\eta^5\text{-C}_5\text{H}_5)$ , producing the  $^{31}\text{P}$  resonance observed at  $\delta$  -26.5. Although the dinuclear species  $\text{Pd}(\mu\text{-2-Me-C}_3\text{H}_4)(\mu\text{-C}_5\text{H}_5)(\text{PMe}_3)_2$  has been reported,<sup>2b</sup> literature  $^1\text{H}$  NMR resonances are not consistent with any of those observed in the currently examined system. Several regions of the  $^1\text{H}$  NMR spectrum showed resonances consistent with the anticipated reductive elimination products (labeled 1 – 3). However, many of these resonances overlapped with additional  $^1\text{H}$  NMR resonances that could not be identified.

This experiment was repeated at  $-55$  °C; the  $^{31}\text{P}$  NMR spectrum obtained (Figure 20) revealed the two species observed above, now as sharp resonances at  $\delta$  -33.2 ( $\text{Pd}(\text{PMe}_3)_4$ ) and  $\delta$  -25.7.

In order to gain insight into the nature of the species at  $^{31}\text{P}$   $\delta$  -25.7, a  $^1\text{H}$  NMR spectrum of the same reaction mixture was obtained 25 minutes after mixing (Figure 21).

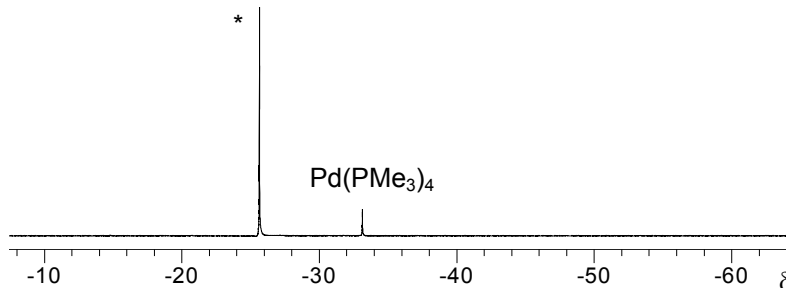


Figure 20.  $^{31}\text{P}$  NMR spectrum (242.9 MHz) of reaction of  $\text{Pd}(\eta^3\text{-C}_3\text{H}_5)(\eta^5\text{-C}_5\text{H}_5)$  and two equivalents of  $\text{PMe}_3$  in toluene- $d_8$  at 20 minutes after mixing at  $-55$  °C. (\* indicates unidentified resonance).

A strong resonance was observed at  $\delta$  5.97, indicative of a Cp containing intermediate species. Several resonances were also consistent with the presence of a  $\eta^1$ -allyl- $\eta^5$ -Cp intermediate (labeled a - e). However, this assignment was tentatively made, as many significant resonances remained unidentified and no corresponding COSY spectrum was obtained to assist in the assignment. The resonance at  $\delta$  1.22 corresponds fairly well in chemical shift to that of  $\text{Pd}(\text{PMe}_3)_4$ .<sup>11</sup> The resonance at  $\delta$  1.02 was assigned as the  $\text{PMe}_3$  bound to the  $\eta^1$ -allyl complex, given its relative intensity to the Cp resonance observed at  $\delta$  5.97.

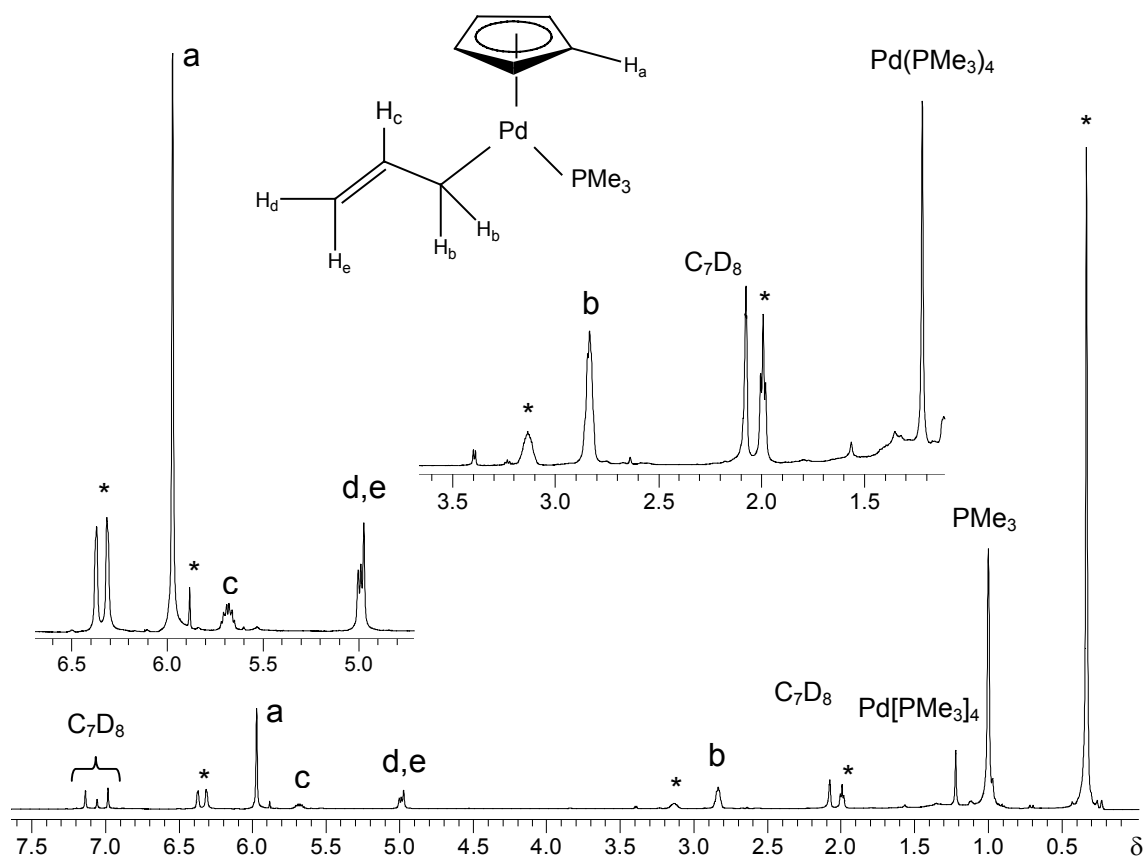


Figure 21.  $^1\text{H}$  NMR spectrum (600 MHz) of reaction of  $\text{Pd}(\eta^3\text{-C}_3\text{H}_5)(\eta^5\text{-C}_5\text{H}_5)$  and two equivalents of  $\text{PMe}_3$  in toluene- $\text{d}_8$  25 minutes after mixing at  $-55^\circ\text{C}$  (\* indicates unidentified resonances).

### 3.1.3.2 L = PPh<sub>3</sub>

<sup>31</sup>P and <sup>1</sup>H NMR experiments were also conducted to observe possible PdL<sub>n</sub> formation (n = 2 - 4) when Pd(η<sup>3</sup>-C<sub>3</sub>H<sub>5</sub>)(η<sup>5</sup>-C<sub>5</sub>H<sub>5</sub>) is reacted with PPh<sub>3</sub>, both at 25 °C and 80 °C. These reactions were first attempted in a 1:1 PPh<sub>3</sub>:Pd(η<sup>3</sup>-C<sub>3</sub>H<sub>5</sub>)(η<sup>5</sup>-C<sub>5</sub>H<sub>5</sub>) ratio to provide the conditions necessary to generate the dinuclear species exclusively,<sup>2a,b,d,f,j</sup> thus facilitating its <sup>1</sup>H NMR assignment. Although Pd<sub>2</sub>(PPh<sub>3</sub>)<sub>2</sub>(μ-C<sub>3</sub>H<sub>5</sub>)(μ-C<sub>5</sub>H<sub>5</sub>) has been reported,<sup>2a</sup> the <sup>1</sup>H NMR data are given in CD<sub>2</sub>Cl<sub>2</sub>, thus providing different chemical shifts than those in toluene-d<sub>8</sub>.

When Pd(η<sup>3</sup>-C<sub>3</sub>H<sub>5</sub>)(η<sup>5</sup>-C<sub>5</sub>H<sub>5</sub>) and PPh<sub>3</sub> were reacted at 25 °C in a 1:1 molar ratio, a <sup>31</sup>P NMR spectrum run approximately 15 minutes after mixing showed a strong resonance at δ 24.9 (Figure 22). This resonance was assigned to Pd<sub>2</sub>(PPh<sub>3</sub>)<sub>2</sub>(μ-C<sub>3</sub>H<sub>5</sub>)(μ-C<sub>5</sub>H<sub>5</sub>), after considering the related <sup>1</sup>H NMR spectra (see below). In addition, no broadened <sup>31</sup>P resonances associated with a Pd(PPh<sub>3</sub>)<sub>n</sub> (n = 3,4) species were observed (δ 22.6, 17.2 respectively),<sup>4</sup> nor was free PPh<sub>3</sub> observed at δ -5.11. The <sup>31</sup>P of free PPh<sub>3</sub> was determined independently in toluene-d<sub>8</sub> and resembles that reported in C<sub>6</sub>D<sub>6</sub> (δ -4.93).<sup>28</sup>

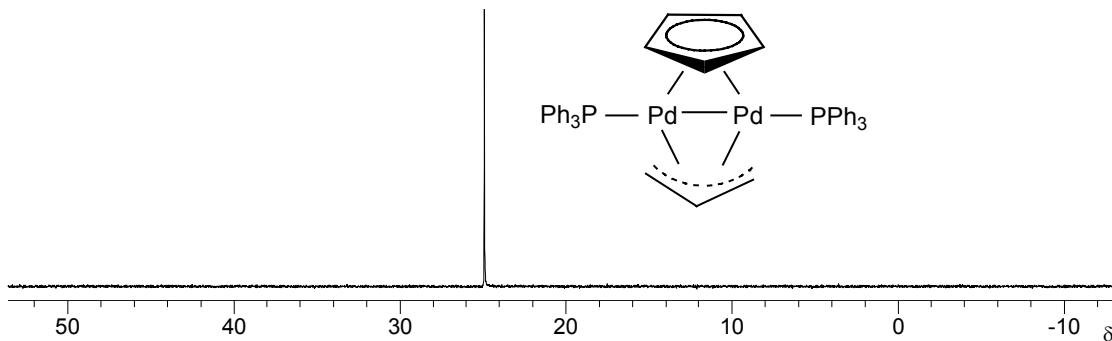


Figure 22. <sup>31</sup>P NMR (242.9 MHz) spectrum of reaction of Pd(η<sup>3</sup>-C<sub>3</sub>H<sub>5</sub>)(η<sup>5</sup>-C<sub>5</sub>H<sub>5</sub>) with one equivalent of PPh<sub>3</sub> in toluene-d<sub>8</sub> at 25 °C 17 minutes after mixing.

A  $^1\text{H}$  NMR spectrum obtained 10 minutes after mixing (Figure 23) showed a singlet at  $\delta$  5.94 with correlated by HSQC to  $^{13}\text{C}$  signal at  $\delta$  91.5, consistent with previously reported  $\mu\text{-C}_5\text{H}_5$ .<sup>2b</sup> One can also see on closer inspection that this  $\mu\text{-C}_5\text{H}_5$  showed a slight shouldering (1.9 Hz), consistent with what was observed by Werner *et al.* in terms of coupling with phosphorus.<sup>2a,b,f</sup> Furthermore, COSY correlated  $^1\text{H}$  resonances appeared upfield from  $\text{Pd}(\eta^3\text{-C}_3\text{H}_5)(\eta^5\text{-C}_5\text{H}_5)$  at  $\delta$  3.35 ( $\text{H}_h$ ),  $\delta$  2.54 ( $\text{H}_g$ ) and  $\delta$  1.18 ( $\text{H}_f$ ). These  $^1\text{H}$  assignments were confirmed by HSQC and HMBC NMR data which showed correlations to  $^{13}\text{C}$  resonances at  $\delta$  32.20 and  $\delta$  82.61 consistent with other reported  $\mu$ -allyl groups in dinuclear species.<sup>2b</sup>

The  $^1\text{H}$  and  $^{13}\text{C}$  NMR assignments for  $\text{Pd}_2(\text{PPh}_3)_2(\mu\text{-C}_3\text{H}_5)(\mu\text{-C}_5\text{H}_5)$  are given in Table 10, along with reported literature data for this species. In addition, resonances (labeled 1-15) associated with the reductive elimination products were observed, with 5-allylcyclopentadiene (Table 9) being the dominant product. Over the course of two hours, this product isomerized and there appeared resonances associated with either 1-allylcyclopentadiene or 2-allylcyclopentadiene (isomer B and C in Table 9). Werner *et al.* observed a similar isomerization when reacting  $\text{Pd}(\eta^3\text{-2-Me-C}_3\text{H}_4)(\eta^5\text{-C}_5\text{H}_5)$  with  $\text{P}(\text{OR})_3$  ( $\text{R} = \text{Me, Et, Ph}$ ) and  $\text{PR}_3$  ( $\text{Bu}^n, \text{Ph}$ ).<sup>2g</sup> The initial reductive elimination product, 5-(2-methylallyl)cyclopentadiene, was reported to rapidly rearrange to 1-(2-methylallyl)cyclopentadiene. Subsequent rearrangement to 2-(2-methylallyl)cyclopentadiene was observed after several days at room temperature.<sup>2g</sup>

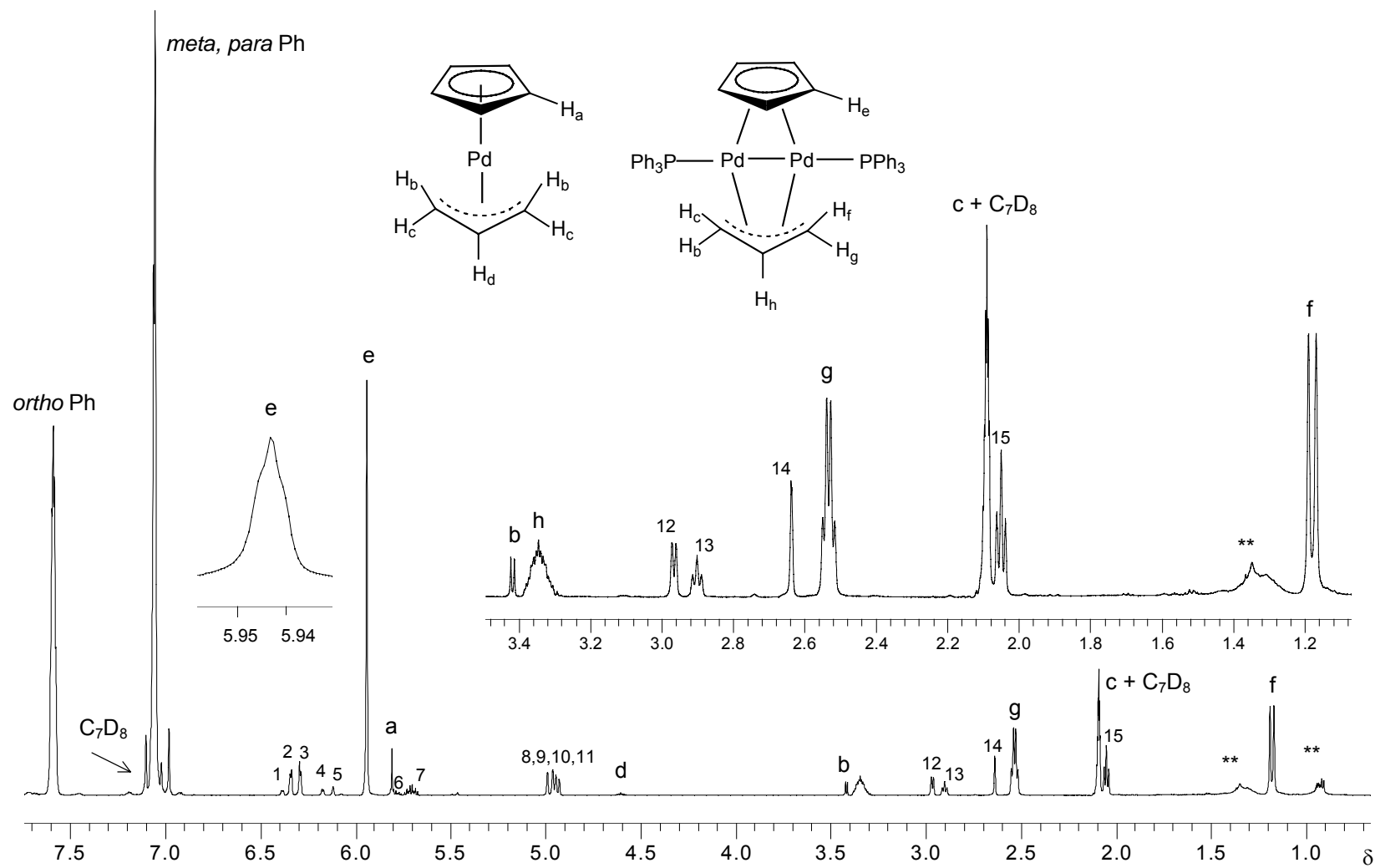
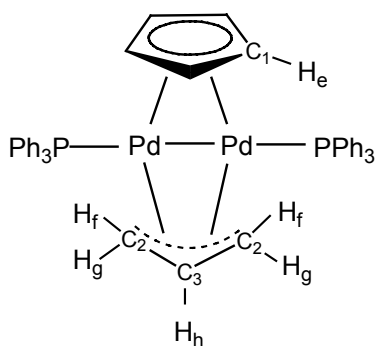


Figure 23.  $^1\text{H}$  NMR (600 MHz) spectrum of reaction of  $\text{Pd}(\eta^3\text{-C}_3\text{H}_5)(\eta^5\text{-C}_5\text{H}_5)$  with one equivalent of  $\text{PPh}_3$  in  $\text{toluene-d}_8$  at  $25^\circ\text{C}$  10 minutes after mixing (\*\* indicates impurity).

Table 10.  $^1\text{H}$  and  $^{13}\text{C}$  NMR assignment for  $\text{Pd}_2(\text{PPh}_3)_2(\mu\text{-C}_3\text{H}_5)(\mu\text{-C}_5\text{H}_5)$  in toluene- $d_8$ .



$\delta$ $^1\text{H}$	Mult.	$J$ (Hz)	Assignment	$\delta$ $^{13}\text{C}$	Mult.	$J$ (Hz)	Assignment
1.18	d	$^3J_{\text{HH}} = 12.5$	f	32.20	s	-	2
2.54	dt	$^3J_{\text{HH}} = 6.8$ $J_{\text{PH}} = 6.8$	g	82.61	t	$^3J_{\text{PC}} = 3.3$	3
3.35	t	$J_{\text{PH}} = 1.9$	e	90.75	s	-	1
5.94	t	$^3J_{\text{HH}} = 12.5$ $^3J_{\text{HH}} = 6.8$ $J_{\text{PH}} = 3.0$	h	128.72	s	-	<i>para</i> Ph
7.05	br. s	-	<i>para</i> Ph	127.65	t	$^3J_{\text{PC}} = 4.7$	<i>meta</i> Ph
7.06	br. s	-	<i>meta</i> Ph	133.50	t	$^3J_{\text{PC}} = 6.9$	<i>ortho</i> Ph
7.58- 7.60	m	-	<i>ortho</i> Ph	134.89	t	$^3J_{\text{PC}} = 15.9$	<i>ipso</i> Ph
<b>Literature:<sup>2a</sup> (<math>\text{CD}_2\text{Cl}_2</math>)</b>							
0.8	d	$J_{\text{HH}} = 12$	f				
2.18	q	$J_{\text{PH}}, J_{\text{HH}} = 8$	g				
2.85	m	-	h				
5.42	t	$J_{\text{PH}} = 1.5$	e				



When a 2:1 ratio of  $\text{PPh}_3:\text{Pd}(\eta^3\text{-C}_3\text{H}_5)(\eta^5\text{-C}_5\text{H}_5)$  was used at 25 °C, a different  $^{31}\text{P}$  NMR spectrum was obtained 22 minutes after mixing (Figure 24).

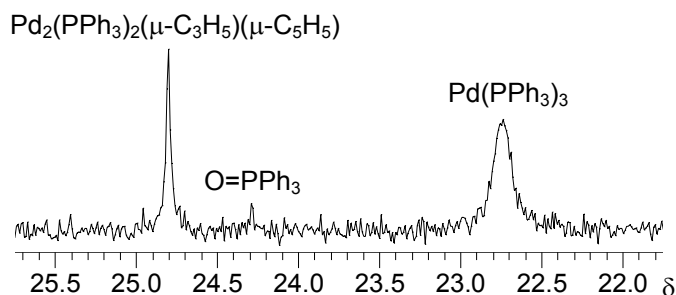


Figure 24.  $^{31}\text{P}$  NMR (163.0 MHz) spectrum of reaction of  $\text{Pd}(\eta^3\text{-C}_3\text{H}_5)(\eta^5\text{-C}_5\text{H}_5)$  with two equivalents of  $\text{PPh}_3$  in toluene- $d_8$  at 25 °C 22 minutes after mixing.

The resonances at  $\delta$  24.8,  $\delta$  24.3 and  $\delta$  22.8 remained unchanged over the course of 2.5 h. The first was assigned to  $\text{Pd}_2(\text{PPh}_3)_2(\mu\text{-C}_3\text{H}_5)(\mu\text{-C}_5\text{H}_5)$ , given the 1:1 experiments described above. The second resonance,  $\delta$  24.3, was assigned to  $\text{O}=\text{PPh}_3$ , according to an independently oxidized sample of  $\text{PPh}_3$  in toluene- $d_8$  (see Section 2.4.1.6). The last of the observed resonances was assigned to  $\text{Pd}(\text{PPh}_3)_3$  ( $\delta$  22.6 in toluene- $d_8$  at  $-70$  °C).<sup>4</sup> A corresponding  $^1\text{H}$  NMR spectrum obtained 2.5 h after mixing showed the anticipated dinuclear species (assigned from Table 10). No free phosphine was observed around  $\delta$   $-5.0$ <sup>12d</sup> nor were resonances observed that were consistent with reports of  $\text{Pd}(\text{PPh}_3)_2$  ( $\delta$  31.0 in toluene- $d_8$ ).<sup>21</sup>

When a 2:1 ratio of  $\text{PPh}_3:\text{Pd}(\eta^3\text{-C}_3\text{H}_5)(\eta^5\text{-C}_5\text{H}_5)$  was reacted at 80 °C, a broad  $^{31}\text{P}$  resonance at  $\delta$  27.1 was observed (Figure 25) and was observed to

shift to  $\delta$  25.1 over 2 h. These resonances are not consistent with  $\text{PdL}_n$  ( $n = 2 - 4$ ),<sup>4,21</sup> perhaps because these species were present but are undergoing rapid exchange on the NMR timescale, producing time averaged signals associated with mixtures of  $\text{Pd}(\text{PPh}_3)_2$ ,  $\text{Pd}(\text{PPh}_3)_3$  and  $\text{Pd}(\text{PPh}_3)_4$ . The rapid equilibration of these species and subsequent resonance broadening is supported by solution stoichiometry studies of  $\text{Pd}(\text{PPh}_3)_4$ , which indicate the reversible dissociation of  $\text{PPh}_3$  to produce  $\text{Pd}(\text{PPh}_3)_3$  and  $\text{Pd}(\text{PPh}_3)_2$ .<sup>4,6</sup> Once again, no free phosphine was observed in the current spectrum, anticipated around  $\delta -5.0$ .<sup>28</sup> The corresponding  $^1\text{H}$  NMR spectra indicated no resonances associated with a dinuclear species.

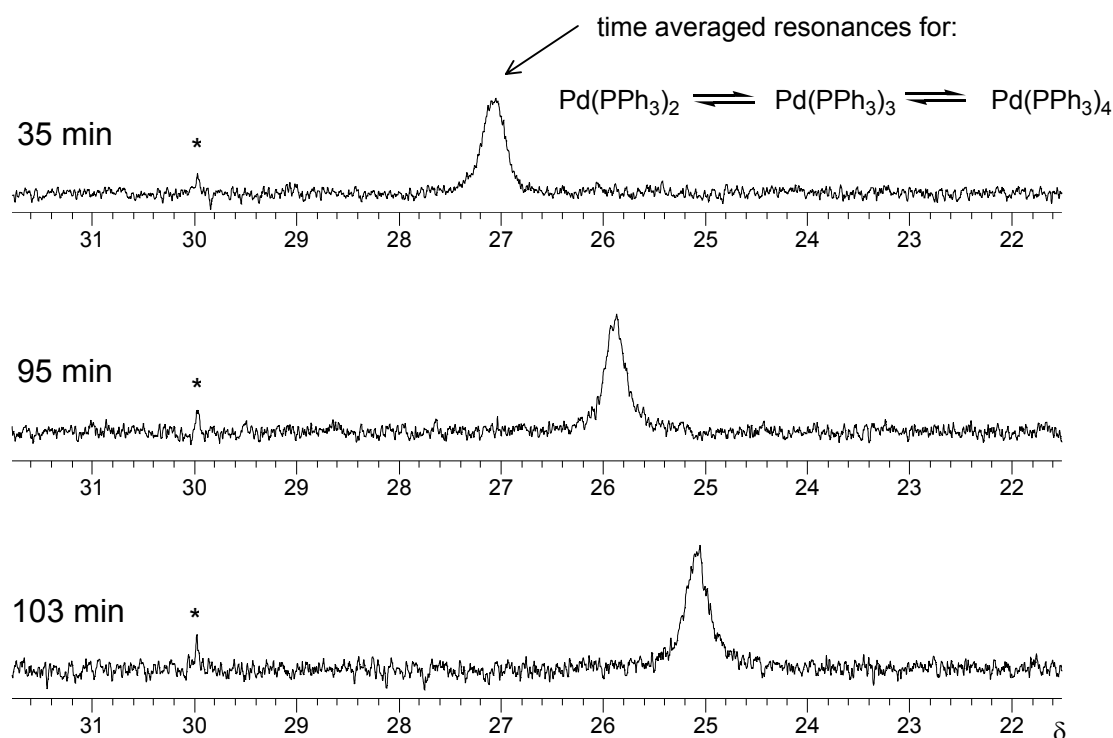


Figure 25.  $^{13}\text{C}$  NMR (163.0 MHz) spectrum of reaction of  $\text{Pd}(\eta^3\text{-C}_3\text{H}_5)(\eta^5\text{-C}_5\text{H}_5)$  with two equivalents of  $\text{PPh}_3$  in  $\text{toluene-d}_8$  at  $80^\circ\text{C}$  (\* indicates unidentified resonance).

It was expected that a 4:1 PPh<sub>3</sub>:Pd ratio would result in the formation of Pd(PPh<sub>3</sub>)<sub>4</sub>. <sup>31</sup>P NMR spectra for the reaction of Pd(η<sup>3</sup>-C<sub>3</sub>H<sub>5</sub>)(η<sup>5</sup>-C<sub>5</sub>H<sub>5</sub>) with four equivalents at 25 °C revealed a single broad resonance at δ 17.2, which corresponds fairly well to Pd(PPh<sub>3</sub>)<sub>4</sub>, reported at δ 18.4 in toluene-d<sub>8</sub> at -70 °C.<sup>4</sup>

Consistent with the observations of Werner *et al.*, it appears that a 1:1 mixture preferably reacts to form only the dinuclear species at 25 °C.<sup>2a,b,d,f,j</sup> However, in the presence of additional phosphine (as is the case in the 2:1 system), the more substituted Pd(PPh<sub>3</sub>)<sub>3</sub> or possibly Pd(PPh<sub>3</sub>)<sub>4</sub> are formed along with the dinuclear species Pd<sub>2</sub>(PPh<sub>3</sub>)<sub>2</sub>(μ-C<sub>3</sub>H<sub>5</sub>)(μ-C<sub>5</sub>H<sub>5</sub>). At an elevated temperature (80 °C), the dinuclear species was undetected favoring Pd(PPh<sub>3</sub>)<sub>n</sub> (n = 2 - 4), which undergoes rapid phosphine exchange on the NMR timescale.

In summary, variable temperature <sup>1</sup>H and <sup>31</sup>P NMR experiments have permitted the evaluation of the optimum conditions in which to produce PdL<sub>n</sub> (n = 2 for PCy<sub>3</sub>, PBu<sup>t</sup><sub>2</sub>Me and PBu<sup>t</sup><sub>3</sub>, n = 3-4 for PPh<sub>3</sub>, PMe<sub>3</sub>) from Pd(η<sup>3</sup>-C<sub>3</sub>H<sub>5</sub>)(η<sup>5</sup>-C<sub>5</sub>H<sub>5</sub>) with L (L = PCy<sub>3</sub>, PBu<sup>t</sup><sub>2</sub>Me, PBu<sup>t</sup><sub>3</sub>, PPh<sub>3</sub>, PMe<sub>3</sub>). The optimized conditions for formation of PdL<sub>2</sub> for L = PCy<sub>3</sub> and PMeBu<sup>t</sup><sub>2</sub> were 77 °C in toluene-d<sub>8</sub> for 1 h, while the PBu<sup>t</sup><sub>3</sub> system examined required only 30 min at this temperature to quantitatively form Pd(PBu<sup>t</sup><sub>3</sub>)<sub>2</sub>. As noted above, this method represents a significant improvement upon many of the previously reported methods for generation of PdL<sub>2</sub>, which vary in temperature and according to the phosphine used. The possibility of generating PdL<sub>n</sub> (L = PPh<sub>3</sub>, PMe<sub>3</sub>, n = 2-4) from Pd(η<sup>3</sup>-C<sub>3</sub>H<sub>5</sub>)(η<sup>5</sup>-C<sub>5</sub>H<sub>5</sub>) was also evaluated by <sup>31</sup>P and <sup>1</sup>H NMR experiments, indicating the presence of many of the intermediate species observed in the PCy<sub>3</sub> and

PMeBu<sup>t</sup><sub>2</sub> systems. However, these systems are complicated by the tendency of these complexes to assume higher coordination numbers, which also results in the broadening of <sup>31</sup>P resonances as a result of rapid phosphine exchange. Nevertheless, PPh<sub>3</sub> and PMe<sub>3</sub> were found to form PdL<sub>n</sub> (n = 3,4) appreciably at room temperature, which contrasts with the higher temperatures required to produce PdL<sub>2</sub> for L = PCy<sub>3</sub>, PMeBu<sup>t</sup><sub>2</sub> and PBu<sup>t</sup><sub>3</sub>. While the conditions for formation of Pd(PMe<sub>3</sub>)<sub>4</sub> were not evaluated at elevated temperature, the examination of the PPh<sub>3</sub> system indicated that Pd(PPh<sub>3</sub>)<sub>n</sub> formed within 35 min of mixing at elevated temperature (80 °C). The current method thus represents a successful means for the *in situ* generation Pd(PPh<sub>3</sub>)<sub>n</sub> (n = 3,4).

### 3.2 Generation of PdL<sub>2</sub> from Pd(η<sup>3</sup>-1-Ph-C<sub>3</sub>H<sub>4</sub>)(η<sup>5</sup>-C<sub>5</sub>H<sub>5</sub>)

Although optimum conditions for PdL<sub>2</sub> generation (L = PCy<sub>3</sub>, PMeBu<sup>t</sup><sub>2</sub>, PBu<sup>t</sup><sub>3</sub>) were established above, it was desirable to find an alternative to Pd(η<sup>3</sup>-C<sub>3</sub>H<sub>5</sub>)(η<sup>5</sup>-C<sub>5</sub>H<sub>5</sub>) as the palladium containing starting material. The efficient preparation and use of Pd(η<sup>3</sup>-C<sub>3</sub>H<sub>5</sub>)(η<sup>5</sup>-C<sub>5</sub>H<sub>5</sub>) presents some difficulty, as it is a thermally unstable (stored at -30 °C) volatile solid (30 mm Hg at 40 °C) with a noxious odour.<sup>29,30</sup> In order to circumvent these inconveniences, the phenyl substituted analogue, Pd(η<sup>3</sup>-1-Ph-C<sub>3</sub>H<sub>4</sub>)(η<sup>5</sup>-C<sub>5</sub>H<sub>5</sub>),<sup>31</sup> was chosen as an alternative starting material for generation of PdL<sub>2</sub>. It was anticipated that the increased mass provided by the phenyl group would result in the reduced volatility of Pd(η<sup>3</sup>-1-Ph-C<sub>3</sub>H<sub>4</sub>)(η<sup>5</sup>-C<sub>5</sub>H<sub>5</sub>) compared to Pd(η<sup>3</sup>-C<sub>3</sub>H<sub>5</sub>)(η<sup>5</sup>-C<sub>5</sub>H<sub>5</sub>). Pd(η<sup>3</sup>-1-Ph-C<sub>3</sub>H<sub>4</sub>)(η<sup>5</sup>-C<sub>5</sub>H<sub>5</sub>) was prepared according to the literature by the

reaction of NaCp with  $[\text{PdCl}(\eta^3\text{-1-Ph-C}_3\text{H}_4)]_2$  and was subsequently characterized by  $^1\text{H}$  and  $^{13}\text{C}$  NMR.<sup>32</sup> Once isolated and purified the physical properties of  $\text{Pd}(\eta^3\text{-1-Ph-C}_3\text{H}_4)(\eta^5\text{-C}_5\text{H}_5)$  were compared with those of  $\text{Pd}(\eta^3\text{-C}_3\text{H}_5)(\eta^5\text{-C}_5\text{H}_5)$ .

While toluene- $d_8$  solutions of  $\text{Pd}(\eta^3\text{-C}_3\text{H}_5)(\eta^5\text{-C}_5\text{H}_5)$  were found to decompose to palladium black, under  $\text{N}_2$  or in air, within 16 hours at 25 °C, solutions of  $\text{Pd}(\eta^3\text{-1-Ph-C}_3\text{H}_4)(\eta^5\text{-C}_5\text{H}_5)$  produced no observable traces of Pd metal under the same conditions and time frame.  $\text{Pd}(\eta^3\text{-1-Ph-C}_3\text{H}_4)(\eta^5\text{-C}_5\text{H}_5)$  thus possesses a similar air stability to  $\text{Pd}(\eta^3\text{-C}_3\text{H}_5)(\eta^5\text{-C}_5\text{H}_5)$ , which has been reported to remain stable in air for several days upon refrigeration.<sup>29</sup> During the work-up of  $\text{Pd}(\eta^3\text{-C}_3\text{H}_5)(\eta^5\text{-C}_5\text{H}_5)$ , noticeable quantities of the compound were regularly found to contaminate the attached vacuum line and solvent traps, even when solvent was removed using a weak vacuum pressure of 0.2 atm. However,  $\text{Pd}(\eta^3\text{-1-Ph-C}_3\text{H}_4)(\eta^5\text{-C}_5\text{H}_5)$  was prepared with no observable deposits in the vacuum line, even when solvent was removed at a measured vacuum pressure of  $1.3 \times 10^{-5}$  atm. The isolation and storage of  $\text{Pd}(\eta^3\text{-1-Ph-C}_3\text{H}_4)(\eta^5\text{-C}_5\text{H}_5)$  was therefore found to be a great deal more convenient than that of  $\text{Pd}(\eta^3\text{-C}_3\text{H}_5)(\eta^5\text{-C}_5\text{H}_5)$ .

Having established its relative convenience compared to  $\text{Pd}(\eta^3\text{-C}_3\text{H}_5)(\eta^5\text{-C}_5\text{H}_5)$ , the reactivity of  $\text{Pd}(\eta^3\text{-1-Ph-C}_3\text{H}_4)(\eta^5\text{-C}_5\text{H}_5)$  with phosphines L ( $\text{L} = \text{PCy}_3, \text{PMeBu}^t_2$ ) was monitored by  $^{31}\text{P}$  and  $^1\text{H}$  NMR spectroscopy, in order to determine the feasibility of  $\text{PdL}_2$  generation from  $\text{Pd}(\eta^3\text{-1-Ph-C}_3\text{H}_4)(\eta^5\text{-C}_5\text{H}_5)$ . However, it was expected that  $\text{Pd}(\eta^3\text{-1-Ph-C}_3\text{H}_4)(\eta^5\text{-C}_5\text{H}_5)$  may require harsher reactions conditions (higher temperature, longer reaction times) to produce  $\text{PdL}_2$

than was observed for  $\text{Pd}(\eta^3\text{-C}_3\text{H}_5)(\eta^5\text{-C}_5\text{H}_5)$ , as a result of its enhanced thermal stability. It was also speculated that the  $\eta^1$ -allyl and dinuclear intermediates<sup>2</sup> observed with  $\text{Pd}(\eta^3\text{-C}_3\text{H}_5)(\eta^5\text{-C}_5\text{H}_5)/\text{L}$  systems may also play a role in reactions involving  $\text{Pd}(\eta^3\text{-1-Ph-C}_3\text{H}_4)(\eta^5\text{-C}_5\text{H}_5)$  with L.

### 3.2.1 L = PCy<sub>3</sub>

When  $\text{Pd}(\eta^3\text{-1-Ph-C}_3\text{H}_4)(\eta^5\text{-C}_5\text{H}_5)$  was reacted with two equivalents of PCy<sub>3</sub> at 25 °C, a <sup>31</sup>P NMR resonance at  $\delta$  54.8 was observed, identified as a stable  $\eta^1$ -allyl species (Figure 26).

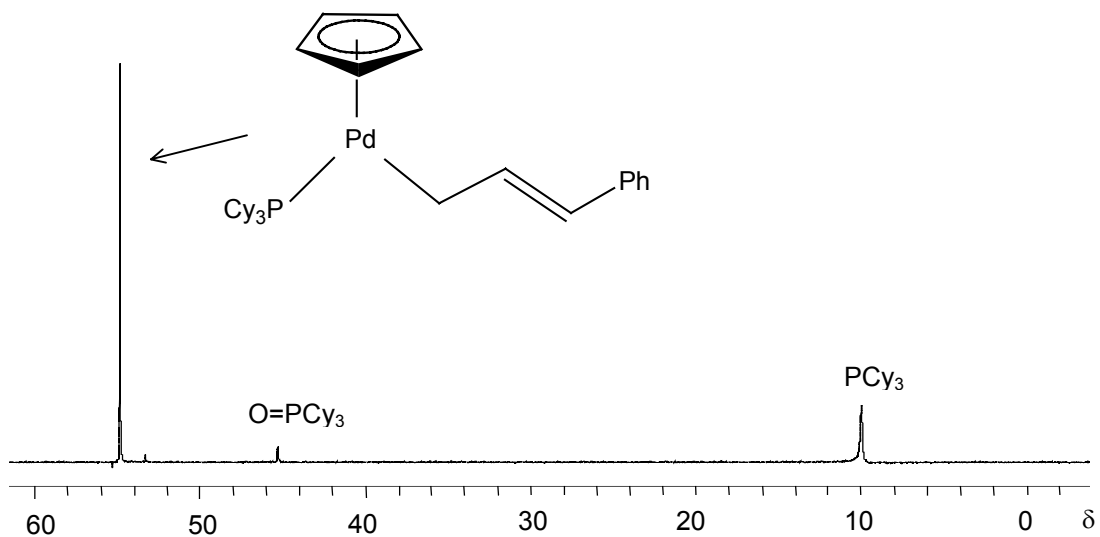


Figure 26. <sup>31</sup>P NMR spectrum (242.9 MHz) for reaction of  $\text{Pd}(\eta^3\text{-1-Ph-C}_3\text{H}_4)(\eta^5\text{-C}_5\text{H}_5)$  with two equivalents of PCy<sub>3</sub> 20 minutes after mixing at 25 °C in toluene-d<sub>8</sub>.

Over the course of 12 h, the free PCy<sub>3</sub> resonance ( $\delta$  10.0)<sup>28</sup> broadened, and a broad resonance at  $\delta$  39.0 appeared, associated with  $\text{Pd}(\text{PCy}_3)_2$  ( $\delta$  39.1).<sup>9</sup> Within 45 h after mixing, the intensity of the  $\eta^1$ -allyl resonance ( $\delta$  54.8) was greatly

diminished, with the dominant species being  $\text{Pd}(\text{PCy}_3)_2$  (Figure 27). Two resonances observed at  $\delta$  22.5 and  $\delta$  54.2 remain unidentified, despite analysis of the corresponding  $^1\text{H}$  and COSY NMR spectra.

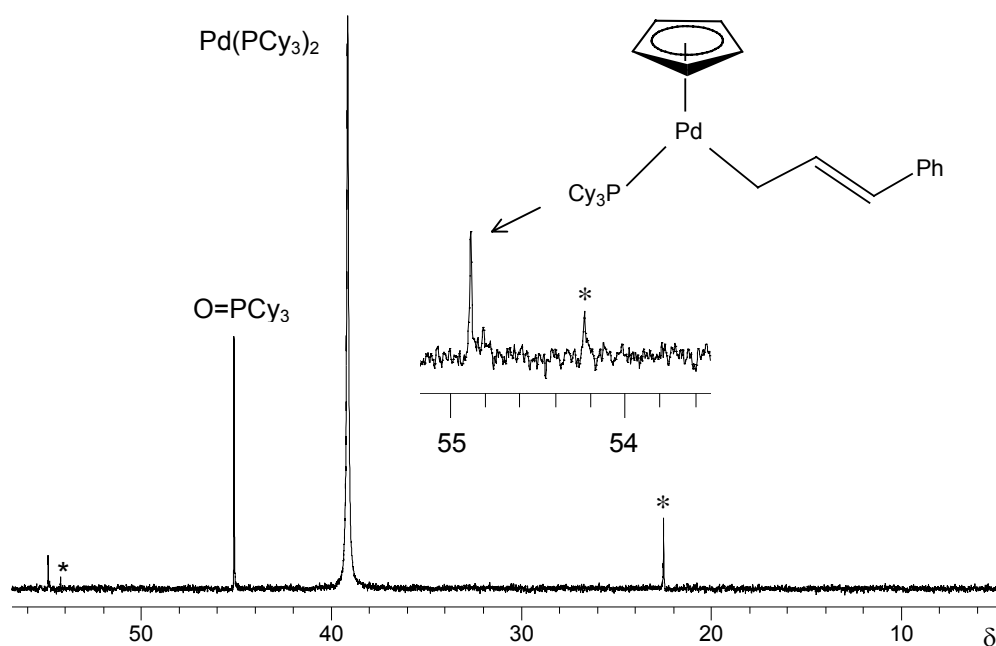


Figure 27.  $^{31}\text{P}$  NMR spectrum (242.9 MHz) for reaction of  $\text{Pd}(\eta^3\text{-1-Ph-C}_3\text{H}_4)(\eta^5\text{-C}_5\text{H}_5)$  with two equivalents of  $\text{PCy}_3$  in toluene- $d_8$  at 25 °C 45 h after mixing ( \* indicates unidentified resonances)

$^1\text{H}$  NMR and COSY spectra confirmed the identity of the species at  $^{31}\text{P}$   $\delta$  54.8 as the  $\eta^1$ -allyl species. The new singlet was observed at  $\delta$  5.77 showed an HSQC correlation  $\delta$   $^{13}\text{C}$   $\delta$  98.1 and was assigned as coordinated  $\eta^5\text{-C}_5\text{H}_5$  (Figure 28). Additionally, three sharp, COSY correlated  $^1\text{H}$  resonances appear at  $\delta$  6.90, 6.40 and 2.58 corresponding to the protons of a  $\eta^1$ -allyl group, along with Ph protons in the region of  $\delta$  7.02-7.40. The obtained  $^1\text{H}$  and  $^{13}\text{C}$  NMR data (Table

11), confirm the presence of a stable  $\eta^1$ -allyl species,  $\text{Pd}(\eta^1\text{-CH}_2\text{CH=CHPh})(\eta^5\text{-C}_5\text{H}_5)(\text{PCy}_3)$ . Furthermore, the value of  $^3J_{\text{H}_d\text{H}_c}$  (15.5 Hz) suggested the *trans* arrangement of the Ph and Pd moiety.

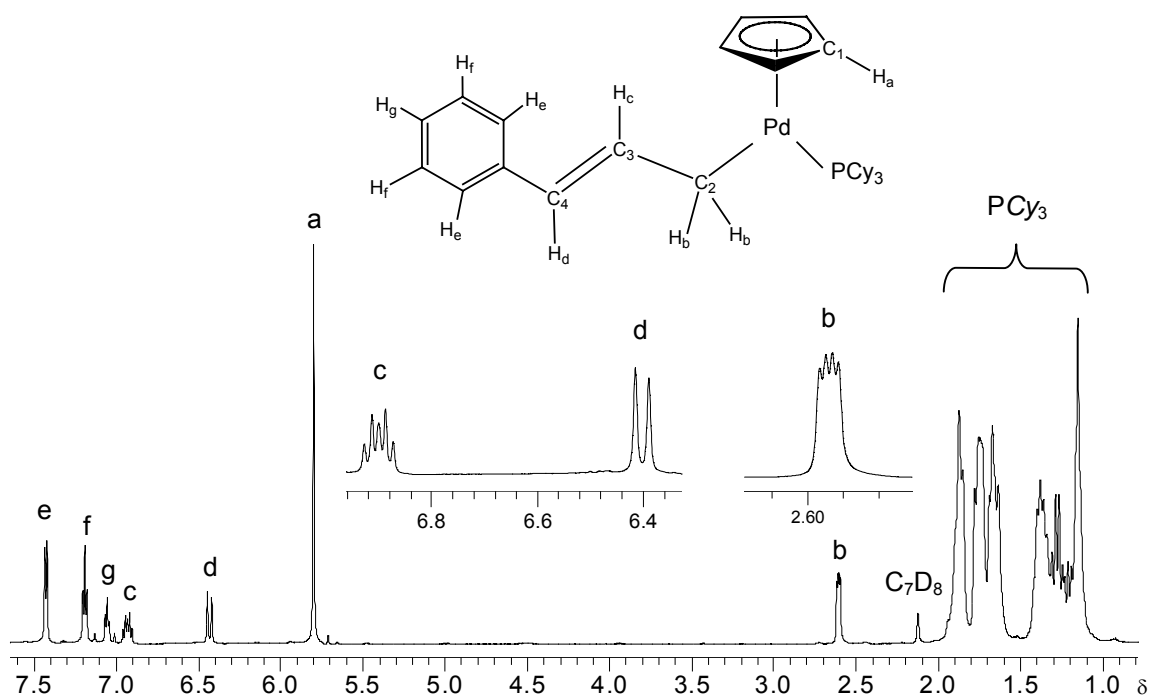
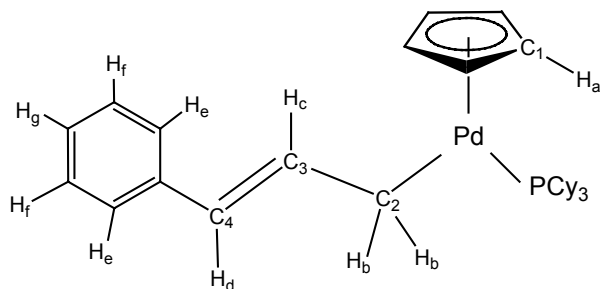


Figure 28.  $^1\text{H}$  NMR spectrum (600 MHz) for reaction of  $\text{Pd}(\eta^3\text{-1-Ph-C}_3\text{H}_4)(\eta^5\text{-C}_5\text{H}_5)$  with two equivalents of  $\text{PCy}_3$  at 25 °C in toluene- $\text{d}_8$  at 20 minutes after mixing.



Table 11.  $^1\text{H}$  and  $^{13}\text{C}$  NMR data for  $\text{Pd}(\eta^1\text{-CH}_2\text{CH=CHPh})(\eta^5\text{-C}_5\text{H}_5)(\text{PCy}_3)$  in toluene- $d_8$ .



$\delta$ $^1\text{H}$	Mult.	J (Hz)	Assignment	$\delta$ $^{13}\text{C}^a$	Mult.	J (Hz)	Assignment
1.12-1.84	-	-	PCy <sub>3</sub>	4.8	d	$^2J_{\text{PC}} = 5.5$	C <sub>2</sub>
2.58	dd	$^3J_{\text{HH}} = 8.7$ $J_{\text{PH}} = 4.2$	b	98.2	s	-	C <sub>1</sub>
5.77	s	-	a	121.0	s	-	C <sub>4</sub>
6.40	d	$^3J_{\text{HH}} = 15.5$	d	125.4	s	-	<i>ortho</i> Ph
6.90	dt	$^3J_{\text{HH}} = 15.5$ $^3J_{\text{HH}} = 8.7$	c	128.9	s	-	<i>meta</i> Ph
7.02	t	$^3J_{\text{HH}} = 7.2$	g	142.0	s	-	C <sub>3</sub>
7.16	dd	$^3J_{\text{HH}} = 7.6$ $^3J_{\text{HH}} = 8.1$	f				
7.40	d	$^3J_{\text{HH}} = 7.8$	e				

a) *ipso* and *para* carbons not assigned due to overlap with C<sub>7</sub>D<sub>8</sub> in  $^{13}\text{C}$  NMR spectrum

This result is in contrast with the observed  $\text{Pd}(\eta^3\text{-C}_3\text{H}_5)(\eta^5\text{-C}_5\text{H}_5)/\text{PCy}_3$  systems. While the  $\text{Pd}(\eta^3\text{-C}_3\text{H}_5)(\eta^5\text{-C}_5\text{H}_5)/\text{PCy}_3$  system at 25 °C produced exchanged broadened resonances associated with a possible  $\eta^1\text{-Cp-}\eta^3\text{-allyl}$  intermediate prior to forming of a dinuclear species,  $\text{Pd}(\eta^3\text{-1-Ph-C}_3\text{H}_4)(\eta^5\text{-C}_5\text{H}_5)$  formed a relatively stable  $\eta^1\text{-allyl}$  complex that remains the dominant species in solution for several hours.

A small number of isolated  $\eta^1$ -allyl complexes have been reported in the literature<sup>33</sup>, many of which involving chelating ligands.<sup>33a,b,d,e</sup> Fewer examples have appeared involving other  $\pi$ -bound ligands, such as the isolation of  $\text{Pd}(\eta^1\text{-C}_3\text{H}_5)(\eta^3\text{-C}_3\text{H}_5)(\text{PPr}^i_3)$ .<sup>33c</sup> It is presumed that the isolation of these  $\eta^1$ -allyl species by a 1:1 reaction of  $\text{Pd}(\eta^3\text{-1-Ph-C}_3\text{H}_4)(\eta^5\text{-C}_5\text{H}_5)$  and L (L =  $\text{PCy}_3$ ) may very well become one of the first examples of a stable  $\eta^1$ -allyl- $\eta^5$ -Cp complex of Pd at ambient temperature.

A  $^1\text{H}$  NMR spectrum obtained 45 h after mixing  $\text{Pd}(\eta^3\text{-1-Ph-C}_3\text{H}_4)(\eta^5\text{-C}_5\text{H}_5)$  with two equivalents of  $\text{PCy}_3$  at 25 °C showed weak resonances for the  $\eta^1$ -allyl species, consistent with its consumption to produce  $\text{Pd}(\text{PCy}_3)_2$  (Figure 29).

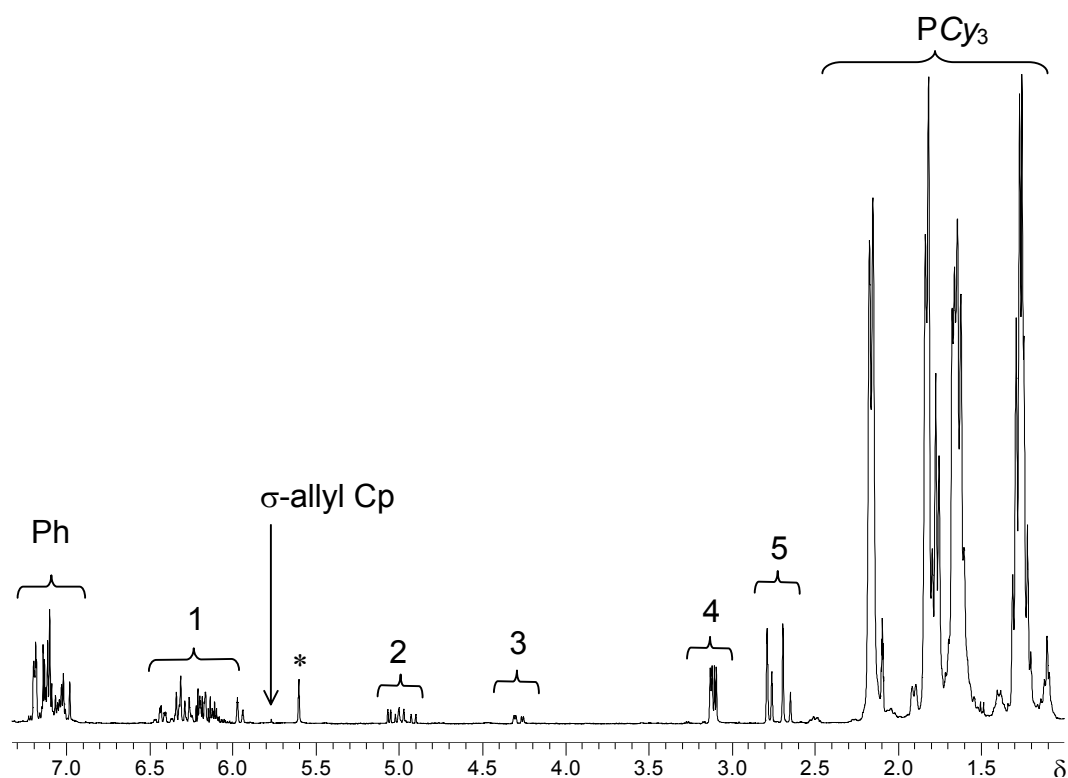
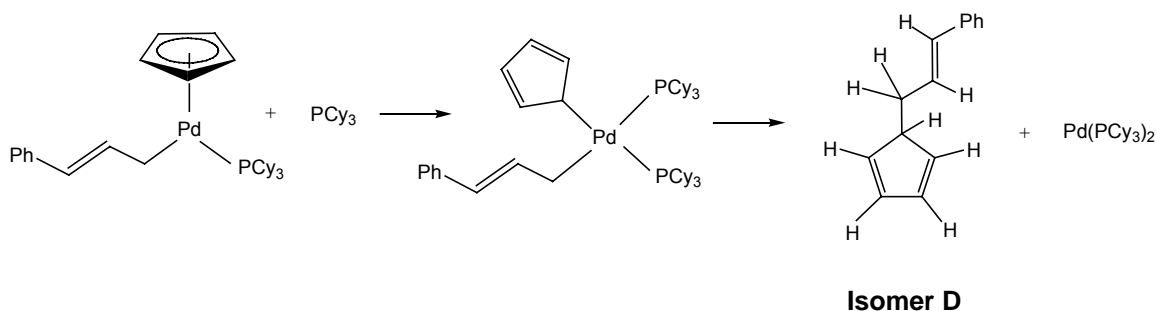


Figure 29.  $^1\text{H}$  NMR spectrum (600 MHz) for reaction of  $\text{Pd}(\eta^3\text{-1-Ph-C}_3\text{H}_4)(\eta^5\text{-C}_5\text{H}_5)$  with two equivalents of  $\text{PCy}_3$  in toluene- $d_8$  at 25 °C at 45 hours after mixing (\* indicates unidentified resonances).

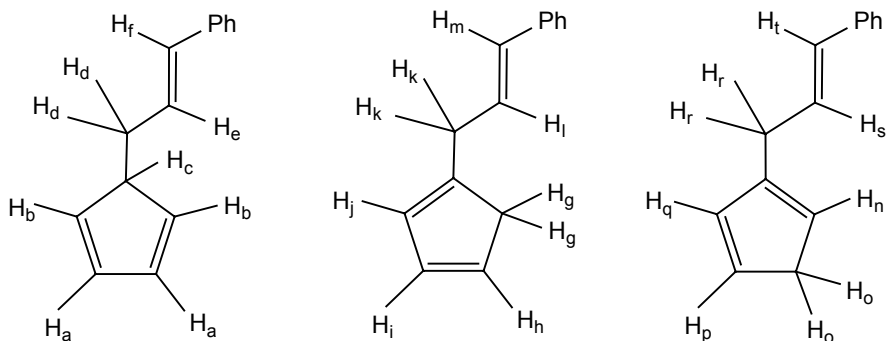
Concurrently, resonances appeared in the phenyl region ( $\delta$  7.03-7.23), as well as in the regions of  $\delta$  6.11-6.48, 4.90-5.07, 4.25-4.31, 3.09-3.13 and 2.65-2.79 (labeled 1-5 respectively). It was anticipated that these resonances would, at least initially, be those of reductive elimination product 5-(3-phenylallyl)cyclopentadiene (labeled isomer D) formed according to Scheme 36, originating from  $\text{Pd}(\eta^1\text{-CH}_2\text{CH=CHPh})(\eta^5\text{-C}_5\text{H}_5)(\text{PCy}_3)_2$ .<sup>2g,d,e</sup>



Scheme 36. Anticipated mechanism of reductive elimination from  $\text{Pd}(\eta^1\text{-CH}_2\text{CH=CHPh})(\eta^5\text{-C}_5\text{H}_5)(\text{PCy}_3)_2$ .

It was anticipated that subsequent 1,5-hydride shifts would produce 1-(3-phenylallyl)cyclopentadiene (isomer E) and 2-(3-phenylallyl)cyclopentadiene (isomer F), whose  $^1\text{H}$  NMR spectra were simulated as described above, using the methods described by Silverstein *et al.*<sup>7</sup> as well as ACD Labs  $^1\text{H}$  NMR Predictor software (Table 12).<sup>8</sup> Upon examination of Figure 29, it became clear that more than one isomeric product was present. However, no multiplets were observed in the area of  $\delta$  5.7, which would correspond to the vinylic protons  $\text{H}_i$  and  $\text{H}_s$  in isomers E and F respectively.

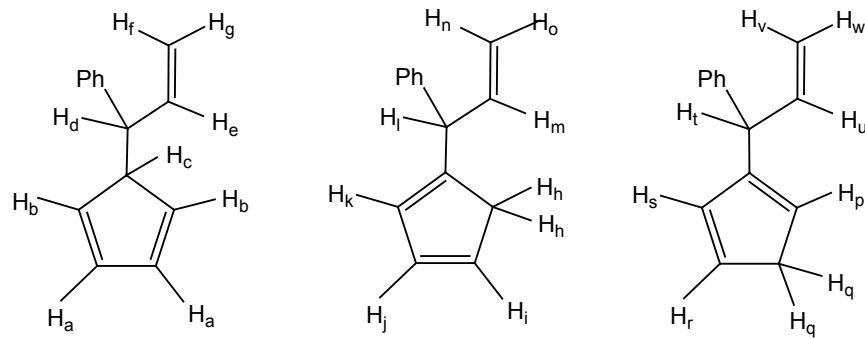
Table 12. Simulated chemical shifts for reductive elimination products derived from 5-(3-phenylallyl)cyclopentadiene.



Isomer D		Isomer E		Isomer F	
$\delta$		$\delta$		$\delta$	
H <sub>a</sub>	6.3	H <sub>g</sub>	2.90	H <sub>n</sub>	6.0
H <sub>b</sub>	6.1	H <sub>n</sub>	6.1	H <sub>o</sub>	2.8
H <sub>c</sub>	1.8	H <sub>i</sub>	6.1	H <sub>p</sub>	6.1
H <sub>d</sub>	2.1	H <sub>j</sub>	6.0	H <sub>q</sub>	6.2
H <sub>e</sub>	6.4	H <sub>k</sub>	2.3	H <sub>r</sub>	2.3
H <sub>f</sub>	6.5	H <sub>l</sub>	5.7	H <sub>s</sub>	5.7
Ph	7.2-7.3	H <sub>m</sub>	6.4	H <sub>t</sub>	6.4
		Ph	7.2-7.3	Ph	7.2-7.3

This implies that while D may be present, E and F are not. Furthermore, simulations of isomers D, E and F could not account for the resonances observed in the regions around  $\delta$  5.0 and 4.3. These resonances can be explained if one considers the alternative reductive elimination products, derived from 5-(1-phenylallyl)cyclopentadiene, whose  $^1\text{H}$  spectra were also simulated (Table 13).

Table 13. Simulated chemical shifts for alternative reductive elimination products derived from 5-(1-phenylallyl)cyclopentadiene.



Isomer G		Isomer H		Isomer I	
$\delta$		$\delta$		$\delta$	
H <sub>a</sub>	6.3	H <sub>h</sub>	2.9	H <sub>p</sub>	6.0
H <sub>b</sub>	6.1	H <sub>i</sub>	6.1	H <sub>q</sub>	2.8
H <sub>c</sub>	1.8	H <sub>j</sub>	6.1	H <sub>r</sub>	6.1
H <sub>d</sub>	4.1	H <sub>k</sub>	5.9	H <sub>s</sub>	6.3
H <sub>e</sub>	6.1	H <sub>l</sub>	2.4	H <sub>t</sub>	2.4
H <sub>f</sub>	5.1	H <sub>m</sub>	5.8	H <sub>u</sub>	5.8
H <sub>g</sub>	5.1	H <sub>n</sub>	5.0	H <sub>v</sub>	5.1
Ph	7.2-7.3	H <sub>o</sub>	5.0	H <sub>w</sub>	5.1
		Ph	7.2-7.3	Ph	7.2-7.3

The resonances observed at  $\delta$  4.25-4.31 (Figure 29) are consistent with that of H<sub>d</sub> in isomer G, while those at  $\delta$  4.90-5.07 are consistent with vinylic methylene protons (H<sub>f, g, n, o, v, w</sub>) in isomers G, H and I respectively. A COSY spectrum was insufficient in further identifying the nature of the isomers present. In addition, the mechanism of formation of these isomers cannot be confirmed, and was quite unexpected given the observed  $\eta^1$ -allyl species Pd( $\eta^1$ -CH<sub>2</sub>CH=CHPh)( $\eta^5$ -C<sub>5</sub>H<sub>5</sub>)(PCy<sub>3</sub>).

Similar studies by Werner *et al.* involved ligand displacement reactions of the asymmetrically substituted complex Pd( $\eta^3$ -1,1,2-Me<sub>3</sub>C<sub>3</sub>H<sub>4</sub>)( $\eta^5$ -C<sub>5</sub>H<sub>5</sub>), in order to determine if reductive elimination occurred at C<sub>1</sub> or C<sub>3</sub> of the  $\eta^3$ -bound

allyl group.<sup>2g</sup> Interestingly, both products, 5-(2,3,3-trimethylallyl)cyclopentadiene and 5-(1,1,2-trimethylallyl)cyclopentadiene were observed, but only at low temperature (−40 °C). It could not be confirmed if either of these products had resulted from the formation and subsequent isomerization of the other. At room temperature, 5-(2,3,3-trimethylallyl)cyclopentadiene was found to dominate, implying that reductive elimination occurred at the less substituted carbon-3. However, it was also noted that the product distribution was dependent on the Lewis base used for ligand displacement.

The reaction of  $\text{Pd}(\eta^3\text{-1-Ph-C}_3\text{H}_4)(\eta^5\text{-C}_5\text{H}_5)$  with two equivalents of  $\text{PCy}_3$  was also monitored by  $^{31}\text{P}$  NMR at 50 °C (Figure 30).

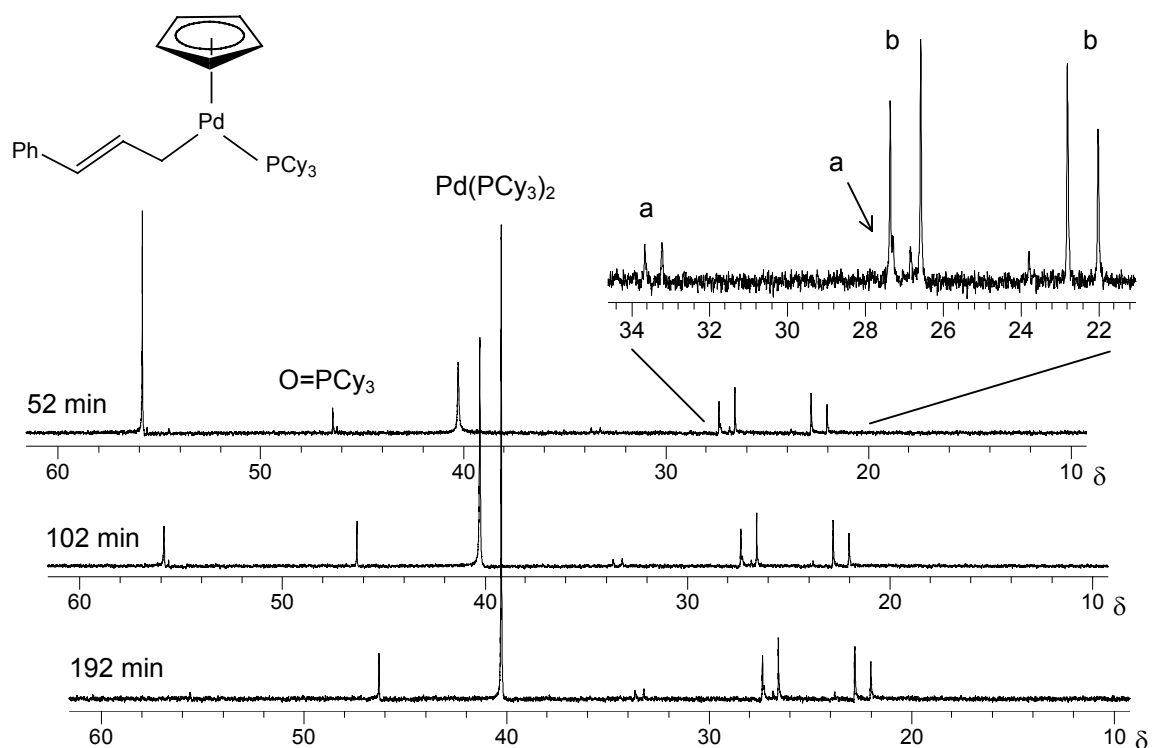


Figure 30. Stacked plots of  $^{31}\text{P}$  NMR spectra (161.9 MHz) for reaction of  $\text{Pd}(\eta^3\text{-1-Ph-C}_3\text{H}_4)(\eta^5\text{-C}_5\text{H}_5)$  with two equivalents  $\text{PCy}_3$  in  $\text{toluene-d}_8$  at 50 °C.

The  $^{31}\text{P}$  NMR data indicated that the  $\eta^1$ -allyl species ( $\delta$  55.8) was consumed, while a new peak at  $\delta$  40.2 emerged, attributed to  $\text{Pd}(\text{PCy}_3)_2$ .<sup>9</sup>

Additionally, two sets of doublets appeared at  $\delta$  22.4, 27.0 (labeled b,  $J_{\text{P-P}} = 127.5$  Hz) and  $\delta$  27.1, 33.4 (labeled a,  $J_{\text{P-P}} = 72.1$  Hz), as confirmed by  $^{31}\text{P}$ - $^{31}\text{P}$  correlation spectroscopy (Figure 31). The presence of two distinct sets of doublets suggested the formation of two different dinuclear species, where the asymmetry of the 1-phenylallyl group results in inequivalent  $^{31}\text{P}$  nuclei. It is conceivable that these dinuclear species exist as conformational isomers (*syn* and *anti* Ph), resulting in two sets of doublets in the spectrum (Figure 32).

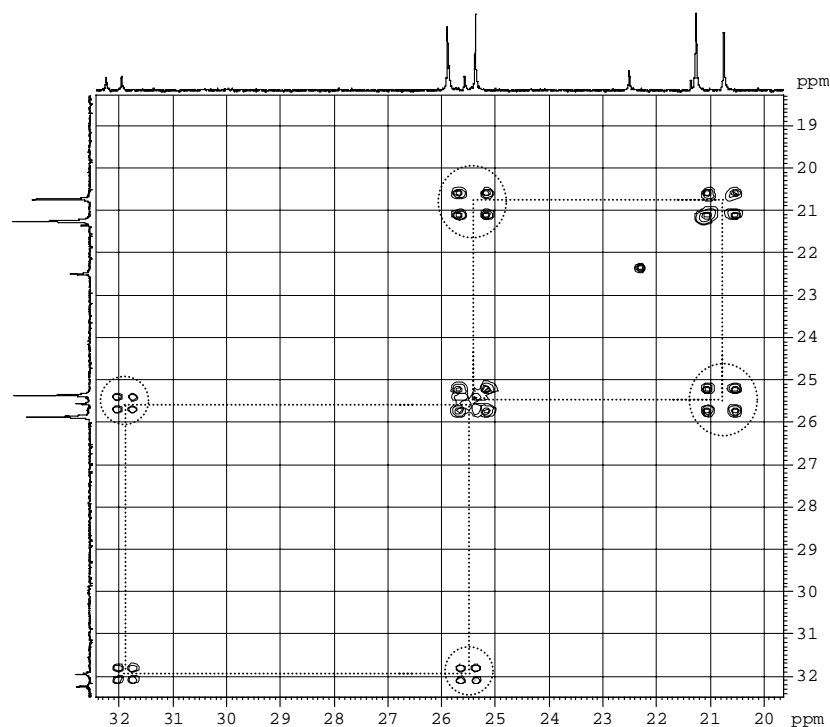


Figure 31.  $^{31}\text{P}$ - $^{31}\text{P}$  correlation spectrum (242.9 MHz) for reaction of  $\text{Pd}(\eta^3\text{-1-Ph-C}_3\text{H}_4)(\eta^5\text{-C}_5\text{H}_5)$  with two equivalents  $\text{PCy}_3$  in toluene- $d_8$  at 50 °C (spectrum obtained upon cooling to 25 °C)

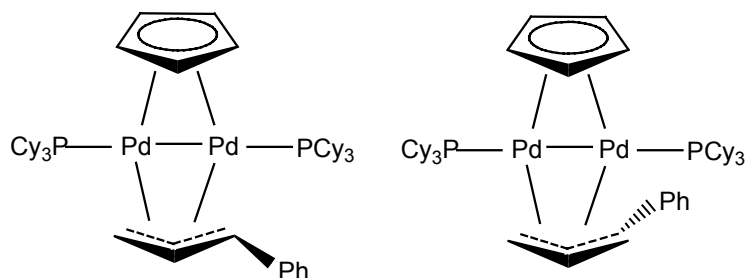


Figure 32. Postulated *anti* and *syn* isomers of  $\text{Pd}(\eta^3\text{-1-Ph-C}_3\text{H}_4)(\eta^5\text{-C}_5\text{H}_5)(\text{PCy}_3)_2$ .

The presence of these complexes is however very difficult to confirm from  $^1\text{H}$  NMR data, as resonances from both reductive elimination products, as well as  $\text{PCy}_3$ , obscure the regions associated with the dinuclear complex. However, a corresponding  $^{13}\text{C}$  NMR spectrum shows a signal at  $\delta$  91.0, typical for a dinuclear species<sup>2b</sup>, which in turn shows an HSQC correlation to a  $^1\text{H}$  signal at  $\delta$  5.98, consistent with an  $\eta^5\text{-Cp}$  ring. Similarly, a  $^{13}\text{C}$  resonance at  $\delta$  89.7 shows an HSQC correlation to  $\delta$   $^1\text{H}$  5.70, supporting the presence of another  $\eta^5\text{-C}_5\text{H}_5$  containing species.<sup>2b</sup>

When  $\text{Pd}(\eta^3\text{-1-Ph-C}_3\text{H}_4)(\eta^5\text{-C}_5\text{H}_5)$  was mixed with two equivalents of  $\text{PCy}_3$  at 77 °C, a  $^{31}\text{P}$  NMR spectrum obtained 12 minutes after mixing shows a broad peak at  $\delta$  40.2 associated with  $\text{Pd}(\text{PCy}_3)_2$ , and a resonance at  $\delta$  46.0 ( $\text{O}=\text{PCy}_3$ ) (Figure 33).<sup>9,28</sup> This was substantially faster than that observed for  $\text{PdL}_2$  generation in  $\text{Pd}(\eta^3\text{-C}_3\text{H}_5)(\eta^5\text{-C}_5\text{H}_5)/\text{PCy}_3$  system (1 h at 77 °C), as described in Section 3.1.2.1.



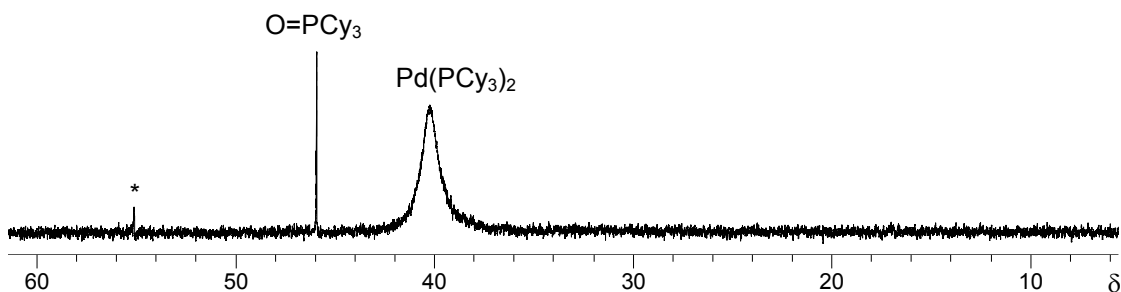


Figure 33. <sup>31</sup>P NMR spectrum (163.0 MHz) for reaction of Pd( $\eta^3$ -1-Ph-C<sub>3</sub>H<sub>4</sub>)( $\eta^5$ -C<sub>5</sub>H<sub>5</sub>) is reacted with two equivalents of PCy<sub>3</sub> in toluene-d<sub>8</sub> at 77 °C 12 minutes after mixing (\* indicates unidentified resonance).

The increased reactivity of Pd( $\eta^3$ -1-Ph-C<sub>3</sub>H<sub>4</sub>)( $\eta^5$ -C<sub>5</sub>H<sub>5</sub>) towards ligand displacement relative to Pd( $\eta^3$ -C<sub>3</sub>H<sub>5</sub>)( $\eta^5$ -C<sub>5</sub>H<sub>5</sub>) is likely due to electronic effects. Previous work has indicated that the metal center of Pd( $\eta^3$ -C<sub>3</sub>H<sub>5</sub>)( $\eta^5$ -C<sub>5</sub>H<sub>5</sub>) is significantly electron deficient,<sup>34</sup> accounting for its reactivity with Lewis bases such as phosphine. As Pd( $\eta^3$ -1-Ph-C<sub>3</sub>H<sub>4</sub>)( $\eta^5$ -C<sub>5</sub>H<sub>5</sub>) reacts much more quickly to produce PdL<sub>2</sub>, this may be a result of a change in electronic character of the  $\eta^3$ -allyl ligand as a result of the phenyl substituent. Much of the work done in assessing the electronic character of the  $\eta^3$ -allyl group in palladium complexes has been performed in the context of catalytically significant cationic  $\eta^3$ -allyl complexes.<sup>35</sup> However, early work performed on *para* substituted phenyl allyl complexes,<sup>36</sup> Pd(1-(*p*-C<sub>6</sub>H<sub>4</sub>X)C<sub>3</sub>H<sub>4</sub>)(L) and Pd(2-(*p*-C<sub>6</sub>H<sub>4</sub>X)C<sub>3</sub>H<sub>4</sub>)(L) (L = acac, Cp, X = Br, Cl, H, CH<sub>3</sub>, CH<sub>3</sub>O) indicates that the 1-position of the  $\eta^3$ -allyl group, bearing the substituted phenyl, is particularly electron poor. Given the behaviour of the 1-Ph complexes described here, it is reasonable to assume that this

enhanced reactivity at the Pd center arises from the electron-withdrawing effect of the phenyl substituent.

An additional explanation for the increased reactivity of the 1-Ph complex towards ligand displacement can be understood by examining the crystal structure of  $\text{Pd}(\eta^3\text{-1-Ph-C}_3\text{H}_4)(\eta^5\text{-C}_5\text{H}_5)$ .<sup>31</sup> Crystallographic studies of  $\text{Pd}(\eta^3\text{-1-Ph-C}_3\text{H}_4)(\eta^5\text{-C}_5\text{H}_5)$  indicate that the Pd-CHPh bond is much longer, and therefore presumably weaker, than the Pd-CH<sub>2</sub> bond.<sup>31</sup> This could cause the former to be a much more reactive position for nucleophilic attack, perhaps through the formation of an  $\eta^1$ -intermediate species.

### 3.2.2 L = P<sup>t</sup>MeBu<sub>2</sub>

Upon reaction of  $\text{Pd}(\eta^3\text{-1-Ph-C}_3\text{H}_4)(\eta^5\text{-C}_5\text{H}_5)$  with two equivalents of P<sup>t</sup>MeBu<sub>2</sub> at 25 °C, similar behavior was observed as with PCy<sub>3</sub>. A <sup>31</sup>P NMR spectrum obtained one hour after mixing at 25 °C showed a strong singlet at  $\delta$  60.6, associated with a  $\eta^1$ -allyl complex, along with a weaker unassigned resonance at  $\delta$  61.6 (Figure 34). Furthermore, there was an extremely broad resonance observed in the region of  $\delta$  41, which implied formation and exchange of the  $\text{Pd}(\text{PMeBu}_2)_2$  complex at room temperature.<sup>11</sup> No free P<sup>t</sup>MeBu<sub>2</sub> was observed at  $\delta$  11.4.<sup>12</sup>

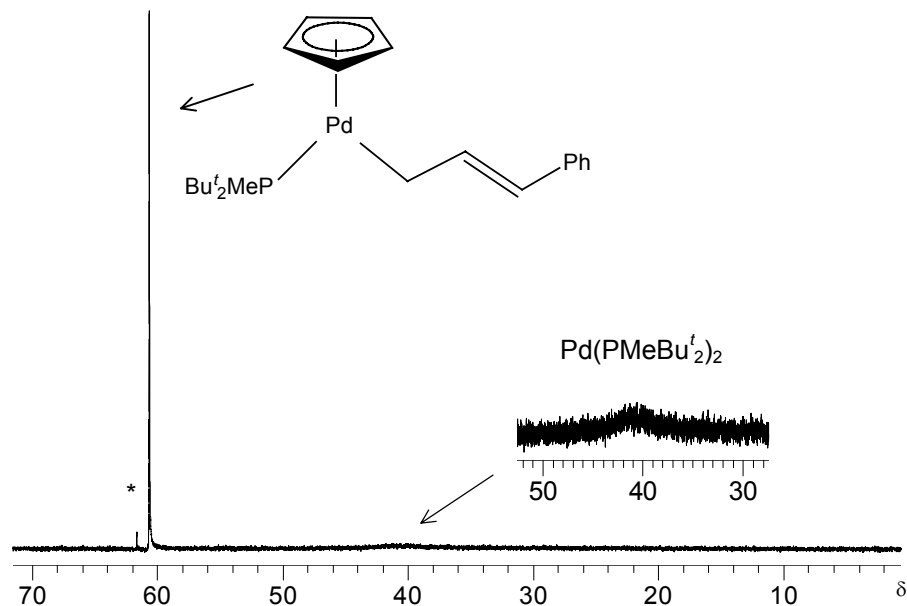


Figure 34.  $^{31}\text{P}$  NMR spectrum (163.0 MHz) for reaction of  $\text{Pd}(\eta^3\text{-1-Ph-C}_3\text{H}_4)(\eta^5\text{-C}_5\text{H}_5)$  with two equivalents of  $\text{PMeBu}_2^t$  in toluene- $d_8$  at 25 °C 1 h after mixing (\* indicates unidentified resonance).

A  $^1\text{H}$  NMR spectrum obtained ten minutes after mixing at 25 °C confirmed the presence of a stable  $\eta^1$ -allyl species, indicated by  $^1\text{H}$  NMR resonances similar to those observed for  $\text{Pd}(\eta^1\text{-CH}_2\text{CH=CHPh})(\eta^5\text{-C}_5\text{H}_5)(\text{PCy}_3)$  (Figure 35). The  $^1\text{H}$  NMR data for  $\text{Pd}(\eta^1\text{-CH}_2\text{CH=CHPh})(\eta^5\text{-C}_5\text{H}_5)(\text{P}^t\text{Bu}_2\text{Me})$  are summarized in Table 14. Two resonances appear in the  $^1\text{H}$  NMR at  $\delta$  1.05 (8.9 Hz) and  $\delta$  0.83 (8.0 Hz) which broaden substantially over the course of the reaction. Although these resonances have chemical shifts similar to those of free  $\text{PMeBu}_2^t$  ( $\delta$  1.04, 10.6 Hz,  $\delta$  0.83, 4.5 Hz),<sup>12</sup> the anticipated  $^{31}\text{P}$  coupling constants are not. These  $\text{PMeBu}_2^t$  resonances are likely associated with the rapidly exchanging  $\text{Pd}(\text{PMeBu}_2^t)_2$ , seen in region of  $^{31}\text{P}$   $\delta$  41.<sup>11</sup>

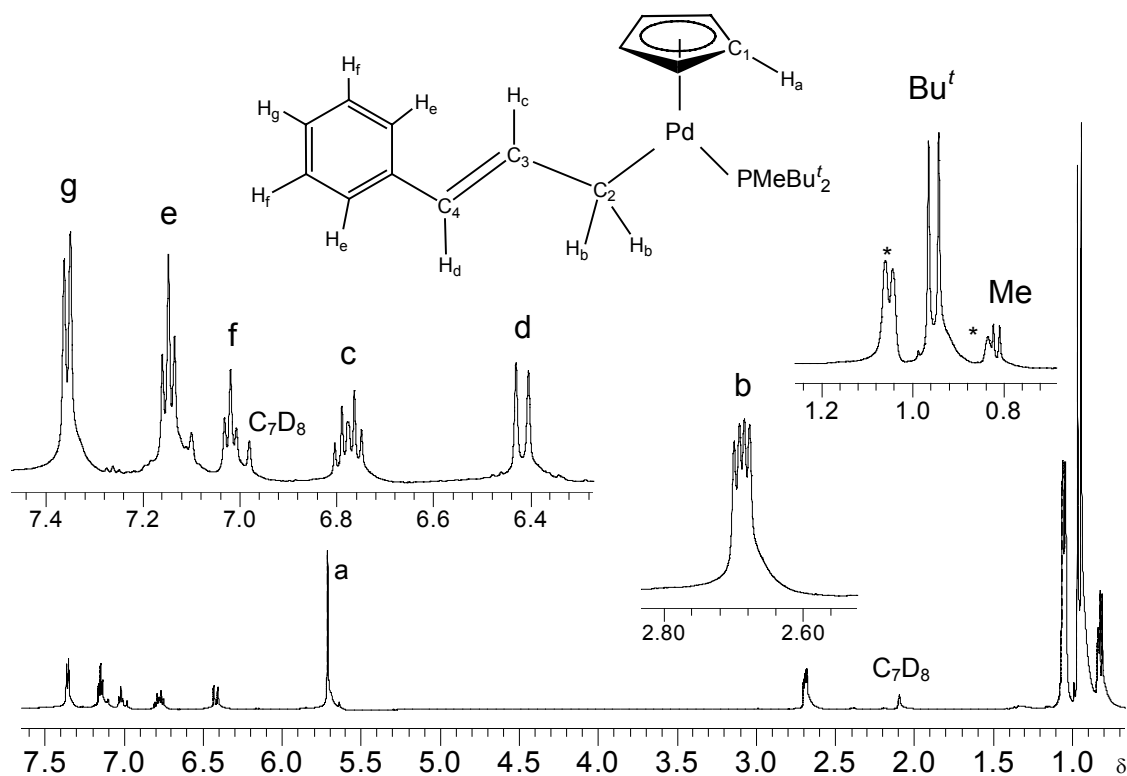


Figure 35.  $^1\text{H}$  NMR spectrum (600 MHz) of  $\text{Pd}(\eta^3\text{-1-Ph-C}_3\text{H}_4)(\eta^5\text{-C}_5\text{H}_5)$  with two equivalents of  $\text{PMeBu}_2$  in toluene- $\text{d}_8$  ten minutes after mixing at  $25^\circ\text{C}$ .

Table 14. Summary of  $^1\text{H}$  NMR data for  $\text{Pd}(\eta^1\text{-CH}_2\text{CH=CHPh})(\eta^5\text{-C}_5\text{H}_5)(\text{P}^t\text{Bu}_2\text{Me})$

$\delta$ $^1\text{H}$	Multiplicity	$J/(\text{Hz})$	Assignment
0.95	d	$^2J_{\text{PH}} = 8.3$	Me
0.82	d	$^3J_{\text{PH}} = 13.6$	$\text{Bu}^t$
2.69	dd	$^3J_{\text{HH}} = 9.1$ $J_{\text{PH}} = 4.5$	b
5.71	s	-	a
6.42	d	$^3J_{\text{HH}} = 15.5$	d
6.78	dt	$^3J_{\text{HH}} = 15.5$ $^3J_{\text{HH}} = 9.1$	c
7.02	t	$^3J_{\text{HH}} = 7.2$	g
7.15	dd	$^3J_{\text{HH}} = 7.6$ $^3J_{\text{HH}} = 7.2$	f
7.36	d	$^3J_{\text{HH}} = 7.6$	e

After 51 hours at 25 °C, the dominant  $\eta^1$ -allyl species  $\text{Pd}(\eta^1\text{-CH}_2\text{CH=CHPh})(\eta^5\text{-C}_5\text{H}_5)(\text{P}^t\text{Bu}_2\text{Me})$  at  $\delta$  60.6 has been partially consumed to produce the anticipated resonance at  $\delta$  41.6, associated with  $\text{Pd}(\text{P}^t\text{MeBu}_2)_2$ .<sup>11</sup> When this sample was then heated to 50 °C, the remaining  $\eta^1$ -allyl species was rapidly consumed within 5 minutes to form  $\text{Pd}(\text{P}^t\text{MeBu}_2)_2$  (Figure 36).

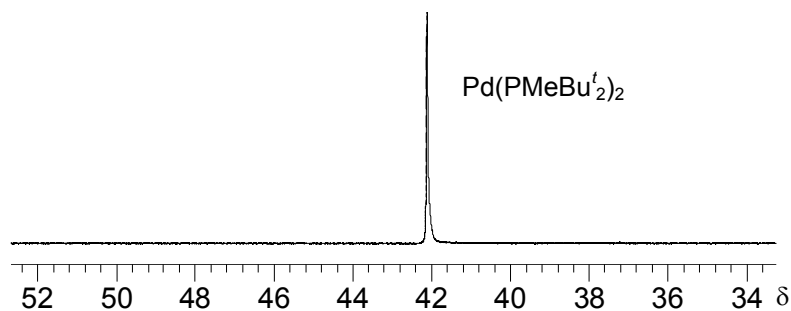


Figure 36. <sup>31</sup>P NMR spectrum (242.9 MHz) for reaction of  $\text{Pd}(\eta^3\text{-1-Ph-C}_3\text{H}_4)(\eta^5\text{-C}_5\text{H}_5)$  with two equivalents of  $\text{P}^t\text{MeBu}_2$  after 51 hours at 25 °C, followed by heating to 50 °C.

As was observed for the  $\text{Pd}(\eta^3\text{-1-Ph-C}_3\text{H}_4)(\eta^5\text{-C}_5\text{H}_5)/\text{PCy}_3$  system, the formation of  $\text{Pd}(\text{P}^t\text{MeBu}_2)_2$  from  $\text{Pd}(\eta^3\text{-1-Ph-C}_3\text{H}_4)(\eta^5\text{-C}_5\text{H}_5)$  occurs much more rapidly at elevated temperature than with the analogous systems using  $\text{Pd}(\eta^3\text{-C}_3\text{H}_5)(\eta^5\text{-C}_5\text{H}_5)$  (1 h at 77 °C).

### 3.2.3 L = PPh<sub>3</sub>

<sup>31</sup>P and <sup>1</sup>H NMR spectra were also obtained for the reaction of  $\text{Pd}(\eta^3\text{-1-PhC}_3\text{H}_4)(\eta^5\text{-C}_5\text{H}_5)$  and two equivalents of  $\text{PPh}_3$  at 25 °C. As was observed with both  $\text{PCy}_3$  and  $\text{P}^t\text{BuMe}_2$ , the stable  $\eta^1$ -allyl species  $\text{Pd}(\eta^1\text{-CH}_2\text{CH=CHPh})(\eta^5\text{-C}_5\text{H}_5)(\text{PPh}_3)$  was detected in the <sup>1</sup>H NMR spectrum (Figure 37) within minutes of

mixing and was confirmed by analysis of the corresponding COSY spectrum (Table 15). The intensity of the  $\eta^1$ -allyl  $^1\text{H}$  resonances diminished over the course of the reaction, consistent with the consumption of  $\eta^1$ -allyl species. In addition, reductive elimination products were observed in the regions labeled 1-10 in Figure 37.

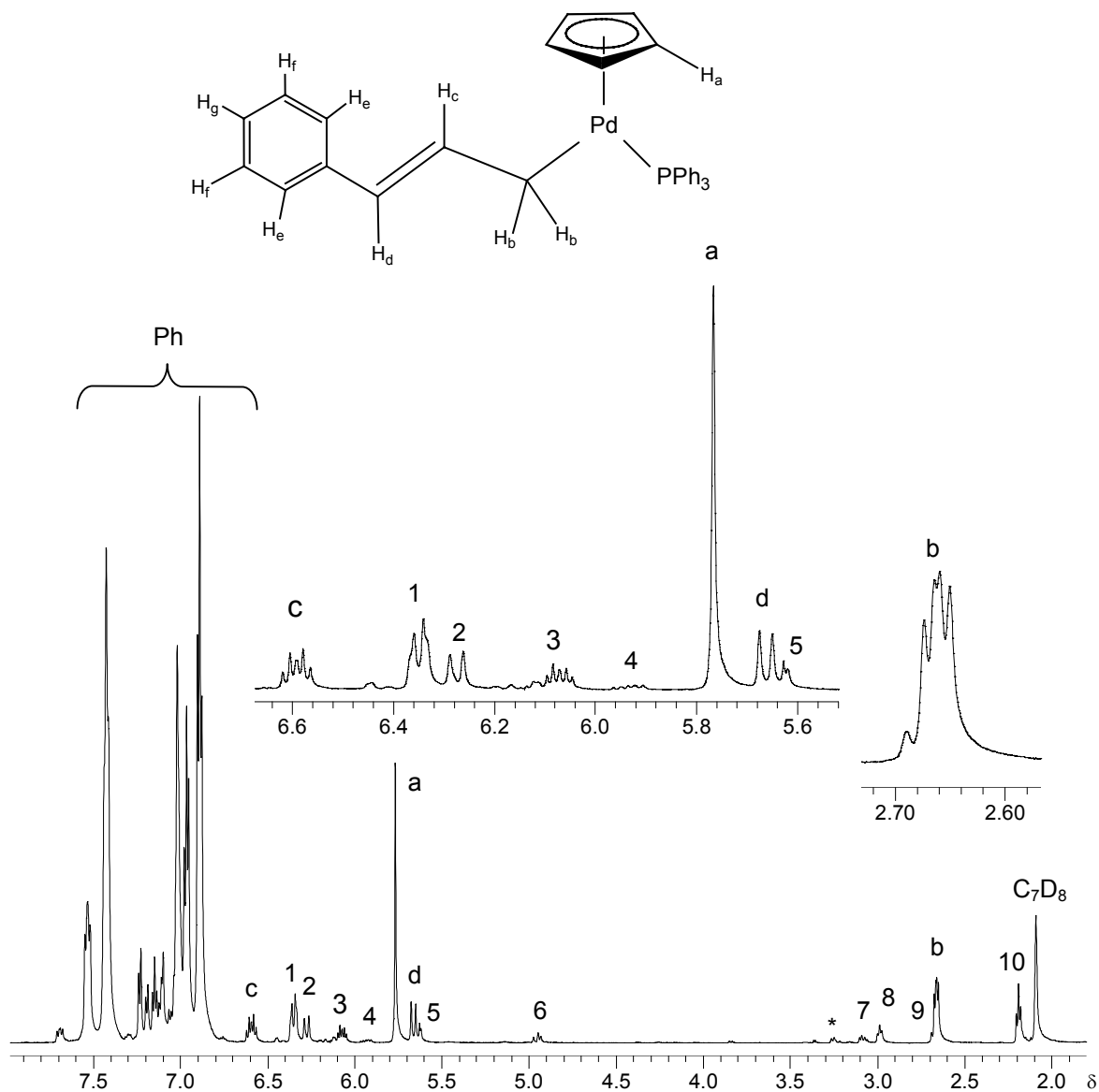
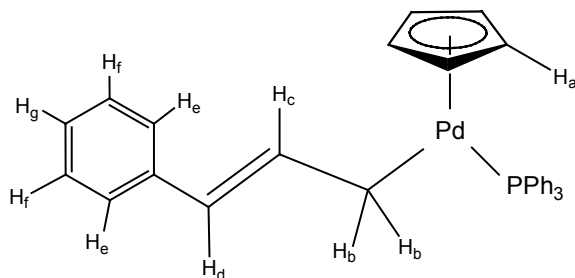


Figure 37.  $^1\text{H}$  NMR spectrum (600 MHz) for reaction of  $\text{Pd}(\eta^3\text{-1-Ph-C}_3\text{H}_4)(\eta^5\text{-C}_5\text{H}_5)$  with two equivalents of  $\text{PPh}_3$  in toluene- $d_8$  7.5 minutes after mixing at 25  $^\circ\text{C}$  (\* indicates unidentified resonances).

Table 15.  $^1\text{H}$  NMR Assignment for  $\text{Pd}(\eta^1\text{-CH}_2\text{CH=CHPh})(\eta^5\text{-C}_5\text{H}_5)(\text{PPh}_3)$ .<sup>a</sup>



$\delta$ $^1\text{H}$	Multiplicity	$J$ (Hz)	Assignment
2.66	dd	$^3J_{\text{HH}} = 9.4$ $J_{\text{PH}} = 5.7$	b
5.66	d	$^3J_{\text{HH}} = 15.1$	d
5.77	s	-	a
6.59	dt	$^3J_{\text{HH}} = 15.1$ $^3J_{\text{HH}} = 8.7$	c

a) Ph peaks not assigned (see text).

The phenyl resonances for the  $\eta^1$ -allyl species could not be assigned with certainty. In addition to the  $\eta^1$ -allyl species,  $^{31}\text{P}$  NMR data (discussed below) indicated the presence of  $\text{Pd}(\text{PPh}_3)_3$ ,  $\text{O}=\text{PPh}_3$ , and dinuclear species. All of these species produced resonances in the phenyl region that overlapped significantly and the obtained  $^1\text{H}$  and COSY NMR were thus insufficient for the identification of the phenyl resonances of the  $\eta^1$ -allyl complex.

The monitoring of this reaction by  $^{31}\text{P}$  NMR revealed a resonance at  $\delta$  44.7, associated with the  $\eta^1$ -allyl species  $\text{Pd}(\eta^1\text{-CH}_2\text{CH=CHPh})(\eta^5\text{-C}_5\text{H}_5)(\text{PPh}_3)$ , which diminished in intensity over time, while that at  $\delta$  22.4 grew in, likely attributable to  $\text{Pd}(\text{PPh}_3)_3$  (Figure 38).<sup>4</sup>

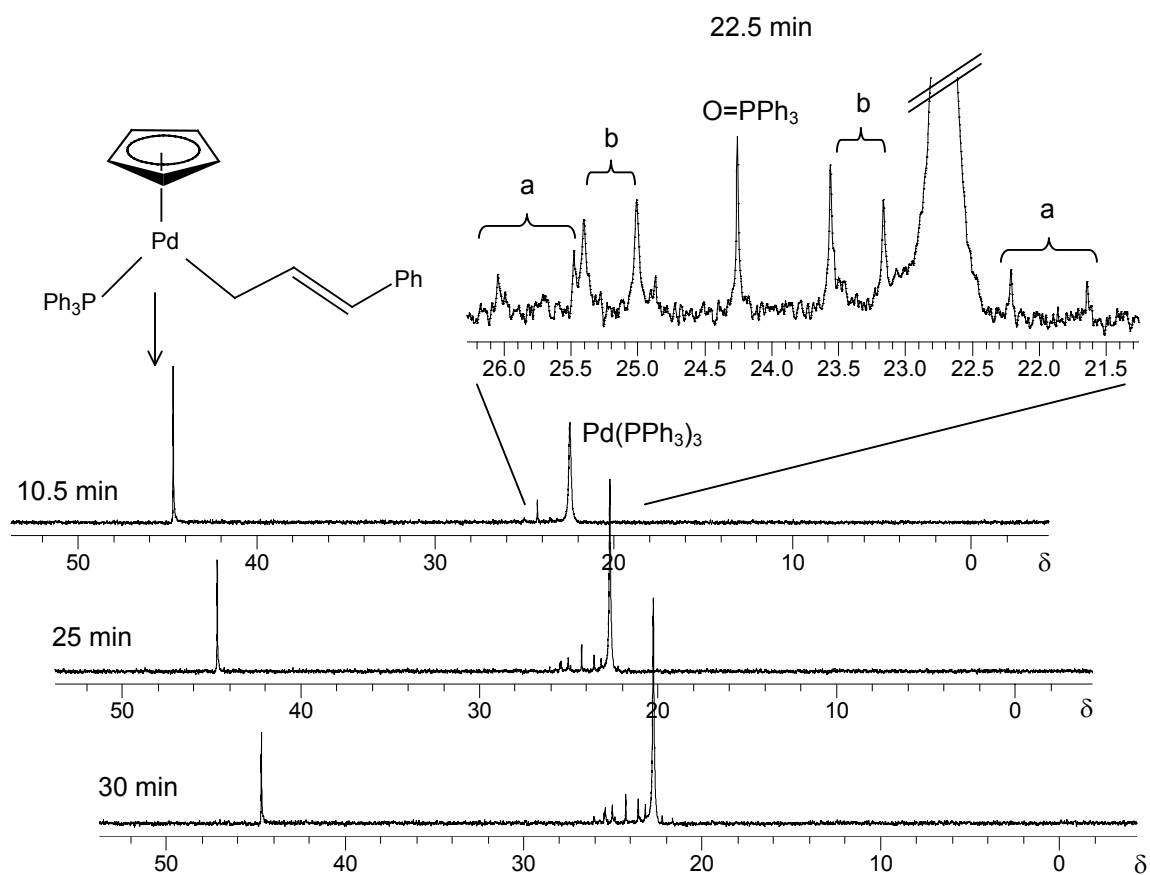


Figure 38.  $^{31}\text{P}$  NMR spectra (242.9 MHz) for reaction of  $\text{Pd}(\eta^3\text{-1-Ph-C}_3\text{H}_4)(\eta^5\text{-C}_5\text{H}_5)$  with two equivalents of  $\text{PPh}_3$  in toluene- $d_8$  at 25 °C.

A sharp resonance was observed at  $\delta$  24.2, identified as  $\text{O=PPh}_3$ , consistent with what was observed in an independently oxidized sample of  $\text{PPh}_3$  in toluene- $d_8$  ( $\delta$  24.3) (see Section 2.4.1.6).

Interestingly, during this time two sets of doublets emerge in the  $^{31}\text{P}$  NMR spectra, the first after ten minutes, at  $\delta$  23.4 and 25.2 (96.3 Hz), and the second after about 15 minutes at  $\delta$  21.9 and 25.8 (138.8 Hz), with respective correlations indicated by  $^{31}\text{P}$ - $^{31}\text{P}$  correlation NMR (Figure 39). As was seen with  $\text{PCy}_3$ , the



presence of two sets of coupled doublets are could be due to *syn* and *anti* isomers of the dinuclear species  $\text{Pd}_2(\text{PPh}_3)_2(\mu\text{-1-Ph-C}_3\text{H}_4)(\mu\text{-C}_5\text{H}_5)$ .

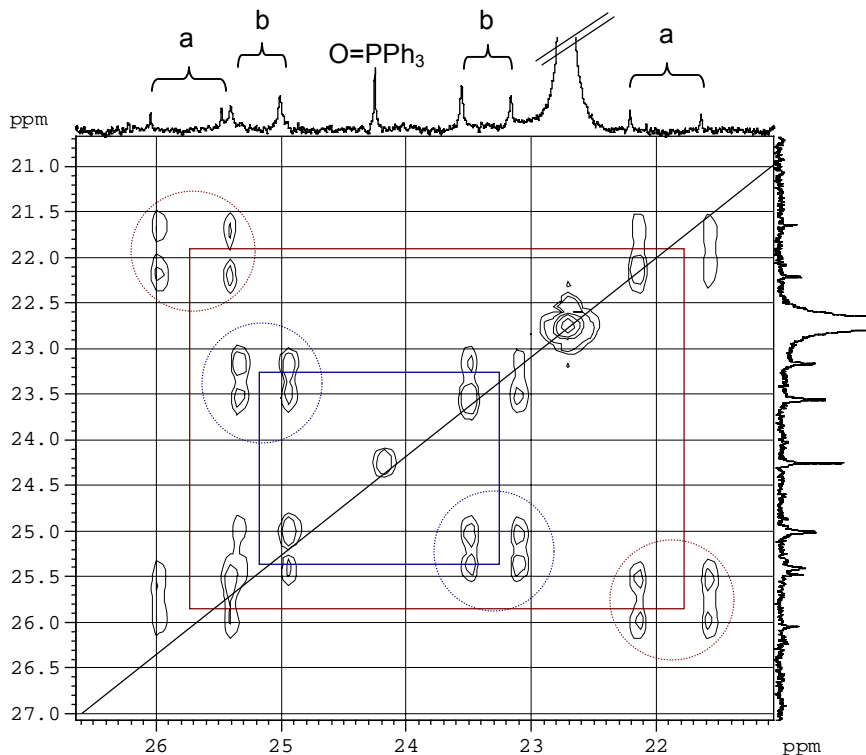


Figure 39.  $^{31}\text{P}$ - $^{31}\text{P}$  correlation spectrum of  $\text{Pd}(\eta^3\text{-1-Ph-C}_3\text{H}_4)(\eta^5\text{-C}_5\text{H}_5)$  and two equivalents  $\text{PPh}_3$  in toluene- $d_8$  at 25 °C.

These coupling constants are comparable to those seen for the presumed dinuclear species generated from  $\text{Pd}(\eta^3\text{-1-Ph-C}_3\text{H}_4)(\eta^5\text{-C}_5\text{H}_5)$  and  $\text{PCy}_3$  (72.1 Hz and 127.5 Hz).

Supporting the formation of two conformationally different dinuclear species, new  $\eta^5\text{-C}_5\text{H}_5$  peaks emerged in the  $^1\text{H}$  NMR spectra at  $\delta$  5.62 and 5.93 (labeled a and b in Figure 40). These  $\delta$   $^1\text{H}$  resonances each showed correlation (HSQC) to  $^{13}\text{C}$  peaks at  $\delta$  92.6 and 91.8 respectively, lending further support to the possibility that two different dinuclear species are present.<sup>2b</sup>

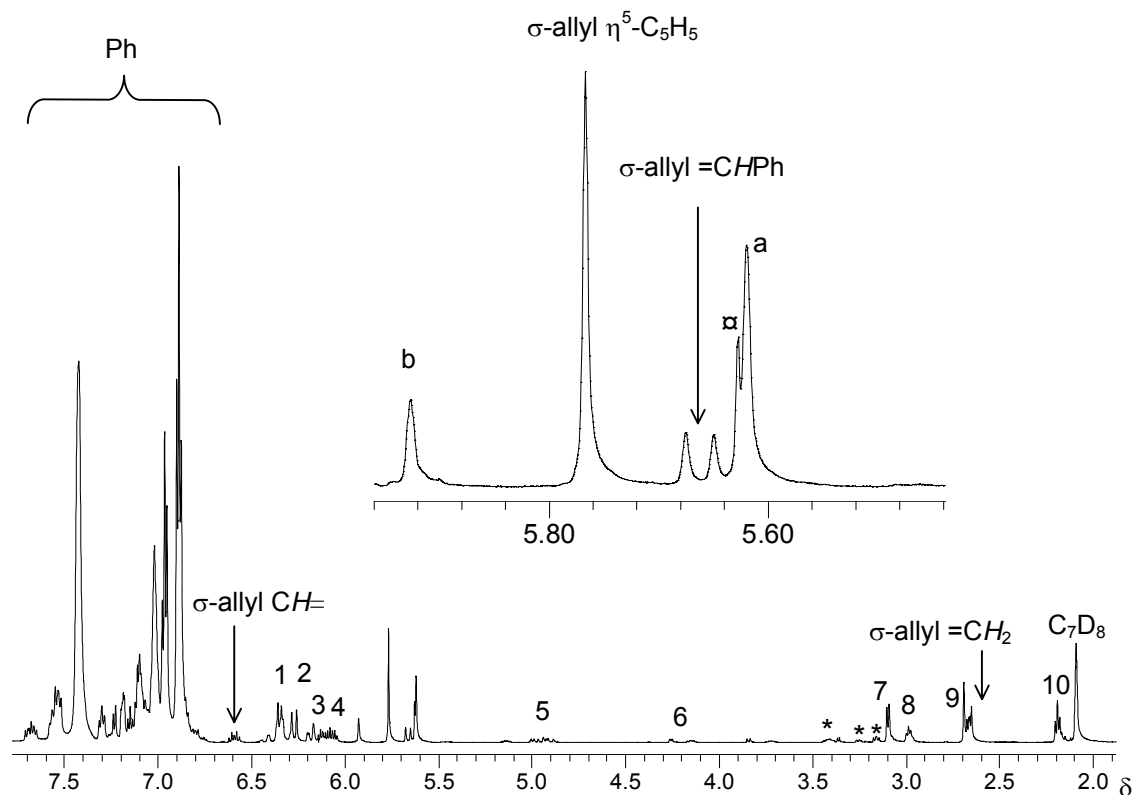
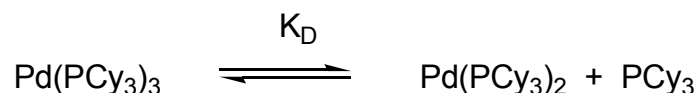


Figure 40. <sup>1</sup>H NMR spectrum (600 MHz) for reaction of Pd(η<sup>3</sup>-1-PhC<sub>3</sub>H<sub>4</sub>)(η<sup>5</sup>-C<sub>5</sub>H<sub>5</sub>) with two equivalents of PPh<sub>3</sub> in toluene-d<sub>8</sub> 35 minutes after mixing at 25 °C in C<sub>7</sub>D<sub>8</sub> (α indicates starting material δ 5.63, \* indicates unidentified resonances).

### 3.3 Homoleptic Compounds PdL<sub>3</sub>; Equilibria between PdL<sub>2</sub> and PdL<sub>3</sub>

The analysis described above often involved the occasional addition of slight excesses or deficiencies of the phosphines because of the small amounts of materials being reacted, and it became apparent that other Pd(0) species were also being formed. In some cases there was observed exchange broadening which implicated species other than the 2:1 compounds of interest, while low temperature spectra sometimes exhibited weak resonances that could not be accounted for.

There is definite precedent for 3:1 compounds PdL<sub>3</sub> existing in solution in equilibrium with the corresponding 2:1 compounds,<sup>4,37</sup> as in Scheme 37, but these usually involve sterically undemanding ligands and would not be expected to be very important in the chemistry of the three relatively large phosphine ligands of interest.



Scheme 37. Dissociation equilibrium for Pd(PCy<sub>3</sub>)<sub>3</sub>.

On the other hand, there is considerable speculation in the literature concerning possible equilibria between 2:1 and 1:1 compounds and the possible role(s) of monophosphine compounds PdL in cross-coupling reactions,<sup>38,39</sup> and it was decided to investigate further the palladium(0) systems being formed. Therefore experiments were carried out in which one equivalent of the phosphine was added to a solution of the PdL<sub>2</sub> compound in toluene-d<sub>8</sub> and the <sup>31</sup>P NMR spectra were obtained at various temperatures.

Although the <sup>31</sup>P NMR spectrum of pure Pd(PCy<sub>3</sub>)<sub>2</sub> at 25 °C exhibits a sharp resonance at δ 39.2, the <sup>31</sup>P NMR spectrum of a solution containing equimolar amounts of Pd(PCy<sub>3</sub>)<sub>2</sub> and PCy<sub>3</sub> at this temperature exhibited broadened resonances at δ 39.7 and 9.4 respectively, very close to the independently observed chemical shifts of Pd(PCy<sub>3</sub>)<sub>2</sub> and PCy<sub>3</sub> alone<sup>9,28</sup> and hence attributed to these compounds undergoing exchange.

On cooling the solution, the two resonances sharpen and shift slightly and at  $-56\text{ }^{\circ}\text{C}$ , a new broad resonance appears at  $\delta\ 26.3$ . At  $-68\text{ }^{\circ}\text{C}$  the latter is clearly visible and of intensity comparable with that of the 2:1 compound (Figure 41).

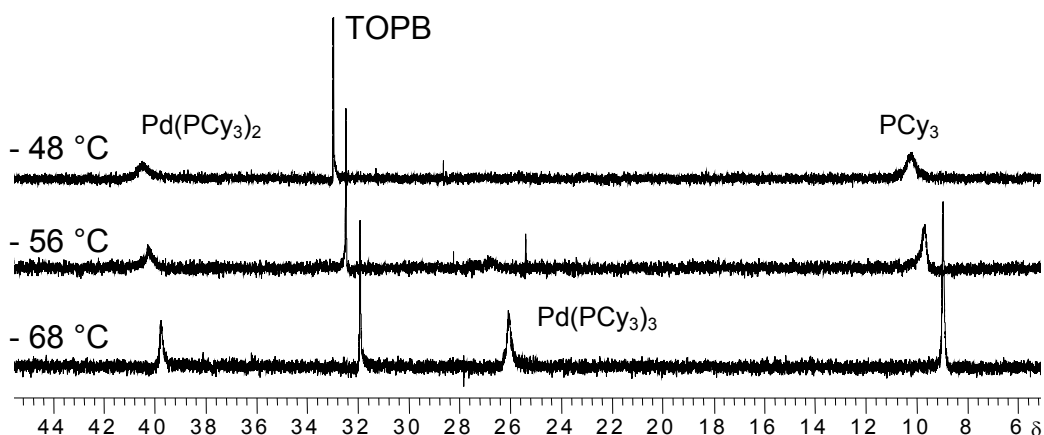


Figure 41. Stacked plots of low temperature  $^{31}\text{P}$  inverse gated NMR spectra (242.9 MHz) for reaction of  $\text{Pd}(\text{PCy}_3)_2$  with one equivalent of  $\text{PCy}_3$  (TOPB indicates tetraoctylphosphonium bromide standard).

This new resonance was not observed in low temperature  $^{31}\text{P}$  NMR spectra containing just  $\text{Pd}(\text{PCy}_3)_2$ , and therefore, consistent with a previous report based on relatively low field spectra ( $^{31}\text{P}$  at 36.43 MHz),<sup>4</sup> it is attributed to the 3:1 compound,  $\text{Pd}(\text{PCy}_3)_3$  rather than the monophosphine complex  $\text{Pd}(\text{PCy}_3)$ .

Since the  $^{31}\text{P}$  resonances of all three compounds,  $\text{PCy}_3$ ,  $\text{Pd}(\text{PCy}_3)_2$  and  $\text{Pd}(\text{PCy}_3)_3$ , are observable over a range of temperatures, it was possible to measure the equilibrium constant  $K_D$  for the dissociation (see Scheme 37) as a function of temperature and obtain thermodynamic data for this system in toluene- $d_8$ . To this end the concentrations of all three species in a 1:1 mixture of

PCy<sub>3</sub> and Pd(PCy<sub>3</sub>)<sub>2</sub> were determined via integrations in the temperature range –68 to –85 °C, mass balances being ensured by relating all intensity measurements to the constant intensity of a very narrow <sup>31</sup>P resonance of a solution of tetraoctylphosphonium bromide (TOPB) standard in toluene-d<sub>8</sub> and contained in a glass capillary inserted into the NMR tube.

A plot of ln K<sub>D</sub> as a function of 1/T was obtained, from which values of ΔH and ΔS were found to be 21 kJ mol<sup>-1</sup> and 59 J K<sup>-1</sup> mol<sup>-1</sup>, respectively (Figure 42).

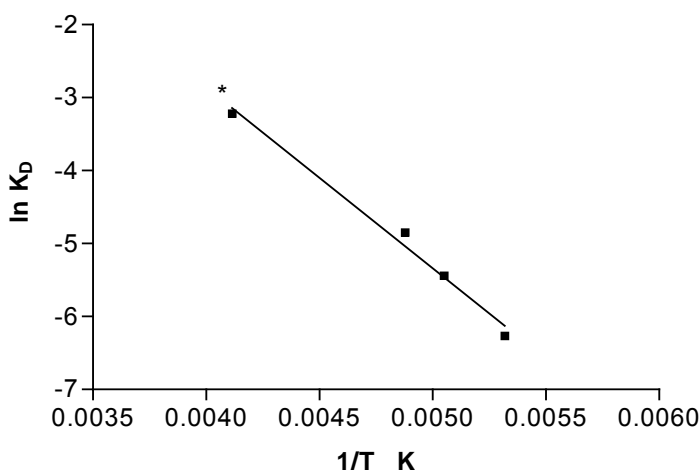


Figure 42. Plot of ln K<sub>D</sub> as a function of 1/T for the dissociation of Pd(PCy<sub>3</sub>)<sub>3</sub> (R<sup>2</sup> = 0.98, \* point from reference 4).

Extrapolation of this plot indicated that K<sub>D</sub> is 0.3 at 25 °C and 1.5 at 100 °C. Thus, for a situation in which the ratio of PCy<sub>3</sub>:Pd(0) in an attempted cross-coupling reaction might be 100:1, the proportion of the total palladium present as Pd(PCy<sub>3</sub>)<sub>3</sub> could be 84 % at 25 °C and 48 % at 100 °C. On the other hand, if the ratio of PCy<sub>3</sub>:Pd(0) were, say, 1000:1, as is likely the case in the very early stages of any cross-coupling reaction involving Pd(II) precatalysts, the proportion

of the total palladium present as Pd(PCy<sub>3</sub>)<sub>3</sub> at 25 °C and 100 °C could be 98 % and 90 %, respectively.

Similar <sup>31</sup>P NMR experiments involving 1:1 mixtures of Pd(PMeBu<sup>t</sup><sub>2</sub>)<sub>2</sub> and PMeBu<sup>t</sup><sub>2</sub> in toluene-d<sub>8</sub> resulted in similar observations, with a resonance attributable to Pd(PMeBu<sup>t</sup><sub>2</sub>)<sub>3</sub> being observed at δ ~30.3 over a range of temperatures. A ln K<sub>D</sub> as a function of 1/T plot was again obtained, from which ΔH and ΔS values 23 kJ mol<sup>-1</sup> and 86 J K<sup>-1</sup> mol<sup>-1</sup>, respectively, were derived (Figure 43).

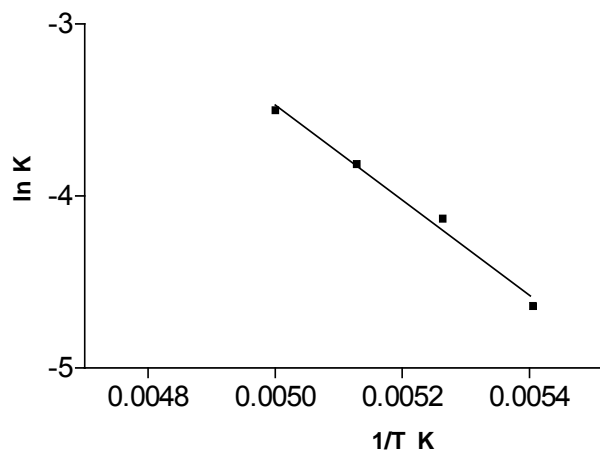


Figure 43. Plot of ln K<sub>D</sub> as a function of 1/T for the dissociation of Pd(PMeBu<sup>t</sup><sub>2</sub>)<sub>3</sub> (R<sup>2</sup> = 0.98).

Extrapolation to 25 °C and 100 °C yielded K<sub>D</sub> values at these temperatures of 3 and 19, respectively. Therefore a 100:1 mixture of PMeBu<sup>t</sup><sub>2</sub> and Pd(PMeBu<sup>t</sup><sub>2</sub>)<sub>2</sub> under the conditions described above could contain 32 % of the total palladium as Pd(PMeBu<sup>t</sup><sub>2</sub>)<sub>3</sub> at 25 °C, 7 % at the higher temperature. Similarly, if the PMeBu<sup>t</sup><sub>2</sub>:Pd(0) ratio were 1000:1, then the total palladium present as Pd(PMeBu<sup>t</sup><sub>2</sub>)<sub>3</sub> at 25 °C and 100 °C could be 83 and 42 % respectively.

In contrast,  $^{31}\text{P}$  NMR spectra of a 1:1 solution of  $\text{PBU}^t_3$  and  $\text{Pd}(\text{PBU}^t_3)_2$  in toluene- $d_8$  exhibited two unbroadened resonances for the two compounds over the temperature range 0 °C to -73 °C, implying that exchange must be slow on the NMR time scale. There is thus no evidence for the formation of  $\text{Pd}(\text{PBU}^t_3)_3$ , reasonable considering the much larger cone angle of this ligand.<sup>18</sup> The large steric bulk of this ligand has been claimed by others<sup>40</sup> to be significant in its role in cross-coupling, producing the monophosphine complex  $\text{Pd}-\text{PBU}^t_3$  as the active catalyst species. No such species could be confirmed in the current system.

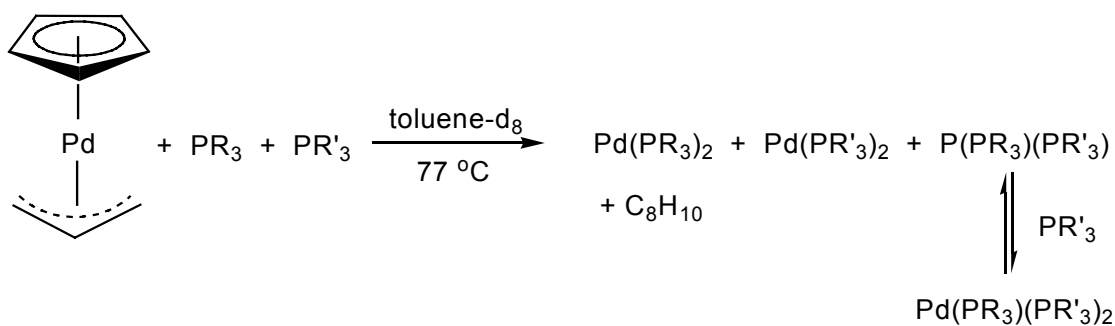
The  $\Delta\text{H}$  values presented above, 21 and 23  $\text{kJ}\cdot\text{mol}^{-1}$  for the  $\text{PCy}_3$  and  $\text{PMeBu}^t_2$  systems, respectively, presumably provide reasonable approximations of the Pd-P bond dissociation energies. If so, then the Pd(0)-phosphine bond energies of these 3:1 compounds are considerably lower than are those determined for many other types of phosphine-transition metal complexes.<sup>41</sup> They are also significantly lower than the only available bond dissociation energy value of a Pd(II)-phosphine compound (54  $\text{kJ mol}^{-1}$ )<sup>41b</sup> and the Pt- $\text{PCy}_3$  bond dissociation energy of the Pt(0) compound  $\text{Pt}[\text{PCy}_3]_3$  (55  $\text{kJ mol}^{-1}$ ).<sup>41c</sup>

### **3.4 Syntheses of the 2:1 Heteroleptic Compounds $\text{PdLL}'$ ( $\text{L}, \text{L}' = \text{PCy}_3, \text{PMeBu}^t_2, \text{PBU}^t_3$ ); Identification of the Corresponding 3:1 Compounds**

As indicated above, *in situ* identification of the 2:1 compounds  $\text{Pd}(\text{PCy}_3)_2$ ,  $\text{Pd}(\text{PMeBu}^t_2)_2$  and  $\text{Pd}(\text{PBU}^t_3)_2$  was readily made on the basis of comparisons with spectra of authentic samples in addition to previously published spectroscopic data for these compounds.<sup>1a,9,11,13</sup> The identification of the homoleptic species

$\text{PdL}_3$  formed *in situ* on addition of excess  $\text{PCy}_3$  or  $\text{PMeBu}^t_2$  to solutions of  $\text{Pd}(\text{PCy}_3)_2$  or  $\text{Pd}(\text{PMeBu}^t_2)_2$ , respectively, seems therefore reasonable, but there is a possibility that the resonances of these two compounds were for some reason severely exchange broadened and therefore unobservable. In this case, since the  $^{31}\text{P}$  nuclei are expected to remain chemically equivalent regardless of the number of ligands coordinated to the palladium, the resonances observed could conceivably be attributable to the  $\text{PdL}_4$  species and the identification of the compounds formed to this point is therefore uncertain.

Unambiguous determinations of coordination numbers could be made via mixed phosphine heteroleptic systems, since the spin-spin coupling patterns observed in the  $^{31}\text{P}$  NMR spectra would provide information concerning the nature of any new species formed (Scheme 38).



Scheme 38. Generation of heteroleptic 2:1 compounds from  $\text{Pd}(\eta^3\text{-C}_3\text{H}_5)(\eta^5\text{-C}_5\text{H}_5)$ .

Thus a compound of the type  $\text{Pd}(\text{PR}_3)(\text{PR}'_3)$  is expected to exhibit the spectrum of an AX or AB spin system, depending on the ratio  $\Delta\nu/J$ ,<sup>42</sup> and a compound of the type  $\text{Pd}(\text{PR}_3)(\text{PR}'_3)_2$  is expected to exhibit the spectrum of an  $\text{AX}_2$  or  $\text{AB}_2$  spin system. Similarly, compounds of the type  $\text{Pd}(\text{PR}_3)_2(\text{PR}'_3)_2$  or  $\text{Pd}(\text{PR}_3)(\text{PR}'_3)_3$  are



expected to exhibit the spectra of  $A_2X_2$  ( $A_2B_2$ ) or  $AX_3$  ( $AB_3$ ) spin systems, respectively.<sup>42</sup>

As it was of interest to determine if heteroleptic 2:1 compounds would form as readily and in the same way as the homoleptic compounds described above - such species have not been studied as cross-coupling catalysts - experiments were carried out that were designed to generate heteroleptic compounds in which different phosphines were bound to palladium.

$Pd(\eta^3-C_3H_5)(\eta^5-C_5H_5)$  was therefore reacted with one equivalent each of  $PCy_3$  and  $PBu^t_3$  for 1 h at 77 °C in toluene- $d_8$  and the resulting  $^{31}P$  NMR spectrum, run at 25 °C after brief cooling, is shown in Figure 44.

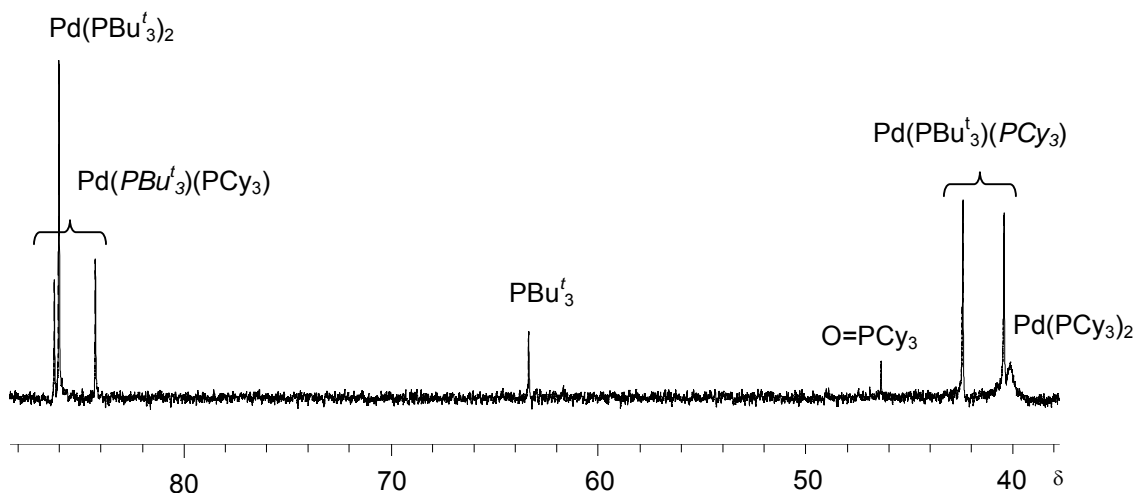


Figure 44.  $^{31}P$  NMR spectrum (121.5 MHz) of the reaction of  $Pd(\eta^3-C_3H_5)(\eta^5-C_5H_5)$  with one equivalent  $PCy_3$  and one equivalent of  $PBu^t_3$  in toluene- $d_8$  at 77 °C (after cooling to 25 °C, assignment indicated in italics).

As can be seen, in addition to the resonances of  $Pd(PCy_3)_2$  ( $\delta$  40.1, exchange broadened),  $Pd(PBu^t_3)_2$  ( $\delta$  86.0, sharp), unreacted  $PBu^t_3$  ( $\delta$  63.3), and a minor amount of  $O=PCy_3$  ( $\delta$  46.3), the spectrum also exhibits an AX pattern

with chemical shifts  $\delta$  41.4 and 85.2 and coupling constant  $^2J_{P-P}$  of 241 Hz ( $\Delta\nu/J = 0.182$ ). An essentially identical  $^{31}\text{P}$  NMR spectrum was obtained on reaction of equimolar amounts of preformed  $\text{Pd}(\text{P}^t\text{Bu}_3)_2$  with  $\text{Pd}(\text{PCy}_3)_2$  in toluene- $d_8$ , and a  $^{31}\text{P}$ - $^{31}\text{P}$  correlation experiment at 25 °C confirms the mutual coupling of the two doublets, supporting their assignment to the new heteroleptic compound  $\text{Pd}(\text{PCy}_3)(\text{P}^t\text{Bu}_3)$  (Figure 45).

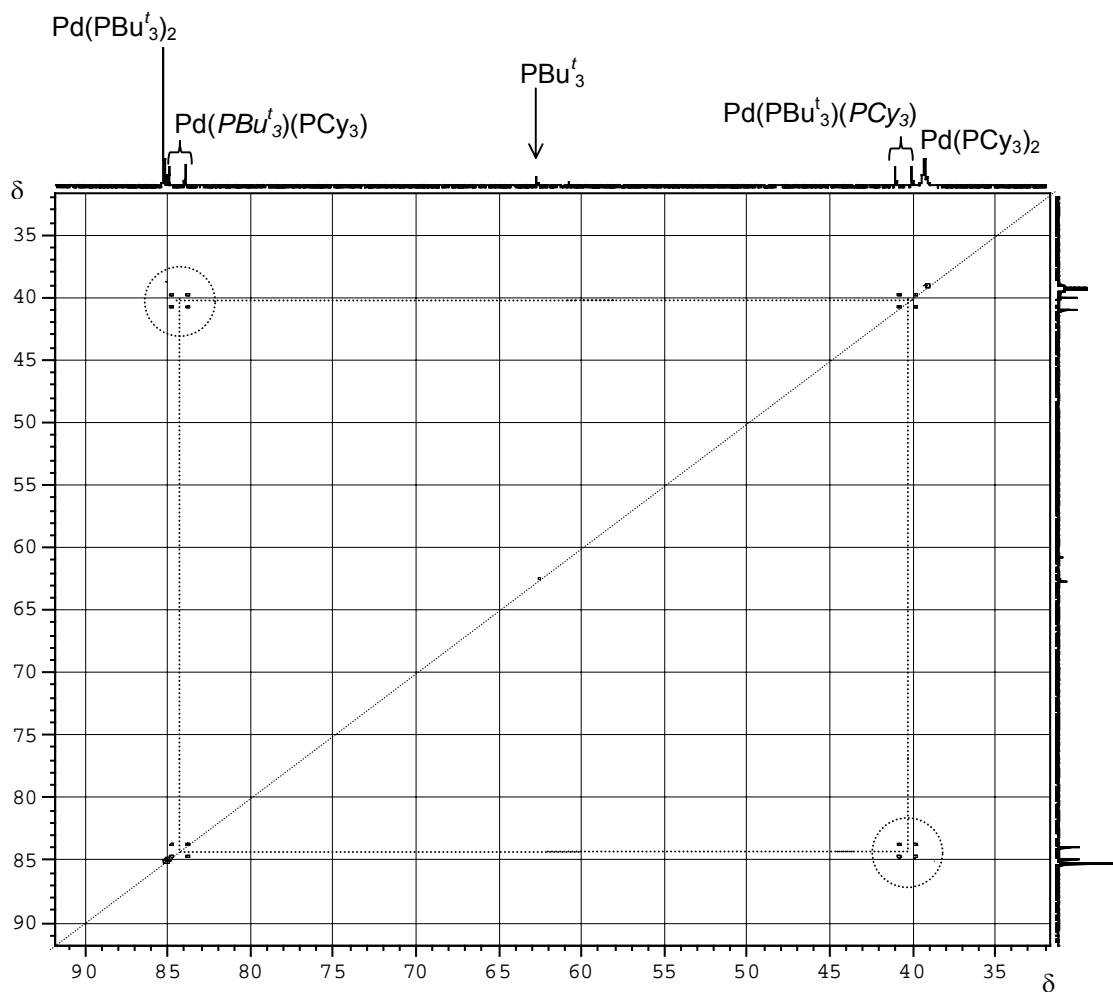


Figure 45.  $^{31}\text{P}$ - $^{31}\text{P}$  correlation spectrum (242.9 MHz) of equimolar quantities of  $\text{Pd}(\text{P}^t\text{Bu}_3)_2$  and  $\text{Pd}(\text{PCy}_3)_2$  in toluene- $d_8$  at 25 °C (assignment indicated in italics).

Formation of  $\text{Pd}(\text{PCy}_3)(\text{P}^t\text{Bu}_3)$  directly from the two homoleptic  $\text{PdL}_2$  precursors shows that ligand exchange is possible in this system, although exchange broadening is observed for only  $\text{Pd}(\text{PCy}_3)_2$ , not for  $\text{Pd}(\text{PCy}_3)(\text{P}^t\text{Bu}_3)$  or  $\text{Pd}(\text{P}^t\text{Bu}_3)_2$ . Similar results were noted above where the  $^{31}\text{P}$  resonance of  $\text{Pd}(\text{PCy}_3)_2$  broadened in the presence of free  $\text{PCy}_3$  while that of  $\text{Pd}(\text{P}^t\text{Bu}_3)_2$  remained sharp in the presence of free  $\text{P}^t\text{Bu}_3$ . Exchange processes are probably associative for compounds  $\text{PdL}_2$ , with the low coordination number of two,<sup>4</sup> and it is likely that compounds containing relatively bulky  $\text{P}^t\text{Bu}_3$  are too sterically hindered to participate in exchange readily.

A very similar result was obtained on reaction of equimolar amounts of  $\text{Pd}(\text{P}^t\text{MeBu}_2)_2$  and  $\text{Pd}(\text{P}^t\text{Bu}_3)_2$  in toluene- $d_8$ . Again an AX spin system with chemical shifts  $\delta$  85.4 and 41.8 and  $^2J_{(\text{P-P})} = 246$  Hz, was attributed to the heteroleptic compound  $\text{Pd}(\text{P}^t\text{MeBu}_2)(\text{P}^t\text{Bu}_3)$ , and again this compound is in equilibrium with its precursors  $\text{Pd}(\text{P}^t\text{MeBu}_2)_2$  ( $\delta$  41.7, exchange broadened) and  $\text{Pd}(\text{P}^t\text{Bu}_3)_2$  ( $\delta$  85.3). As above, a  $^{31}\text{P}$ - $^{31}\text{P}$  correlation spectrum of  $\text{Pd}(\text{P}^t\text{MeBu}_2)(\text{P}^t\text{Bu}_3)$  confirmed the assignments (Figure 46).

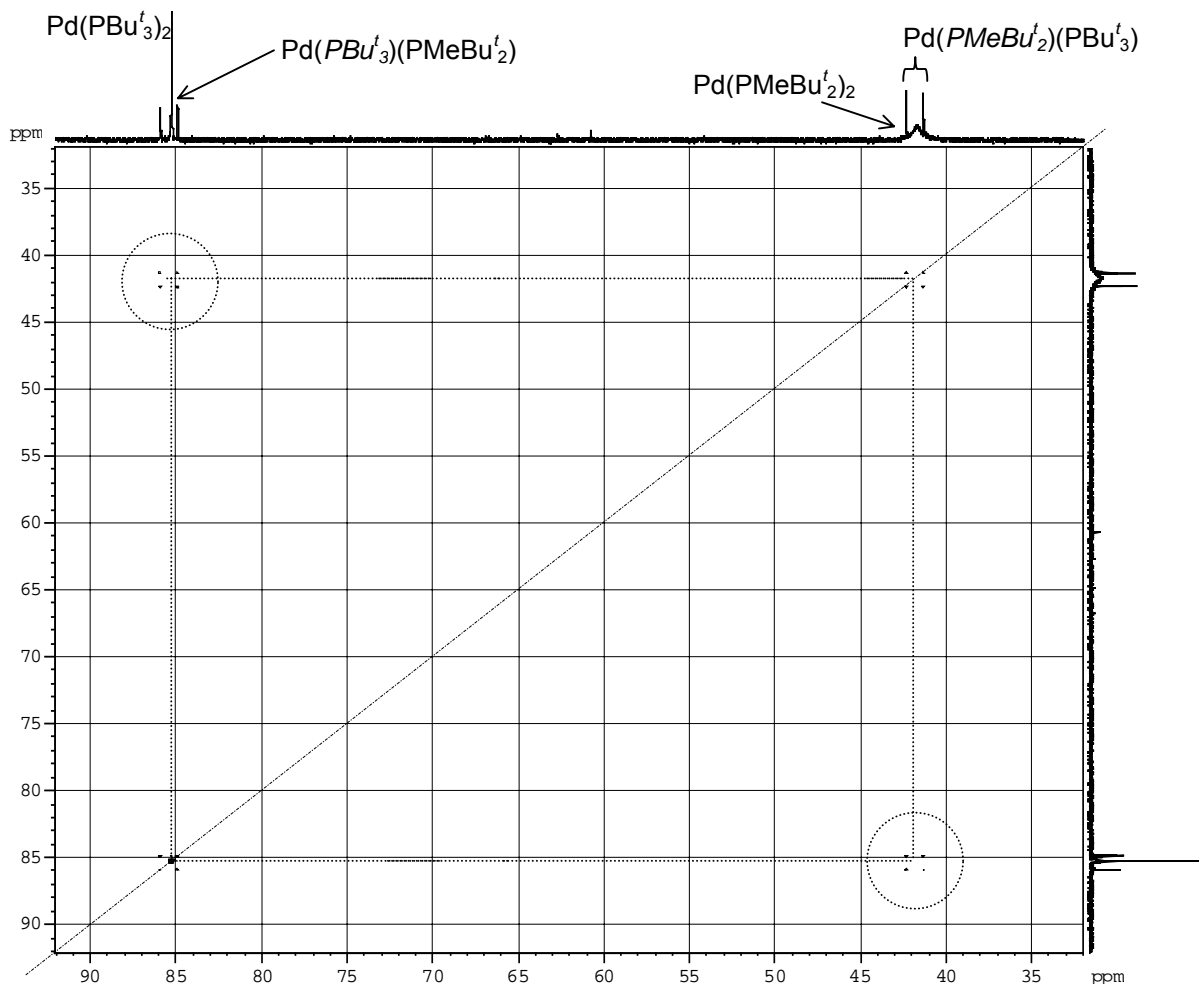


Figure 46.  $^{31}\text{P}$ - $^{31}\text{P}$  correlation spectrum (242.9 MHz) of equimolar amounts of  $\text{Pd}(\text{PBu}^t_3)_2$  with  $\text{Pd}(\text{PMeBu}^t_2)_2$  in toluene- $d_8$  at 25 °C (assignment indicated in italics).

In the interest of varying the size and donating ability of the phosphine,  $\text{Pd}(\eta^3\text{-C}_3\text{H}_5)(\eta^5\text{-C}_5\text{H}_5)$  was also reacted with one equivalent each of  $\text{PPh}_3$  and  $\text{PCy}_3$  for 2.5 hours at 77 °C in toluene- $d_8$ . Once cooled to 21 °C, a  $^{31}\text{P}$  NMR spectrum was obtained, showing two exchange broadened resonances at  $\delta$  22.8

and  $\delta$  39.8, consistent with  $\text{Pd}(\text{PPh}_3)_3$  and  $\text{Pd}(\text{PCy}_3)_2$  (Figure 47).<sup>4,9</sup> It seems that, while the above mentioned heteroleptic systems undergo relatively slow exchange to produce distinctly observable spin systems at 25 °C, heteroleptic systems involving  $\text{PPh}_3$  undergo rapid exchange on the NMR timescale. Such systems would require low temperature  $^{31}\text{P}$  NMR to produce useful spin systems for analysis, but this was not attempted.

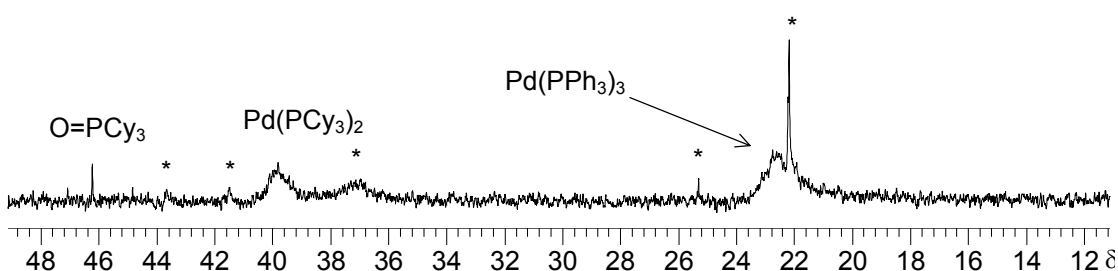


Figure 47.  $^{31}\text{P}$  NMR spectrum (121.5 MHz) of reaction of  $\text{Pd}(\eta^3\text{-C}_3\text{H}_5)(\eta^5\text{-C}_5\text{H}_5)$  with one equivalent each of  $\text{PCy}_3$  and  $\text{PPh}_3$  after cooling to 21 °C (\* indicates unidentified resonances).

The last of the heteroleptic systems examined involves  $\text{PCy}_3$  and  $\text{PMeBu}^t_2$ , both with cone angles significantly smaller than that of  $\text{P}^t\text{Bu}_3$  (170°, 160° and 182° respectively).<sup>11</sup> Complicating matters, while the  $^{31}\text{P}$  chemical shifts of coordinated  $\text{P}^t\text{Bu}_3$  generally lie ~20 - 40 ppm downfield from the chemical shifts of coordinated  $\text{PCy}_3$  and  $\text{PMeBu}^t_2$  (Table 16), giving rise to first order  $^{31}\text{P}$  NMR spectra, the  $^{31}\text{P}$  chemical shifts of  $\text{Pd}(\text{PCy}_3)_2$  and  $\text{Pd}(\text{PMeBu}^t_2)_2$  differ by only ~2 ppm. This (~486 Hz at a probe frequency of ~243 MHz) is comparable in magnitude to the values of  $^2J_{(\text{P-P})}$  discussed above for  $\text{Pd}(\text{PCy}_3)(\text{P}^t\text{Bu}_3)$ , and it was therefore anticipated that a second order  $^{31}\text{P}$  spectrum would be observed<sup>42</sup> for the compound  $\text{Pd}(\text{PCy}_3)(\text{PMeBu}^t_2)$ .

The Pd(0)/PCy<sub>3</sub>/PMeBu<sup>t</sup><sub>2</sub> system turned out to be much more complex and interesting than anticipated, and it was thus investigated in more detail than the other systems described. In the first experiment carried out, a <sup>31</sup>P NMR spectrum of a toluene-d<sub>8</sub> solution containing equimolar amounts of Pd(PMeBu<sup>t</sup><sub>2</sub>)<sub>2</sub> and Pd(PCy<sub>3</sub>)<sub>2</sub> was run at 25 °C (Figure 48a) and showed four resonances of comparable intensity at δ 41.8, 40.6, 40.5 and 39.3, very similar to the <sup>31</sup>P chemical shifts of the corresponding homoleptic PdL<sub>2</sub> compounds.

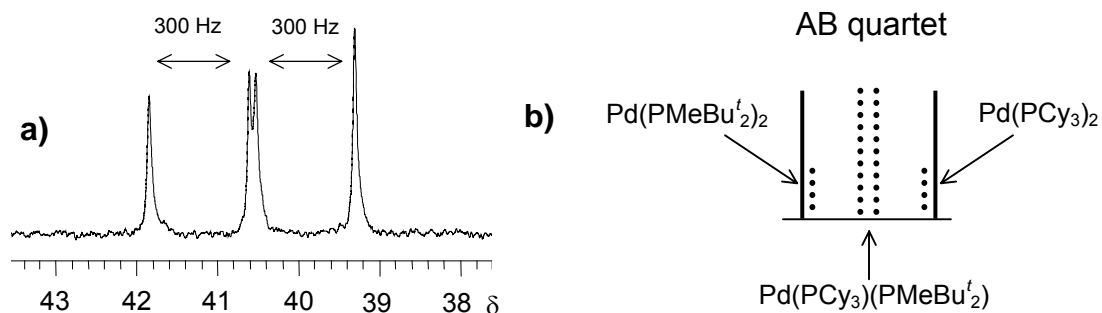


Figure 48. a) <sup>31</sup>P NMR spectrum (242.9 MHz) at 25 °C of a solution containing equimolar quantities of Pd(PCy<sub>3</sub>)<sub>2</sub> and Pd(PMeBu<sup>t</sup><sub>2</sub>)<sub>2</sub> b) Representation of postulated AB quartet.

The two apparent <sup>2</sup>J<sub>(P-P)</sub> separations (i.e. the differences in Hz between the resonances at δ 41.8 and 40.6, and between those at δ 40.5 and 39.3) were identically 300 Hz, greater than the values of <sup>2</sup>J<sub>(P-P)</sub> found above for Pd(PMeBu<sup>t</sup><sub>2</sub>)(PBU<sup>t</sup><sub>3</sub>) and Pd(PCy<sub>3</sub>)(PBU<sup>t</sup><sub>3</sub>). Therefore Δν appears comparable to <sup>2</sup>J<sub>(P-P)</sub> for the presumed species Pd(PCy<sub>3</sub>)(PMeBu<sup>t</sup><sub>2</sub>) in solution. However, if the two very closely spaced central lines at δ 40.6 and 40.5 are taken as the two center peaks of an AB quartet (Figure 48b), then the two outside peaks should exhibit much lower intensities than are observed.<sup>42</sup> It therefore seems likely that

most of the intensity of each of the resonances at  $\delta$  41.8 and 39.3 results from the presence of significant amounts of the two homoleptic compounds Pd(PMeBu<sup>t</sup><sub>2</sub>)<sub>2</sub> and Pd(PCy<sub>3</sub>)<sub>2</sub>, respectively. Supporting this conclusion, a <sup>31</sup>P-<sup>31</sup>P correlation experiment showed that the central peaks at  $\delta$  40.6 and 40.5 correlate with resonances at  $\delta$  41.8 and 39.3 respectively, hidden under the main resonances with these chemical shifts (Figure 49).

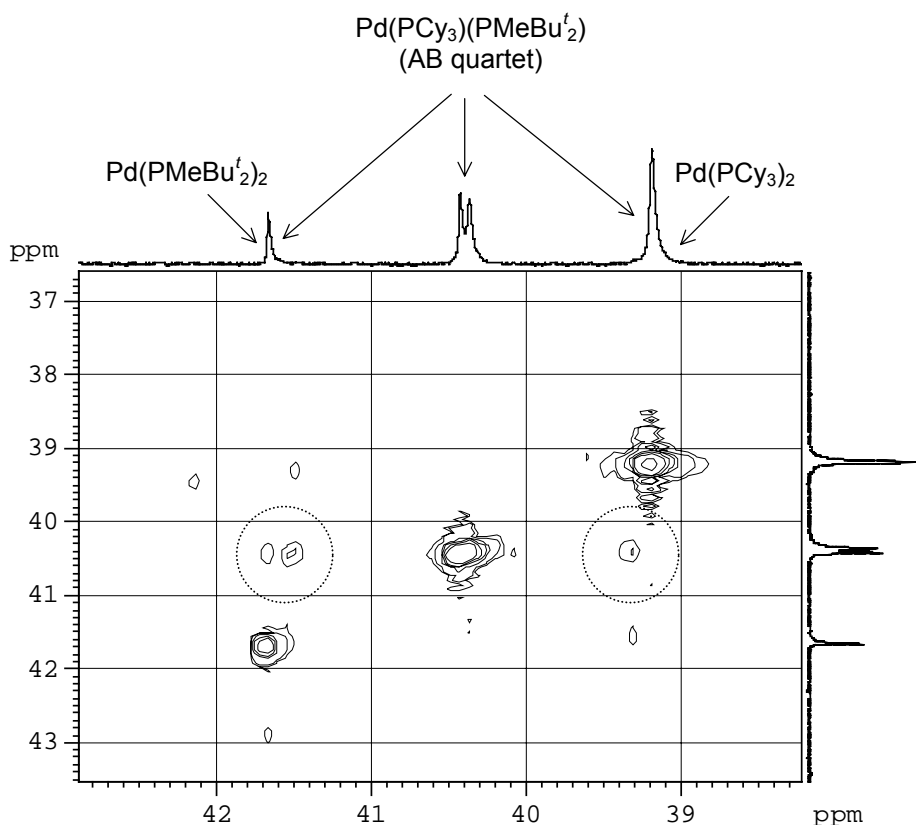


Figure 49. <sup>31</sup>P-<sup>31</sup>P correlation spectrum (242.9 MHz) of Pd(PMeBu<sup>t</sup><sub>2</sub>)<sub>2</sub> and Pd(PCy<sub>3</sub>)<sub>2</sub> at 25 °C.

Furthermore the chemical shifts of the two “outside” resonances are essentially identical to those of Pd(PMeBu<sup>t</sup><sub>2</sub>)<sub>2</sub> and Pd(PCy<sub>3</sub>)<sub>2</sub> respectively. It can also be seen (Figure 45) that the chemical shifts of the two “outside” resonances

of the quartet in the spectrum of  $\text{Pd}(\text{PCy}_3)(\text{P}^t\text{Bu}_3)$  are very similar to those of the two homoleptic compounds  $\text{Pd}(\text{P}^t\text{Bu}_3)_2$  and  $\text{Pd}(\text{PCy}_3)_2$ .

Consistent with the described observations for the  $\text{P}^t\text{MeBu}_2/\text{P}^t\text{Bu}_3$  and  $\text{PCy}_3/\text{P}^t\text{Bu}_3$  systems, it is not surprising to find significant amounts of the two homoleptic compounds present in equilibrium with the heteroleptic species. It should be noted that the  $^{31}\text{P}$  chemical shifts of the AB spin system do not, of course, coincide with any of the four observed resonances, but are calculated to be  $\delta$  40.3 and 40.8.<sup>42</sup>

In a second experiment carried out to understand this system, a solution containing  $\text{Pd}(\text{PCy}_3)_2$  (0.015 mmol) and one equivalent of  $\text{P}^t\text{MeBu}_2$  was prepared in 0.5 mL toluene- $d_8$  at 21 °C and  $^{31}\text{P}$  NMR spectra were obtained over the temperature range +25 to -93 °C (Figure 50).

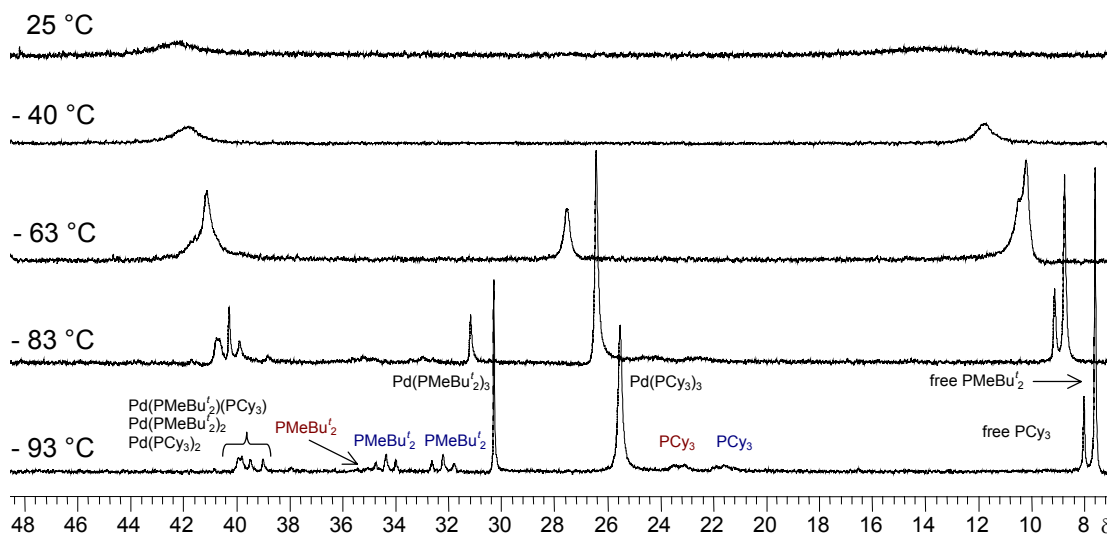


Figure 50. Stacked plots of variable temperature  $^{31}\text{P}$  NMR spectra (242.9 MHz) of the reaction of  $\text{Pd}(\text{PCy}_3)_2$  with one equivalent of  $\text{P}^t\text{MeBu}_2$  in toluene- $d_8$  ( $\text{Pd}(\text{P}^t\text{MeBu}_2)_2(\text{PCy}_3)$  in blue,  $\text{Pd}(\text{P}^t\text{MeBu}_2)(\text{PCy}_3)_2$  in red).



As can be seen, the  $^{31}\text{P}$  NMR spectrum at 25 °C exhibited two very broad resonances at  $\delta \sim 14$  and  $\sim 42$ . On cooling to  $-40$  °C these narrowed and shifted upfield slightly and by  $-63$  °C both had begun to decoalesce. At  $-93$  °C, many more resolved features can be observed. The dominant features of the spectrum at  $-93$  °C are singlets at  $\delta$  7.52 and 7.95 which are assigned respectively to free  $\text{PMeBu}^t_2$  and  $\text{PCy}_3$  shifted from the room temperature chemical shifts (Table 16) by temperature effects. There were also strong singlets at  $\delta$  25.5 and 30.3 which are assigned to the homoleptic compounds  $\text{Pd}(\text{PCy}_3)_3$  and  $\text{Pd}(\text{PMeBu}^t_2)_3$ , respectively (see above).

Much weaker resonances present in the spectrum at  $-93$  °C include several resonances in the region  $\delta$  39 - 40; these are consistent with the anticipated presence of  $\text{Pd}(\text{PCy}_3)_2$ ,  $\text{Pd}(\text{PMeBu}^t_2)_2$  and  $\text{Pd}(\text{PCy}_3)(\text{PMeBu}^t_2)$ . Two very broad resonances were also observed at  $\delta \sim 23.3$  and  $\sim 21.6$ , along with two less broadened 1:2:1 triplets at  $\delta \sim 32.2$  and  $\sim 34.4$  and an extremely broad resonance at  $\delta \sim 35$ , partially obscured by the triplet at  $\delta \sim 34.4$ . None of these resonances appeared in spectra of solutions containing only  $\text{PCy}_3$  or  $\text{PMeBu}^t_2$ . These resonances thus suggest the presence of several of the possible heteroleptic compounds,  $\text{Pd}(\text{PCy}_3)(\text{PMeBu}^t_2)_2$ ,  $\text{Pd}(\text{PCy}_3)_2(\text{PMeBu}^t_2)$ ,  $\text{Pd}(\text{PCy}_3)_2(\text{PMeBu}^t_2)_2$ ,  $\text{Pd}(\text{PCy}_3)(\text{PMeBu}^t_2)_3$  and/or  $\text{Pd}(\text{PCy}_3)_3(\text{PMeBu}^t_2)$ . The initial interpretation of the pair of 1:2:1 triplets at  $\delta \sim 32.2$  and  $\sim 34.4$  was that they comprised an  $A_2X_2$  spin system, attributed to the 4:1 compound  $\text{Pd}(\text{PCy}_3)_2(\text{PMeBu}^t_2)_2$ . This was surprising, given that  $\text{PCy}_3$  and  $\text{PMeBu}^t_2$  are

similar, sterically demanding phosphines that are not known to form homoleptic  $\text{PdL}_4$  species.

In order to obtain better resolved 1D spectra and 2D  $^{31}\text{P}$ - $^{31}\text{P}$  correlation spectra, the described NMR experiment was repeated utilizing a higher concentration of  $\text{Pd}(\text{PCy}_3)_2$  (0.025 mmol in 0.5 mL toluene- $d_8$ ) and two equivalents of  $\text{PMeBu}^t_2$ . The spectra obtained at the various temperatures were similar to those shown in Figure 50, although the exchange broadening at 25 °C was so severe due to the large excess of  $\text{PMeBu}^t_2$  that the two resonances at  $\delta \sim 14$  and  $\sim 42$  were barely distinguishable from the baseline. A spectrum run at  $-88$  °C (Figure 51) is similar to that shown in Figure 50 at  $-93$  °C except that the resonance of free  $\text{PMeBu}^t_2$  at  $\delta 7.71$  is (as expected) more intense than that of free  $\text{PCy}_3$  ( $\delta 8.14$ ).

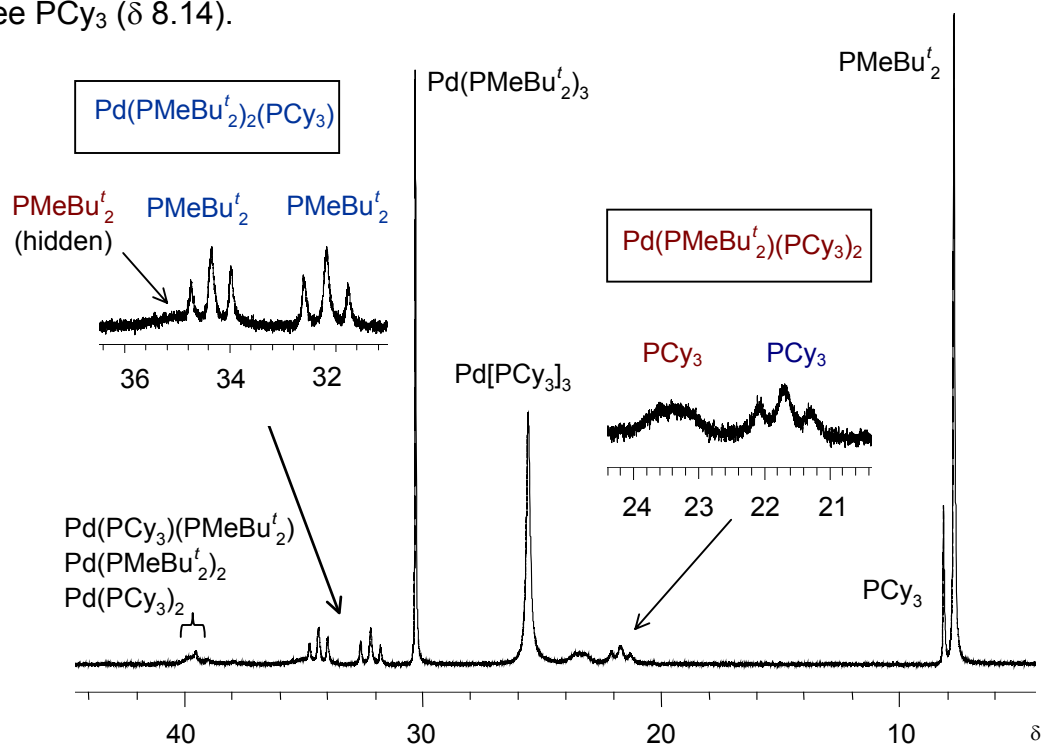


Figure 51.  $^{31}\text{P}$  NMR spectra (242.9 MHz) of the reaction of  $\text{Pd}(\text{PCy}_3)_2$  with two equivalents of  $\text{PMeBu}^t_2$  at  $-88$  °C.

More importantly, the triplets at  $\delta \sim 32.2$  and  $\sim 34.3$  are now much more intense than the resonances of the 2:1 compounds in the region  $\delta$  39 - 40, consistent with their assignment as species of higher coordination number. In addition, these resonances are well resolved enough that the splittings can be accurately measured:  $\sim 90.7$  Hz for that centered at  $\delta \sim 34.3$  and  $\sim 101.6$  Hz for that centered at  $\delta \sim 32.2$ . Furthermore, both the center lines were also found to be broader than the corresponding outside lines, and thus the two resonance patterns were found not to be 1:2:1 triplets (associated with an unlikely  $\text{PdL}_4$  complex) but pairs of overlapping doublets.

The two broad resonances at  $\delta \sim 23.6$  and  $\sim 21.7$  gained in intensity relative to the resonances at  $\delta$  39 - 40. However, while the resonance at  $\delta \sim 23.6$  was featureless, the resonance at  $\delta \sim 21.7$  became a broadened triplet, with splittings of  $\sim 90.4$  Hz and therefore also appeared to be a set of overlapping doublets. The resonances at  $\delta \sim 32.2$ ,  $\sim 34.3$ ,  $\sim 23.6$  and  $\sim 21.7$  were all of comparable intensities and the extremely broad resonance at  $\delta \sim 35$  remained barely visible.

A  $^{31}\text{P}$ - $^{31}\text{P}$  correlation experiment of the sample was then obtained at  $-88$  °C (Figure 52) and several features are important to note. The resonances in the region  $\delta$  39 - 40 did not correlate with any resonances at higher field, consistent with their assignment as the homoleptic and heteroleptic 2:1 compounds. The proposed sets of doublets at  $\delta \sim 32.2$ ,  $\sim 34.3$  and  $\sim 21.7$  were all mutually coupled,

implying that they comprise an AMX spin system and were thus assigned to one of the three coordinate compounds  $\text{Pd}(\text{PCy}_3)_2(\text{PMeBu}^t_2)$  or  $\text{Pd}(\text{PCy}_3)(\text{PMeBu}^t_2)_2$ .

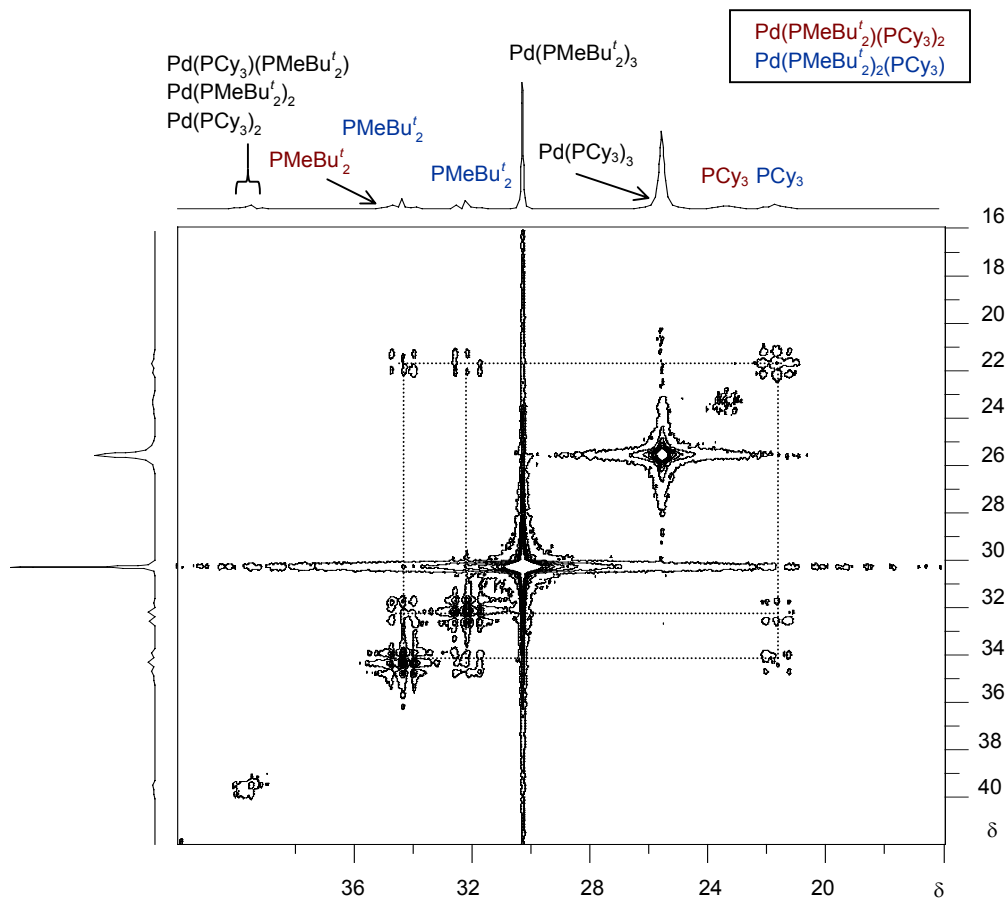


Figure 52.  $^{31}\text{P}$ - $^{31}\text{P}$  correlation spectrum (242.9 MHz) of a solution containing  $\text{Pd}(\text{PCy}_3)_2$  and two equivalents  $\text{PMeBu}^t_2$  in toluene- $d_8$  at  $-88\text{ }^\circ\text{C}$ .

Since the  $^{31}\text{P}$  resonance of  $\text{Pd}(\text{PMeBu}^t_2)_3$  was downfield from and was sharper than that of  $\text{Pd}(\text{PCy}_3)_3$  (Figure 52), it seems likely that the compound giving rise to the AMX spin system was  $\text{Pd}(\text{PCy}_3)(\text{PMeBu}^t_2)_2$ , with the multiplets at  $\delta \sim 32.2$  and  $\sim 34.3$  attributed to two  $\text{PMeBu}^t_2$  rendered nonequivalent. This non-

equivalence may originate because the  $\text{PMeBu}^t_2$  groups are “frozen” at this low temperature in different rotational conformations relative to the  $\text{PCy}_3$ .

In support of this suggestion, it was noted that the room temperature  $^{31}\text{P}$  NMR spectrum of *trans*- $\text{PdCl}_2(\text{PMeBu}^t_2)_2$  (Section 3.8.1) showed two singlets of unequal intensity because of the presence of two different rotamers in solution, resulting from a significant steric barrier to rotation about the Pd-P bond.<sup>43</sup> It is thus reasonable to suppose that the two  $\text{PMeBu}^t_2$  ligands in  $\text{Pd}(\text{PCy}_3)(\text{PMeBu}^t_2)_2$  adopt different orientations with significant barriers to interconversion at low temperature. Alternatively, the two  $\text{PMeBu}^t_2$  ligands may be magnetically nonequivalent (diastereotopic) by virtue of the chirality of the coordinated  $\text{PCy}_3$ .<sup>44</sup>

Assuming, that the magnitudes of  $^2J_{(\text{P-P})}$  in these palladium(0) compounds are governed mainly by the Fermi contact term,<sup>45</sup> the decrease in  $^2J_{(\text{P-P})}$  from 486 Hz for  $\text{Pd}(\text{PCy}_3)(\text{PMeBu}^t_2)$  to ~96 Hz for  $\text{Pd}(\text{PCy}_3)(\text{PMeBu}^t_2)_2$  is consistent with the change from the linear  $sp$  hybridized structure to the trigonal  $sp^2$  analogue. This supports the suggestion of an increase in the coordination number from  $\text{PdL}_2$  to  $\text{PdL}_3$ . The weakening of the Pd-P  $\sigma$  bonds due greater steric crowding in the 3:1 compound should also result in a decrease in  $^2J_{(\text{P-P})}$ .<sup>45</sup> Observation of a near first order pattern between the resonances at  $\delta \sim 32.2$  and  $\sim 34.3$  occurs because  $\Delta\nu \sim 500$  Hz and  $J \sim 90$  Hz, and therefore  $\Delta\nu/J \approx 5.6$ , much larger than was the case with  $\text{Pd}(\text{PCy}_3)(\text{PMeBu}^t_2)$ .

By process of elimination, the very broad resonance at  $\delta \sim 23.6$  was assigned to the  $\text{PCy}_3$  ligands of the compound  $\text{Pd}(\text{PCy}_3)_2(\text{PMeBu}^t_2)$ , with the  $\text{PMeBu}^t_2$  resonance being the very broad resonance at  $\delta \sim 35$ .

In summary,  $^{31}\text{P}$  NMR experiments at variable temperature involving homoleptic and heteroleptic phosphine systems serve to confirm the tendency of many systems to assume 3:1 coordination complexes. The observed species in these systems along with their  $^{31}\text{P}$  chemical shifts are summarized in Table 16.

Table 16.  $^{31}\text{P}$  NMR data for homoleptic and heteroleptic complexes of  $\text{PdL}_n$  at 25 °C in toluene- $d_8$  (L =  $\text{PCy}_3$ ,  $\text{PMeBu}^t_2$ ,  $\text{PBU}^t_3$ )

Compound	$\delta$ (Free L)	$\delta$ ( $\text{PCy}_3$ )	$\delta$ ( $\text{PMeBu}^t_2$ )	$\delta$ ( $\text{PBU}^t_3$ )	$^2J$ (P-P) (Hz)
$\text{Pd}(\text{PCy}_3)_2$	9.9	39.2	-	-	-
$\text{Pd}(\text{PCy}_3)_3$		25.5 <sup>a</sup>			
$\text{Pd}(\text{PMeBu}^t_2)_2$	11.4	-	41.9	-	-
$\text{Pd}(\text{PMeBu}^t_2)_3$			30.3 <sup>b</sup>		
$\text{Pd}(\text{PBU}^t_3)_2$	63.3	-	-	84.7	-
$\text{Pd}(\text{PCy}_3)(\text{PMeBu}^t_2)$	-	40.3 <sup>c</sup>	40.8 <sup>c</sup>		300
$\text{Pd}(\text{PMeBu}^t_2)(\text{PBU}^t_3)$	-		41.8	85.4	246
$\text{Pd}(\text{PCy}_3)(\text{PBU}^t_3)$	-	41.4	-	85.2	241

a. At -68 °C.

b. At -88 °C.

c. In benzene- $d_6$  at 25 °C; calculated as an AB spin system

The formation of such complexes has significant implications for cross-coupling processes involving 2:1 bisphosphine complexes. This is because relative catalyst activities may vary, not necessarily due to a steric or electronic property of the phosphine, as is often assumed, but because of differing degrees to which the initially very small amounts of generated Pd(0) species may be present as a

unreactive tris-phosphine complex rather than the assumed bisphosphine species. The tendency of a particular phosphine to form a more highly coordinated and presumable less reactive species may thus be a determining factor in the overall efficiency of a cross-coupling process.

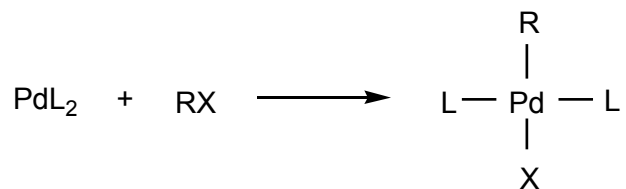
### 3.5 Investigative Experiments In Oxidative Addition

With the intention of investigating the kinetics of oxidative addition, preliminary experiments were performed in which oxidative addition of  $\text{PdL}_2$  ( $\text{L} = \text{PCy}_3, \text{PMeBu}^t_2, \text{PBu}^t_3$ ) was monitored by  $^1\text{H}$  and  $^{31}\text{P}$  NMR with a variety of substrates  $\text{RX}$  (allyl chloride, 1-bromoethylbenzene, bromobenzene, chlorobenzene). Experiments of this kind were performed by two different methods: from previously isolated  $\text{PdL}_2$  and from *in situ* generated  $\text{PdL}_2$  (from  $\text{Pd}(\eta^3\text{-C}_3\text{H}_5)(\eta^5\text{-C}_5\text{H}_5)$ ). Furthermore, given reports of anionic bisphosphine complexes  $\text{PdL}_2\text{X}^-$ , generated upon reduction of  $\text{Pd(II)}$ ,<sup>46</sup> it was of interest to determine if added halide affected the nature of species observed during oxidative addition.

#### 3.5.1 Oxidative Addition with Isolated $\text{PdL}_2$

Reactions were performed with isolated  $\text{PdL}_2$  ( $\text{L} = \text{PCy}_3, \text{PMeBu}^t_2, \text{PBu}^t_3$ ) and several different organic halides (bromobenzene, chlorobenzene, allyl chloride and 1-bromoethylbenzene), with the goal of observing the tendency of the bisphosphine complexes towards oxidative addition. A generalized scheme

for oxidative addition is shown in Scheme 39, and the attempted oxidative addition reactions are summarized in Table 17 for Pd(PCy<sub>3</sub>)<sub>2</sub> and Pd(PMeBu<sup>t</sup>)<sub>2</sub>.



Scheme 39. Oxidative addition reaction involving PdL<sub>2</sub>.

Table 17. Attempted oxidative addition reactions involving PdL<sub>2</sub> (L = PCy<sub>3</sub>, PMeBu<sup>t</sup>) at 21 °C.

Entry	PdL <sub>2</sub>	RX	Pd:RX	Solvent	Reaction Time /h
1	Pd(PCy <sub>3</sub> ) <sub>2</sub>	C <sub>6</sub> H <sub>5</sub> CH(CH <sub>3</sub> )Br	1:3	C <sub>6</sub> D <sub>6</sub>	2
2	Pd(PCy <sub>3</sub> ) <sub>2</sub>	CH <sub>2</sub> CHCH <sub>2</sub> Cl	1:0.4	C <sub>6</sub> D <sub>6</sub>	3
3	Pd(PCy <sub>3</sub> ) <sub>2</sub>	C <sub>6</sub> H <sub>5</sub> Cl	1:11	C <sub>7</sub> D <sub>8</sub>	1
4	Pd(PCy <sub>3</sub> ) <sub>2</sub>	C <sub>6</sub> H <sub>5</sub> Br	1:1	C <sub>6</sub> D <sub>6</sub>	2
5	Pd(PCy <sub>3</sub> ) <sub>2</sub>	C <sub>6</sub> H <sub>5</sub> Br	1:10	C <sub>7</sub> D <sub>8</sub>	0.5
6	Pd(PMeBu <sup>t</sup> ) <sub>2</sub>	C <sub>6</sub> H <sub>5</sub> Br	1:1	C <sub>7</sub> D <sub>8</sub>	3

The reaction of Pd(PCy<sub>3</sub>)<sub>2</sub> and bromobenzene in a 1:1 molar ratio proceeded rapidly at room temperature, producing a resonance at δ 21.3 consistent with *trans*-Pd(PCy<sub>3</sub>)<sub>2</sub>(Ph)(Br) (<sup>31</sup>P δ 20.6),<sup>47</sup> seen in (Figure 53). Pd(PCy<sub>3</sub>)<sub>2</sub> was no longer visible after two hours after mixing, indicating the completion of the reaction. The presence of the *trans*-Pd(PCy<sub>3</sub>)<sub>2</sub>(Ph)(Br) was also confirmed by the appearance of three resonances (δ 6.89, 7.01, 7.61) in the aromatic region of the associated <sup>1</sup>H NMR spectrum (Figure 54) However, residual bromobenzene was observed, indicating that an excess has been added to the NMR scale reaction.



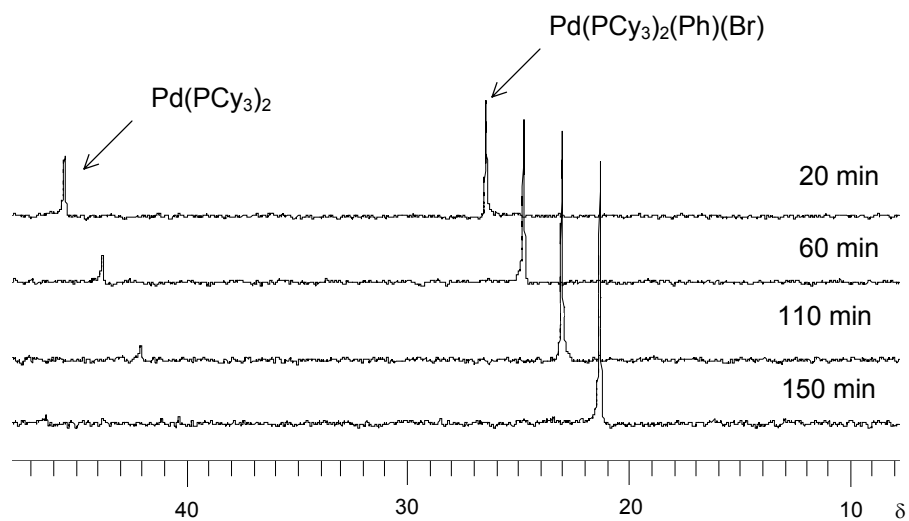


Figure 53.  $^{31}\text{P}$  NMR spectrum (163.0 MHz) for reaction of equimolar quantities of  $\text{Pd}(\text{PCy}_3)_2$  and bromobenzene in benzene- $\text{d}_6$  at 25 °C.

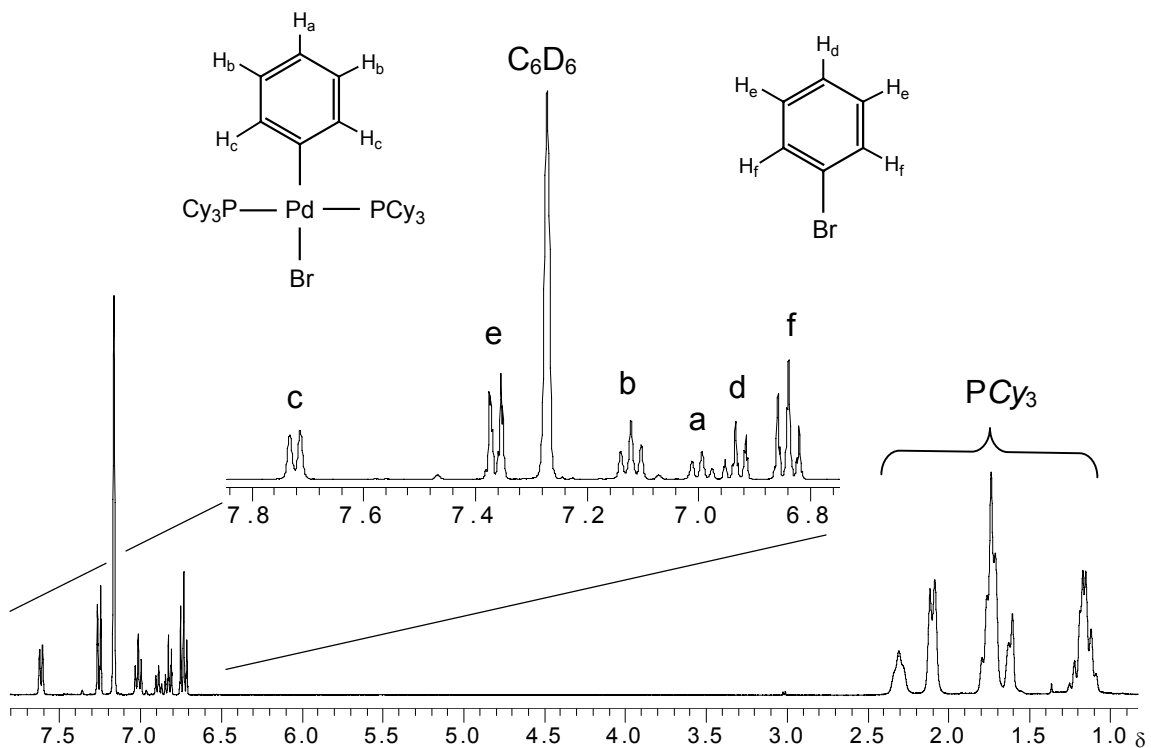


Figure 54.  $^1\text{H}$  NMR spectrum (400 MHz) for reaction of equimolar quantities of  $\text{Pd}(\text{PCy}_3)_2$  and bromobenzene in benzene- $\text{d}_6$  at 25 °C two hours after mixing.

When the reaction was repeated in a 1:10 Pd(PCy<sub>3</sub>)<sub>2</sub>/PhBr ratio, the oxidative addition reaction was complete in approximately 30 minutes at room temperature.

Similar studies were repeated with Pd(PCy<sub>3</sub>)<sub>2</sub> and (1-bromo)ethylbenzene (C<sub>6</sub>H<sub>5</sub>CH(CH<sub>3</sub>)Br), of interest due to the presence of a β-hydrogen, which may undergo β-hydride elimination following oxidative addition. While β-hydrogen elimination has been acknowledged as a difficulty associated with cross-coupling reactions involving alkyl halides,<sup>48</sup> recent work has shown that β-hydride elimination can be avoided to produce isolable *trans* complexes at room temperature, as shown with Pd(PMeBu<sup>t</sup><sub>2</sub>)<sub>2</sub>.<sup>8</sup> A <sup>1</sup>H NMR spectrum was obtained two hours after mixing Pd(PCy<sub>3</sub>)<sub>2</sub> with three equivalents of (1-bromo)ethylbenzene (C<sub>6</sub>H<sub>5</sub>CH(CH<sub>3</sub>)Br) at 21 °C, showing residual (1-bromoethyl)benzene, along with weak styrene resonances in the regions of δ 5.07, 5.60 and δ 6.50-6.63 (Figure 55). In addition, a hydride resonance at δ -13.21 was observed, consistent with the literature reports for [Pd(PCy<sub>3</sub>)<sub>2</sub>HBr] (δ -13.3),<sup>49</sup> indicating that oxidative addition had occurred, followed by subsequent β-hydride elimination. A <sup>31</sup>P NMR spectrum taken 2.5 hours after mixing showed a resonance at δ 25.1, presumably [Pd(PCy<sub>3</sub>)<sub>2</sub>HBr], as well as unreacted Pd(PCy<sub>3</sub>)<sub>2</sub> and O=PCy<sub>3</sub> at δ 40.5 and 45.9 respectively (Figure 56).

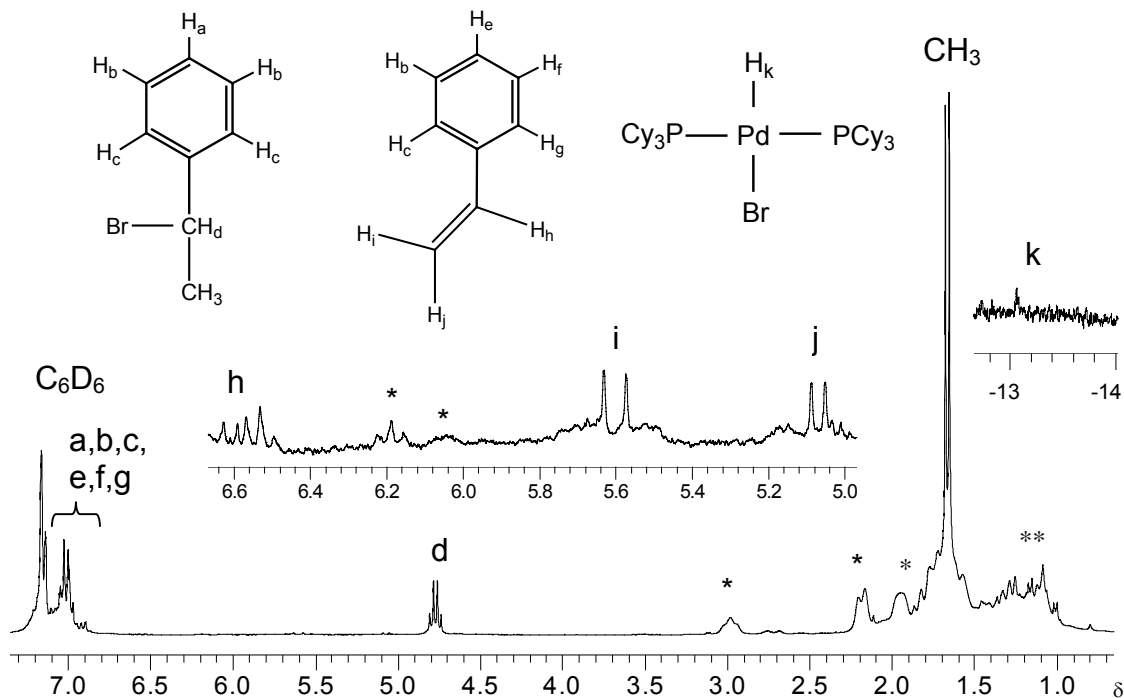


Figure 55.  $^1\text{H}$  NMR spectrum (300 MHz) for reaction of  $\text{Pd}(\text{PCy}_3)_2$  and three equivalents (1-bromo)ethylbenzene in benzene- $\text{d}_6$  two hours after mixing at  $21^\circ\text{C}$  (\* indicates unidentified resonance, \*\* indicates impurity).

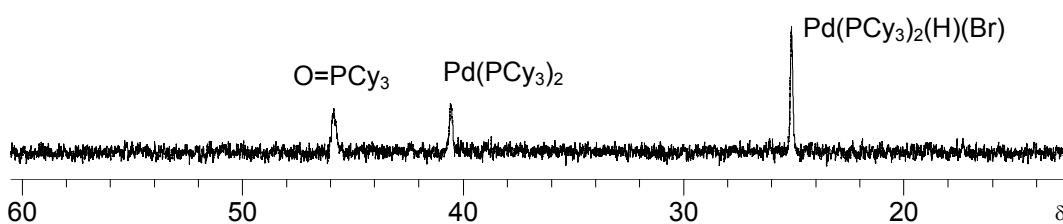


Figure 56.  $^{31}\text{P}$  NMR (163.0 MHz) for reaction of  $\text{Pd}(\text{PCy}_3)_2$  and three equivalents (1-bromo)ethylbenzene 2.5 hours after mixing at  $21^\circ\text{C}$ .

$^1\text{H}$  and  $^{31}\text{P}$  NMR experiments were performed to observe potential oxidative addition with chlorides, specifically chlorobenzene and allyl chloride. Aryl and alkyl chlorides are desirable coupling partners in Suzuki-Miyaura reactions as they are widely available and inexpensive.<sup>50</sup>

However, their weakness remains their poor reactivity towards oxidative addition, and numerous efforts have been made to effect coupling with aryl and alkyl chlorides.<sup>50</sup> As was anticipated, the reaction with Pd(PCy<sub>3</sub>)<sub>2</sub> and allyl chloride for five hours at 21 °C did not produce any evidence of oxidative addition in the <sup>1</sup>H or <sup>31</sup>P NMR spectra. Only the <sup>1</sup>H resonances associated with unreacted allyl chloride and Pd(PCy<sub>3</sub>)<sub>2</sub> (<sup>31</sup>P δ 39.1) were observed. Similarly, no reaction was observed when Pd(PCy<sub>3</sub>)<sub>2</sub> and chlorobenzene were combined at 21 °C.

Pd(PMeBu<sup>t</sup><sub>2</sub>)<sub>2</sub> was also found to react with bromobenzene in a 1:1 molar ratio producing a resonance at δ 26.2, as seen in the <sup>31</sup>P NMR (Figure 57). This species was assigned to *trans*-Pd(PMeBu<sup>t</sup><sub>2</sub>)<sub>2</sub>(Ph)(Br), and it consistent with the appearance of three new phenyl resonances in the <sup>1</sup>H NMR spectrum (Figure 58).

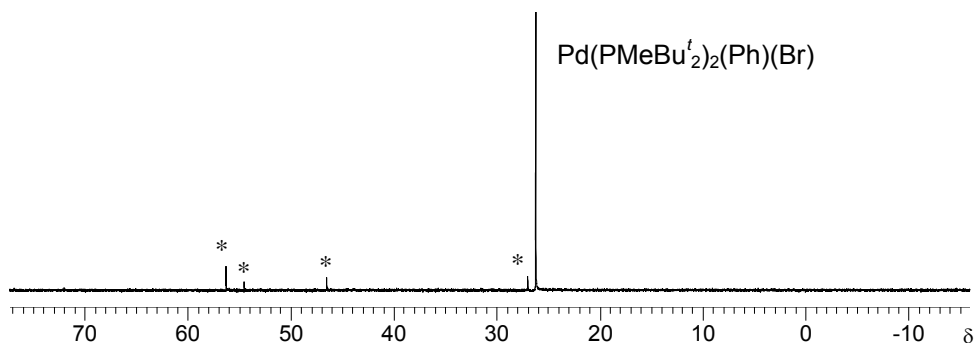


Figure 57. <sup>31</sup>P NMR spectrum (163.0 MHz) for reaction of Pd(PMeBu<sup>t</sup><sub>2</sub>)<sub>2</sub> with one equivalent bromobenzene in benzene-d<sub>6</sub> at 25 °C (\* indicates unidentified resonances).

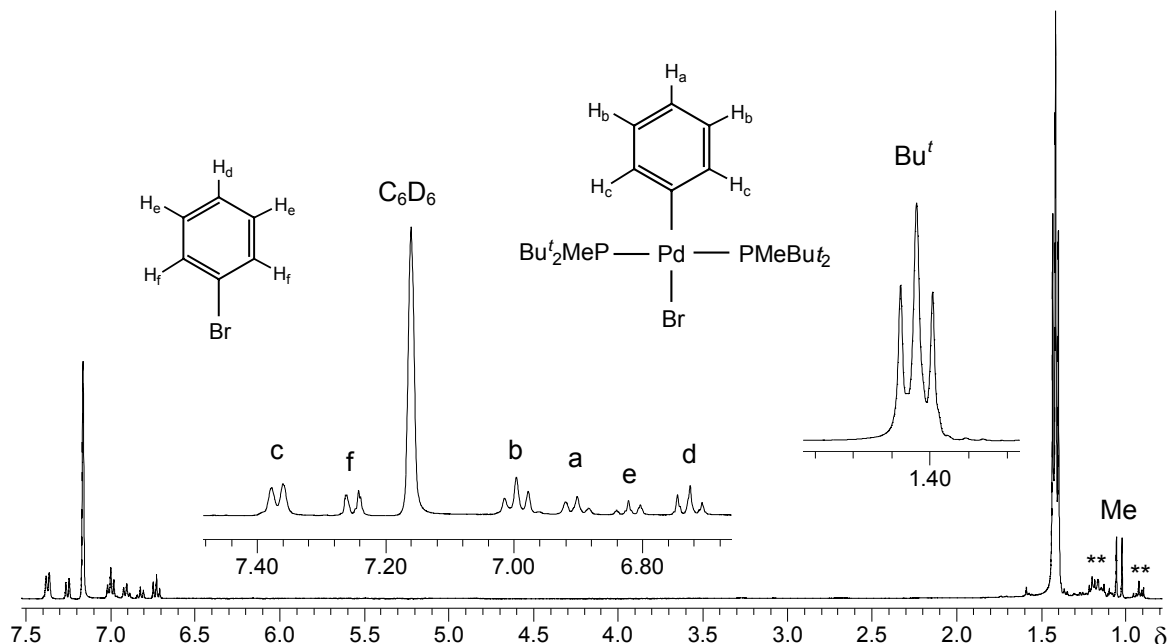


Figure 58. <sup>1</sup>H NMR spectrum (400 MHz) for reaction of Pd(PMeBu<sup>t</sup><sub>2</sub>)<sub>2</sub> with one equivalent bromobenzene at 25 °C (\*\* indicates impurity).

Given these results, bromobenzene was chosen as an appropriate substrate to pursue kinetics studies of oxidative addition (see section 3.6), as it underwent rapid oxidative addition at 21 °C with both Pd(PCy<sub>3</sub>)<sub>2</sub> and Pd(PMeBu<sup>t</sup><sub>2</sub>)<sub>2</sub>.

Many attempts were made to observe oxidative addition with Pd(P<sup>t</sup>Bu<sub>3</sub>)<sub>2</sub> and bromobenzene, at a variety of experimental conditions, shown in Table 18. When performed at 25 °C in toluene-d<sub>8</sub> (entries 1 and 3), no reaction was observed, as was indicated by a single, unchanged <sup>31</sup>P resonance for Pd(P<sup>t</sup>Bu<sub>3</sub>)<sub>2</sub> appearing at δ 85.1.<sup>13</sup>

Table 18. Attempted oxidative addition experiments involving Pd(PBu<sup>t</sup><sub>3</sub>)<sub>2</sub>.

Entry	Pd(PBu <sup>t</sup> <sub>3</sub> ) <sub>2</sub> :PhBr	Solvent	Time /h	Temp/°C
1	1:1	C <sub>7</sub> D <sub>8</sub>	1	25
2	1:1	C <sub>6</sub> D <sub>6</sub>	0.33	60
3	1:10	C <sub>7</sub> D <sub>8</sub>	2.5	25
4	1:10	1:1.5 C <sub>7</sub> D <sub>8</sub> /THF	2.5	25
5	1:10	1:1.5 C <sub>7</sub> D <sub>8</sub> /1,4-dioxane	3	25
6	1:10	1:1.5 C <sub>7</sub> D <sub>8</sub> /THF	1	60
7	1:10	1,4-dioxane	2.75	25
8	1:10	THF	3	25

When this reaction was instead heated for 20 min in C<sub>6</sub>D<sub>6</sub> (entry 2), the resonance at  $\delta$  85.1 (Pd(P<sup>t</sup>Bu<sub>3</sub>)<sub>2</sub>) was observed unchanged, along with a minor peak at  $\delta$  62.3 consistent with PBu<sup>t</sup><sub>3</sub> (Figure 59).<sup>18</sup>

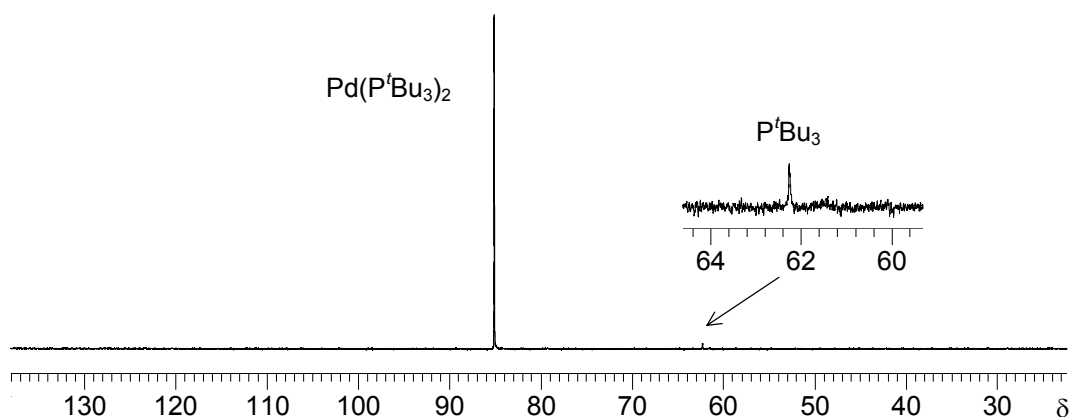


Figure 59. <sup>31</sup>P NMR spectrum (163.0 MHz) for attempted reaction of Pd(PBu<sup>t</sup><sub>3</sub>)<sub>2</sub> with one equivalent bromobenzene at 60 °C 20 minutes after mixing.

Oxidative addition of Pd(PBu<sup>t</sup><sub>3</sub>)<sub>2</sub> was also attempted toluene-d<sub>8</sub>/THF (entry 4) and pure THF (entry 8) at 25 °C, and both experiments revealed only the resonance for Pd(PBu<sup>t</sup><sub>3</sub>)<sub>2</sub> ( $\delta$  85.0). However, when Pd(PBu<sup>t</sup><sub>3</sub>)<sub>2</sub> was reacted with bromobenzene in toluene-d<sub>8</sub>/THF at 60 °C (entry 6), a <sup>31</sup>P NMR spectrum

revealed  $\text{Pd}(\text{P}^t\text{Bu}_3)_2$  ( $\delta$  85.2) and two very close signals at  $\delta$  62.4 and 62.8 (Figure 60). It is possible that these resonances are due to free  $\text{P}^t\text{Bu}_3$  as well as the oxidative addition product  $[\text{Pd}(\text{P}^t\text{Bu}_3)\text{PhBr}]$ , ( $^{31}\text{P}$   $\delta$  63.0) described by Hartwig *et al.*<sup>31</sup> The quite minor amount of this product in the current work is consistent with the harsh conditions reported for quantitative formation of  $[\text{Pd}(\text{P}^t\text{Bu}_3)\text{PhBr}]$  (neat bromobenzene at 77 °C).

In much the same way, reactions performed in 1,4-dioxane (entries 5 and 7) produced two species with  $^{31}\text{P}$  resonances in the region of  $\delta \sim 63$ . In all of these instances however, the assignment of these species cannot be confirmed, as corresponding  $^1\text{H}$  NMR spectra (in protonated THF and 1,4-dioxane respectively) do not show the associated proton resonances for  $\text{Pd}(\text{P}^t\text{Bu}_3)_2$ ,  $\text{P}^t\text{Bu}_3$  or  $\text{Pd}(\text{P}^t\text{Bu}_3)(\text{Ph})(\text{Br})$ .

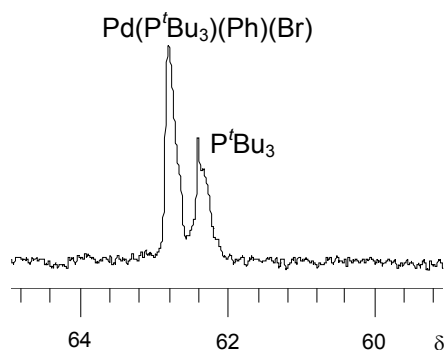


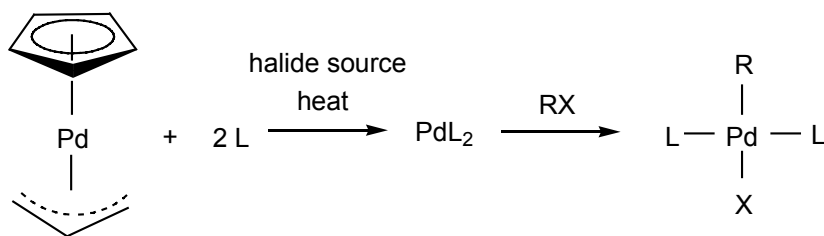
Figure 60.  $^{31}\text{P}$  NMR spectrum (242.9 MHz) for reaction of  $\text{Pd}(\text{P}^t\text{Bu}_3)_2$  with bromobenzene in toluene- $d_8$ /THF at 60 °C.

The relative lack of oxidative addition in systems involving  $\text{Pd}(\text{P}^t\text{Bu}_3)_2$  is consistent with the work of Hartwig *et al.*, who noted that oxidative addition under these conditions is unfavorable for  $\text{Pd}(\text{P}^t\text{Bu}_3)_2$ , requiring 40 equivalents of bromobenzene at 70 °C for greater than 16 hours.<sup>47</sup> The poor reactivity of

$\text{Pd}(\text{PBU}_3)_2$  towards oxidative addition observed here is however consistent with the systems for Suzuki coupling that have been reported with  $\text{PBU}_3$ .<sup>21b,c</sup> The authors note that the catalyst generated *in situ* from  $\text{Pd}_2(\text{dba})_3$  and  $\text{PBU}_3$  in a 1:1 Pd: $\text{PBU}_3$  ratio produces a highly active species (i.e.  $\text{Pd-PBU}_3$ ), while that generated with a 2:1 Pd: $\text{PBU}_3$  ratio (presumably  $\text{Pd}(\text{PBU}_3)_2$ ) produces an extremely slow rate of coupling.<sup>40c</sup>

### 3.5.2 Oxidative Addition with *In Situ* Generated $\text{PdL}_2$

Oxidative addition experiments with *in situ* generated  $\text{PdL}_2$  also of interest as it was desirable, prior to beginning a quantitative kinetic analysis, to determine if the addition of a halide had any effect on the nature of Pd complexes formed, as well as any subsequent oxidative addition products. A generalized representation of these experiments is shown in Scheme 40 and the varied experimental conditions are described in Table 19.



Scheme 40. Generalized representation of *in situ* oxidative addition reaction.



Table 19. Oxidative addition experiments performed with *in situ* PdL<sub>2</sub>

Entry	L	<i>In Situ</i> Conditions*	Pd:PhBr	Halide	Solvent
1	PCy <sub>3</sub>	60 °C, 180 min	1:10	TBAB	THF
2*	PCy <sub>3</sub>	75 °C, 180 min	1:10	TOPB	C <sub>7</sub> D <sub>8</sub>
3	PMeBu <sup>t</sup> <sub>2</sub>	60 °C, 60 min	1:10	TBAB	THF
4*	PMeBu <sup>t</sup> <sub>2</sub>	75 °C, 150 min	1:10	TOPB	C <sub>7</sub> D <sub>8</sub>

\* halide source added after heating, prior to PhBr

Experiments were performed with added tetraoctylphosphonium bromide (TOPB) in toluene-d<sub>8</sub>, or tetrabutylammonium bromide (TBAB) in THF as the halide source (Figure 61).

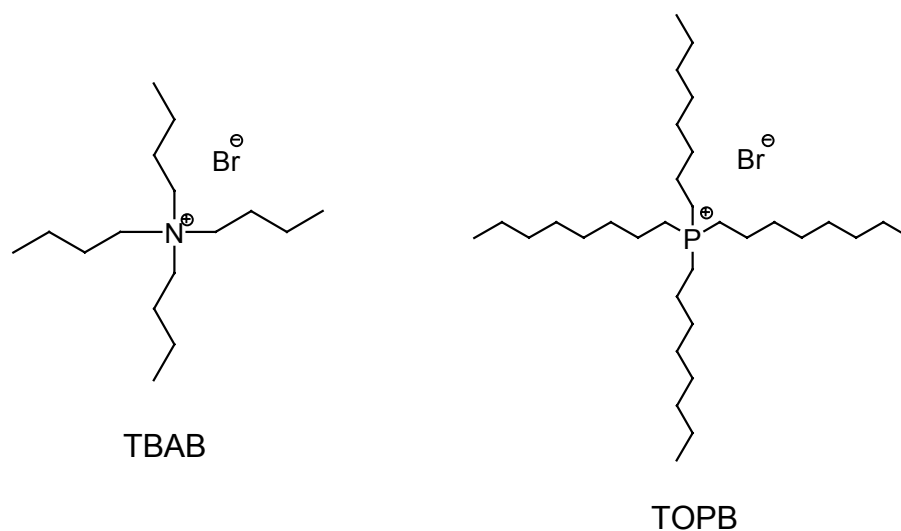


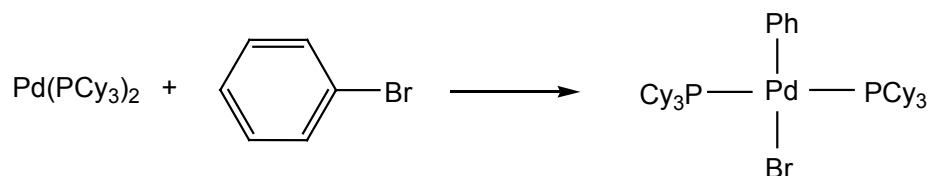
Figure 61. Tetrabutylammonium bromide (TBAB) and tetraoctylphosphonium bromide (TOPB).

It was found that in each instance the addition of halide (TBAB or TOPB) during the *in situ* formation of PdL<sub>2</sub> from Pd( $\eta^3$ -C<sub>3</sub>H<sub>5</sub>)( $\eta^5$ -C<sub>5</sub>H<sub>5</sub>) did not produce new or unanticipated <sup>31</sup>P containing Pd species observed in solution, indicated by unchanged <sup>31</sup>P chemical shifts for Pd(PCy<sub>3</sub>)<sub>2</sub> and Pd(PMeBu<sup>t</sup>)<sub>2</sub>. Furthermore, subsequent addition of bromobenzene produced only the anticipated peaks for

$\text{Pd}(\text{PCy}_3)_2(\text{Ph})(\text{Br})$  and  $\text{Pd}(\text{PMeBu}^t_2)_2(\text{Ph})(\text{Br})$ , as reported above. The purposeful addition of halide as TOPB or TBAB therefore failed to produce any changes in the species typically observed in the  $^{31}\text{P}$  NMR spectra during oxidative addition.

### 3.6 Kinetic Analyses of Oxidative Addition of PhBr to $\text{Pd}(\text{PCy}_3)_2$

Kinetic experiments on oxidative addition reactions involving  $\text{Pd}(\text{PCy}_3)_2$  and bromobenzene were performed with a two-fold purpose in mind (Scheme 41). Firstly, while added halide did not noticeably alter the nature of the species observed during oxidative addition (Section 3.5.2), it remained of interest to determine if the presence of halide ion altered the rate of oxidative addition, given the reported existence of anionic bisphosphine complexes  $\text{PdL}_2\text{X}^-$ .<sup>46</sup>



Scheme 41. Oxidative addition of  $\text{Pd}(\text{PCy}_3)_2$  and bromobenzene.

TOPB was a convenient choice as a halide source in these systems as it has good solubility in toluene- $d_8$  while also acting as a  $^{31}\text{P}$  NMR internal standard by virtue of the tetraoctylphosphonium cation. Secondly, it was of interest to establish the kinetic parameters and mechanistic details of the oxidative addition step. The relative ease with which oxidative addition of PhBr to  $\text{Pd}(\text{PCy}_3)_2$  occurs

at room temperature is in direct contrast with the high temperatures and long reaction times often used in cross-coupling processes, perhaps indicating that the rate-determining step of the catalytic process is reduction of typically used Pd(II) precursors.

The rate expression for oxidative addition was expected to be a function of both [PhBr] and [PdL<sub>2</sub>]. By conducting experiments under pseudo first order conditions (large [PhBr]), one can assume that [PhBr] remains essentially constant, allowing for the isolation of the rate expression as a function of [PdL<sub>2</sub>]. The rate of reaction will thus be equal to  $k_{\text{obs}}[\text{PdL}_2]$ , where the dependence of  $k_{\text{obs}}$  on [PhBr] can be established by plotting  $k_{\text{obs}}$  as a function of [PhBr].

In a typical kinetics experiment, a toluene-d<sub>8</sub> solution of Pd(PCy<sub>3</sub>)<sub>2</sub> was transferred to an NMR tube containing a sealed glass capillary of TOPB in toluene. The added TOPB solution was of known concentration and thus served as an external standard from which relative integrations could be made. In order to obtain pseudo-first order data, the amount of PhBr that was injected into the NMR tube was varied, and experiments were performed at several PhBr concentrations (PhBr: Pd ratios of 13:1, 22:1, 32:1, 38:1 and 51:1). Prior to injection of PhBr, the probe was first tuned using a separate sample of toluene-d<sub>8</sub>. After the appropriate amount of PhBr was injected into the NMR tube, the time was noted and the sample was introduced into the NMR probe at 25 °C. <sup>31</sup>P inverse gated spectra were then obtained at 94 s intervals. In order to obtain sufficient kinetic data, spectra were obtained in each experiment for greater than two half-lives of Pd(PCy<sub>3</sub>)<sub>2</sub>. Typically, Prism software<sup>51</sup> was then utilized to

perform either linear or non-linear regression to analyze the obtained kinetic data.

The obtained  $^{31}\text{P}$  inverse-gated NMR spectra showed the disappearance of the  $\text{Pd}(\text{PCy}_3)_2$  resonance at  $\delta$  39.0 with the concurrent growth of a resonance at  $\delta$  21.3, associated with  $\text{Pd}(\text{PCy}_3)_2(\text{Ph})(\text{Br})$ . The integration of these resonances relative to the external TOPB standard allowed one to calculate the concentration of each of these species over time. A representative example of the obtained kinetic data in these experiments is shown in Figure 62.

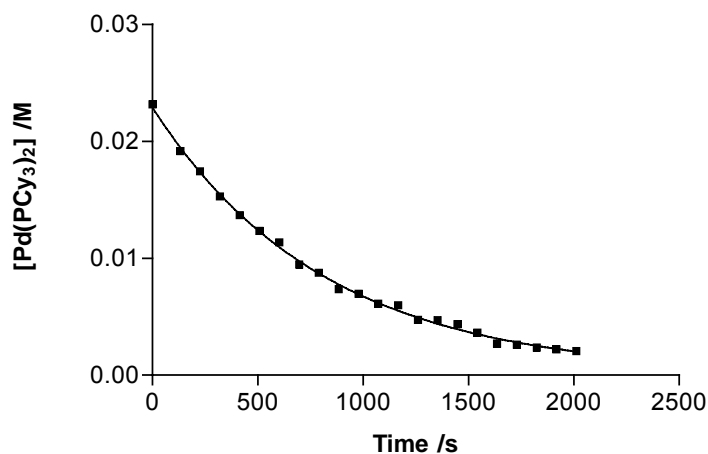


Figure 62. Concentration of  $\text{Pd}(\text{PCy}_3)_2$  as a function of time for the oxidative addition of PhBr (0.483 M) to  $\text{Pd}(\text{PCy}_3)_2$  ( $[\text{Pd}(\text{PCy}_3)_2]_0 = 0.0232$  M) at 25 °C in toluene- $d_8$ .

Subsequent analysis of the obtained concentration data revealed linear plots of  $\ln[\text{Pd}(\text{PCy}_3)_2]$  as a function of time (at varied  $[\text{PhBr}]$ ), suggesting that the reaction is first order in  $\text{Pd}(\text{PCy}_3)_2$  (see Appendix 1 for data). A representative example of this linear plot is shown in Figure 63. Linear regression provided slope values for each of these linear plots, which corresponded to the observed rate constants  $k_{\text{obs}}$  (see Appendix 1).

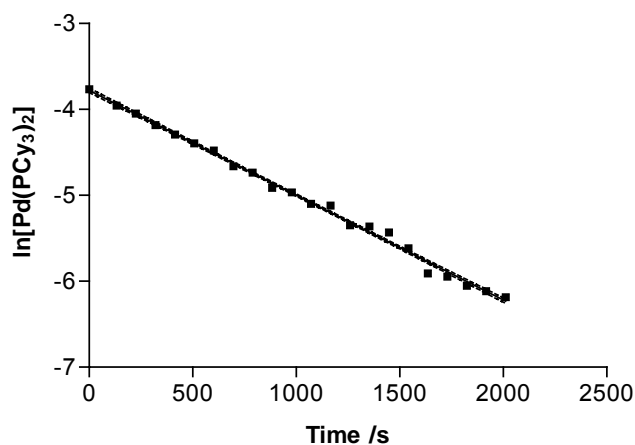


Figure 63.  $\ln[\text{Pd}(\text{PCy}_3)_2]$  as a function of time for oxidative addition of PhBr (0.483 M) to  $\text{Pd}(\text{PCy}_3)_2$  ( $[\text{Pd}(\text{PCy}_3)_2]_0 = 0.0232 \text{ M}$ ) at 25 °C in toluene- $d_8$ .

The obtained values of  $k_{\text{obs}}$  were then plotted as a function of  $[\text{PhBr}]$  and produced a linear plot with a y-intercept, having the general form  $k_{\text{obs}} = k' + k[\text{PhBr}]$  (Figure 64).

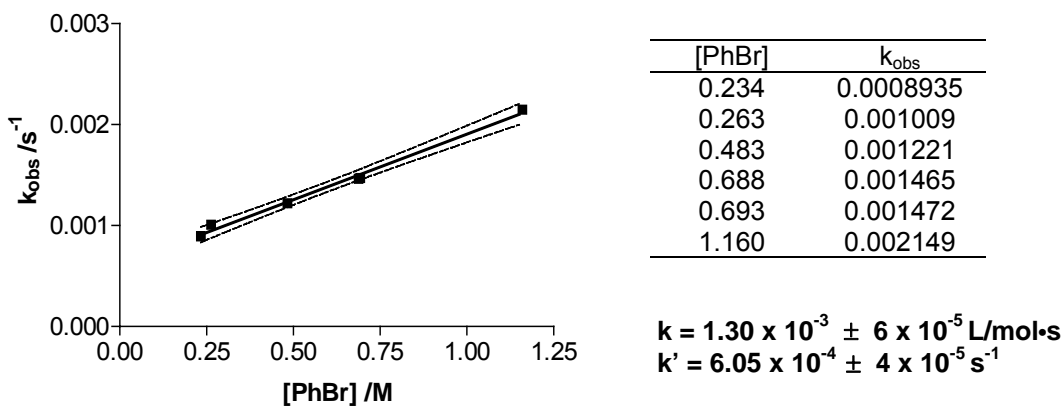


Figure 64.  $k_{\text{obs}}$  as a function of time for the oxidative addition of  $\text{Pd}(\text{PCy}_3)_2$  and PhBr at 25 °C in toluene- $d_8$  (--- represents 95% confidence intervals,  $R^2 = 0.99$ ).

With this general form for the rate law in mind, such experiments were repeated in the presence of added halide in order to assess its effect of the rate

of oxidative addition (Section 3.6.1). Similarly, experiments were also repeated in the presence of one equivalent of PCy<sub>3</sub> (with respect to Pd(PCy<sub>3</sub>)<sub>2</sub> = 0.0021M) (Section 3.6.2). These kinetic results and related rate expressions were then interpreted in the context of a proposed mechanistic scheme (Section 3.6.3), revealing significant insight into the mechanism for the formation of the oxidative addition product *trans*-[Pd(PCy<sub>3</sub>)<sub>2</sub>PhBr].

### 3.6.1 Assessment of The Effect of Added Halide as TOPB

To assess the effect of added bromide ion, oxidative addition experiments were performed as described above, except that the Pd(PCy<sub>3</sub>)<sub>2</sub> solution was added to an NMR tube containing a solution of TOPB (0.15 mL of 0.10 M in toluene-d<sub>8</sub>). The added TOPB thus served as the Br<sup>-</sup> source (one equivalent of TOPB with respect to Pd(PCy<sub>3</sub>)<sub>2</sub>), as well as an internal standard. The concentrations of the Pd containing species were monitored by <sup>31</sup>P inverse-gated NMR spectroscopy over time by integration relative to the internal TOPB standard. The value of k<sub>obs</sub> was then determined as described above (at varied [PhBr]) and a plot of k<sub>obs</sub> as a function of [PhBr] was obtained (Figure 65). As was observed above in the absence of TOPB (Figure 64), a plot of k<sub>obs</sub> as a function of [PhBr] with added TOPB produced a linear plot with a y-intercept, once again with a general form k<sub>obs</sub> = k + k'[PhBr] (Figure 65). A comparison of the data in the absence of TOPB (k = 1.30 x 10<sup>-3</sup> L/mol·s and k' = 6.05 x 10<sup>-4</sup> s<sup>-1</sup>) and presence of TOPB (k = 1.27 x 10<sup>-3</sup> L/mol·s and k' = 6.20 x 10<sup>-4</sup> s<sup>-1</sup>) showed

no significant difference in the values of  $k$  and  $k'$ , indicating that added TOPB had no effect on the oxidative addition reaction of  $\text{Pd}(\text{PCy}_3)_2$  with bromobenzene.

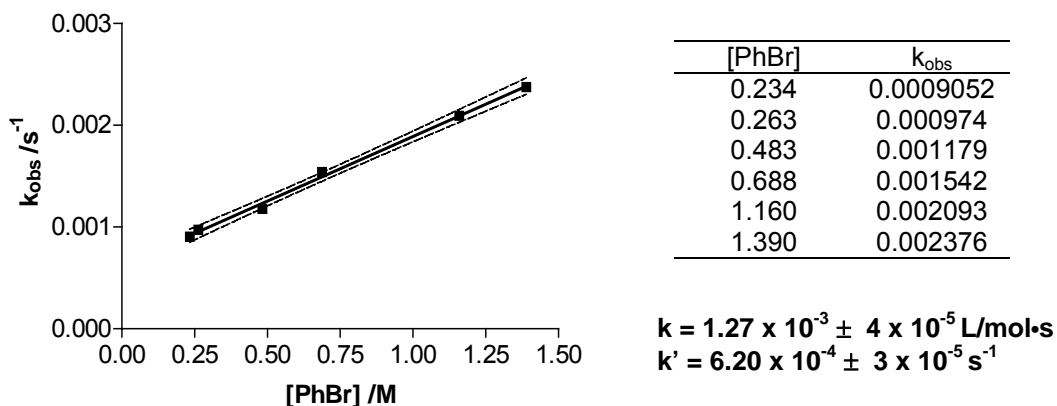


Figure 65.  $k_{\text{obs}}$  as a function of time for the oxidative addition of PhBr to  $\text{Pd}(\text{PCy}_3)_2$  in the presence of TOPB (--- represents 95% confidence intervals,  $R^2 = 0.99$ ).

### 3.6.2 Oxidative Addition in the Presence of Additional $\text{PCy}_3$

Oxidative addition of  $\text{Pd}(\text{PCy}_3)_2$  with bromobenzene was also monitored by  $^{31}\text{P}$  NMR spectroscopy in the presence of one equivalent of  $\text{PCy}_3$  (with respect to  $[\text{Pd}(\text{PCy}_3)_2]_0 = 0.021 \text{ M}$ ) in order to elucidate the mechanistic details of the oxidative addition step, as well as associated kinetic parameters. Such experiments were performed as above except that a toluene- $d_8$  solution of  $\text{Pd}(\text{PCy}_3)_2$  was added to an NMR tube containing a toluene- $d_8$  solution of  $\text{PCy}_3$  prior to injection of PhBr. In each instance, the concentration of the product *trans*- $\text{Pd}(\text{PCy}_3)_2(\text{Ph})(\text{Br})$  was determined by integration relative to the included TOPB standard. Two replicate experiments were performed at each value of [PhBr]. The concentration data were then plotted as a function of time for a given [PhBr]. The obtained concentration data for [PhBr] = 0.272 M are shown in

Figure 66a. For purposes of comparison, data obtained in the absence of free PCy<sub>3</sub> ([PhBr] = 0.272 M) are also shown (Figure 66b).

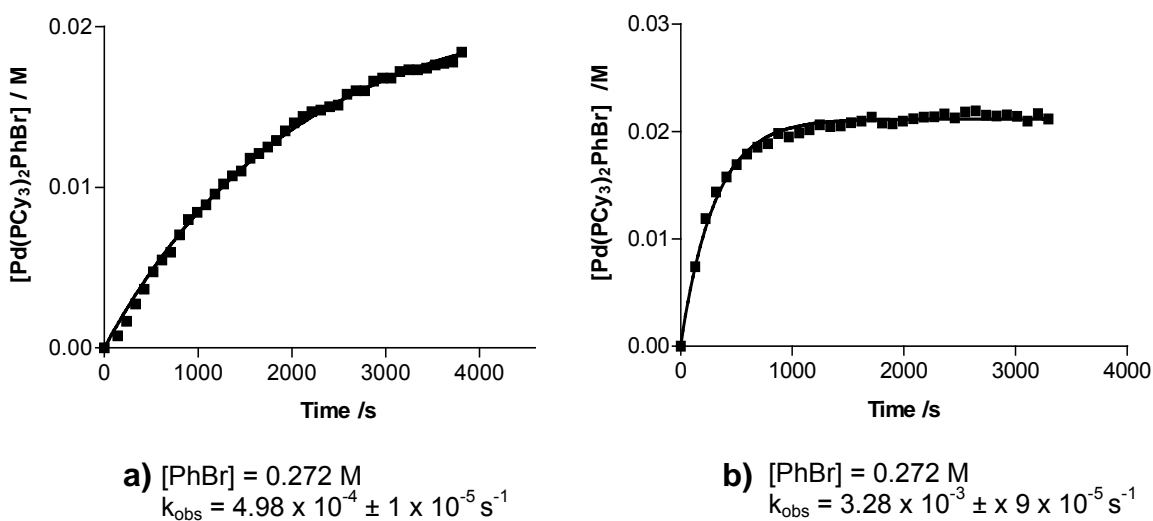
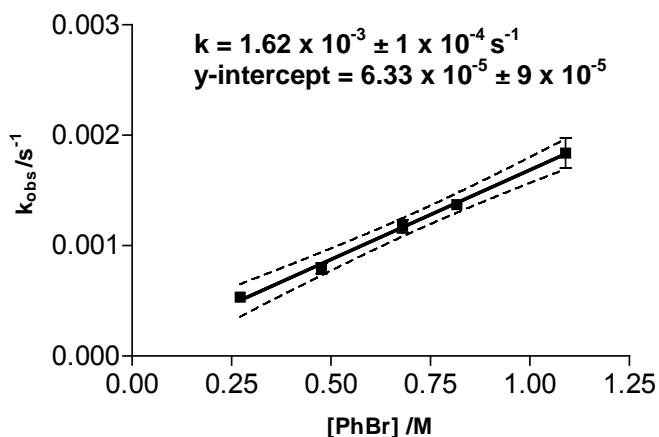


Figure 66. Plot of [Pd(PCy<sub>3</sub>)<sub>2</sub>PhBr] as a function of time for oxidative addition of PhBr (0.272 M) to Pd(PCy<sub>3</sub>)<sub>2</sub> ([Pd(PCy<sub>3</sub>)<sub>2</sub>]<sub>0</sub> = 0.021 M) a) in the presence of one equivalent of PCy<sub>3</sub> ([PCy<sub>3</sub>] = 0.021 M) b) in the absence of one equivalent of PCy<sub>3</sub>.

A comparison of the data obtained at [PhBr] = 0.272 M with 0 or 0.021 M PCy<sub>3</sub> revealed significant inhibition of oxidative addition in the presence of additional PCy<sub>3</sub>. The values of  $k_{\text{obs}}$  at varied [PhBr] were obtained by the non-linear regression of the concentration data, allowing one to produce a plot of  $k_{\text{obs}}$  as a function of [PhBr] (Figure 67). The plot of  $k_{\text{obs}}$  as a function of [PhBr] was found to be linear and lacked a y-intercept, thus having the general form  $k_{\text{obs}} = k[\text{PhBr}]$ . This plot contrasts with that obtained in the absence of added PCy<sub>3</sub> (Figure 64), which has the general form  $k_{\text{obs}} = k' + k[\text{PhBr}]$ .





[PhBr]	$k_{\text{obs}}$	
	Trial 1	Trial 2
0.272	0.000572	0.000498
0.476	0.000746	0.000841
0.680	0.001118	0.001233
0.816	0.001360	0.001382
1.09 <sup>a</sup>	0.001630	0.002096

a) [PhBr] = 1.09 M performed with a third replicate where  $k_{\text{obs}} = 0.001793 \text{ s}^{-1}$

Figure 67.  $k_{\text{obs}}$  as a function of time for the oxidative addition of PhBr to  $\text{Pd}(\text{PCy}_3)_2$  in the presence of one equivalent of  $\text{PCy}_3$  (--- represents 95% confidence intervals,  $R^2 = 0.95$ ).

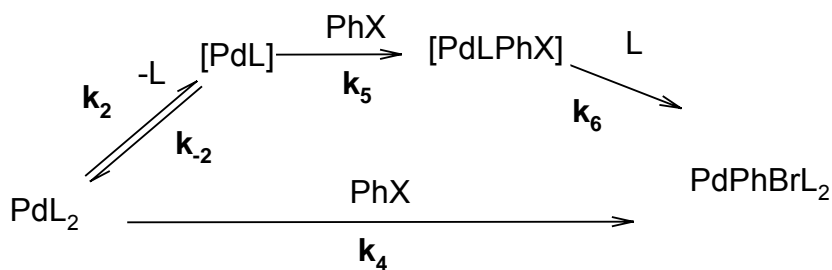
A comparison of these plots indicates that while they possess similar slope values ( $k$ ), their values for the y-intercept are significantly different. This difference was then interpreted in the context of the possible mechanistic pathways to product formation (Section 3.6.3).

### 3.6.3 Mechanistic Interpretation of Kinetic Data for Oxidative Addition

Given the observed difference in the experimental rate laws in the absence ( $k_{\text{obs}} = k' + k[\text{PhBr}]$ ) and presence of  $\text{PCy}_3$  ( $k_{\text{obs}} = k[\text{PhBr}]$ ), the possible mechanistic pathways for the oxidative addition were considered. The rate expressions for each of these pathways were derived, with the aim of comparing plots based on these expressions to the experimentally obtained plots of  $k_{\text{obs}}$  as a function of  $[\text{PhBr}]$ . If one or more of the derived rate expressions produces a linear plot that corresponds to the obtained kinetic data, one can say that the

related pathway is a viable mechanism for oxidative addition of  $\text{Pd}(\text{PCy}_3)_2$  and  $\text{PhBr}$ .

The first mechanistic scenario considered was that in which oxidative addition occurs in the absence of additional  $\text{PCy}_3$ , as is visualized in Scheme 42.



Scheme 42. Possible mechanistic pathways for the oxidative addition of  $\text{PhBr}$  to  $\text{PdL}_2$  ( $\text{L} = \text{PCy}_3$ ).

Two reasonable pathways can be conceived for oxidative addition to  $\text{PdL}_2$  ( $\text{L} = \text{PCy}_3$ ). The first involves direct oxidative addition to  $\text{PdL}_2$  ( $k_4$ ), while the second involves a reversible dissociation of  $\text{PCy}_3$  to produce a monophosphine complex, which subsequently undergoes oxidative addition ( $k_5$ ) and association of  $\text{PCy}_3$  ( $k_6$ ) to form the product. The associated rate laws were derived using the assumption of a rapid pre-equilibrium ( $k_2, k_{-2} > k_5$ ), as well as the steady state approximation for  $[\text{PdLPhBr}]$  (for all derivations, see Appendix 1). It was then possible to further simplify the rate equations to reflect each of the following mechanistic possibilities; a)  $\text{PdL}_2$  is unreactive, b)  $\text{PdL}$  is unreactive, c) both  $\text{PdL}_2$  and  $\text{PdL}$  are reactive. A summary of these assumptions and the resulting rate expressions appear in Table 20.

Table 20. Summary of rate expression derivations for oxidative addition of PhBr to Pd(PCy<sub>3</sub>)<sub>2</sub> in the absence of additional PCy<sub>3</sub>.

		Mechanistic Possibilities		
Pre-equilibrium Assumption for K <sub>2</sub>	Rate Law	a) PdL <sub>2</sub> is unreactive (k <sub>4</sub> = 0)	b) PdL is unreactive (k <sub>5</sub> = 0)	c) PdL <sub>2</sub> and PdL are reactive (k <sub>4</sub> , k <sub>5</sub> ≠ 0)
Rapid	$k_{\text{obs}} = k_4[\text{ArX}] + \frac{k_2 K_5 [\text{ArX}]}{[\text{L}]}$	$k_{\text{obs}} = \frac{k_5 K_2 [\text{ArX}]}{[\text{L}]}$	$k_{\text{obs}} = k_4 [\text{ArX}]$	$k_{\text{obs}} = \left( k_4 + \frac{k_5 K_2}{[\text{L}]} \right) [\text{ArX}]$
Non-rapid	$k_{\text{obs}} = k_4 [\text{ArX}] + \frac{k_2 k_5 [\text{ArX}]}{k_{-2} [\text{L}] + k_5 [\text{ArX}]}$	$k_{\text{obs}} = \frac{k_2 k_5 [\text{ArX}]}{k_{-2} [\text{L}] + k_5 [\text{ArX}]}$ <b>1. if <math>k_{-2} [\text{L}] \gg k_5 [\text{ArX}]</math> then:</b> $k_{\text{obs}} = \frac{k_2 k_5 [\text{ArX}]}{k_{-2} [\text{L}]}$ <b>2. if <math>k_{-2} [\text{L}] \ll k_5 [\text{ArX}]</math> then:</b> $k_{\text{obs}} = \frac{k_2 k_5 [\text{ArX}]}{k_5 [\text{ArX}]} = k_2$	$k_{\text{obs}} = k_4 [\text{ArX}]$	<b>1. if <math>k_{-2} [\text{L}] \gg k_5 [\text{ArX}]</math> then:</b> $k_{\text{obs}} = \left( k_4 + \frac{k_2 k_5}{k_{-2} [\text{L}]} \right) [\text{ArX}]$ <b>2. if <math>k_{-2} [\text{L}] \ll k_5 [\text{ArX}]</math> then:</b> $k_{\text{obs}} = k_4 [\text{ArX}] + k_2$

Based upon the proposed mechanistic scheme, there are eight possible expressions that must be compared to the experimentally obtained plot of  $k_{\text{obs}}$  as a function of  $[\text{PhBr}]$  (Table 20). In examining these expressions, it is possible to predict whether a zero or non-zero y-intercept would result if  $k_{\text{obs}}$  was plotted as a function of  $[\text{PhBr}]$ . These possibilities and the nature of the related y-intercept are summarized in Table 21.

Table 21. Possible rate expressions describing oxidative addition of PhBr to  $\text{Pd}(\text{PCy}_3)_2$  under pseudo first order conditions.

Entry	Assumptions	Rate Law	y-intercept
1	$K_2$ rapid $k_4 = 0$	$k_{\text{obs}} = \frac{k_5 K_2 [\text{ArX}]}{[\text{L}]}$	zero
2	$K_2$ rapid $k_5 = 0$	$k_{\text{obs}} = k_4 [\text{ArX}]$	zero
3	$K_2$ rapid $k_4, k_5 \neq 0$	$k_{\text{obs}} = \left( k_4 + \frac{k_5 K_2}{[\text{L}]} \right) [\text{ArX}]$	zero
4	$K_2$ non-rapid $k_4 = 0$ $k_{-2} [\text{L}] \gg k_5 [\text{ArX}]$	$k_{\text{obs}} = \frac{k_2 k_5 [\text{ArX}]}{k_{-2} [\text{L}]}$	zero
5	$K_2$ non-rapid $k_4 = 0$ $k_{-2} [\text{L}] \ll k_5 [\text{ArX}]$	$k_{\text{obs}} = k_2$	non-zero
6	$K_2$ non-rapid $k_5 = 0$	$k_{\text{obs}} = k_4 [\text{ArX}]$	zero
7	$K_2$ non-rapid $k_4, k_5 \neq 0$ $k_{-2} [\text{L}] \gg k_5 [\text{ArX}]$	$k_{\text{obs}} = \left( k_4 + \frac{k_2 k_5}{k_{-2} [\text{L}]} \right) [\text{ArX}]$	zero
8	$K_2$ non-rapid $k_4, k_5 \neq 0$ $k_{-2} [\text{L}] \ll k_5 [\text{ArX}]^a$	$k_{\text{obs}} = k_4 [\text{ArX}] + k_2$	non-zero

a)  $[\text{L}]$  is assumed to be extremely small (no  $[\text{PdL}]$  is observed spectroscopically), thus the assumption holds true for very small  $[\text{ArX}]$

Of all these expressions, that which is represented in entry 8 is the only equation which adequately predicts the experimental pseudo first order plot, namely, where  $k_{\text{obs}}$  varies as a function of  $[\text{PhBr}]$  and possesses a non-zero y-intercept ( $k_{\text{obs}} = k' + k[\text{PhBr}]$ ). One can therefore conclude that  $k$  in the observed rate law is in fact  $k_4$ , while  $k'$  corresponds to  $k_2$ . This result is particularly significant in that it suggests the existence of two separate pathways, involving oxidative addition of PhBr to  $\text{PdL}_2$  ( $k_4$ ) or  $\text{PdL}$  ( $k_5$ ), both of which produce the oxidative addition product.

This result is in contrast to that reported for the kinetics of oxidative addition of  $\text{Pd}(\text{PCy}_3)_2$  with both PhI and PhOTf.<sup>52</sup> The rate of reaction of PhI with  $\text{Pd}(\text{PCy}_3)_2$  in THF was noted to remain unaffected by excess of  $\text{PCy}_3$ , implying a single path for oxidative addition involving only  $\text{Pd}(\text{PCy}_3)_2$ . Similarly, the rate of addition of PhOTf was also unchanged with additional phosphine.<sup>52</sup> However, the existence of two pathways for oxidative addition (from Pd-L and  $\text{PdL}_2$ ) has been shown for the reaction of the more sterically hindered complex  $\text{Pd}(\text{P}(o\text{-Tol})_3)_2$  (cone angle  $194^\circ$ )<sup>11</sup> with  $p\text{-Bu}^t\text{-C}_6\text{H}_4\text{Br}$ .<sup>53</sup> Interestingly, others have reported that for  $\text{Pd}(\text{Q-phos})_2$  (Q-phos =  $\text{Fe}(\eta^5\text{-C}_5\text{H}_4\text{P}(\text{Bu}^t)_2)(\eta^5\text{-C}_5(\text{CH}_3)_5)$ ) the mechanism for oxidative addition depends upon the nature of the substrate.<sup>54</sup> It was found that while oxidative addition with PhI proceeds directly from  $\text{Pd}(\text{Q-phos})_2$ , the addition involving PhBr occurs through the monophosphine complex  $\text{Pd-Q-phos}$ , formed by irreversible dissociation of Q-phos from  $\text{Pd}(\text{Q-phos})_2$ . The oxidative addition of PhCl behaved similarly, proceeding via the monophosphine complex after a reversible dissociation of Q-phos from  $\text{Pd}(\text{Q-phos})_2$ . Such

studies, taken along with the currently described kinetic system, thus serve to highlight the difficulty in making generalizations regarding of the mechanism of oxidative addition to bisphosphine complexes of Pd(0).

Using the selected rate expression (entry 8) and values obtained from the pseudo first order plot, it was possible to determine the percentage of product formed by each pathway. Since the overall rate constant for product formation ( $k_{\text{obs}}$ ) can be expressed as the sum of individual contributions from the PdL<sub>2</sub> path ( $k_4[\text{ArX}]$ ) and the PdL path ( $k_2$ ), the proportion of product formed by each pathway can be determined as a percentage of the overall rate constant  $k_{\text{obs}}$ , as seen in Figure 68. Thus, as an example, when  $[\text{PhBr}] = 0.693 \text{ M}$ , 60% of the product is formed from oxidative addition of PdL<sub>2</sub>, while 40 % is formed by dissociation of PdL<sub>2</sub>, followed by reaction of PhBr and PdL.

$$\text{Product from } k_4 \text{ path} = \left( \frac{k_4[\text{ArX}]}{k_4[\text{ArX}] + k_2} \right) 100\% \approx 60\%$$

$$\text{Product from } k_2 \text{ path} = \left( \frac{k_2}{k_4[\text{ArX}] + k_2} \right) 100\% \approx 40\%$$

Figure 68. Percentage of produced by pathway for oxidative addition of PhBr to Pd(PCy<sub>3</sub>)<sub>2</sub> ( $[\text{PhBr}] = 0.693 \text{ M}$ ).

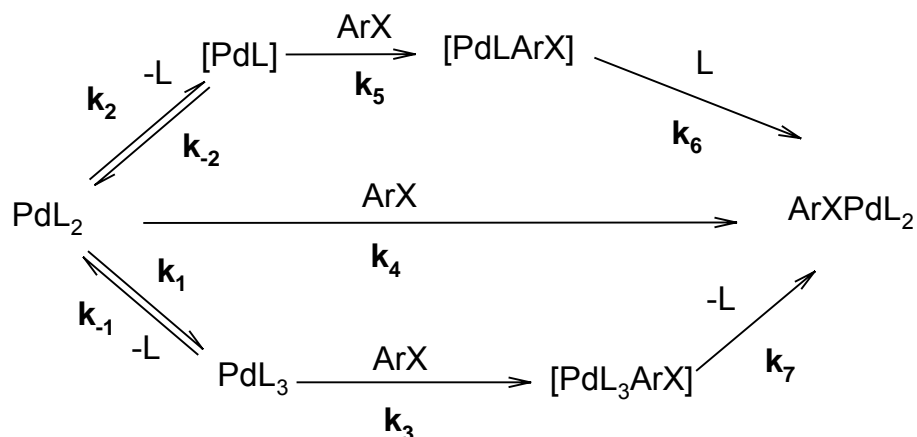
Interestingly, if the product distribution is calculated at other  $[\text{PhBr}]$ , it can be seen that the proportion of product derived from the PdL pathway is expected to decrease as  $[\text{PhBr}]$  increases (Table 22).

Table 22. Percentage of product produced by each pathway at varied [ArX] for the oxidative addition of PhBr to Pd(PCy<sub>3</sub>)<sub>2</sub>.

[PhBr]	0.234 M	0.693 M	1.16 M
% from PdL <sub>2</sub> (k <sub>4</sub> )	33	60	71
% from PdL (k <sub>2</sub> )	66	40	29

If one considers the conditions for catalytic oxidative addition, one would expect a large excess of PhBr compared to the Pd species present. At larger [PhBr], the PdL pathway may be essentially shut down, favoring instead the PdL<sub>2</sub> pathway. For example, in a given coupling protocol where [ArX] is 5.0 M, the PdL<sub>2</sub> pathway would account for 91 % of product formed, while that of PdL would only provide 9%. This is particularly significant in the context of recent reports of monophosphine catalyst systems.<sup>38</sup> The current results indicate (at least for the Pd(PCy<sub>3</sub>)<sub>2</sub> system) that oxidative addition of Pd-L may play a minor role in product formation if the associated PdL<sub>2</sub> complex can undergo direct and facile oxidative addition and if the concentration of ArX is large.

The second mechanistic scenario to be considered was that which involved oxidative addition in the presence of additional PCy<sub>3</sub>. Such a scheme must now account for the presence of a tris-substituted species Pd(PCy<sub>3</sub>)<sub>3</sub>. The associated mechanistic possibilities for oxidative addition with additional PCy<sub>3</sub> are described in Scheme 43.



Scheme 43. Possible mechanistic pathways for the oxidative addition of PhBr to Pd(PCy<sub>3</sub>)<sub>2</sub> in the presence of excess PCy<sub>3</sub>.

In addition to pathways involving PdL<sub>2</sub> and PdL, the proposed mechanistic scheme now accounts for the possible reactivity of PdL<sub>3</sub> towards oxidative addition. The possible rate expressions for each of these pathways were derived as described above (see Appendix 1 for derivations) with the added complication of assuming either rapid or non-rapid pre-equilibria for both K<sub>1</sub> and K<sub>2</sub>. It was assumed that both PdL<sub>2</sub> and PdL would always be reactive species (i.e. k<sub>4</sub>, k<sub>5</sub> ≠ 0), as was the case in the absence of additional PCy<sub>3</sub>. A summary of these rate laws appears in Table 23.



Table 23. Summary of rate law possibilities for oxidative addition of PhBr to Pd(PCy<sub>3</sub>)<sub>2</sub> in the presence of excess PCy<sub>3</sub>.

Pre-equilibrium Assumption		Rate Law	If PdL <sub>3</sub> is unreactive (k <sub>3</sub> = 0)	If all species are reactive (k <sub>3</sub> , k <sub>4</sub> , k <sub>5</sub> ≠ 0)
K <sub>1</sub>	K <sub>2</sub>			
Rap id	Rapid	$k_{\text{obs}} = \left( \frac{k_3[\text{L}]}{K_1} + k_4 + \frac{k_5 K_2}{[\text{L}]} \right) [\text{ArX}]$	$k_{\text{obs}} = \left( k_4 + \frac{k_5 K_2}{[\text{L}]} \right) [\text{ArX}]$	$k_{\text{obs}} = \left( \frac{k_3[\text{L}]}{K_1} + k_4 + \frac{k_5 K_2}{[\text{L}]} \right) [\text{ArX}]$
Rap id	Non-Rapid	$k_{\text{obs}} = \left( \frac{k_3[\text{L}]}{K_1} + k_4 + \frac{k_2 k_5}{k_{-2}[\text{L}] + k_5[\text{ArX}]} \right) [\text{ArX}]$	$k_{\text{obs}} = \left( k_4 + \frac{k_2 k_5}{k_{-2}[\text{L}] + k_5[\text{ArX}]} \right) [\text{ArX}]$ <p>1. If <math>k_{-2}[\text{L}] &gt; k_5[\text{ArX}]</math>, then:</p> $k_{\text{obs}} = \left( k_4 + \frac{k_2 k_5}{k_{-2}[\text{L}]} \right) [\text{ArX}]$ <p>2. If <math>k_{-2}[\text{L}] &lt; k_5[\text{ArX}]</math>, then:</p> $k_{\text{obs}} = k_4[\text{ArX}] + k_2$	<p>1. If <math>k_{-2}[\text{L}] &gt; k_5[\text{ArX}]</math>, then:</p> $k_{\text{obs}} = \left( \frac{k_3[\text{L}]}{K_1} + k_4 + \frac{k_2 k_5}{k_{-2}[\text{L}]} \right) [\text{ArX}]$ <p>2. If <math>k_{-2}[\text{L}] &lt; k_5[\text{ArX}]</math>, then:</p> $k_{\text{obs}} = \left( \frac{k_3[\text{L}]}{K_1} + k_4 \right) [\text{ArX}] + k_2$

Table 23. Continued.

Pre-equilibrium Assumption		Rate Law	If PdL <sub>3</sub> is unreactive (k <sub>3</sub> = 0)	If all species are reactive (k <sub>3</sub> , k <sub>4</sub> , k <sub>5</sub> ≠ 0)
K <sub>1</sub>	K <sub>2</sub>			
Non-Rapid	Rapid	$k_{\text{obs}} = \left( \frac{k_3 k_{-1} [\text{L}]}{k_1 + k_3 [\text{ArX}]} + k_4 + \frac{k_5 K_2}{[\text{L}]} \right) [\text{ArX}]$	$k_{\text{obs}} = \left( k_4 + \frac{k_5 K_2}{[\text{L}]} \right) [\text{ArX}]$	<p>1. If <math>k_1 &gt; k_3 [\text{ArX}]</math>, then:</p> $k_{\text{obs}} = \left( \frac{k_3 k_{-1} [\text{L}]}{k_1} + k_4 + \frac{k_5 K_2}{[\text{L}]} \right) [\text{ArX}]$ <p>2. If <math>k_1 &lt; k_3 [\text{ArX}]</math>, then:</p> $k_{\text{obs}} = \left( \frac{k_{-1} [\text{L}]}{[\text{ArX}]} + k_4 + \frac{k_5 K_2}{[\text{L}]} \right) [\text{ArX}]$

Table 23. Continued.

Pre-equilibrium Assumption		Rate Law	If PdL <sub>3</sub> is unreactive (k <sub>3</sub> = 0)	If all species are reactive (k <sub>3</sub> , k <sub>4</sub> , k <sub>5</sub> ≠ 0)
K <sub>1</sub>	K <sub>2</sub>			
Non-Rapid	Non-Rapid	$k_{\text{obs}} = \left( \frac{k_{-1}k_3[\text{L}]}{k_1 + k_3[\text{ArX}]} + k_4 \dots + \frac{k_2k_5}{k_{-2}[\text{L}] + k_5[\text{ArX}]} \right) [\text{ArX}]$	$k_{\text{obs}} = \left( k_4 + \frac{k_2k_5}{k_{-2}[\text{L}] + k_5[\text{ArX}]} \right) [\text{ArX}]$ <p>1. If k<sub>-2</sub>[L] &gt; k<sub>5</sub>[ArX], then:</p> $k_{\text{obs}} = \left( k_4 + \frac{k_2k_5}{k_{-2}[\text{L}]} \right) [\text{ArX}]$ <p>2. If k<sub>-2</sub>[L] &lt; k<sub>5</sub>[ArX], then:</p> $k_{\text{obs}} = k_4[\text{ArX}] + k_2$	<p>1. If k<sub>-2</sub>[L] &gt; k<sub>5</sub>[ArX], then:</p> <p>a) If K<sub>1</sub> &gt; k<sub>3</sub>[ArX], then:</p> $k_{\text{obs}} = \left( \frac{k_{-1}k_3[\text{L}]}{k_1} + k_4 + \frac{k_2k_5}{k_{-2}[\text{L}]} \right) [\text{ArX}]$ <p>b) If K<sub>1</sub> &lt; k<sub>3</sub>[ArX], then:</p> $k_{\text{obs}} = \left( \frac{k_{-1}[\text{L}]}{[\text{ArX}]} + k_4 + \frac{k_2k_5}{k_{-2}[\text{L}]} \right) [\text{ArX}]$ <p>2. If k<sub>-2</sub>[L] &lt; k<sub>5</sub>[ArX], then:</p> <p>a) If K<sub>1</sub> &gt; k<sub>3</sub>[ArX], then:</p> $k_{\text{obs}} = \left( \frac{k_{-1}k_3[\text{L}]}{k_1} + k_4 \right) [\text{ArX}] + k_2$ <p>b) If K<sub>1</sub> &lt; k<sub>3</sub>[ArX], then:</p> $k_{\text{obs}} = \left( \frac{k_{-1}[\text{L}]}{k_3[\text{ArX}]} + k_4 \right) [\text{ArX}] + k_2$

Having derived all possible rate expressions, it was necessary to compare them to the obtained kinetic data for oxidative addition in the presence of additional  $\text{PCy}_3$ . The pseudo first order plot of  $k_{\text{obs}}$  as a function of  $[\text{PhBr}]$  for oxidative addition in the presence of one equivalent of  $\text{PCy}_3$  was linear and lacked the y-intercept (Figure 67) that had been observed in the absence of  $\text{PCy}_3$  (Figure 64). The derived rate equation(s) that meet these requirements (linear plot of  $k_{\text{obs}}$  as a function of  $[\text{ArX}]$ , zero y-intercept for the same plot) were therefore possible expressions for the rate of formation of product. Given that experiments in the absence of  $\text{PCy}_3$  indicated that  $K_2$  involved a non-rapid equilibration relative to subsequent steps, rate equations derived with a similar non-rapid equilibration were considered the most reasonable in describing the experimental rate law (i.e. those in which attainment of  $K_2$  is slow, but the nature of  $K_1$  is varied). These “candidate” rate equations and related assumptions are summarized in Table 24. For each of these rate expressions, the nature of the y-intercept is described.

The rate expression described in entry 5 is not consistent with the observed pseudo first order plot, as it predicts a non-zero y-intercept at large values of  $[\text{ArX}]$ . Furthermore, the rate expressions based on the assumption of an unreactive  $\text{PdL}_3$  species (entries 1 and 3), as well as those that assume a reactive  $\text{PdL}_3$  (entries 2 and 4) both predict zero y-intercepts for a pseudo first order plot ( $k_{\text{obs}}$  as a function of  $[\text{PhBr}]$ ). The current kinetic data are thus insufficient and the rate law derivations inconclusive in determining the reactivity of  $\text{PdL}_3$  towards oxidative addition.

Table 24. Possible rate equations for oxidative addition of PhBr to Pd(PCy<sub>3</sub>)<sub>2</sub> in the presence of excess PCy<sub>3</sub>.

Entry	Pre-equilibrium Assumptions	Rate Law	y-intercept
1	K <sub>1</sub> rapid K <sub>2</sub> non-rapid k <sub>3</sub> = 0	$k_{\text{obs}} = \left( k_4 + \frac{k_2 k_5}{k_{-2}[\text{L}] + k_5[\text{ArX}]} \right) [\text{ArX}]$	zero
2	K <sub>1</sub> rapid K <sub>2</sub> non-rapid k <sub>3</sub> ≠ 0 k <sub>-2</sub> [L] > k <sub>5</sub> [ArX]	$k_{\text{obs}} = \left( \frac{k_3[\text{L}]}{K_1} + k_4 + \frac{k_2 k_5}{k_{-2}[\text{L}]} \right) [\text{ArX}]$	zero
3	K <sub>1</sub> non-rapid K <sub>2</sub> non-rapid k <sub>3</sub> = 0	$k_{\text{obs}} = \left( k_4 + \frac{k_2 k_5}{k_{-2}[\text{L}]} \right) [\text{ArX}]$	zero
4	K <sub>1</sub> non-rapid K <sub>2</sub> non-rapid k <sub>3</sub> ≠ 0 k <sub>1</sub> > k <sub>3</sub> [ArX]	$k_{\text{obs}} = \left( \frac{k_{-1} k_3 [\text{L}]}{k_1} + k_4 + \frac{k_2 k_5}{k_{-2}[\text{L}]} \right) [\text{ArX}]$	zero
5	K <sub>1</sub> non-rapid K <sub>2</sub> non-rapid k <sub>3</sub> ≠ 0 k <sub>1</sub> < k <sub>3</sub> [ArX]	$k_{\text{obs}} = \left( \frac{k_{-1}[\text{L}]}{[\text{ArX}]} + k_4 + \frac{k_2 k_5}{k_{-2}[\text{L}]} \right) [\text{ArX}]$	non-zero

The possibility of varying [L] under the current pseudo first order conditions (excess PhBr) was also considered as a means to gain insight into the mechanistic details of this system. In order to assess reactivity of PdL<sub>3</sub> in oxidative addition, one would have to distinguish between the rate expressions that assume an unreactive PdL<sub>3</sub> (k<sub>3</sub> = 0, entries 1 and 3) and those that do not (k<sub>3</sub> ≠ 0, entries 2 and 4). For small values of [L], the last term in each of the expressions assuming k<sub>3</sub> ≠ 0 (entries 2 and 4) is anticipated to be small, given that k<sub>-2</sub>[L] should be small, as phosphine coordination to PdL to reform PdL<sub>2</sub> is expected to be quite facile. With this last term being negligible, those expressions that assume k<sub>3</sub> ≠ 0 (entries 2 and 4) might be expected to

demonstrate a first order variation with [L], as a result of the first term of these rate expressions ( $k_3[L]/K_1$  and  $k_{-1}k_3[L]/k_1$  for entries 2 and 4 respectively). However, should  $\text{Pd}(\text{PCy}_3)_3$  be reactive, it is anticipated that the rate constant for its oxidative addition with PhBr ( $k_3$ ) is quite small, given the steric bulk of  $\text{PCy}_3$ . The first term of these expressions, which depends on  $k_3$  and  $K_1$  ( $K_1 = 0.3$ , see Section 2.5.1), may therefore also be negligible. As a result, these expressions may be indistinguishable from those that assume  $k_3 = 0$  (entries 1 and 3).

One might anticipate that this difficulty could be circumvented by utilizing larger [L] under pseudo first order conditions (excess PhBr). However, the interpretation of experiments conducted at large values of [L] would be complicated by the necessity to re-express all derived rate expressions in terms of  $[\text{Pd}]_{\text{T}}$  rather than  $[\text{PdL}_2]$ . This is because  $[\text{PdL}_3]$  is no longer negligible at large values of [L].

The described rate expressions were thus rewritten in terms of  $[\text{Pd}]_{\text{T}}$ , which was taken to be equal to the sum of  $[\text{PdL}_3]$  and  $[\text{PdL}_2]$  (see Appendix 1). Although mass balance considerations would require that one also include  $[\text{PdL}]$ , it was assumed that  $[\text{PdL}]$ , being a highly reactive  $12 e^-$  species, would never appreciably accumulate to significant levels. The new rate expressions, derived for large [L], are described in Table 25.

The rate equations thus obtained cannot be expressed linearly as a function of [L]. They are instead asymptotic functions, where  $k_{\text{obs}}$  would be expected to approach a particular value as the value of [L] was increased. In order to determine the reactivity of  $\text{PdL}_3$  for oxidative addition, one would need to

distinguish between the set of expressions derived assuming  $k_3 = 0$  (entries 1 and 3) and those that assume  $k_3 \neq 0$  (entries 2 and 4). Those expressions that assume  $\text{PdL}_3$  is a reactive participant in oxidative addition (entries 2 and 4) all possess an additional term independent of  $[\text{L}]$ , containing  $k_3$  (entry 2 has a  $k_3$  term, while entry 4 possesses a  $k_{-1}k_3K_1/(k_1 + k_3[\text{ArX}])$  term).

Table 25. Possible rate equations at large values of  $[\text{L}]$  for oxidative addition of PhBr to  $\text{Pd}(\text{PCy}_3)_2$  in the presence of excess  $\text{PCy}_3$ .

Entry	Pre-equilibrium Assumptions	Rate Law
1	$K_1$ rapid $K_2$ non-rapid $k_3 = 0$	$k_{\text{obs}} = \left( \frac{k_2k_5K_1}{(k_{-2}K_1 + k_5[\text{ArX}])[\text{L}] + k_{-2}[\text{L}]^2} \right) [\text{ArX}]$
2	$K_1$ rapid $K_2$ non-rapid $k_3 \neq 0$	$k_{\text{obs}} = \left( k_3 + \frac{k_2k_5K_1}{(k_{-2}K_1 + k_5[\text{ArX}])[\text{L}] + k_{-2}[\text{L}]^2} \right) [\text{ArX}]$
3	$K_1$ non-rapid $K_2$ non-rapid $k_3 = 0$	$k_{\text{obs}} = \left( \frac{k_4K_1}{[\text{L}]} + \frac{k_2k_5K_1}{(k_{-2}K_1 + k_5[\text{ArX}])[\text{L}] + k_{-2}[\text{L}]^2} \right) [\text{ArX}]$
4	$K_1$ non-rapid $K_2$ non-rapid $k_3 \neq 0$	$k_{\text{obs}} = \left( \frac{k_{-1}k_3K_1}{k_1 + k_3[\text{ArX}]} + \frac{k_4K_1}{[\text{L}]} + \frac{k_2k_5K_1}{(k_{-2}K_1 + k_5[\text{ArX}])[\text{L}] + k_{-2}[\text{L}]^2} \right) [\text{ArX}]$

The overall rate expressions would thus be expected to approach the value of this term at large values of  $[\text{L}]$ . One can contrast this behaviour with those expressions that assume an unreactive  $\text{PdL}_3$  species (entries 1 and 3), which approach zero at large values of  $[\text{L}]$ .

Although this discussion provides, in theory, a method with which one could distinguish between these two possible mechanistic scenarios ( $k_3 = 0$  or  $k_3 \neq 0$ ), in practice such an approach is probably doomed to failure. If  $\text{PdL}_3$  is in

fact a reactive species in these systems, one would expect that its reaction with PhBr would be relatively slow, given the large barrier to oxidative addition that would result from the steric bulk of three PCy<sub>3</sub> ligands surrounding the palladium(0) centre. One must therefore anticipate that the value of  $k_3$  would be very small compared to that observed for PdL<sub>2</sub> ( $k_4 = 0.0013$  L/mol·s in the absence of additional PCy<sub>3</sub>). In these instances, a plot of  $k_{\text{obs}}$  as a function of [L] might also appear to approach zero at large [L] and it seems unlikely that the value of the asymptote could be determined accurately. As a result, the two mechanistic scenarios described would not be distinguishable within the limits of experimental accuracy. Kinetic experiments of oxidative addition with large variable [L] were therefore deemed without merit and were not pursued. The current work was therefore unsuccessful in assessing the reactivity of Pd(PCy<sub>3</sub>)<sub>3</sub> in oxidative addition.

It seems reasonable to suspect, given the steric bulk surrounding Pd, that PdL<sub>3</sub> is in fact an unreactive species in oxidative addition. The formation of a tris species in the presence of additional PCy<sub>3</sub> would be expected to reduce the amounts of PdL<sub>2</sub> and PdL available for oxidative addition and subsequently inhibit the reaction and lower the rate of product formation. This is consistent with the slowed rate of formation of *trans*-Pd(PCy<sub>3</sub>)<sub>2</sub>(Ph)(Br) in the presence of PCy<sub>3</sub>, as seen in Figure 66. Such an explanation appears consistent with the experimentally obtained kinetic data as well as with the observed lack of reactivity of Pd(PPh<sub>3</sub>)<sub>3</sub>, a complex possessing less sterically hindered phosphines.<sup>6</sup> However, such a comparison should be tenuously made, as PPh<sub>3</sub>



is a poorer electron donor than PCy<sub>3</sub>, thus reducing the tendency of the metal towards oxidative addition.

### 3.7 Studies Initiated to Examine Transmetallation

As mentioned previously, the transmetallation step as it relates to Suzuki-Miyaura cross-coupling has been the subject of relatively limited study.<sup>55</sup> In response to this deficiency, several preliminary studies were initiated with the long-term goal of establishing a better understanding of the transmetallation process as it relates to Suzuki-Miyaura cross-coupling.

#### 3.7.1 Attempted GC study

In an effort to develop further methods to monitor transmetallation processes, work was initiated to establish a protocol suitable to observe transmetallation by gas chromatography. The organotrifluoroborate salt (K[PhBF<sub>3</sub>]) was selected as a coupling partner of interest, as it has recently received greater attention in the area of SM cross-coupling.<sup>56</sup> It was anticipated that K[PhBF<sub>3</sub>] could be combined with *trans*-Pd(PCy<sub>3</sub>)<sub>2</sub>(Ph)(Br) under a wide variety of reactions conditions, and subsequent products, likely biphenyl, analyzed to by GC analysis. However, several preliminary experiments were necessary in order to institute an effective protocol.

It was recognized that, at the high injector temperatures required to volatilize the reaction components, it was quite possible that *trans*-Pd(PCy<sub>3</sub>)<sub>2</sub>(Ph)(Br) itself would produce a certain amount of biphenyl under these

conditions. It was therefore decided to qualitatively assess the formation of biphenyl from samples of exclusively *trans*-Pd(PCy<sub>3</sub>)<sub>2</sub>(Ph)(Br). A sample containing 1.3 x 10<sup>-2</sup> M *trans*-Pd(PCy<sub>3</sub>)<sub>2</sub>(Ph)(Br) in toluene was introduced into the GC injection port at 300 °C, producing numerous species with a variety of retention times. Notably, biphenyl was observed to elute under the conditions of analysis at 4.56 minutes, established previously from a biphenyl sample of known concentration in toluene. Subsequent samples (2 - 4) containing K[PhBF<sub>3</sub>] were heated for different lengths of time, and results are summarized in Table 26.

Table 26. Summary of GC experiments in toluene (unless otherwise indicated).

Entry	Pd(PCy <sub>3</sub> ) <sub>2</sub> (Ph)(Br)	K[PhBF <sub>3</sub> ]	Conditions <sup>a</sup>	Area of biphenyl <sup>b</sup>
1	1.3 x 10 <sup>-2</sup> M	-	c	1
2	1.3 x 10 <sup>-2</sup> M	1.3 x 10 <sup>-2</sup> M	I. 10 min, 50 °C	1.1
			II. 19 hrs, 21 °C	1.0
3	1.3 x 10 <sup>-2</sup> M	1.2 x 10 <sup>-2</sup> M	I. 2 hrs, 80 °C	0
			II. 1hr, 80 °C	0
4 <sup>d</sup>	1.0 x 10 <sup>-2</sup> M	1.0 x 10 <sup>-2</sup> M	c	0.71

a) conditions described by I, II were applied consecutively on same sample

b) normalized area based on sample 1

c) injected immediately after preparation

d) performed in 5:1 toluene/THF

Despite the variation in reaction conditions, the obtained data did not provide any meaningful assessment of the amount of biphenyl produced. In fact, the data indicated that injection of exclusively *trans*-Pd(PCy<sub>3</sub>)<sub>2</sub>(Ph)(Br) produced an equal, or in one instance a greater quantity of biphenyl than samples also

containing K[PhBF<sub>3</sub>]. This method was therefore set aside in order to establish a method to monitor transmetallation by NMR spectroscopy.

### 3.7.2 Study and Attempted Preparation of [TOP][PhBF<sub>3</sub>]

Given the successful monitoring of oxidative addition by NMR spectroscopy, it was desirable to initiate similar studies involving transmetallation. Organotrifluoroborate salts (K[PhBF<sub>3</sub>]) were once again selected as convenient substrates meriting further study.<sup>56</sup>

With the eventual goal of simply and effectively monitoring transmetallation between *trans*-PdL<sub>2</sub>PhBr and organotrifluoroborates, it was desirable to obtain a borate salt whose cation possessed an easily monitored, NMR active nucleus. Furthermore, it was of interest to obtain a borate salt that possessed greater solubility in organic solvents. The preparation of tetraoctylphosphonium phenyltrifluoroborate, [TOP][PhBF<sub>3</sub>] was therefore chosen as a starting point from which to prepare a convenient substrate for NMR studies of transmetallation.

[TOP][PhBF<sub>3</sub>] has not been previously reported in the literature, although a variety of tetraalkylammonium salts of borate anions are known and have been prepared through counter ion exchange.<sup>57</sup> It was therefore decided to attempt a similar preparation of [TOP][PhBF<sub>3</sub>] using tetraoctylphosphonium bromide (TOPB) and K[PhBF<sub>3</sub>].

This cation exchange was first attempted in water and CH<sub>2</sub>Cl<sub>2</sub>, resulting in a biphasic solution that was allowed to stir at 25 °C for 1.5 hours. Extraction with

CH<sub>2</sub>Cl<sub>2</sub> produced a viscous, colourless oil with a <sup>31</sup>P resonance at δ 32.6, consistent with the presence of TOP<sup>+</sup>. A <sup>1</sup>H NMR spectrum of this oil suggested the presence of two phenyl containing species, indicated by additional peaks in the aromatic region (Figure 69).

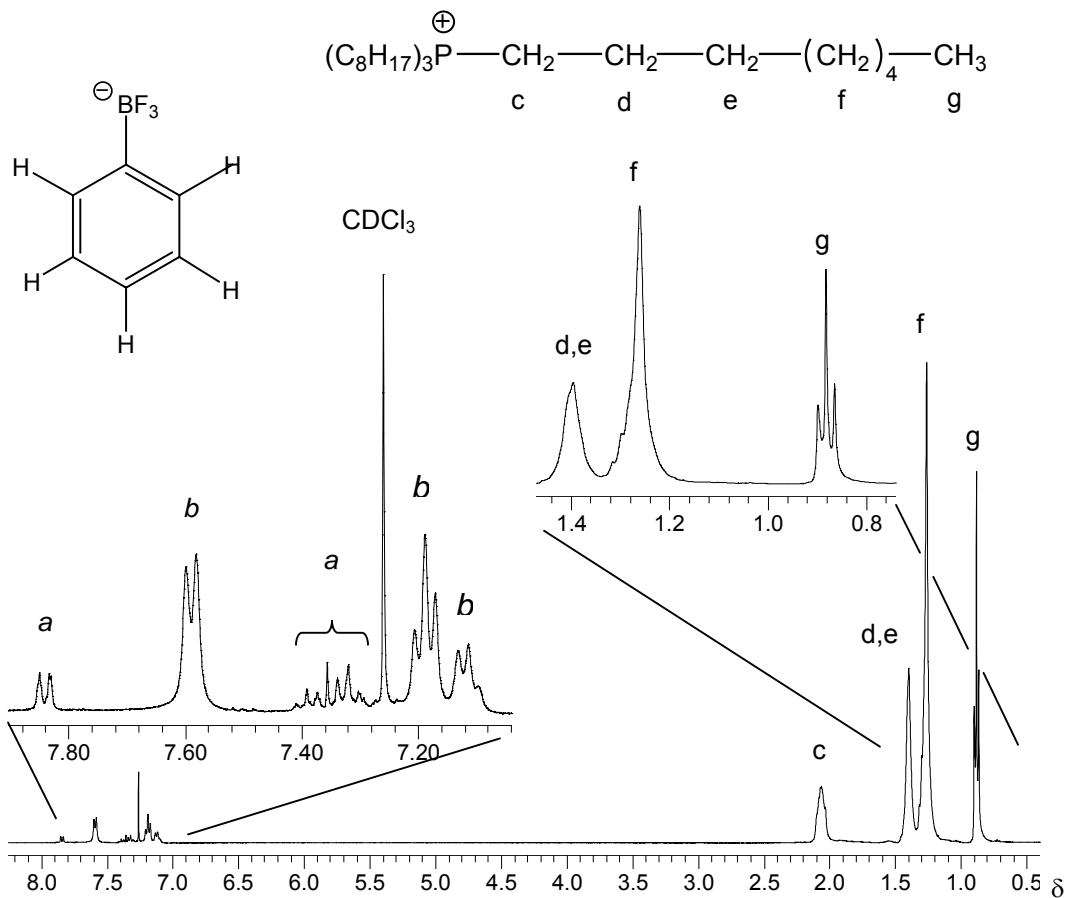


Figure 69. <sup>1</sup>H NMR spectrum (400 MHz) of colourless oil in CDCl<sub>3</sub> obtained as product in the attempted preparation of [TOP][PhBF<sub>3</sub>] (\* indicates unidentified phenyl resonances).

Furthermore, COSY experiments indicated that the resonances labeled *a* were correlated to each other, as were the resonances labeled *b*. Both these sets of resonances were inconsistent with those that have been reported for K[PhBF<sub>3</sub>] in

dmso-d<sub>6</sub> ( $\delta$  7.01, 3H,  $\delta$  7.30 2H)<sup>58</sup> or acetonitrile-d<sub>3</sub> ( $\delta$  7.22-7.05 3H,  $\delta$  7.44-7.41 2H).<sup>59</sup> Furthermore, a <sup>1</sup>H NMR spectrum of K[PhBF<sub>3</sub>] in D<sub>2</sub>O prior to the performed cation exchange showed resonances at  $\delta$  7.57 and 7.41-7.33, also inconsistent with the resonances observed here and those reported in the literature. These highly solvent dependent phenyl resonances therefore do not conclusively establish the presence of PhBF<sub>3</sub><sup>-</sup>. The accompanying <sup>11</sup>B NMR spectrum (referenced to BF<sub>3</sub>·H<sub>2</sub>O) showed two featureless resonances at  $\delta$  3.9 and  $\delta$  30.3. While the resonance observed at  $\delta$  3.9 was consistent with an aryl containing trifluoroborate salt ( $\delta$  1.7-5.0),<sup>57</sup> it lacked the characteristic 1:3:3:1 quartet pattern anticipated for boron.

It was thus hypothesized that the two sets of phenyl resonances in the <sup>1</sup>H NMR were the result of the hydrolysis of K[PhBF<sub>3</sub>], producing species of the type PhBF<sub>2</sub>(OH) or PhBF(OH)<sub>2</sub>, as discussed previously in the literature.<sup>56a,57,60</sup> Srebnik *et al.* indicates the partial hydrolysis (2-10%) of aryltrifluoroborates in D<sub>2</sub>O over 24 hours, determined by <sup>1</sup>H, <sup>11</sup>B and <sup>19</sup>F NMR.<sup>58</sup> Furthermore, in the context of Suzuki-Miyaura cross-coupling reactions, it has been noted that transmetallation is not possible with organotrifluoroborate salts in the absence of water, possibly because the actual species that undergo transmetallation are in fact PhBF<sub>2</sub>(OH) or PhBF(OH)<sub>2</sub>.<sup>57</sup>

With this possibility in mind, cation exchange was repeated anhydrously in dry methanol and the obtained viscous, colourless oil was dissolved in CDCl<sub>3</sub> and a <sup>1</sup>H NMR spectrum was obtained (Figure 70).

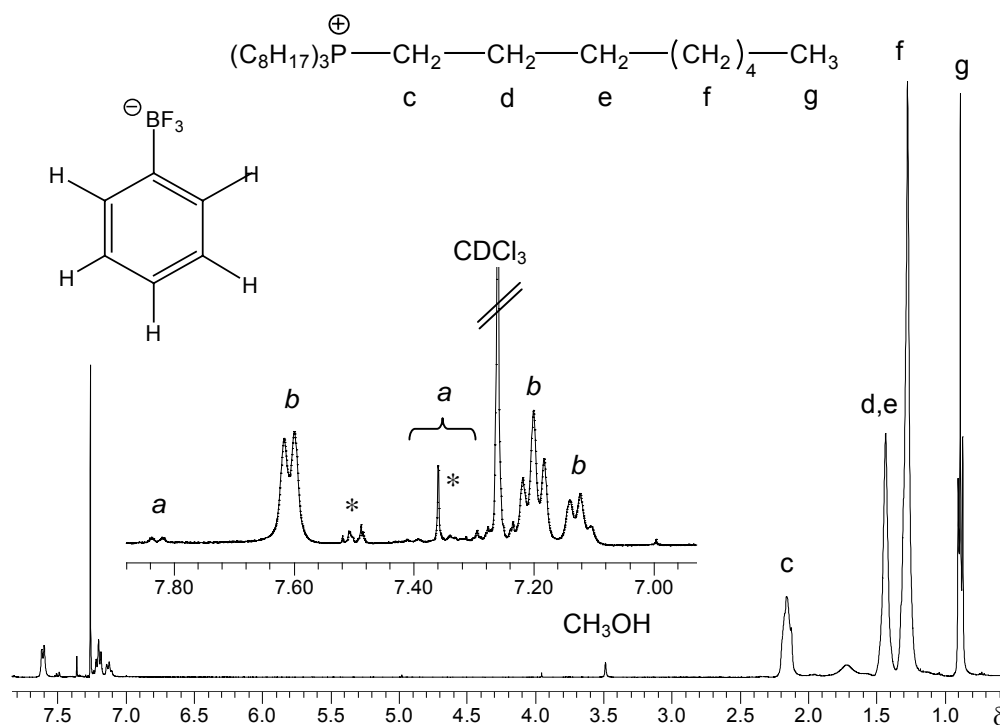


Figure 70.  $^1\text{H}$  NMR spectrum (400 MHz) in  $\text{CDCl}_3$  for attempted preparation of  $[\text{TOP}][\text{PhBF}_3]$  from anhydrous  $\text{MeOH}$  (\* indicates unidentified resonances).

Along with the peaks associated with  $\text{TOP}^+$ , the obtained  $^1\text{H}$  spectrum showed strong phenyl resonances labeled *b*, the same as those observed in Figure 67. The phenyl resonances (labeled *a*) that had been observed previously were significantly diminished when the exchange was performed anhydrously, which supports the presence of the hypothesized hydrolysis products of  $\text{PhBF}_3^-$  when performed in water. A corresponding  $^{11}\text{B}$  NMR spectrum showed only a broad resonance at  $\delta$  3.90, consistent with an aryltrifluoroborate anion.<sup>57</sup> It thus seems that cation exchange performed anhydrously favors the formation of a major phenyl containing species, possibly  $\text{PhBF}_3^-$ .

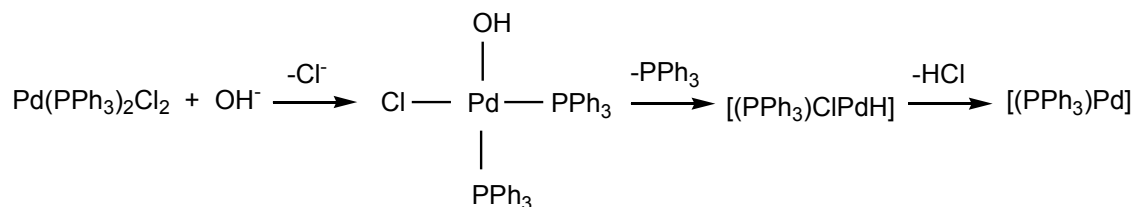
Should hydrolysis be occurring in these systems, it may or may not occur prior to cation exchange; while Batey *et al.* have noted instantaneous cation exchange with  $\text{K}[\text{ArBF}_3]$  and  $[\text{Bu}^n_4\text{N}][\text{OH}]$  ( $\text{CH}_2\text{Cl}_2/\text{H}_2\text{O}$ ),<sup>57</sup> Vedejs *et al.* have noted that effective cation between  $\text{K}[\text{o-C}_6\text{H}_4\text{BF}_3]$  and  $[\text{BnNMe}_3][\text{Br}]$  required 18 h using the same solvent system.<sup>59</sup> The currently described method for the preparation of  $[\text{TOP}][\text{PhBF}_3]$  is therefore ineffective, possibly complicated by hydrolysis of the associated anion.<sup>56a,57,60</sup>

Presumably, any meaningful future study of transmetallation involving  $[\text{TOP}][\text{PhBF}_3]$ , or any trifluoroborate salt, would require experiments performed in which both the absence and presence of water, and any resulting hydrolysis products characterized. Such a study therefore demands a method with which to obtain viable, pure  $[\text{TOP}][\text{PhBF}_3]$ , uncompromised by prior contamination.

### 3.8 Preparation and Reduction Experiments Involving $\text{PdL}_2\text{Cl}_2$

As was expressed earlier, reduction of Pd(II) precursors to form catalytically active Pd(0) species has remained a topic of minimal attention in the literature. While significant work by Amatore *et al.*<sup>46</sup> has addressed the nature of species resulting from the reduction of Pd(II) precursors, little has been done to determine what brings about such reduction in the greater context of an actual Suzuki-Miyaura reaction protocol. In such a protocol one must consider not only the nature of the Pd(II) precursor, but also other reaction variables. In this work, an assessment of the effect of the boron containing reagent  $(\text{PhB}(\text{OH})_2$  and  $\text{K}[\text{PhBF}_3])$  on reduction of  $\text{PdL}_2\text{Cl}_2$  ( $\text{L} = \text{Cy}_3, \text{PMeBu}^t_2$ ) was undertaken.

Grushin and Alper have reported the alkali-induced disproportionation of complexes of the type  $\text{PdL}_2\text{Cl}_2$  ( $\text{L} = \text{PCy}_3, \text{PPh}_3$ ) to produce  $\text{Pd}(0)$  species.<sup>61</sup> Extensive work revealed that  $\text{OH}^-$  can undergo ligand exchange with  $\text{Cl}^-$  in  $\text{Pd}(\text{PPh}_3)_2\text{Cl}_2$ , resulting in formation of  $\text{O}=\text{PPh}_3$ ,  $[\text{PdH}(\text{PPh}_3)\text{Cl}]$  and subsequently the presumed species  $[(\text{PPh}_3)\text{Pd}]$ , which then underwent oxidative addition with  $\text{PhI}$  (Scheme 44).



Scheme 44. Mechanism proposed for alkali induced reduction of  $\text{Pd}(\text{PPh}_3)_2\text{Cl}_2$ .<sup>61</sup>

Given that Suzuki-Miyaura cross-coupling is generally performed in the presence of aqueous base, such investigations are also pertinent to Suzuki-Miyaura reactions utilizing precatalysts of the type  $\text{PdL}_2\text{Cl}_2$ . An assessment of the effect of aqueous base ( $\text{K}_2\text{CO}_3$ ) on the reduction of  $\text{Pd}(\text{PCy}_3)_2\text{Cl}_2$  and  $\text{Pd}(\text{PMeBu}^t)_2\text{Cl}_2$  in the presence of  $\text{PhB}(\text{OH})_2$  was therefore undertaken in the current work. Similarly, the effect of added  $\text{K}[\text{PhBF}_3]$  was also considered.

### 3.8.1 Spectroscopic Characteristics of *trans*- $\text{Pd}(\text{PMeBu}^t)_2\text{Cl}_2$

The preparation and spectroscopic properties of  $\text{Pd}(\text{PCy}_3)_2\text{Cl}_2$  have been previously described in the literature.<sup>9</sup> However, for complexes where  $\text{L} = \text{PMeBu}^t$ , only the platinum analogue  $\text{Pt}(\text{PMeBu}^t)_2\text{Cl}_2$  has received significant



attention in the literature.<sup>43,62</sup> The spectroscopic characteristics of *trans*-Pd(PMeBu<sup>t</sup><sub>2</sub>)<sub>2</sub>Cl<sub>2</sub> are therefore described herein. This compound was isolated by the reaction of NaCl and PdCl<sub>2</sub> and PMeBu<sup>t</sup><sub>2</sub> for at room temperature in dry MeOH. A yellow crystalline solid was isolated by recrystallization (CH<sub>2</sub>Cl<sub>2</sub>/MeOH), and a <sup>31</sup>P NMR spectrum was obtained at 25 °C, revealing two <sup>31</sup>P resonances at δ 28.4 and 30.9 at 25 °C (Figure 71a). When heated to 77 °C, these resonances coalesce to produce a single broad resonance at δ 30.5 (Figure 71b). The spectral data suggest that at 25 °C, as seen for Pt[PMeBu<sup>t</sup><sub>2</sub>]Cl<sub>2</sub>,<sup>43,62</sup> the Pd complex is present as two conformational isomers undergoing slow exchange on the NMR timescale.

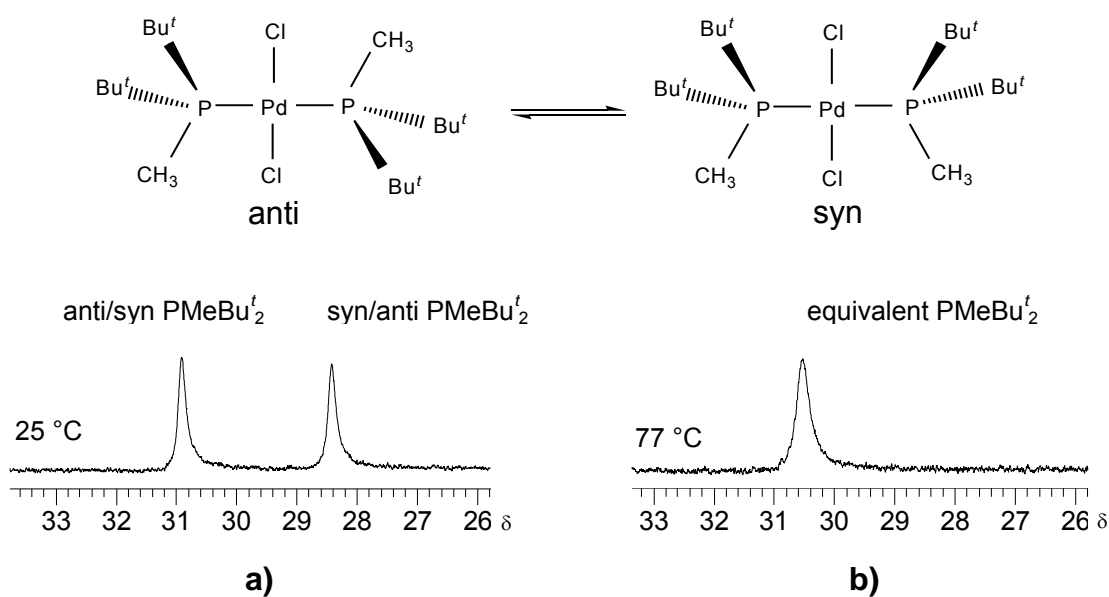


Figure 71. a) <sup>31</sup>P NMR spectra (163.0 MHz) of Pd(PMeBu<sup>t</sup><sub>2</sub>)Cl<sub>2</sub> in TCE-d<sub>2</sub> at 25 °C and b) at 77 °C.

Evidence for conformational exchange was also seen in the  $^{13}\text{C}$  NMR spectra. At 25 °C, two broad resonances were observed at  $\delta$  2.4 and 3.6, corresponding to the inequivalent P-CH<sub>3</sub> groups (Figure 72). At 77 °C, these resonances coalesce and show the anticipated virtual triplet pattern associated with *trans*-Pd(PMeBu<sup>t</sup><sub>2</sub>)Cl<sub>2</sub> (Figure 73). These rotational conformers presumably result from the restricted rotation within the phosphine, as a result of the steric bulk provided by the *trans* chlorines. Of note, in this work equilibrating conformational isomers of this type were absent in samples of Pd(PMeBu<sup>t</sup><sub>2</sub>)<sub>2</sub>.

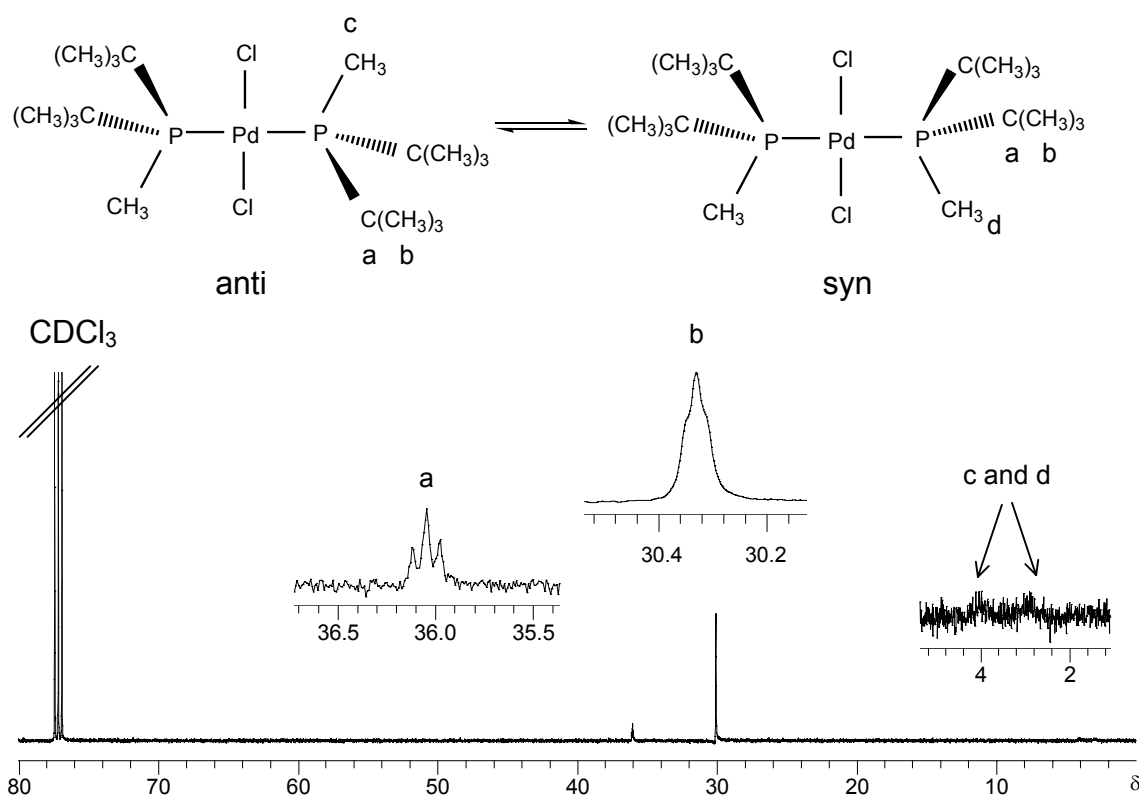


Figure 72.  $^{13}\text{C}$  NMR spectrum (125.7 MHz) of Pd(PMeBu<sup>t</sup><sub>2</sub>)Cl<sub>2</sub> in CDCl<sub>3</sub> at 25 °C.

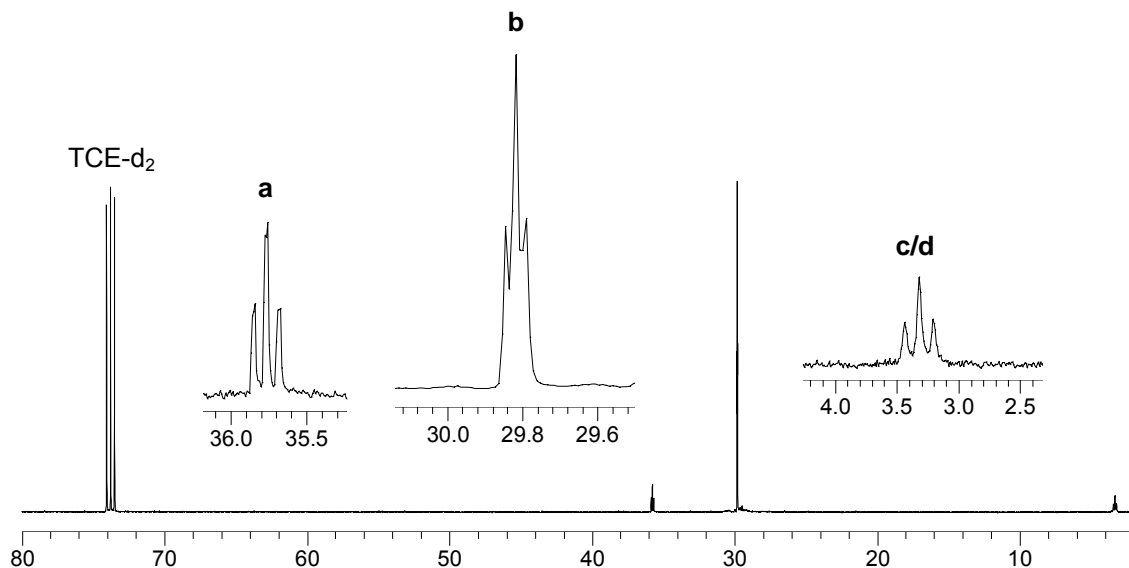


Figure 73.  $^{13}\text{C}$  NMR spectrum (100.6 MHz) of  $\text{Pd}(\text{PMeBu}^t_2)\text{Cl}_2$  ( $\text{TCE-d}_2$  at  $77\text{ }^\circ\text{C}$ ).

### 3.8.2 Reduction Experiments Involving $\text{PdL}_2\text{Cl}_2$ ( $\text{L} = \text{PCy}_3, \text{PMeBu}^t_2$ )

Multiple experiments were performed in order to ascertain the conditions under which  $\text{PdL}_2\text{Cl}_2$  ( $\text{L} = \text{PCy}_3, \text{PMeBu}^t_2$ ) is reduced to  $\text{Pd}(0)$ . The temperature of the reaction was varied (from  $21\text{ }^\circ\text{C}$  to  $80\text{ }^\circ\text{C}$ ), as well as the solvent system (toluene, 5:1 toluene/ $\text{H}_2\text{O}$ , DMF, 5:1 DMF/ $\text{H}_2\text{O}$ ). Two equivalents of either  $\text{K}[\text{PhBF}_3]$  or  $\text{PhB}(\text{OH})_2/\text{K}_2\text{CO}_3$  (1:1) were used as the boron containing substrate. After a reaction was complete, the solvent was removed and the residue was dissolved in  $\text{C}_6\text{D}_6$  and  $^{31}\text{P}$  NMR spectra were obtained at  $25\text{ }^\circ\text{C}$ . A summary of these experiments is shown in Table 27 and Table 28.

Table 27. Summary of reduction experiments with PdCl<sub>2</sub>[PCy<sub>3</sub>]<sub>2</sub>.

Entry	Reagent	Solvent	Temp/°C	Time/ h	PdL <sub>2</sub> <sup>a</sup>	Pd black <sup>b</sup>
1	K[PhBF <sub>3</sub> ]	toluene	21	24	none	none
2	K[PhBF <sub>3</sub> ]	toluene/H <sub>2</sub> O	21	18	none	none
3	K[PhBF <sub>3</sub> ]	toluene	65	18	none	none
4	K[PhBF <sub>3</sub> ]	toluene/H <sub>2</sub> O	65	18	none	none
5	K[PhBF <sub>3</sub> ]	DMF	21	23.5	none	none
6	K[PhBF <sub>3</sub> ]	DMF/H <sub>2</sub> O	21	18	none	none
7	K[PhBF <sub>3</sub> ]	DMF	65	24	none	none
8	K[PhBF <sub>3</sub> ]	DMF/H <sub>2</sub> O	65	24	none	none

a) determined by <sup>31</sup>P NMR (Pd[PCy<sub>3</sub>]<sub>2</sub> at δ 39)

b) determined visually

Table 28. Summary of reduction experiments with PdCl<sub>2</sub>[PMeBu<sup>t</sup>]<sub>2</sub>.

Entry	Reagent	Solvent	Base	Temp /°C	Time /h	PdL <sub>2</sub> <sup>a</sup>	Pd black <sup>b</sup>
1	K[PhBF <sub>3</sub> ]	toluene	-	21	22	-	-
2	K[PhBF <sub>3</sub> ]	toluene/H <sub>2</sub> O	-	21	22	-	-
3	K[PhBF <sub>3</sub> ]	toluene	-	80	18	-	-
4	K[PhBF <sub>3</sub> ]	toluene/H <sub>2</sub> O	-	80	24	-	Yes
5	PhB(OH) <sub>2</sub>	toluene	K <sub>2</sub> CO <sub>3</sub>	21	24	-	-
6	PhB(OH) <sub>2</sub>	toluene/H <sub>2</sub> O	K <sub>2</sub> CO <sub>3</sub>	21	24	-	-
7	PhB(OH) <sub>2</sub>	toluene	K <sub>2</sub> CO <sub>3</sub>	80	18	-	-
8	PhB(OH) <sub>2</sub>	toluene/H <sub>2</sub> O	K <sub>2</sub> CO <sub>3</sub>	80	16.5	Yes	Yes
9	-	toluene/H <sub>2</sub> O	-	80	4	-	-
10	-	toluene/H <sub>2</sub> O	K <sub>2</sub> CO <sub>3</sub>	80	20	-	Yes
11 <sup>c</sup>	-	toluene/H <sub>2</sub> O	K <sub>2</sub> CO <sub>3</sub>	80	23	Yes	Yes

a) determined by <sup>31</sup>P NMR Pd[MeBu<sup>t</sup>]<sub>2</sub> at δ 42

b) determined visually

c) 4 eq. K<sub>2</sub>CO<sub>3</sub> used

None of the conditions tested with Pd(PCy<sub>3</sub>)<sub>2</sub>Cl<sub>2</sub> produced any evidence of Pd(PCy<sub>3</sub>)<sub>2</sub> or Pd(0) black, indicating that solvent variation, as well as the presence or absence of water, did not bring about reduction of Pd(PCy<sub>3</sub>)<sub>2</sub>Cl<sub>2</sub>. In addition, heating to 65 °C produced no visible evidence for Pd(0) black or Pd(PCy<sub>3</sub>)<sub>2</sub>. However, it is possible that 65 °C was insufficient to bring about reduction, given that reactions with Pd(MeBu<sup>t</sup>)<sub>2</sub>Cl<sub>2</sub> produced Pd(0) at 80 °C (see below).

A  $^{31}\text{P}$  NMR spectrum (entry 8, Table 28) showed that  $\text{Pd}(\text{PMeBu}^t_2)_2\text{Cl}_2$  ( $\delta$  27.8, 30.1) produced  $\text{Pd}(\text{PMeBu}^t_2)_2$  ( $\delta$  41.7) in the presence of  $\text{PhB}(\text{OH})_2$ ,  $\text{K}_2\text{CO}_3$  in toluene/ $\text{H}_2\text{O}$  at  $80^\circ\text{C}$  (Figure 74).

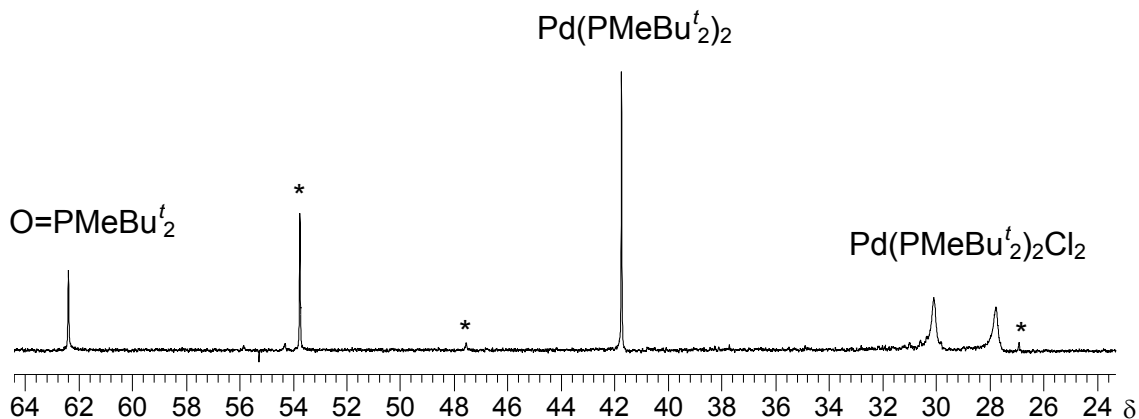


Figure 74.  $^{31}\text{P}$  NMR spectrum (242.9 MHz) of the attempted reduction of  $\text{Pd}(\text{MeBu}^t_2)_2\text{Cl}_2$  in the presence of  $\text{PhB}(\text{OH})_2$ , toluene,  $\text{H}_2\text{O}$  and  $\text{K}_2\text{CO}_3$ , heated to  $80^\circ\text{C}$  prior to acquisition (\* unidentified resonances).

Two significant  $^{31}\text{P}$  resonances ( $\delta$  62.4, 53.7) were observed that could not be assigned with certainty. One can compare these resonances to that observed for partial oxidation of a sample of  $\text{PMeBu}^t_2$  in toluene- $d_8$  ( $\delta$  61.7) (Section 2.4.1.6). The resonance at  $\delta$  62.4 corresponds fairly well to that observed in oxidized  $\text{PMeBu}^t_2$  ( $\delta$  61.7), and both are similar to literature reports for  $\text{O}=\text{PMeBu}^t_2$  ( $\delta$  60.0 in  $\text{CCl}_4$ ).<sup>63</sup> The presence of phosphine oxide is consistent with the observations made by Grushin and Alper for the reduction other  $\text{PdL}_2\text{Cl}_2$  complexes in alkali solutions.<sup>61</sup>

When the reaction was repeated without  $\text{PhB}(\text{OH})_2$  (entry 10), deposition of  $\text{Pd}(0)$  was observed without the formation of  $\text{Pd}(\text{PMeBu}^t_2)_2$  (Figure 75a). However, when the number of equivalents of  $\text{K}_2\text{CO}_3$  were doubled (4 eq. instead

of 2 eq.), Pd(PMeBu<sup>t</sup><sub>2</sub>)<sub>2</sub> was observed (δ 41.7) (Figure 75b). However, numerous resonances appear in both spectra, implying the presence of several phosphorus containing species that remain unidentified.

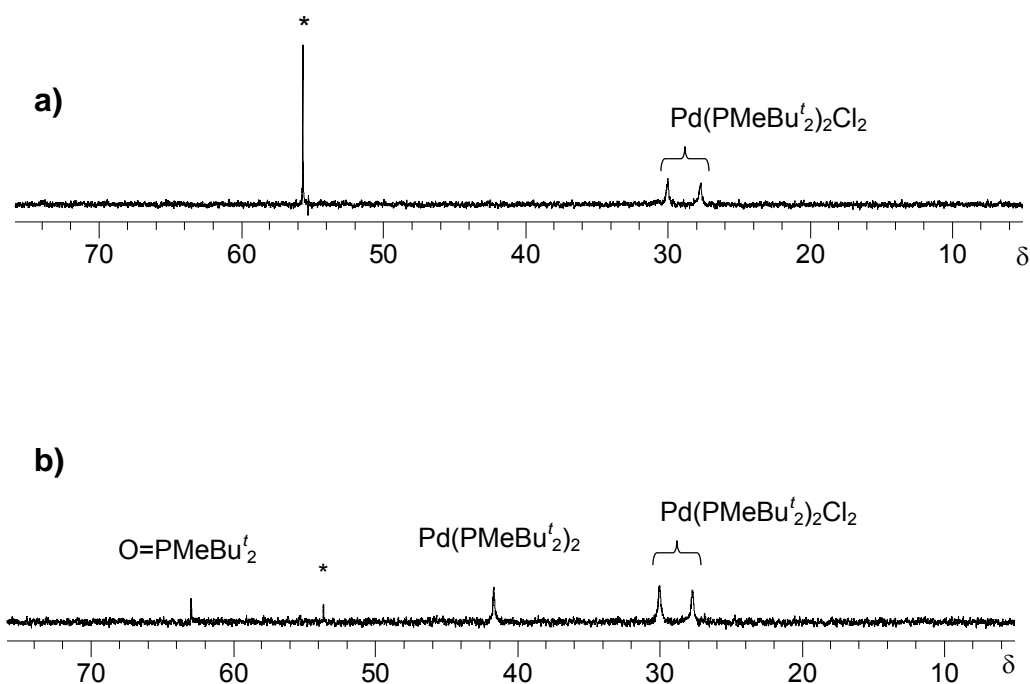


Figure 75. a) <sup>31</sup>P NMR spectrum (242.9 MHz) of the attempted reduction of Pd(PMeBu<sup>t</sup><sub>2</sub>)<sub>2</sub>Cl<sub>2</sub> in the presence of toluene, H<sub>2</sub>O and K<sub>2</sub>CO<sub>3</sub> (2 eq.) b) in the presence of toluene, H<sub>2</sub>O and K<sub>2</sub>CO<sub>3</sub> (4 eq.) heated to 80 °C prior to acquisition (\* indicates unidentified resonances).

The results indicate that the reduction Pd(PMeBu<sup>t</sup><sub>2</sub>)<sub>2</sub>Cl<sub>2</sub> is possible in both the presence (entry 8) and absence of PhB(OH)<sub>2</sub>, provided additional base is used (entry 11). Interestingly, Pd(PMeBu<sup>t</sup><sub>2</sub>)<sub>2</sub> was observed when PhB(OH)<sub>2</sub>/K<sub>2</sub>CO<sub>3</sub> was used (entry 8), while only Pd(0) black was observed with K[PhBF<sub>3</sub>] (entry 4).

This is a particularly significant result to in the context of Suzuki-Miyaura cross-coupling, since it implies that the nature of the boron reagent can have an impact on the Pd(0) species generated in solution. Furthermore, under the

conditions applied in a typical SM reaction, the boron reagent is used in stoichiometric quantities and is therefore in significant excess compared to the catalytic amounts of Pd(II) present. Under these conditions it is thus reasonable to anticipate that full reduction of  $\text{Pd}(\text{PMeBu}^t_2)_2\text{Cl}_2$  is possible.

A possible mechanism for  $\text{Pd}(\text{PMeBu}^t_2)_2$  formation could involve the formation of a hydroxyl complex, as was proposed by Grushin and Alper.<sup>61</sup> However, one could also envision successive transfer of a phenyl group from  $\text{PhB}(\text{OH})_3^-$  (produced in solution from  $\text{PhB}(\text{OH})_2$ ,  $\text{H}_2\text{O}$  and  $\text{K}_2\text{CO}_3$ ) to  $\text{Pd}(\text{PMeBu}^t_2)_2\text{Cl}_2$ , eventually yielding biphenyl and  $\text{Pd}(\text{PMeBu}^t_2)_2$  by means of reductive elimination. An in depth *in situ* NMR study of reduction in these systems may provide more mechanistic details, as current results are insufficient in elucidating the mechanism of reduction.

In a entirely different context, experiments were performed in an attempt to prepare  $\text{Pd}(\text{PBu}^t_3)_2\text{Br}_2$  by reacting  $\text{Pd}(\text{COD})\text{Br}_2$  with  $\text{PBu}^t_3$  at 21 °C. Attempts to isolate  $\text{Pd}(\text{PBu}^t_3)_2\text{Br}_2$  were unsuccessful, and produced solutions containing Pd black and a variety of  $^{31}\text{P}$  containing species, including  $\text{Pd}(\text{PBu}^t_3)_2$  ( $\delta$  85.3) (Figure 76).

In the context of the abovementioned reduction experiments, this result is quite significant. While reduction was not observed for  $\text{Pd}(\text{PCy}_3)_2\text{Cl}_2$ ,  $\text{Pd}(\text{PMeBu}^t_2)_2\text{Cl}_2$  produced  $\text{Pd}(\text{PMeBu}^t_2)_2$  when heated to 80 °C. In contrast, reactions with  $\text{Pd}(\text{COD})\text{Br}_2$  with  $\text{PBu}^t_3$  produced  $\text{Pd}(\text{PBu}^t_3)_2$ , even when cooled to (5 °C). This result serves to emphasize the wide variation in terms of the ease and conditions of reduction of Pd(II) complexes.

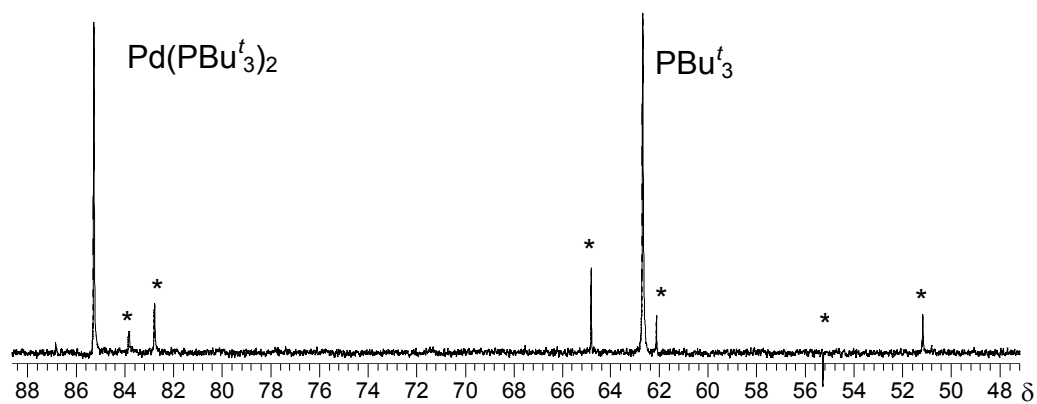


Figure 76.  $^{31}\text{P}$  NMR spectrum (242.9 MHz,  $\text{CD}_2\text{Cl}_2$ ) of residue of the reaction of  $\text{Pd}(\text{COD})\text{Br}_2$  and two eq.  $\text{PBu}^t_3$  at  $5^\circ\text{C}$  for 1 h.



### 3.9 References

1. (a) Yoshida, T.; Otsuka, S. *Inorg. Synth.* **1990**, *28*, 113. (b) Yoshida, T.; Otsuka, S. *Inorg. Synth.* **1979**, *19*, 101. (c) Matsumoto, M.; Yoshioka, H.; Nakatsu, K.; Yoshida, T.; Otsuka, S. *J. Am. Chem. Soc.* **1974**, *96*, 3322. (d) Otsuka, S.; Yoshida, T.; Matsumoto, M.; Nakatsu, K. *J. Am. Chem. Soc.* **1976**, *98*, 5850.
2. (a) Werner, H.; Kühn, A.; Tune, D. *J. Chem. Ber.* **1977**, *110*, 1763. (b) Kühn, A.; Werner, H. *J. Organomet. Chem.* **1979**, *179*, 421. (c) Werner, H.; Kühn, A.; Burschka, C. *Chem. Ber.* **1980**, *113*, 2291. (d) Werner, H. *Angew. Chem. Int. Ed.* **1977**, *16*, 1 (e) Werner, H. *Adv. Organomet. Chem.* **1981**, *19*, 155. (f) Werner, H.; Tune, D.; Parker, G.; Krüger, C.; Brauer, D. *J. Angew. Chem. Int. Ed.* **1975**, *14*, 185. (g) Parker, G.; Werner, H. *Helv. Chim. Act.* **1973**, *56*, 2819. (h) Werner, H.; Kühn, A. *Angew. Chem. Int. Ed.* **1979**, *18*, 416. (i) Harder, V.; Werner, H. *Helv. Chim. Act.* **1973**, *56*, 549. (j) Werner, H. Kuhn, A. *Angew. Chem. Int. Ed.* **1977**, *16*, 412.
3. Hughes, R.P.; Powell, J. *J. Am. Chem. Soc.* **1972**, *94*, 7723.
4. Mann, B. E.; Musco, A. *J. C. S. Dalton*, **1975**, 1673.
5. Pflüger, F.; Amatore, C. *Organometallics* **1990**, *9*, 2276.
6. Fauvarque, J-F.; Pflüger, F.; Troupel, M. *J. Organomet. Chem.* **1981**, *208*, 419.

7. Silverstein, R. M.; Webster, F. X.; Kiemle, D. J. *Spectrometric Identification of Organic Compounds*. 7<sup>th</sup> Ed. John Wiley and Sons, New York, **2005**.
8. Advanced Chemistry Development ACD/H NMR Predictor Version 4.5 for Windows.
9. Grushin, V. V.; Benismon, C.; Alper, H. *Inorg. Chem.* **1994**, *33*, 4804.
10. Van Gaal, H. L. M.; Van den Bekerom, F. L. A. *J. Organomet. Chem.* **1977**, *134*, 237.
11. Kirchoff, J. H.; Netherton, M. R.; Hills, I. D.; Fu, G. C. *J. Am. Chem. Soc.* **2002**, *124*, 13662.
12. Wang, K.; Goldman, M. E.; Emge, T. J.; Goldman, A. S. *J. Organomet. Chem.* **1996**, *518*, 55.
13. Dai, C.; Fu, G. C. *J. Am. Chem. Soc.* **2001**, *123*, 2719.
14. a) Netherton, M. R.; Fu, G. C. *Angew. Chem. Int. Ed.* **2002**, *41*, 3910. b) Hills, I. D.; Netherton, M. R.; Fu, G. C. *Angew. Chem. Int. Ed.* **2003**, *42*, 5749.
15. Kuran, W.; Musco, A. *Inorg. Chim. Acta*, **1975**, *12*, 187.
16. Paul, F.; Patt, J.; Hartwig, J. F. *Organometallics* **1995**, *14*, 3030.
17. Goel, R. G.; Montemayor, R. G. *Inorg. Chem.* **1977**, *16*, 2183.
18. Tolman, C. A. *Chem. Rev.* **1977**, *77*, 313.
19. Musco, A.; Kuran, W.; Silvani, A.; Anker, M. W. *J.C.S. Chem. Comm.* **1973**, 938.
20. Coulson, D.R. *Inorg. Synth.* **1971**, *13*, 121.

21. Urata, H.; Suzuki, H.; Moro-oka, Y.; Ikawa, T. *J. Organomet. Chem.* **1989**, *364*, 235.
22. Adrianov, V.G; Akhrem, I.S.; Chistovalova, N.M.; Struchkov, T.Y. *Zh. Strukt. Chem.*, **1976**, *17*, 135.
23. Tolman, C.A.; Seidel, W.C.; Gerlach, D.H. *J. Am. Chem. Soc.* **1972**, *94*, 2669.
24. Sergienko, V.S.; Porai-Koshits, M.A.; *Zh. Strukt. Khim.* **1987**, *28*, 103.
25. Amatore, C.; Jutand, A.; Khalil, F.; M'Barki, M.A.; Mottier, L. *Organometallics*, **1993**, *12*, 3168.
26. a) Negishi, E.; Takahashi, T.; Akiyoshi, K. *J. Chem. Soc., Chem. Comm.* **1986**, 1338. b) Enders, M.; Kohl, G.; Pritzkow, H. *J. Organomet. Chem.* **2001**, *622*, 66. c) Huttenloch, M. E.; Dielbold, J.; Rief, U.; Brintzinger, H. H.; Gilbert, A. M.; Katz, T. *J. Organometallics*, **1992**, *11*, 3600. d) Röder, J. C.; Meyer, F.; Winter, R. F.; Kaifer, E. *J. Organomet. Chem.* **2002**, *641*, 113. e) Köcher, S.; Van Klink, G. P. M.; Van Koten, G.; Lang, H. *J. Organomet. Chem.* **2003**, *684*, 230.
27. Mann, B. E. *J. Chem. Soc. Perkin II*, **1972**, 30.
28. Potyen, M. C.; Rothwell, I. P. *J. Chem. Soc. Chem. Comm.* **1995**, 849-852.
29. Shaw, B. L. *Proc. Chem. Soc.* **1960**, 247.
30. Tatsuno, Y.; Yoshida, T.; Otsuka, S. *Inorg. Synth.* **1990**, **28**, 342.
31. Murrall, N. W.; Welch, A. J. *J. Organomet. Chem.* **1986**, *301*, 109.

32. Auburn, P. R.; Mackenzie, P. B.; Bosnich, B. *J. Am. Chem. Soc.* **1985**, *107*, 2033.
33. (a) Zhang, J.; Braustein, P.; Welter, R. *Inorg. Chem.* **2004**, *43*, 4172. (b) Numata, S.; Okawara, R.; Kurosawa, H. *Inorg. Chem.* **1977**, *16*, 1737. (c) Krause, J.; Goddard, R.; Mynott, R.; Pörscheke, R. *Organometallics* **2001**, *20*, 1992. (d) Rülke, R.E.; Kassjager, V. E.; Wehman, P.; Elsevier, C. J.; Van Leeuwen, P.W.N.M.; Vrieze, K.; Fraanje, J.; Goubitz, K.; Spek, A.L. *Organometallics* **1996**, *15*, 3022. (e) Braustein, P.; Naud, F.; Dedieu, A.; Rohmer, M.-M.; DeCian, A.; Rettig, S.J. *Organometallics*, **2001**, *20*, 2966.
34. Gubin, S. P.; Rubezhov, A.Z.; Winch, B. L.; Nesmeyanov, A.N. *Tet. Lett.* **1964**, 2881.
35. Takahashi, Y.; Akahori, H.; Sakai, S.; Ishii, Y. *Bull. Chem. Soc. Jpn.* **1971**, *44*, 2703.
36. Malet, R.; Moreno-Manas, M.; Pajuelo, F.; Parella, T.; Pleixtas, R. *Mag. Res. Chem.* **1997**, *35*, 227 and references therein.
37. Cotton, F. A.; Wilkinson, G.; Murillo, C. A.; Bochmann, M.; *Advanced Inorganic Chemistry*, 6<sup>th</sup> Ed. John Wiley and Sons, New York, 1999, 1065.
38. Christmann, U.; Vilar, R. *Angew. Chem. Int. Ed.* **2005**, *44*, 366, and references therein.
39. (a) Ahlquist, M.; Norrby, P. *Organometallics*, **2007**, *26*, 550. (b) Ahlquist, M.; Fristrup, P. Tanner, D.; Norrby, P. *Organometallics*, **2006**, *25*, 2066.

40. (a) Stambuli, J. P.; Buhl, M.; Hartwig, J. F. *J. Am. Chem. Soc.* **2002**, *124*, 9346. (b) Littke, A. F.; Fu, G. C. *Angew. Chem. Int. Ed.* **1998**, *37*, 3387. (c) Littke, A. F.; Dai, C.; Fu, G. C. *J. Am. Chem. Soc.* **2000**, *122*, 4020.
41. (a) Dias, P. B.; Minas de Piedade, M. E.; Simões, J. A. M. *Coord. Chem. Rev.* **1994**, *135/136*, 737. (b) Sen, A.; Chen, J.; Vetter, W. M.; Whittle, R. R. *J. Am. Chem. Soc.* **1987**, *109*, 148. (c) Immiri, A.; Musco, A.; Mann, B. E. *Inorg. Chim. Acta* **1977**, *21*, L37.
42. Bovey, F. A. *Nuclear Magnetic Resonance Spectroscopy*. Academic Press: New York and London, U.K., 1969.
43. (a) Luck, L. A.; Elcesser, W. L.; Hubbard, J. L.; Bushweller, C. H. *Magn. Res. Chem.* **1989**, *27*, 488. (b) Dimeglio, C. M.; Luck, L. A.; Rithner, C. D.; Rheingold, A. L.; Elcesser, W. L.; Hubbard, J. L.; Bushweller, C. H. *J. Phys. Chem.* **1990**, *94*, 6255.
44. Bowmaker, G. A.; Brown, C. L.; Hart, R. D.; Healy, P. C.; Rickard, C. E. F.; White, A. H. *J. Chem. Soc., Dalton Trans.* **1999**, 881.
45. a) Pregosin, P. S.; Kinz, R. W. In *NMR Basic Principles and Progress*; Diehl, P.; Fluck, E.; Kosfeld, R., Eds.; Springer-Verlag: New York, USA, 1979; Vol 16:  $^{31}\text{P}$  and  $^{13}\text{C}$  NMR of Transition Metal Phosphine Complexes, chap. B. (b) Harris, R. K. *Nuclear Magnetic Resonance Spectroscopy*, Pitman, London, 1983, chap. 8B.
46. Amatore, C.; Jutand, A. *Acc. Chem. Res.* **2000**, *33*, 314.
47. Stambuli, J. P.; Incarvito, C. D.; Bühl, M.; Hartwig, J. F. *J. Am. Chem. Soc.* **2004**, *126*, 1184.

48. Cárdenas, D. J. *Angew. Chem. Int. Ed.* **1999**, 38, 3018.
49. Green, M. L. H.; Munakata, H.; Saito, T. *J. Chem. Soc. A., Inorg. Phys. Theor.* **1971**, 469.
50. Littke, A.F.; Fu, G. C. *Angew. Chem. Int. Ed.* **2002**, 41, 4176.
51. GraphPad Software Prism Version 3.02
52. Galardon, E.; Ramdeehul, S.; Brown, J. M.; Cowley, A.; Hii, K. K.; Jutand, A. *Angew. Chem. Int. Ed.* **2002**, 41, 1760.
53. Hartwig, J.F.; Paul, F.; *J. Am. Chem. Soc.* **1995**, 117, 5373.
54. Barrios-Landeros, F.; Hartwig, J.F. *J. Am. Chem. Soc.* **2005**, 127, 6944.
55. Miyaura, N. *J. Organomet. Chem.* **2002**, 653, 54.
56. (a) Molander, G. A.; Ellis, N. *Acc. Chem. Res.* **2007**, 40, 275. (b) Stefani, H. A.; Cella, R.; Vieira, A. S. *Tetrahedron*, **2007**, 63, 3623.
57. Batey, R. A.; Quach, T. D. *Tet. Lett.* **2001**, 42, 9099.
58. Smoum, R.; Rubinstein, A.; Srebnik, M. *Org. Biomol. Chem.* **2005**, 3, 941.
59. Vedejs, E.; Fields, C.S. Hayashi, R.; Hitchcock, S. R.; Powell, D.R.; Schrimpf, M. R. *J. Am. Chem. Soc.* **1999**, 121, 2460.
60. Darses, S.; Genet, J. P. *Eur. J. Org. Chem.*, **2003**, 4313.
61. Grushin, V. V.; Alper, H. A. *Organometallics*, **1993**, 12, 1890.
62. Mann, B. E.; Shaw, B. L.; Slade, R. M. *J. Chem. Soc. A. Inorg. Phys. Chem.*, **1971**, 2976.
63. Ionkin, A. S.; Marshall, W. J.; Fish, B. M.; Schiffhauer, M. F.; Davidson, F. *J. Am. Chem. Soc.* **2007**, 129, 9210.

## Chapter 4

### Summary and Conclusions

It is without doubt that the large body of research regarding Pd-catalyzed cross coupling reactions, particularly the SM reaction, has shed greater light on the synthetic utility and mechanistic details of the process. However, the extent to which the supposed catalyst is formed from common precatalysts has not been well addressed in the literature and to date there has been little evidence that popular catalyst precursors do in fact produce the assumed active catalyst, namely bis-ligated Pd(0) complexes. It is therefore conceivable that the forcing conditions (high temperature, long reaction times) required by many cross-coupling protocols are a necessity due to rate limiting factor may be catalyst formation.

This work has attempted to address this issue by the development of an optimized method for forming the catalytic species under mild conditions. Research efforts succeeded in determining the optimum (i.e. minimum temperature, maximum time required) conditions under which the compounds PdL<sub>2</sub> (L = PCy<sub>3</sub>, PMeBu<sup>t</sup><sub>2</sub>, PBu<sup>t</sup><sub>3</sub>) are generated cleanly and essentially quantitatively by Pd(η<sup>3</sup>-C<sub>3</sub>H<sub>5</sub>)(η<sup>5</sup>-C<sub>5</sub>H<sub>5</sub>), based on a method previously reported in the literature by Otuska *et al.*<sup>1</sup> Although reactions of Pd(η<sup>3</sup>-C<sub>3</sub>H<sub>5</sub>)(η<sup>5</sup>-C<sub>5</sub>H<sub>5</sub>) with two equivalents each of PCy<sub>3</sub>, PMeBu<sup>t</sup><sub>2</sub> or PBu<sup>t</sup><sub>3</sub> are slow at room temperature and produce η<sup>1</sup>-allyl and dinuclear intermediates in the cases of PCy<sub>3</sub> and PMeBu<sup>t</sup><sub>2</sub>, reactions of all three ligands at 77 °C proceed cleanly and at very

useful rates to give  $\text{Pd}(\text{PCy}_3)_2$  and  $\text{Pd}(\text{PMeBu}^t_2)_2$  within 1 h, while  $\text{Pd}(\text{PBu}^t_3)_2$  reacts within 30 min. While application of this methodology to syntheses of analogous Pd(0) compounds of other phosphines would ideally be preceded by a brief  $^{31}\text{P}$  NMR spectroscopic assessment similar to those described above, the known lability of  $\text{Pd}(\eta^3\text{-C}_3\text{H}_5)(\eta^5\text{-C}_5\text{H}_5)_2$  suggests that 1 h at 77 °C will normally suffice. The procedure outlined here appears to provide the only reliable method available to date for generating known concentrations of  $\text{PdL}_2$  quickly, reliably and under mild conditions.

A similar assessment was performed utilizing  $\text{Pd}(\eta^3\text{-1-Ph-C}_3\text{H}_4)(\eta^5\text{-C}_5\text{H}_5)$ , which was found to be a more conveniently prepared and handled precursor to  $\text{PdL}_2$  than  $\text{Pd}(\eta^3\text{-C}_3\text{H}_5)(\eta^5\text{-C}_5\text{H}_5)$ .  $^{31}\text{P}$  NMR studies revealed the existence of stable  $\eta^1$ -allyl species  $\text{Pd}(\eta^1\text{-CH}_2\text{CH=CHPh})(\eta^5\text{-C}_5\text{H}_5)\text{L}$  (L =  $\text{PCy}_3$ ,  $\text{PMeBu}^t_2$ ,  $\text{PPh}_3$ ) at 25 °C. However, at 77 °C  $\text{PdL}_2$  is generated quickly from  $\text{Pd}(\eta^3\text{-1-Ph-C}_3\text{H}_4)(\eta^5\text{-C}_5\text{H}_5)$  within minutes (12 minutes after mixing for  $\text{PCy}_3$ ).  $\text{Pd}(\eta^3\text{-1-Ph-C}_3\text{H}_4)(\eta^5\text{-C}_5\text{H}_5)$  thus demonstrates significantly increased reactivity towards ligand displacement relative to  $\text{Pd}(\eta^3\text{-C}_3\text{H}_5)(\eta^5\text{-C}_5\text{H}_5)$ .

The solution stoichiometry of compounds of the type  $\text{PdL}_{1,2,3}$ , was also successfully assessed. The conditions under which 3:1 compounds  $\text{PdL}_3$  may be in equilibrium with the 2:1 species  $\text{PdL}_2$  were also defined, as well as the thermodynamic parameters for dissociation of  $\text{PdL}_3$  when L =  $\text{PCy}_3$ . Interestingly, and consistent with its greater steric bulk,  $\text{Pd}(\text{PBu}^t_3)_2$  is not inclined to increase its coordination number, its  $^{31}\text{P}$  NMR resonance being completely unaffected by added  $\text{PCy}_3$ ,  $\text{PMeBu}^t_2$  or  $\text{PBu}^t_3$ . In contrast, the  $^{31}\text{P}$  NMR resonances of



$\text{Pd}(\text{PCy}_3)_2$  and  $\text{Pd}(\text{PMeBu}^t_2)_2$  are both broadened significantly by added  $\text{PCy}_3$  or  $\text{PMeBu}^t_2$  and both ligands form 3:1 coordination compounds. The homoleptic compounds  $\text{Pd}(\text{PCy}_3)_3$  and  $\text{Pd}(\text{PMeBu}^t_2)_3$  appear to be the dominant species in the presence of excess phosphines at low temperatures. Further confirming the existence of tris substituted complexes, the heteroleptic compounds  $\text{Pd}(\text{PCy}_3)_2(\text{PMeBu}^t_2)$  and  $\text{Pd}(\text{PCy}_3)(\text{PMeBu}^t_2)_2$  have been shown to exist at low temperature.

Equilibrium constants for dissociation of the compounds  $\text{PdL}_3$  to  $\text{PdL}_2$  and free L (L =  $\text{PCy}_3$ ,  $\text{PMeBu}^t_2$ ) were measured over a range of temperatures and  $\Delta\text{H}$  and  $\Delta\text{S}$  values of  $21 \text{ kJ mol}^{-1}$  and  $59 \text{ J deg}^{-1} \text{ mol}^{-1}$  respectively were found for the  $\text{PCy}_3$  system, while values of  $23 \text{ kJ mol}^{-1}$  and  $86 \text{ J deg}^{-1} \text{ mol}^{-1}$  respectively were found for  $\text{PMeBu}^t_2$ . The enthalpy values are to a first approximation a measure of the Pd-P bond dissociation energies. These Pd(0)-phosphine bond energies are lower than those reported previously for a Pd(II)- $\text{PPh}_3$  bond ( $54 \text{ kJ mol}^{-1}$ )<sup>3a</sup> and a Pt(0)- $\text{PCy}_3$  bond ( $55 \text{ kJ mol}^{-1}$ ).<sup>3b</sup>

The formation of the 3:1 compounds has serious implications for catalysis involving  $\text{PdL}_2$  catalysts. As outlined in the introduction, such catalysts are most often presumed to be generated via reductions of palladium(II) precursors in processes which are largely of an unknown nature, proceeding at unknown rates and resulting in unknown yields. Relative catalytic activities are often deduced on the basis of yields of cross-coupling products and then rationalized on the basis of steric and/or electronic properties of the phosphines used. This research was initiated with the notion that relative catalytic activities may rather reflect the

relative rates of reduction of palladium(II), but now it must be realized also that reactivities may vary because of differing degrees to which the initially very small amounts of generated palladium(0) species may be present as tris-phosphine compounds rather than the generally assumed bis-phosphine species.

The proportion of palladium(0) present at 25 °C as  $\text{PdL}_3$  if the  $\text{PCy}_3$ :Pd ratio lies in the range 100:1 to 1000:1, as would be expected the early stages of a cross-coupling reaction involving Pd(II) precatalysts, Thus the fraction of the total added palladium present as the tris complex in catalytic solutions can be quite significant. The relative tendency of a particular phosphine to form the more highly coordinated, presumably much less reactive species, may be a determining factor on the overall efficiency of a cross-coupling process, one which should be considered during the optimization of a catalytic cross-coupling protocol.

A successful study of the kinetics of oxidative addition PhBr to of  $\text{Pd}(\text{PCy}_3)_2$  was also performed. It was found that oxidative addition is first order in  $\text{Pd}(\text{PCy}_3)_2$  and that added bromide, as the toluene soluble tetraoctylphosphonium salt, had no effect on the rate of oxidative addition. A linear plot of  $k_{\text{obs}}$  as a function of  $[\text{PhBr}]$  under pseudo first order conditions possessed a y-intercept, suggesting the existence of two distinct pathways for oxidative addition of PhBr to  $\text{Pd}(\text{PCy}_3)_2$ . While  $\text{Pd}(\text{PCy}_3)_2$  adds directly to PhBr to form *trans*- $\text{Pd}(\text{PCy}_3)_2(\text{Ph})(\text{Br})$ , the kinetic data also support a concurrent pathway in which dissociation of  $\text{PCy}_3$  from  $\text{Pd}(\text{PCy}_3)_2$  produces the monophosphine complex  $\text{Pd}(\text{PCy}_3)$ , which subsequently adds to PhBr. Added  $\text{PCy}_3$  was found to

inhibit oxidative addition, possibly by converting some of the available Pd(0) to the kinetically inactive (or less active) 3:1 compound. Although the reactivity of PdL<sub>3</sub> towards oxidative addition could not be confirmed with the current kinetic data, the observed inhibition of oxidative addition is significant. If the presence of one equivalent of free phosphine relative to PdL<sub>2</sub> is sufficient to inhibit the rate of oxidative addition, one might anticipate that this effect would be much more significant if, as might be expected in the context of a catalytic protocol where [L] is large. The obtained kinetic results thus serve to highlight the necessity of considering the potential role of PdL<sub>3</sub> in a given catalytic protocol. Future research to assess the reactivity (or lack therefore) of PdL<sub>3</sub> (L = PCy<sub>3</sub>) towards oxidative addition would thus be invaluable in further elucidating the role of PdL<sub>3</sub> in the context of catalysis.

Having shown that the presumed active catalyst species PdL<sub>2</sub> can in fact be generated in under milder conditions, research efforts were then directed towards assessing the conditions under which PdL<sub>2</sub>Cl<sub>2</sub> (L = PCy<sub>3</sub>, PMeBu<sup>t</sup><sub>2</sub>) is reduced to Pd(0). While reduction was not observed for Pd(PCy<sub>3</sub>)<sub>2</sub>Cl<sub>2</sub>, Pd(PMeBu<sup>t</sup><sub>2</sub>)<sub>2</sub>Cl<sub>2</sub> produced Pd(PMeBu<sup>t</sup><sub>2</sub>)<sub>2</sub> when heated to 80 °C. In contrast, reactions with Pd(COD)Br<sub>2</sub> with PBu<sup>t</sup><sub>3</sub> produced Pd(PBu<sup>t</sup><sub>3</sub>)<sub>2</sub>, even when cooled to 5 °C. The obtained results thus highlight the great difference in terms of the ease and reaction conditions required for the reduction of Pd(II) complexes. A thorough, future NMR study of reduction in these systems may provide a more in depth understanding of the mechanistic details surrounding reduction to Pd(0).

## 4.1 References

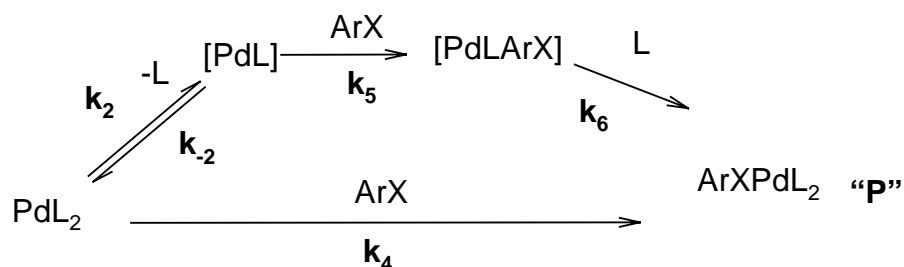
1. Tatsuno, Y.; Yoshida, T.; Otsuka, S. *Inorg. Synth.* **1990**, *28*, 342.
2. a) Liang, C.; Xia, W.; Soltani-Ahamdi, H.; Schlüter, O.; Fischer, R.; Muhler, M. *Chem. Comm.* **2005**, 282. b) Niklewski, A.; Strunskus, T.; Witte, G.; Wöll, C.; *Chem. Mater.* **2005**, *17*, 861. c) Xia, W.; Schlüter, O.; Liang, C.; Van den Berg, M. W. E.; Guraya, M.; Muhler, M. *Catal. Today* **2005**, *102-103*, 34.
3. a) Sen, A.; Chen, J.; Vetter, W. M.; Whittle, R. R. *J. Am. Chem. Soc.* **1987**, *109*, 148. b) Immiri, A.; Musco, A.; Mann, B. E.; *Inorg. Chim. Acta* **1977**, *21*, L37.

## Appendix 1

### A.1 Rate Law Derivations

The following describes the rate law derivations for the oxidative addition reaction of ArX with PdL<sub>2</sub> (L = PCy<sub>3</sub>). The derivations were first completed for oxidative addition in the absence of added L and were subsequently performed for oxidative addition in the presence of additional L. In each instance, a mechanistic scheme describing all relevant intermediates is shown.

#### A.1.1 Derivation of Rate Expressions for the Oxidative Addition of ArX to PdL<sub>2</sub> in the Absence of Excess Phosphine



Scheme 45. Mechanistic pathways proposed for rate law derivation for the oxidative addition of ArX to PdL<sub>2</sub> in the absence of additional L.

The mechanistic pathways for oxidative addition were proposed (Scheme 45) and the derivation of rate expressions was performed first assuming a rapid pre-equilibrium for K<sub>2</sub>. This was followed by derivations which assumed that K<sub>2</sub> is comparable in rate to the other pathways (i.e. non-rapid). The obtained rate

expressions were then simplified based on assumptions regarding the reactivity of each of the product forming pathways ( $k_4$  and  $k_5$ )

#### A.1.1.1 Rate Expressions Assuming Rapid $K_2$

The rate of product formation, P, can be expressed as follows:

$$\frac{d[P]}{dt} = k_4[ArX][PdL_2] + k_6[PdLArX][L]$$

The  $[PdLArX]$  term, an intermediate, can be replaced using the steady state approximation:

$$\frac{d[PdLArX]}{dt} = k_5[ArX][PdL] - k_6[PdLArX][L] = 0$$

$$k_5[ArX][PdL] = k_6[PdLArX][L]$$

$$\frac{d[P]}{dt} = k_4[ArX][PdL_2] + k_5[ArX][PdL]$$

The  $[PdL]$  term can then be replaced by using the equilibrium expression for  $K_2$ :

$$\frac{d[P]}{dt} = k_4[ArX][PdL_2] + \frac{k_5K_2[ArX][PdL_2]}{[L]} \quad \text{since } K_2 = \frac{[PdL][L]}{[PdL_2]}$$

Factoring yields an expression for  $k_{obs}$ :

$$\frac{d[P]}{dt} = k_4[ArX][PdL_2] + \frac{k_5K_2[ArX][PdL_2]}{[L]}$$

$$\frac{d[P]}{dt} = \left( k_4 + \frac{k_5K_2}{[L]} \right) [ArX][PdL_2]$$

Since  $\frac{d[P]}{dt} = k_{obs}[PdL_2]$  under pseudo first order conditions,

$$k_{\text{obs}} = \left( k_4 + \frac{k_5 K_2}{[L]} \right) [\text{ArX}]$$

Several simplifications can then be made to the rate expression, assuming the reactive nature of the involved species:

**a) If PdL<sub>2</sub> is unreactive (k<sub>4</sub> = 0)**

The k<sub>4</sub> term is thus negligible and the rate expression can be re-written:

$$k_{\text{obs}} = \left( k_4 + \frac{k_5 K_2}{[L]} \right) [\text{ArX}] \text{ thus simplifies to } k_{\text{obs}} = \frac{k_5 K_2 [\text{ArX}]}{[L]}$$

This rate expression predicts first order dependence on [ArX] and inverse in [L].

**b) If PdL is unreactive (k<sub>5</sub> = 0)**

$$k_{\text{obs}} = \left( k_4 + \frac{k_5 K_2}{[L]} \right) [\text{ArX}] \text{ simplifies to } k_{\text{obs}} = k_4 [\text{ArX}]$$

This predicts first order dependence on [ArX] and zero order in [L].

**c) If both PdL<sub>2</sub> and PdL are reactive (k<sub>4</sub>, k<sub>5</sub> > 0)**

The rate expression remains unchanged:

$$k_{\text{obs}} = \left( k_4 + \frac{k_5 K_2}{[L]} \right) [\text{ArX}]$$

This rate expression predicts first order dependence on [ArX] and the dependence on [L] would vary from 0 to -1.

**A.1.1.2 Rate Expressions Assuming Non-rapid K<sub>2</sub>**

$$\frac{d[\text{P}]}{dt} = k_4 [\text{ArX}][\text{PdL}_2] + k_6 [\text{PdLArX}][\text{L}]$$

Using the steady state approximation:

$$\frac{d[\text{PdLArX}]}{dt} = k_5[\text{ArX}][\text{PdL}] - k_6[\text{PdLArX}][\text{L}] = 0$$

$$k_5[\text{ArX}][\text{PdL}] = k_6[\text{PdLArX}][\text{L}]$$

Substituting into the expression for product formation:

$$\frac{d[\text{P}]}{dt} = k_4[\text{ArX}][\text{PdL}_2] + k_5[\text{ArX}][\text{PdL}]$$

The steady state approximation must be used to express [PdL]:

$$\frac{d[\text{PdL}]}{dt} = k_2[\text{PdL}_2] - k_{-2}[\text{PdL}][\text{L}] - k_5[\text{PdL}][\text{ArX}] = 0$$

$$[\text{PdL}] = \frac{k_2[\text{PdL}_2]}{k_{-2}[\text{L}] + k_5[\text{ArX}]}$$

Again substituting into the expression for product formation:

$$\frac{d[\text{P}]}{dt} = k_4[\text{ArX}][\text{PdL}_2] + \frac{k_2k_5[\text{ArX}][\text{PdL}_2]}{k_{-2}[\text{L}] + k_5[\text{ArX}]}$$

The expression can then be written in terms of  $k_{\text{obs}}$ :

$$k_{\text{obs}} = k_4[\text{ArX}] + \frac{k_2k_5[\text{ArX}]}{k_{-2}[\text{L}] + k_5[\text{ArX}]}$$

As seen above, several simplifications can then be made, assuming the reactive nature of the involved species:

**a) If PdL<sub>2</sub> is unreactive ( $k_4 = 0$ )**

$$k_{\text{obs}} = k_4[\text{ArX}] + \frac{k_2k_5[\text{ArX}]}{k_{-2}[\text{L}] + k_5[\text{ArX}]} \quad \text{becomes} \quad k_{\text{obs}} = \frac{k_2k_5[\text{ArX}]}{k_{-2}[\text{L}] + k_5[\text{ArX}]}$$

Further simplifications can then be made:

*i.* If  $k_{-2}[\text{L}] \gg k_5[\text{ArX}]$ , then:



$$k_{\text{obs}} = \frac{k_2 k_5 [\text{ArX}]}{k_{-2} [\text{L}]}$$

This expression predicts first order dependence on [ArX] and inverse order in [L].

ii. If  $k_{-2} [\text{L}] \ll k_5 [\text{ArX}]$ , then:

$$k_{\text{obs}} = \frac{k_2 k_5 [\text{ArX}]}{k_5 [\text{ArX}]} = k_2$$

This expression predicts zero order in both [ArX] and [L].

**b) If PdL is unreactive ( $k_5 = 0$ )**

$$k_{\text{obs}} = k_4 [\text{ArX}] + \frac{k_2 k_5 [\text{ArX}]}{k_{-2} [\text{L}] + k_5 [\text{ArX}]} \text{ becomes } k_{\text{obs}} = k_4 [\text{ArX}]$$

This expression is first order in [ArX] and zero order in [L].

**c) If both PdL<sub>2</sub> and PdL are reactive ( $k_4, k_5 > 0$ )**

i. If  $k_{-2} [\text{L}] \gg k_5 [\text{ArX}]$ , then:

$$k_{\text{obs}} = k_4 [\text{ArX}] + \frac{k_2 k_5 [\text{ArX}]}{k_{-2} [\text{L}] + k_5 [\text{ArX}]} \text{ simplifies to } k_{\text{obs}} = \left( k_4 + \frac{k_2 k_5}{k_{-2} [\text{L}]} \right) [\text{ArX}]$$

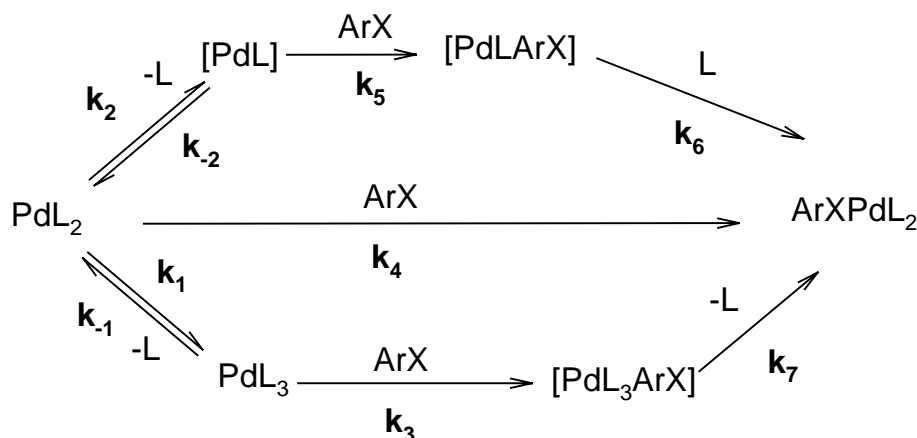
The expression is first order in [ArX] and varies from 0 to -1 for [L].

ii. If  $k_{-2} [\text{L}] \ll k_5 [\text{ArX}]$ , then:

$$k_{\text{obs}} = k_4 [\text{ArX}] + \frac{k_2 k_5 [\text{ArX}]}{k_{-2} [\text{L}] + k_5 [\text{ArX}]} \text{ simplifies to } k_{\text{obs}} = k_4 [\text{ArX}] + k_2$$

The expression is first order in [ArX] and zero order in [L].

**A.1.2 Derivation of Rate Expressions for the Oxidative Addition of ArX to PdL<sub>2</sub> in the Presence of L**

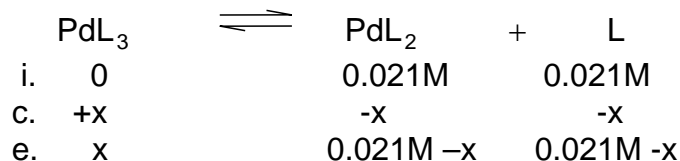


Scheme 46. Mechanistic pathways proposed for rate law derivation for the oxidative addition of ArX to PdL<sub>2</sub> in the presence of additional L.

As seen in Scheme 46, PdL<sub>3</sub> can form as a result of additional L. Four different pre-equilibrium assumptions will be considered in turn. If K<sub>2</sub> is a rapid pre-equilibrium, K<sub>1</sub> may or may not be a rapid equilibrium. Similarly, if K<sub>2</sub> is not a rapid equilibrium, K<sub>1</sub> may or may not be a rapid equilibrium.

In addition, one must determine the necessity of expressing the rate in terms of total Pd concentration, [Pd]<sub>T</sub>. This is because in adding L, [PdL<sub>2</sub>] may be affected by accumulation of PdL<sub>3</sub>. One can however assume that PdL does not accumulate as it is anticipated to be a highly reactive species. In the described oxidative addition experiments, [PdL<sub>2</sub>] = [L] = 0.021M, where L = PCy<sub>3</sub>. Furthermore, the K<sub>D</sub> value for PdL<sub>3</sub> (L= PCy<sub>3</sub>) has been approximated to be 0.3

(Section 2.5.1). One can therefore calculate  $[\text{PdL}_3]$  and determine the percentage of total palladium present bound as  $\text{PdL}_3$ :



$$K_D = \frac{(0.021\text{M} - x)^2}{x} = 0.3$$

$$x^2 - 0.342x + 0.000441 = 0$$

$$x = \frac{0.342 \pm \sqrt{(-0.342)^2 - 4(1)(0.000441)}}{2(1)}$$

$$x = 0.001295 \text{ M} \quad \text{or} \quad x = 0.68141 \text{ M}$$

$$\% \text{ of } [\text{Pd}]_T \text{ as } \text{PdL}_3 = \frac{[\text{PdL}_3]}{[\text{PdL}_2]_0} = \frac{0.001295 \text{ M}}{0.021\text{M}} \times 100\% = 6\%$$

Thus,  $[\text{PdL}_3]$  is 6 % of the initial  $[\text{PdL}_2]$  concentration and can be considered negligible. Rate laws may in this case be reasonably expressed as a function of  $[\text{PdL}_2]$  only.

#### A.1.2.1 Rate Expressions for Rapid $K_2$ and $K_1$

Assuming that the steps producing the desired product P are irreversible, the rate of formation of product is as follows:

$$\frac{d[\text{P}]}{dt} = k_3[\text{PdL}_3][\text{ArX}] + k_4[\text{ArX}][\text{PdL}_2] + k_6[\text{PdLArX}][\text{L}]$$

Using the steady state assumption:

$$\frac{d[\text{PdLArX}]}{dt} = k_5[\text{ArX}][\text{PdL}] - k_6[\text{PdLArX}][\text{L}] = 0$$

$$k_5[\text{ArX}][\text{PdL}] = k_6[\text{PdLArX}][\text{L}]$$

Substituting for [PdLArX]:

$$\frac{d[\text{P}]}{dt} = k_3[\text{PdL}_3][\text{ArX}] + k_4[\text{ArX}][\text{PdL}_2] + k_5[\text{ArX}][\text{PdL}]$$

Both expressions can then be used to substitute for [PdL<sub>3</sub>] and [PdL<sub>2</sub>]:

$$K_1 = \frac{[\text{PdL}_2][\text{L}]}{[\text{PdL}_3]} \quad K_2 = \frac{[\text{PdL}][\text{L}]}{[\text{PdL}_2]}$$

$$\frac{d[\text{P}]}{dt} = \frac{k_3[\text{PdL}_2][\text{L}][\text{ArX}]}{K_1} + k_4[\text{ArX}][\text{PdL}_2] + \frac{k_5K_2[\text{ArX}][\text{PdL}_2]}{[\text{L}]}$$

The rate expression can then be written in terms of  $k_{\text{obs}}$ :

$$k_{\text{obs}} = \frac{k_3[\text{L}][\text{ArX}]}{K_1} + k_4[\text{ArX}] + \frac{k_5K_2[\text{ArX}]}{[\text{L}]}$$

$$k_{\text{obs}} = \left( \frac{k_3[\text{L}]}{K_1} + k_4 + \frac{k_5K_2}{[\text{L}]} \right) [\text{ArX}]$$

This represents the rate law provided  $k_3$ ,  $k_4$  and  $k_5$  are all non-zero. It is reasonable to assume that  $k_4$  and  $k_5$  are non-zero, thus, we must therefore consider a only a scenario in which PdL<sub>3</sub> is unreactive (i.e.  $k_3 = 0$ ).

**a) If PdL, PdL<sub>2</sub> are reactive ( $k_4, k_5 > 0$ ) and PdL<sub>3</sub> is unreactive ( $k_3 = 0$ )**

$$k_{\text{obs}} = \left( \frac{k_3[\text{L}]}{K_1} + k_4 + \frac{k_5K_2}{[\text{L}]} \right) [\text{ArX}] \text{ simplifies to } k_{\text{obs}} = \left( k_4 + \frac{k_5K_2}{[\text{L}]} \right) [\text{ArX}]$$

In this case the rate expression would be first order in [ArX] and would vary from -1 to 0 in [L].

### A.1.2.2 Rate Expressions for Rapid $K_2$ and Non-rapid $K_1$

$$\frac{d[P]}{dt} = k_3[PdL_3][ArX] + k_4[ArX][PdL_2] + k_6[PdLArX][L]$$

Using the steady state approximation and substituting in for  $[PdLArX]$ :

$$\frac{d[PdLArX]}{dt} = k_5[ArX][PdL] - k_6[PdLArX][L] = 0$$

$$k_5[ArX][PdL] = k_6[PdLArX][L]$$

$$\frac{d[P]}{dt} = k_3[PdL_3][ArX] + k_4[ArX][PdL_2] + k_5[ArX][PdL]$$

One can then use the equilibrium expression for  $K_2$  to substitute for  $[PdL]$  and the steady state approximation to express  $[PdL_3]$ :

$$K_2 = \frac{[PdL][L]}{[PdL_2]} \quad \text{and} \quad \frac{d[PdL_3]}{dt} = k_{-1}[L][PdL_2] - k_3[PdL_3][ArX] - k_1[PdL_3] = 0$$

$$[PdL_3] = \frac{k_{-1}[PdL_2][L]}{k_1 + k_3[ArX]}$$

Substituting these terms into the expression for product formation gives:

$$\frac{d[P]}{dt} = \frac{k_3k_{-1}[PdL_2][L][ArX]}{k_1 + k_3[ArX]} + k_4[ArX][PdL_2] + \frac{k_5K_2[ArX][PdL_2]}{[L]}$$

The expression can then be written in terms of  $k_{obs}$ :

$$k_{obs} = \frac{k_3k_{-1}[L][ArX]}{k_1 + k_3[ArX]} + k_4[ArX] + \frac{k_5K_2[ArX]}{[L]}$$

$$k_{obs} = \left( \frac{k_3k_{-1}[L]}{k_1 + k_3[ArX]} + k_4 + \frac{k_5K_2}{[L]} \right) [ArX]$$

As described above, simplification can be made depending upon the reactivity of the involved species.

**a) If PdL and PdL<sub>2</sub> are reactive (k<sub>4</sub>, k<sub>5</sub> > 0) but PdL<sub>3</sub> is unreactive (k<sub>3</sub> = 0)**

$$k_{\text{obs}} = \left( \frac{k_3 k_{-1} [\text{L}]}{k_1 + k_3 [\text{ArX}]} + k_4 + \frac{k_5 K_2}{[\text{L}]} \right) [\text{ArX}] \text{ simplifies to } k_{\text{obs}} = \left( k_4 + \frac{k_5 K_2}{[\text{L}]} \right) [\text{ArX}]$$

**b) If PdL<sub>2</sub>, PdL and PdL<sub>3</sub> are reactive (k<sub>3</sub>, k<sub>4</sub>, k<sub>5</sub> ≠ 0), then:**

*i.* If  $k_1 > k_3 [\text{ArX}]$ , then:

$$k_{\text{obs}} = \left( \frac{k_3 k_{-1} [\text{L}]}{k_1 + k_3 [\text{ArX}]} + k_4 + \frac{k_5 K_2}{[\text{L}]} \right) [\text{ArX}] \text{ simplifies to}$$

$$k_{\text{obs}} = \left( \frac{k_3 k_{-1} [\text{L}]}{k_1} + k_4 + \frac{k_5 K_2}{[\text{L}]} \right) [\text{ArX}]$$

*ii.* If  $k_1 < k_3 [\text{ArX}]$ , then:

$$k_{\text{obs}} = \left( \frac{k_3 k_{-1} [\text{L}]}{k_1 + k_3 [\text{ArX}]} + k_4 + \frac{k_5 K_2}{[\text{L}]} \right) [\text{ArX}] \text{ simplifies to}$$

$$k_{\text{obs}} = \left( \frac{k_{-1} [\text{L}]}{[\text{ArX}]} + k_4 + \frac{k_5 K_2}{[\text{L}]} \right) [\text{ArX}]$$

### A.1.2.3 Rate Expressions for Non-rapid K<sub>2</sub> and Rapid K<sub>1</sub>

$$\frac{d[\text{P}]}{dt} = k_3 [\text{PdL}_3] [\text{ArX}] + k_4 [\text{ArX}] [\text{PdL}_2] + k_6 [\text{PdLArX}] [\text{L}]$$

From the steady state approximation:

$$\frac{d[\text{PdLArX}]}{dt} = k_5 [\text{ArX}] [\text{PdL}] - k_6 [\text{PdLArX}] [\text{L}] = 0$$

$$k_5[\text{ArX}][\text{PdL}] = k_6[\text{PdLArX}][\text{L}]$$

Substituting into the rate expression for product formation:

$$\frac{d[\text{P}]}{dt} = k_3[\text{PdL}_3][\text{ArX}] + k_4[\text{ArX}][\text{PdL}_2] + k_5[\text{ArX}][\text{PdL}]$$

The equilibrium expression for  $K_1$  can be used to substituted for  $[\text{PdL}_3]$ , while the steady state approximation must be used for  $[\text{PdL}]$ :

$$\frac{d[\text{PdL}]}{dt} = k_2[\text{PdL}_2] - k_{-2}[\text{PdL}][\text{L}] - k_5[\text{PdL}][\text{ArX}] = 0$$

$$[\text{PdL}] = \frac{k_2[\text{PdL}_2]}{k_{-2}[\text{L}] + k_5[\text{ArX}]}$$

$$K_1 = \frac{[\text{PdL}_2][\text{L}]}{[\text{PdL}_3]}$$

Making the required substitutions gives:

$$\frac{d[\text{P}]}{dt} = \frac{k_3[\text{PdL}_2][\text{L}][\text{ArX}]}{K_1} + k_4[\text{ArX}][\text{PdL}_2] + \frac{k_2k_5[\text{ArX}][\text{PdL}_2]}{k_{-2}[\text{L}] + k_5[\text{ArX}]}$$

The rate expression can then be written for  $k_{\text{obs}}$ :

$$k_{\text{obs}} = \frac{k_3[\text{L}][\text{ArX}]}{K_1} + k_4[\text{ArX}] + \frac{k_2k_5[\text{ArX}]}{k_{-2}[\text{L}] + k_5[\text{ArX}]}$$

$$k_{\text{obs}} = \left( \frac{k_3[\text{L}]}{K_1} + k_4 + \frac{k_2k_5}{k_{-2}[\text{L}] + k_5[\text{ArX}]} \right) [\text{ArX}]$$

**a) If PdL and PdL<sub>2</sub> are reactive ( $k_4, k_5 > 0$ ) but PdL<sub>3</sub> is unreactive ( $k_3 = 0$ )**

$k_{\text{obs}} = \left( \frac{k_3[\text{L}]}{K_1} + k_4 + \frac{k_2k_5}{k_{-2}[\text{L}] + k_5[\text{ArX}]} \right) [\text{ArX}]$  simplifies to the following expression:

$$k_{\text{obs}} = \left( k_4 + \frac{k_2 k_5}{k_{-2}[\text{L}] + k_5[\text{ArX}]} \right) [\text{ArX}]$$

which produces the same expressions derived above in Derivation 1.2 c:

*i.* If  $k_{-2}[\text{L}] \gg k_5[\text{ArX}]$ , then:

$$k_{\text{obs}} = \left( k_4 + \frac{k_2 k_5}{k_{-2}[\text{L}]} \right) [\text{ArX}]$$

*ii.* If  $k_{-2}[\text{L}] \ll k_5[\text{ArX}]$ , then:

$$k_{\text{obs}} = k_4[\text{ArX}] + k_2$$

**b) If PdL<sub>2</sub>, PdL and PdL<sub>3</sub> are reactive ( $k_3, k_4, k_5 \neq 0$ ):**

*i.* If  $k_{-2}[\text{L}] > k_5[\text{ArX}]$ , then:

$$k_{\text{obs}} = \left( \frac{k_3[\text{L}]}{K_1} + k_4 + \frac{k_2 k_5}{k_{-2}[\text{L}] + k_5[\text{ArX}]} \right) [\text{ArX}] \text{ simplifies to}$$

$$k_{\text{obs}} = \left( \frac{k_3[\text{L}]}{K_1} + k_4 + \frac{k_2 k_5}{k_{-2}[\text{L}]} \right) [\text{ArX}]$$

*ii.* If  $k_{-2}[\text{L}] < k_5[\text{ArX}]$ , then:

$$k_{\text{obs}} = \left( \frac{k_3[\text{L}]}{K_1} + k_4 + \frac{k_2 k_5}{k_{-2}[\text{L}] + k_5[\text{ArX}]} \right) [\text{ArX}] \text{ simplifies to}$$

$$k_{\text{obs}} = \left( \frac{k_3[\text{L}]}{K_1} + k_4 \right) [\text{ArX}] + k_2$$

#### A.1.2.4 Rate Expressions for Non-rapid K<sub>2</sub> and K<sub>1</sub>

$$\frac{d[\text{P}]}{dt} = k_3[\text{PdL}_3][\text{ArX}] + k_4[\text{ArX}][\text{PdL}_2] + k_6[\text{PdLArX}][\text{L}]$$

Using the steady state approximation for each species:



$$\frac{d[\text{PdLArX}]}{dt} = k_5[\text{ArX}][\text{PdL}] - k_6[\text{PdLArX}][\text{L}] = 0$$

$$\frac{d[\text{PdL}]}{dt} = k_2[\text{PdL}_2] - k_{-2}[\text{PdL}][\text{L}] - k_5[\text{PdL}][\text{ArX}] = 0$$

$$\frac{d[\text{PdL}_3]}{dt} = k_{-1}[\text{L}][\text{PdL}_2] - k_3[\text{PdL}_3][\text{ArX}] - k_1[\text{PdL}_3] = 0$$

Solving for  $[\text{PdLArX}]$ ,  $[\text{PdL}]$  and  $[\text{PdL}_3]$  respectively then allows one to substitute these into the rate expression:

$$\frac{d[\text{P}]}{dt} = \frac{k_{-1}k_3[\text{PdL}_2][\text{ArX}][\text{L}]}{k_1 + k_3[\text{ArX}]} + k_4[\text{ArX}][\text{PdL}_2] + \frac{k_2k_5[\text{PdL}_2][\text{ArX}]}{k_{-2}[\text{L}] + k_5[\text{ArX}]}$$

The expression can then be written in terms of  $k_{\text{obs}}$

$$k_{\text{obs}} = \frac{k_{-1}k_3[\text{ArX}][\text{L}]}{k_1 + k_3[\text{ArX}]} + k_4[\text{ArX}] + \frac{k_2k_5[\text{ArX}]}{k_{-2}[\text{L}] + k_5[\text{ArX}]}$$

$$k_{\text{obs}} = \left( \frac{k_{-1}k_3[\text{L}]}{k_1 + k_3[\text{ArX}]} + k_4 + \frac{k_2k_5}{k_{-2}[\text{L}] + k_5[\text{ArX}]} \right) [\text{ArX}]$$

**a) If PdL and PdL<sub>2</sub> are reactive ( $k_4, k_5 > 0$ ) but PdL<sub>3</sub> is unreactive ( $k_3 = 0$ )**

$$k_{\text{obs}} = \left( \frac{k_{-1}k_3[\text{L}]}{k_1 + k_3[\text{ArX}]} + k_4 + \frac{k_2k_5}{k_{-2}[\text{L}] + k_5[\text{ArX}]} \right) [\text{ArX}] \text{ then simplifies to}$$

$$k_{\text{obs}} = \left( k_4 + \frac{k_2k_5}{k_{-2}[\text{L}] + k_5[\text{ArX}]} \right) [\text{ArX}]$$

*i.* If  $k_{-2}[\text{L}] > k_5[\text{ArX}]$ , then:

$$k_{\text{obs}} = \left( k_4 + \frac{k_2k_5}{k_{-2}[\text{L}]} \right) [\text{ArX}]$$

*ii.* If  $k_{-2}[\text{L}] < k_5[\text{ArX}]$ , then:

$$k_{\text{obs}} = \left( k_4 + \frac{k_2}{[\text{ArX}]} \right) [\text{ArX}]$$

$$k_{\text{obs}} = k_4[\text{ArX}] + k_2$$

**b) If PdL<sub>2</sub>, PdL and PdL<sub>3</sub> are reactive (k<sub>3</sub>, k<sub>4</sub>, k<sub>5</sub> ≠ 0), then:**

$$k_{\text{obs}} = \left( \frac{k_{-1}k_3[\text{L}]}{k_1 + k_3[\text{ArX}]} + k_4 + \frac{k_2k_5}{k_{-2}[\text{L}] + k_5[\text{ArX}]} \right) [\text{ArX}]$$

*i.* If  $k_{-2}[\text{L}] < k_5[\text{ArX}]$ , then:

$$k_{\text{obs}} = \left( \frac{k_{-1}k_3[\text{L}]}{k_1 + k_3[\text{ArX}]} + k_4 + \frac{k_2}{[\text{ArX}]} \right) [\text{ArX}]$$

$$k_{\text{obs}} = \left( \frac{k_{-1}k_3[\text{L}]}{k_1 + k_3[\text{ArX}]} + k_4 \right) [\text{ArX}] + k_2$$

- If  $k_1 > k_3[\text{ArX}]$ , then:

$$k_{\text{obs}} = \left( \frac{k_{-1}k_3[\text{L}]}{k_1} + k_4 \right) [\text{ArX}] + k_2$$

- If  $k_1 < k_3[\text{ArX}]$ , then:

$$k_{\text{obs}} = \left( \frac{k_{-1}[\text{L}]}{k_3[\text{ArX}]} + k_4 \right) [\text{ArX}] + k_2$$

*ii.* If  $k_{-2}[\text{L}] > k_5[\text{ArX}]$ , then:

$$k_{\text{obs}} = \left( \frac{k_{-1}k_3[\text{L}]}{k_1 + k_3[\text{ArX}]} + k_4 + \frac{k_2k_5}{k_{-2}[\text{L}]} \right) [\text{ArX}]$$

- If  $k_1 > k_3[\text{ArX}]$ , then:

$$k_{\text{obs}} = \left( \frac{k_{-1}k_3[\text{L}]}{k_1} + k_4 + \frac{k_2k_5}{k_{-2}[\text{L}]} \right) [\text{ArX}]$$

- If  $k_1 < k_3[\text{ArX}]$ , then:

$$k_{\text{obs}} = \left( \frac{k_{-1}[\text{L}]}{[\text{ArX}]} + k_4 + \frac{k_2 k_5}{k_{-2}[\text{L}]} \right) [\text{ArX}]$$

### A.1.3 Rate Expression Derivations In Terms of $[\text{Pd}]_{\text{T}}$ for Large $[\text{L}]$

While Scheme 46 remains valid for large values of  $[\text{L}]$ , one must anticipate in this case the formation of sufficient  $\text{PdL}_3$  such that  $[\text{PdL}_2]$  is affected. Rate law derivations must therefore be expressed as a function of total  $\text{Pd}(0)$  concentration ( $[\text{Pd}]_{\text{T}}$ ) as follows:

$$[\text{Pd}]_{\text{T}} = [\text{PdL}_3] + [\text{PdL}_2] + [\text{PdL}]$$

It can be assumed in this system that  $[\text{PdL}]$  is negligible, as it quickly reacts to form product. Thus  $[\text{Pd}^0]_{\text{T}}$  becomes:

$$[\text{Pd}]_{\text{T}} = [\text{PdL}_3] + [\text{PdL}_2]$$

$$[\text{Pd}]_{\text{T}} - [\text{PdL}_3] = [\text{PdL}_2]$$

$$[\text{Pd}]_{\text{T}} - \frac{[\text{PdL}_2][\text{L}]}{K_1} = [\text{PdL}_2]$$

$$[\text{PdL}_2] = \frac{K_1 [\text{Pd}]_{\text{T}}}{K_1 + [\text{L}]}$$

This relationship now allows for the rate expressions to be expressed in terms of  $[\text{Pd}]_{\text{T}}$ . Of all of the above mentioned rate expressions, those that produced a zero y-intercept for a pseudo first order plot in the presence of additional L were

consistent with the observed kinetic data (see Table 24, Section 3.6.3). In the interest of determining the reactivity of PdL<sub>3</sub> (i.e. k<sub>3</sub> = 0 or > 0), only these expressions were then re-derived with [Pd]<sub>T</sub>, with the aim of assessing the possibility of distinguishing between them at large values of [L]. The assumptions made for each of these derivations are re-iterated below.

### A.1.3.1 Rate Expressions for Rapid K<sub>1</sub> and Non-rapid K<sub>2</sub> at Large [L]

From Derivation A.1.2.3:

$$\frac{d[P]}{dt} = \left( \frac{k_3[L]}{K_1} + k_4 + \frac{k_2k_5}{k_{-2}[L] + k_5[ArX]} \right) [ArX][PdL_2]$$

One can then substitute for [PdL<sub>2</sub>] using the expression written in terms of [Pd]<sub>T</sub>:

$$\frac{d[P]}{dt} = \left( \frac{k_3[L]}{K_1} + k_4 + \frac{k_2k_5}{k_{-2}[L] + k_5[ArX]} \right) \left( \frac{K_1[Pd]_T}{K_1 + [L]} \right)$$

$$\frac{d[P]}{dt} = \left( \frac{k_3[L]}{K_1 + [L]} + \frac{k_4K_1}{K_1 + [L]} + \frac{k_2k_5K_1}{k_{-2}K_1[L] + k_{-2}[L]^2 + k_5K_1[ArX] + k_5[ArX][L]} \right) [ArX][Pd]_T$$

Writing as in terms of k<sub>obs</sub> gives:

$$k_{obs} = \left( \frac{k_3[L] + k_4K_1}{K_1 + [L]} + \frac{k_2k_5K_1}{k_{-2}K_1[L] + k_{-2}[L]^2 + k_5K_1[ArX] + k_5[ArX][L]} \right) [ArX]$$

#### a) If PdL<sub>3</sub> is unreactive (k<sub>3</sub> = 0) and [L] is large:

The expression above can be simplified as follows for large [L]:

$$k_{obs} = \left( k_3 + \frac{k_2k_5K_1}{(k_{-2}K_1 + k_5[ArX])[L] + k_{-2}[L]^2} \right) [ArX]$$

Given that k<sub>3</sub> = 0, this reduces to:

$$k_{\text{obs}} = \left( \frac{k_2 k_5 K_1}{(k_{-2} K_1 + k_5 [\text{ArX}]) [\text{L}] + k_{-2} [\text{L}]^2} \right) [\text{ArX}]$$

**b) If PdL<sub>3</sub> is reactive (k<sub>3</sub> > 0) and [L] is large:**

This is the expression derived above in a):

$$k_{\text{obs}} = \left( k_3 + \frac{k_2 k_5 K_1}{(k_{-2} K_1 + k_5 [\text{ArX}]) [\text{L}] + k_{-2} [\text{L}]^2} \right) [\text{ArX}]$$

### A.1.3.2 Rate Expressions for Non-rapid K<sub>1</sub> and K<sub>2</sub> at Large [L]

From Derivation A.1.2.4:

$$\frac{d[\text{P}]}{dt} = \left( \frac{k_{-1} k_3 [\text{L}]}{k_1 + k_3 [\text{ArX}]} + k_4 + \frac{k_2 k_5}{k_{-2} [\text{L}] + k_5 [\text{ArX}]} \right) [\text{ArX}] [\text{PdL}_2]$$

One can then substitute for [PdL<sub>2</sub>] using the expression written in terms of [Pd]<sub>T</sub>:

$$\frac{d[\text{P}]}{dt} = \left( \frac{k_{-1} k_3 [\text{L}]}{k_1 + k_3 [\text{ArX}]} + k_4 + \frac{k_2 k_5}{k_{-2} [\text{L}] + k_5 [\text{ArX}]} \right) \left( \frac{K_1 [\text{Pd}]_{\text{T}}}{K_1 + [\text{L}]} \right)$$

$$\frac{d[\text{P}]}{dt} = \left( \frac{k_{-1} k_3 K_1 [\text{L}]}{k_1 K_1 + k_1 [\text{L}] + k_3 K_1 [\text{ArX}] + k_3 [\text{ArX}] [\text{L}]} + \frac{k_4 K_1}{K_1 + [\text{L}]} + \dots \right)$$

$$\left. \frac{k_2 k_5 K_1}{k_{-2} K_1 [\text{L}] + k_{-2} [\text{L}]^2 + k_1 k_5 [\text{ArX}] + k_5 [\text{ArX}] [\text{L}]} \right) [\text{ArX}] [\text{Pd}]_{\text{T}}$$

$$k_{\text{obs}} = \left( \frac{k_{-1} k_3 K_1 [\text{L}]}{k_1 K_1 + k_1 [\text{L}] + k_3 K_1 [\text{ArX}] + k_3 [\text{ArX}] [\text{L}]} + \frac{k_4 K_1}{K_1 + [\text{L}]} + \dots \right. \\ \left. \frac{k_2 k_5 K_1}{k_{-2} K_1 [\text{L}] + k_{-2} [\text{L}]^2 + k_1 k_5 [\text{ArX}] + k_5 [\text{ArX}] [\text{L}]} \right) [\text{ArX}]$$

a) If PdL<sub>3</sub> is unreactive (k<sub>3</sub> = 0) and [L] is large:

One can eliminate the term containing k<sub>3</sub>, since k<sub>3</sub> = 0. This becomes:

$$k_{\text{obs}} = \left( \frac{k_4 K_1}{K_1 + [L]} + \frac{k_2 k_5 K_1}{k_{-2} K_1 [L] + k_{-2} [L]^2 + k_1 k_5 [\text{ArX}] + k_5 [\text{ArX}] [L]} \right) [\text{ArX}]$$

Simplifying for large [L]:

$$k_{\text{obs}} = \left( \frac{k_4 K_1}{[L]} + \frac{k_2 k_5 K_1}{(k_{-2} K_1 + k_5 [\text{ArX}]) [L] + k_{-2} [L]^2} \right) [\text{ArX}]$$

b) If PdL<sub>3</sub> is reactive (k<sub>3</sub> > 0) and [L] is large:

$$k_{\text{obs}} = \left( \frac{k_{-1} k_3 K_1}{k_1 + k_3 [\text{ArX}]} + \frac{k_4 K_1}{[L]} + \frac{k_2 k_5 K_1}{(k_{-2} K_1 + k_5 [\text{ArX}]) [L] + k_{-2} [L]^2} \right) [\text{ArX}]$$

#### A.1.4 Kinetic Data for Oxidative Addition of PhBr to Pd(PCy<sub>3</sub>)<sub>2</sub>

##### A. 1.4.1 ln[Pd(PCy<sub>3</sub>)<sub>2</sub>] as a Function of Time without TOPB

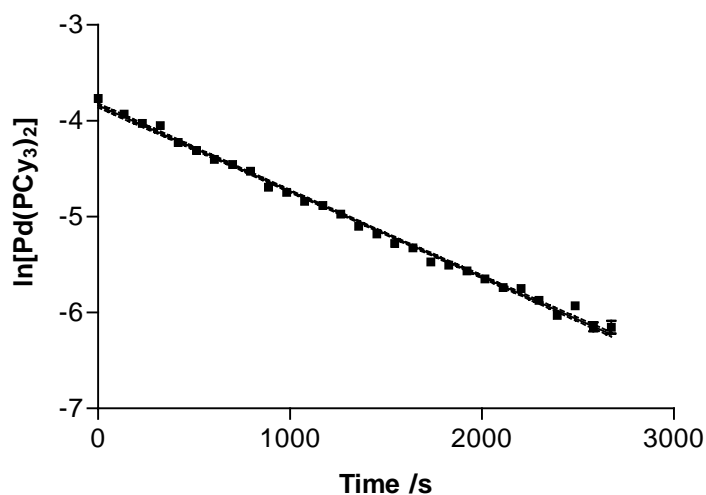


Figure 77. ln[Pd(PCy<sub>3</sub>)<sub>2</sub>] as a function of time for oxidative addition of PhBr (0.234 M) to Pd(PCy<sub>3</sub>)<sub>2</sub> ([Pd(PCy<sub>3</sub>)<sub>2</sub>]<sub>0</sub> = 0.0232 M) at 25 °C in toluene-d<sub>8</sub>.

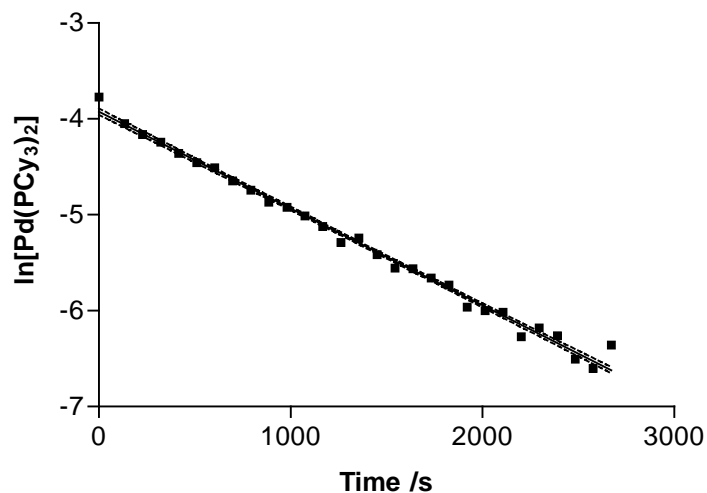


Figure 78.  $\ln[\text{Pd}(\text{PCy}_3)_2]$  as a function of time for oxidative addition of PhBr (0.263 M) to  $\text{Pd}(\text{PCy}_3)_2$  ( $[\text{Pd}(\text{PCy}_3)_2]_0 = 0.0232 \text{ M}$ ) at 25 °C in toluene- $\text{d}_8$ .

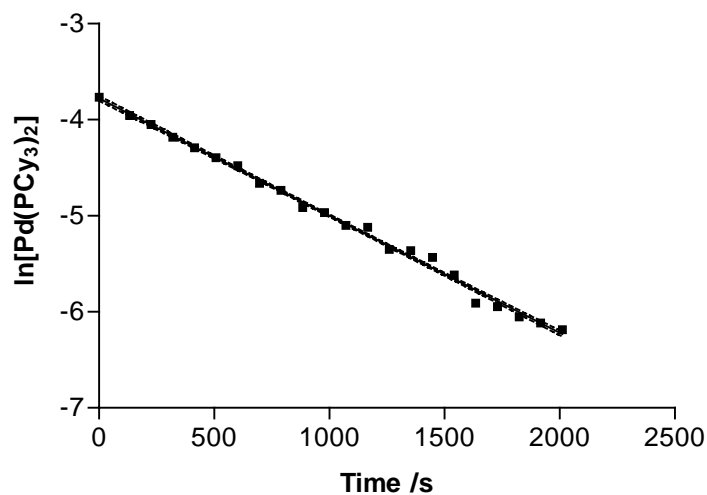


Figure 79.  $\ln[\text{Pd}(\text{PCy}_3)_2]$  as a function of time for oxidative addition of PhBr (0.483 M) to  $\text{Pd}(\text{PCy}_3)_2$  ( $[\text{Pd}(\text{PCy}_3)_2]_0 = 0.0232 \text{ M}$ ) at 25 °C in toluene- $\text{d}_8$ .

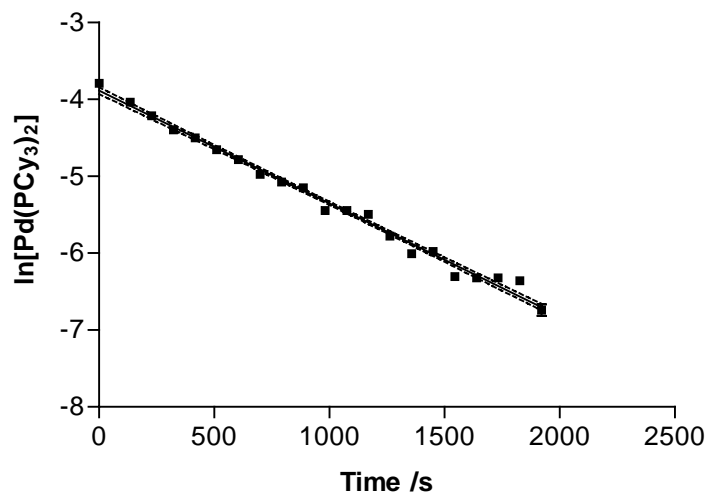


Figure 80.  $\ln[\text{Pd}(\text{PCy}_3)_2]$  as a function of time for oxidative addition of PhBr (0.688 M) to  $\text{Pd}(\text{PCy}_3)_2$  ( $[\text{Pd}(\text{PCy}_3)_2]_0 = 0.0226 \text{ M}$ ) at 25 °C in toluene- $\text{d}_8$ .

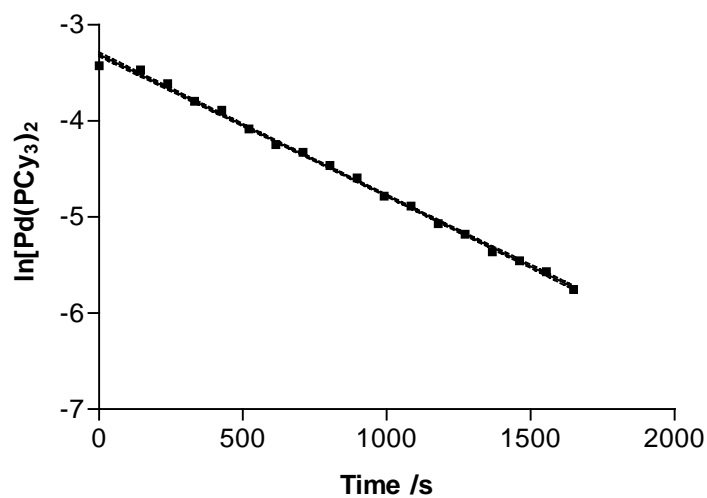


Figure 81.  $\ln[\text{Pd}(\text{PCy}_3)_2]$  as a function of time for oxidative addition of PhBr (0.693 M) to  $\text{Pd}(\text{PCy}_3)_2$  ( $[\text{Pd}(\text{PCy}_3)_2]_0 = 0.0326 \text{ M}$ ) at 25 °C in toluene- $\text{d}_8$ .



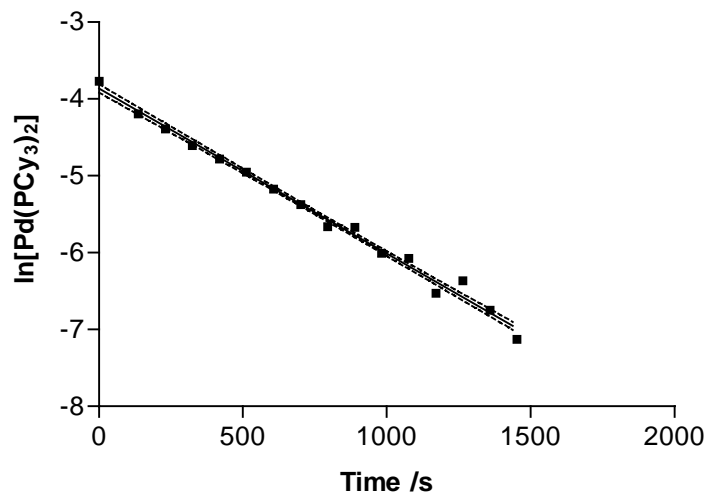


Figure 82.  $\ln[\text{Pd}(\text{PCy}_3)_2]$  as a function of time for oxidative addition of PhBr (1.16 M) to  $\text{Pd}(\text{PCy}_3)_2$  ( $[\text{Pd}(\text{PCy}_3)_2]_0 = 0.0232 \text{ M}$ ) at 25 °C in toluene- $d_8$ .

#### A.1.4.2 $\ln[\text{Pd}(\text{PCy}_3)_2]$ as a Function of Time with TOPB

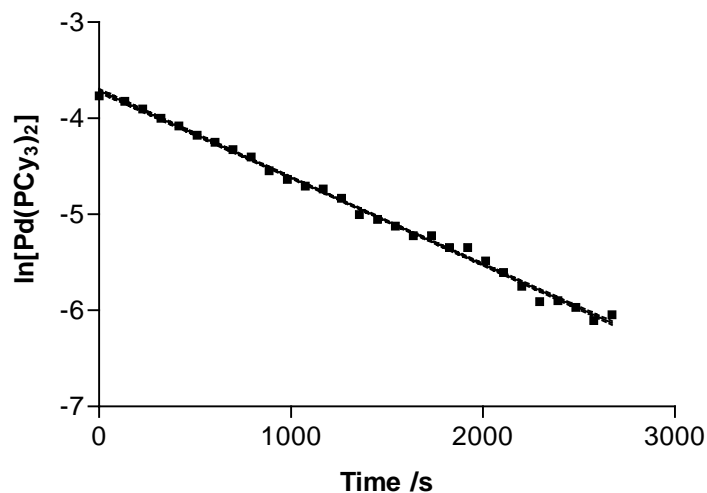


Figure 83.  $\ln[\text{Pd}(\text{PCy}_3)_2]$  as a function of time for oxidative addition of PhBr (0.234 M) to  $\text{Pd}(\text{PCy}_3)_2$  in the presence of TOPB ( $[\text{Pd}(\text{PCy}_3)_2]_0 = 0.0232 \text{ M}$ ,  $[\text{TOPB}] = 0.0231 \text{ M}$ ) at 25 °C in toluene- $d_8$ .

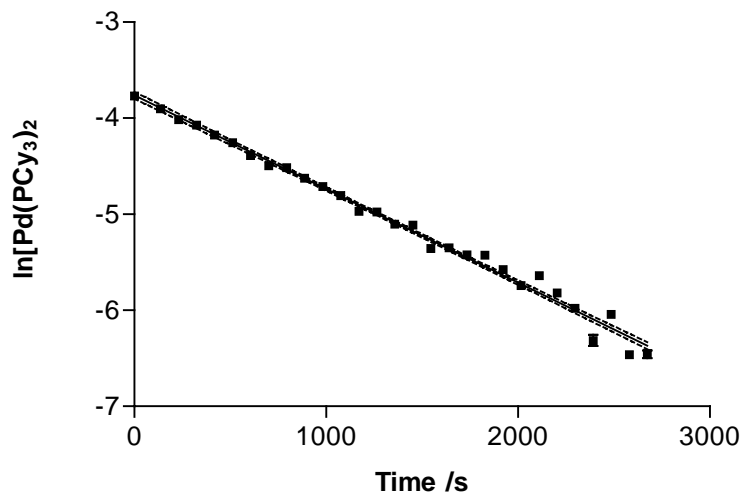


Figure 84.  $\ln[\text{Pd}(\text{PCy}_3)_2]$  as a function of time for oxidative addition of PhBr (0.263 M) to  $\text{Pd}(\text{PCy}_3)_2$  in the presence of TOPB ( $[\text{Pd}(\text{PCy}_3)_2]_0 = 0.0232 \text{ M}$ ,  $[\text{TOPB}] = 0.0231 \text{ M}$ ) at 25 °C in toluene- $d_8$ .

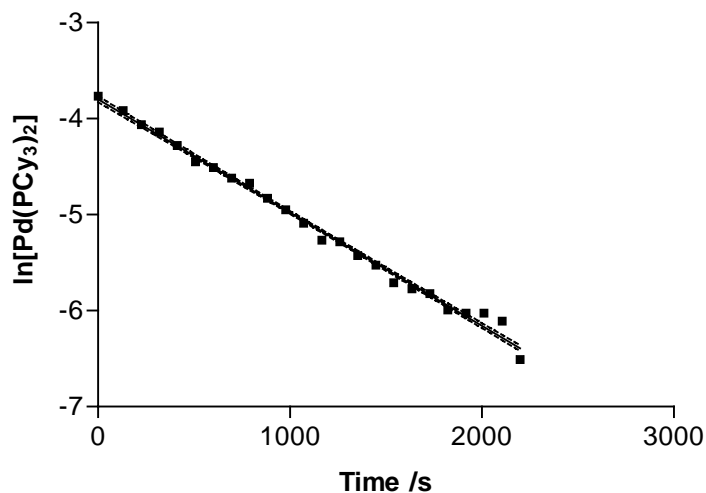


Figure 85.  $\ln[\text{Pd}(\text{PCy}_3)_2]$  as a function of time for oxidative addition of PhBr (0.483 M) to  $\text{Pd}(\text{PCy}_3)_2$  in the presence of TOPB ( $[\text{Pd}(\text{PCy}_3)_2]_0 = 0.0232 \text{ M}$ ,  $[\text{TOPB}] = 0.0231 \text{ M}$ ) at 25 °C in toluene- $d_8$ .

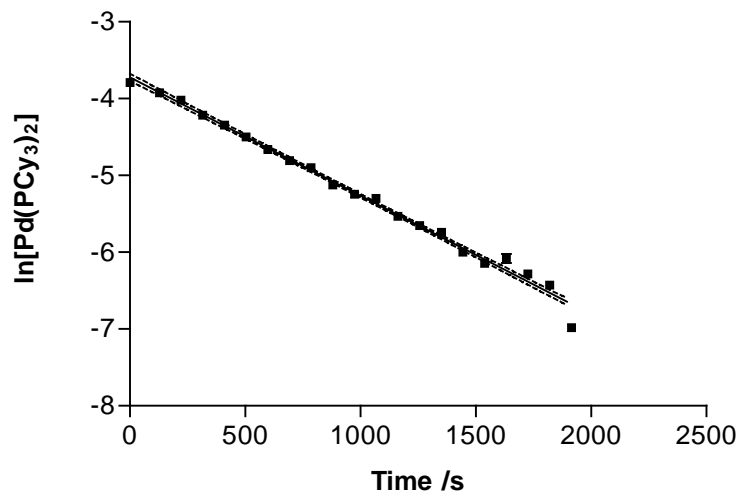


Figure 86.  $\ln[\text{Pd}(\text{PCy}_3)_2]$  as a function of time for oxidative addition of PhBr (0.688 M) to  $\text{Pd}(\text{PCy}_3)_2$  in the presence of TOPB ( $[\text{Pd}(\text{PCy}_3)_2]_0 = 0.0226 \text{ M}$ ,  $[\text{TOPB}] = 0.0231 \text{ M}$ ) at 25 °C in toluene- $\text{d}_8$ .

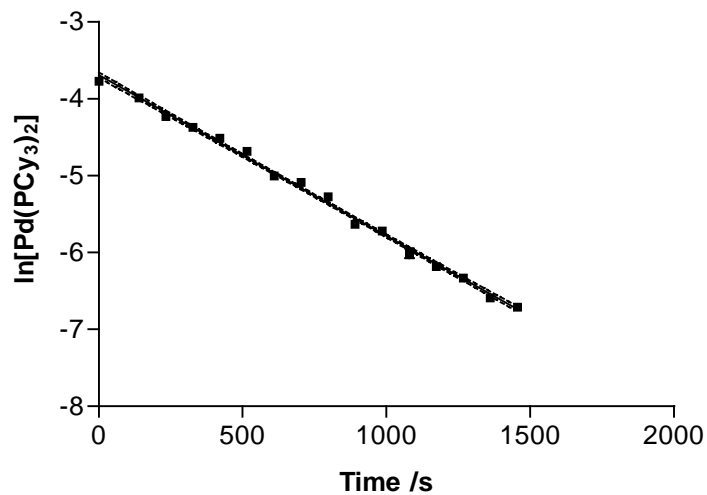


Figure 87.  $\ln[\text{Pd}(\text{PCy}_3)_2]$  as a function of time for oxidative addition of PhBr (1.16 M) to  $\text{Pd}(\text{PCy}_3)_2$  in the presence of TOPB ( $[\text{Pd}(\text{PCy}_3)_2]_0 = 0.0232 \text{ M}$ ,  $[\text{TOPB}] = 0.0231 \text{ M}$ ) at 25 °C in toluene- $\text{d}_8$ .

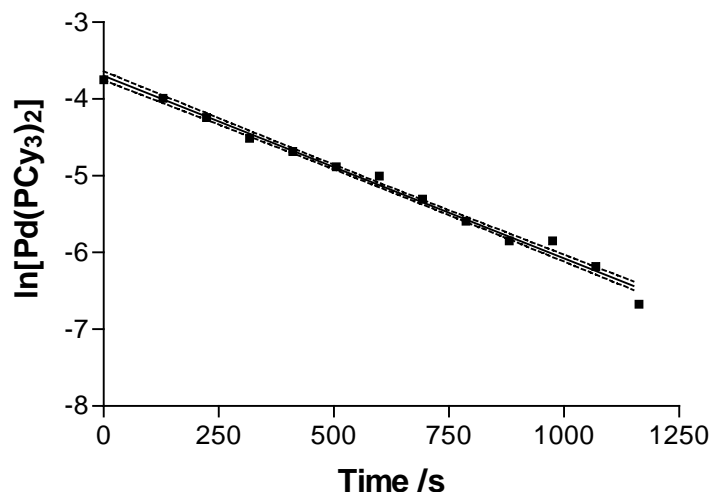


Figure 88.  $\ln[\text{Pd}(\text{PCy}_3)_2]$  as a function of time for oxidative addition of PhBr (1.39 M) to  $\text{Pd}(\text{PCy}_3)_2$  in the presence of TOPB ( $[\text{Pd}(\text{PCy}_3)_2]_0 = 0.0235 \text{ M}$ ,  $[\text{TOPB}] = 0.0231 \text{ M}$ ) at  $25^\circ\text{C}$  in toluene- $\text{d}_8$ .

#### A. 1.4.3 $[\text{Pd}(\text{PCy}_3)_2\text{PhBr}]$ as a Function of Time for Oxidative Addition of PhBr to $\text{Pd}(\text{PCy}_3)_2$ in the Presence of $\text{PCy}_3$

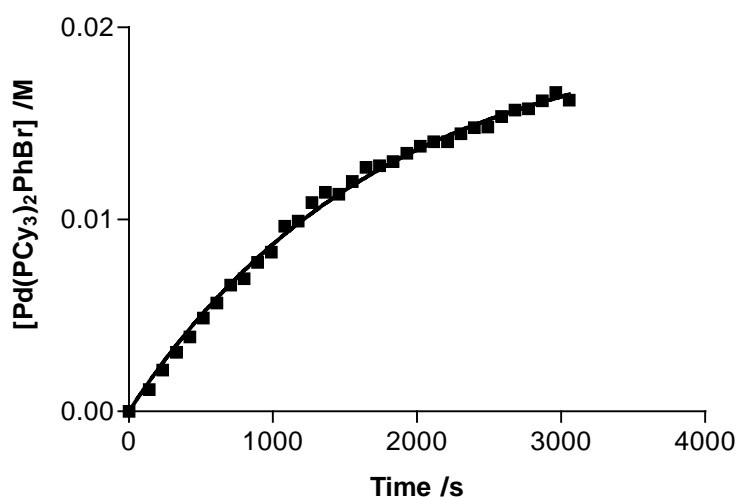


Figure 89. Concentration of  $\text{Pd}(\text{PCy}_3)_2(\text{Ph})(\text{Br})$  as a function of time for the oxidative addition of PhBr (0.272 M) to  $\text{Pd}(\text{PCy}_3)_2$  in the presence of added  $\text{PCy}_3$  ( $[\text{Pd}(\text{PCy}_3)_2]_0 = 0.0213 \text{ M}$ ,  $[\text{PCy}_3]_0 = 0.0214 \text{ M}$ ) at  $25^\circ\text{C}$  in toluene- $\text{d}_8$  (Trial 1).

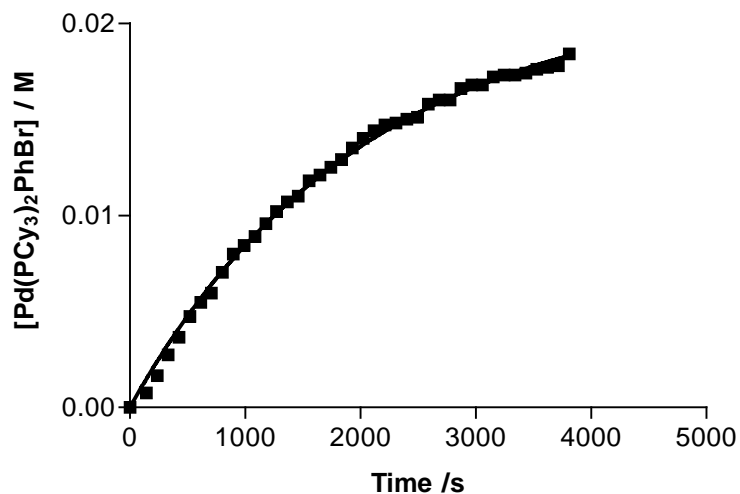


Figure 90. Concentration of Pd(PCy<sub>3</sub>)<sub>2</sub>(Ph)(Br) as a function of time for the oxidative addition of PhBr (0.272 M) to Pd(PCy<sub>3</sub>)<sub>2</sub> in the presence of added PCy<sub>3</sub> ([Pd(PCy<sub>3</sub>)<sub>2</sub>]<sub>0</sub> = 0.0213 M, [PCy<sub>3</sub>]<sub>0</sub> = 0.0214 M) at 25 °C in toluene-d<sub>8</sub> (Trial 2).

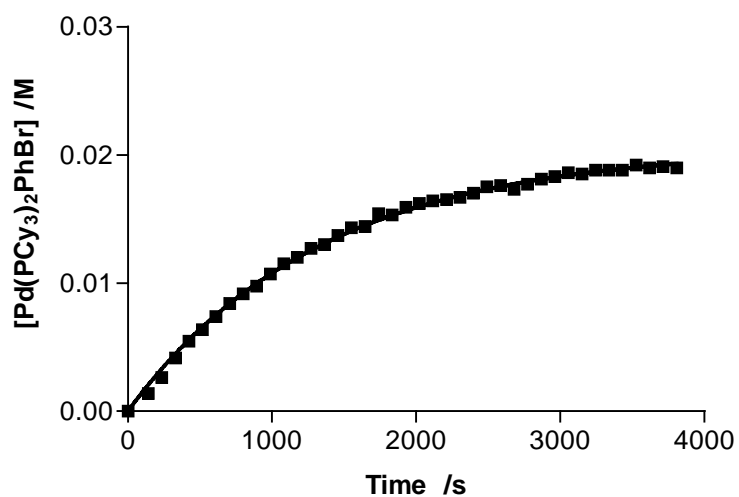


Figure 91. Concentration of Pd(PCy<sub>3</sub>)<sub>2</sub>(Ph)(Br) as a function of time for the oxidative addition of PhBr (0.476 M) to Pd(PCy<sub>3</sub>)<sub>2</sub> in the presence of added PCy<sub>3</sub> ([Pd(PCy<sub>3</sub>)<sub>2</sub>]<sub>0</sub> = 0.0214 M, [PCy<sub>3</sub>]<sub>0</sub> = 0.0214 M) at 25 °C in toluene-d<sub>8</sub> (Trial 1).

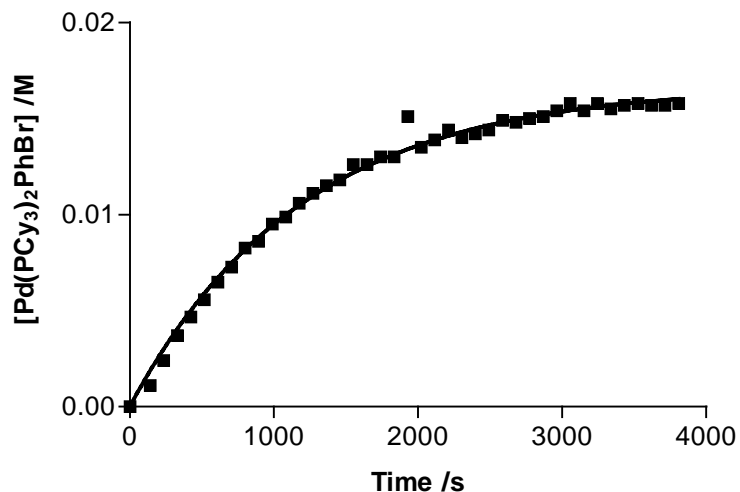


Figure 92. Concentration of Pd(PCy<sub>3</sub>)<sub>2</sub>(Ph)(Br) as a function of time for the oxidative addition of PhBr (0.476 M) to Pd(PCy<sub>3</sub>)<sub>2</sub> in the presence of added PCy<sub>3</sub> ([Pd(PCy<sub>3</sub>)<sub>2</sub>]<sub>o</sub> = 0.0214 M, [PCy<sub>3</sub>]<sub>o</sub> = 0.0214 M) at 25 °C in toluene-d<sub>8</sub> (Trial 2).

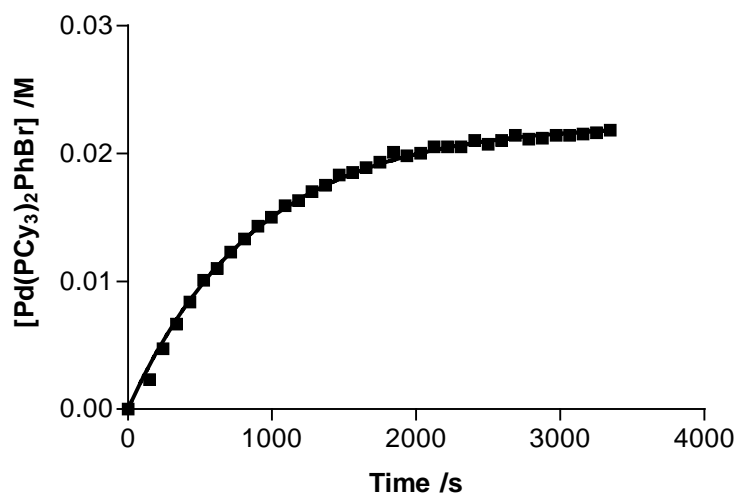


Figure 93. Concentration of Pd(PCy<sub>3</sub>)<sub>2</sub>(Ph)(Br) as a function of time for the oxidative addition of PhBr (0.680 M) to Pd(PCy<sub>3</sub>)<sub>2</sub> in the presence of added PCy<sub>3</sub> ([Pd(PCy<sub>3</sub>)<sub>2</sub>]<sub>o</sub> = 0.0219 M, [PCy<sub>3</sub>]<sub>o</sub> = 0.0214 M) at 25 °C in toluene-d<sub>8</sub> (Trial 1).

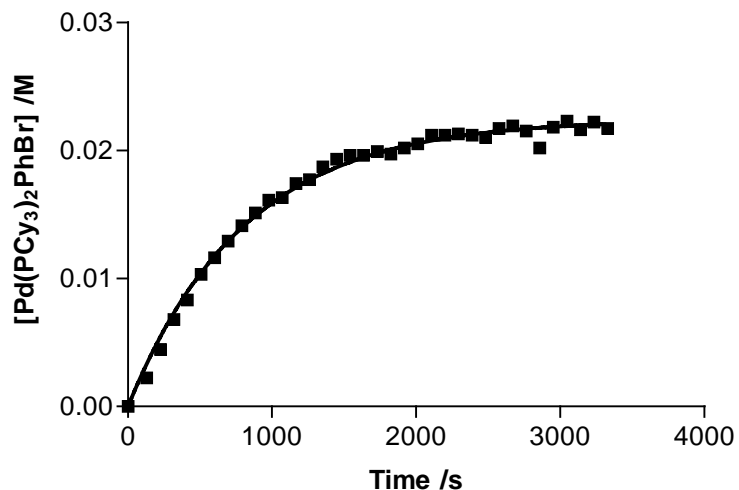


Figure 94. Concentration of Pd(PCy<sub>3</sub>)<sub>2</sub>(Ph)(Br) as a function of time for the oxidative addition of PhBr (0.680 M) to Pd(PCy<sub>3</sub>)<sub>2</sub> in the presence of added PCy<sub>3</sub> ([Pd(PCy<sub>3</sub>)<sub>2</sub>]<sub>0</sub> = 0.0219 M, [PCy<sub>3</sub>]<sub>0</sub> = 0.0214 M) at 25 °C in toluene-d<sub>8</sub> (Trial 2).

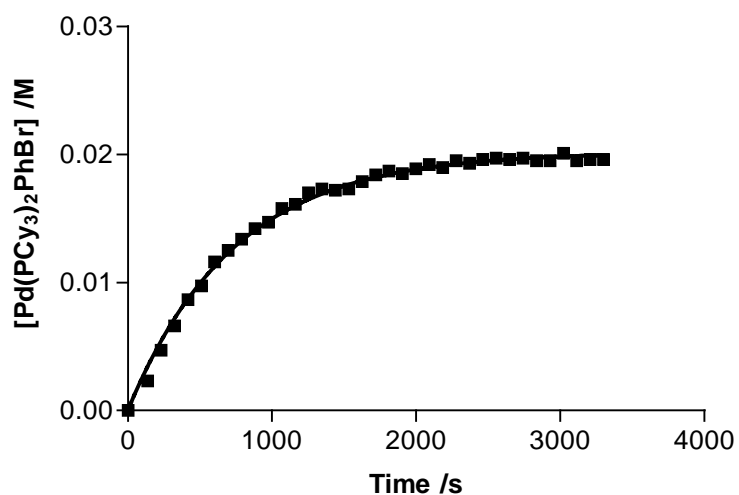


Figure 95. Concentration of Pd(PCy<sub>3</sub>)<sub>2</sub>(Ph)(Br) as a function of time for the oxidative addition of PhBr (0.816 M) to Pd(PCy<sub>3</sub>)<sub>2</sub> in the presence of added PCy<sub>3</sub> ([Pd(PCy<sub>3</sub>)<sub>2</sub>]<sub>0</sub> = 0.0214 M, [PCy<sub>3</sub>]<sub>0</sub> = 0.0214 M) at 25 °C in toluene-d<sub>8</sub> (Trial 1).

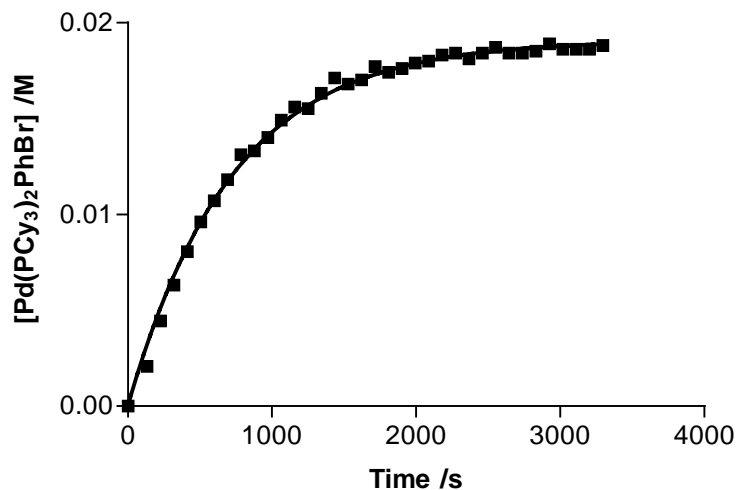


Figure 96. Concentration of Pd(PCy<sub>3</sub>)<sub>2</sub>(Ph)(Br) as a function of time for the oxidative addition of PhBr (0.816 M) to Pd(PCy<sub>3</sub>)<sub>2</sub> in the presence of added PCy<sub>3</sub> ([Pd(PCy<sub>3</sub>)<sub>2</sub>]<sub>0</sub> = 0.0214 M, [PCy<sub>3</sub>]<sub>0</sub> = 0.0214 M) at 25 °C in toluene-d<sub>8</sub> (Trial 2).

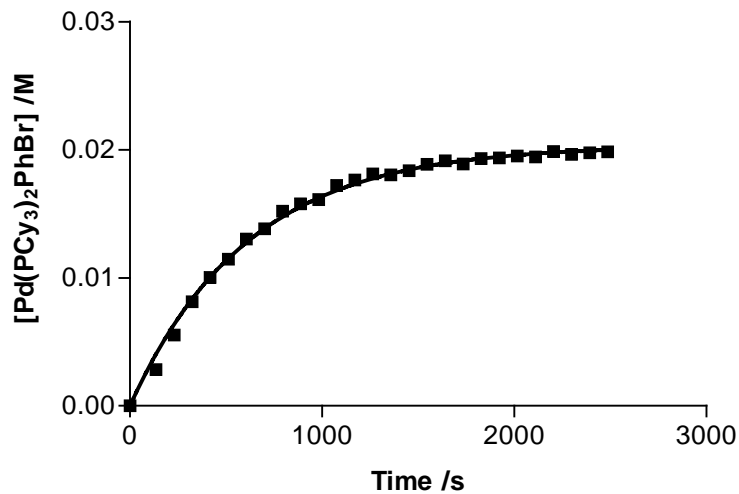


Figure 97. Concentration of Pd(PCy<sub>3</sub>)<sub>2</sub>(Ph)(Br) as a function of time for the oxidative addition of PhBr (1.09 M) to Pd(PCy<sub>3</sub>)<sub>2</sub> in the presence of added PCy<sub>3</sub> ([Pd(PCy<sub>3</sub>)<sub>2</sub>]<sub>0</sub> = 0.0212 M, [PCy<sub>3</sub>]<sub>0</sub> = 0.0214 M) at 25 °C in toluene-d<sub>8</sub> (Trial 1).



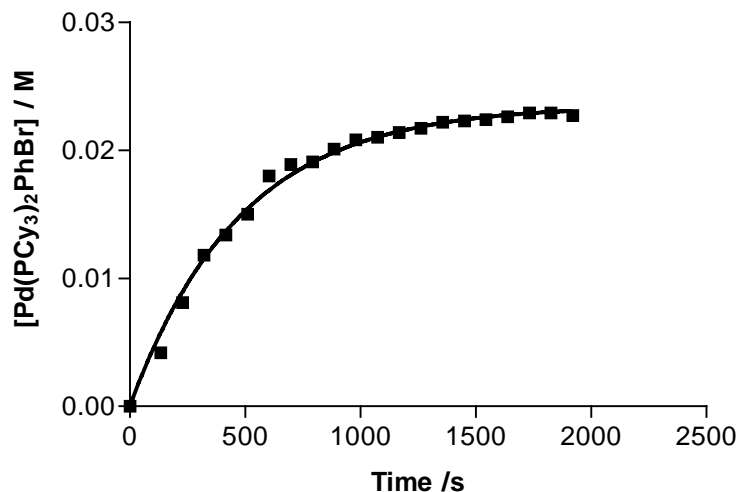


Figure 98. Concentration of Pd(PCy<sub>3</sub>)<sub>2</sub>(Ph)(Br) as a function of time for the oxidative addition of PhBr (1.09 M) to Pd(PCy<sub>3</sub>)<sub>2</sub> in the presence of added PCy<sub>3</sub> ([Pd(PCy<sub>3</sub>)<sub>2</sub>]<sub>0</sub> = 0.0219 M, [PCy<sub>3</sub>]<sub>0</sub> = 0.0214 M) at 25 °C in toluene-d<sub>8</sub> (Trial 2).

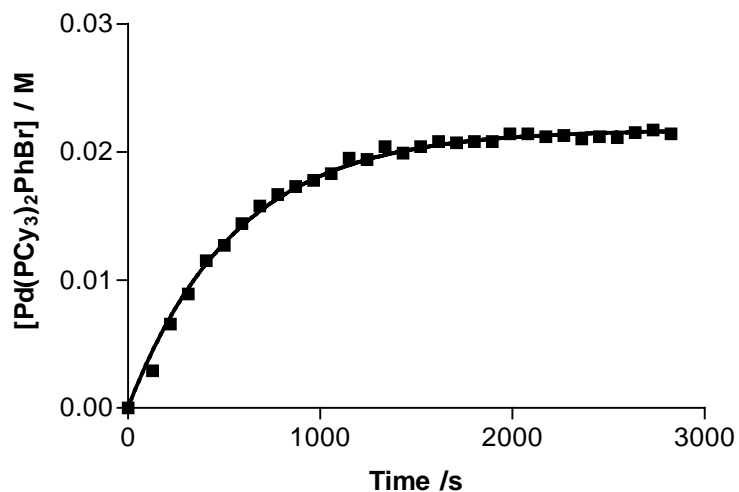


Figure 99. Concentration of Pd(PCy<sub>3</sub>)<sub>2</sub>(Ph)(Br) as a function of time for the oxidative addition of PhBr (1.09 M) to Pd(PCy<sub>3</sub>)<sub>2</sub> in the presence of added PCy<sub>3</sub> ([Pd(PCy<sub>3</sub>)<sub>2</sub>]<sub>0</sub> = 0.0214 M, [PCy<sub>3</sub>]<sub>0</sub> = 0.0214 M) at 25 °C in toluene-d<sub>8</sub> (Trial 3).